

Advances in Polymer Science 282

Maria Laura Di Lorenzo
René Androsch *Editors*

Industrial Applications of Poly(lactic acid)

 Springer

Editorial Board:

- A. Abe, Yokohama, Kanagawa, Japan
- A.-C. Albertsson, Stockholm, Sweden
- G.W. Coates, Ithaca, NY, USA
- J. Genzer, Raleigh, NC, USA
- S. Kobayashi, Kyoto, Japan
- K.-S. Lee, Daejeon, South Korea
- L. Leibler, Paris, France
- T.E. Long, Blacksburg, VA, USA
- M. Möller, Aachen, Germany
- O. Okay, Istanbul, Turkey
- V. Percec, Philadelphia, PA, USA
- B.Z. Tang, Hong Kong, China
- E.M. Terentjev, Cambridge, UK
- P. Theato, Karlsruhe, Germany
- M.J. Vicent, Valencia, Spain
- B. Voit, Dresden, Germany
- U. Wiesner, Ithaca, NY, USA
- X. Zhang, Beijing, China

Aims and Scope

The series *Advances in Polymer Science* presents critical reviews of the present and future trends in polymer and biopolymer science. It covers all areas of research in polymer and biopolymer science including chemistry, physical chemistry, physics, material science.

The thematic volumes are addressed to scientists, whether at universities or in industry, who wish to keep abreast of the important advances in the covered topics.

Advances in Polymer Science enjoys a longstanding tradition and good reputation in its community. Each volume is dedicated to a current topic, and each review critically surveys one aspect of that topic, to place it within the context of the volume. The volumes typically summarize the significant developments of the last 5 to 10 years and discuss them critically, presenting selected examples, explaining and illustrating the important principles, and bringing together many important references of primary literature. On that basis, future research directions in the area can be discussed. *Advances in Polymer Science* volumes thus are important references for every polymer scientist, as well as for other scientists interested in polymer science - as an introduction to a neighboring field, or as a compilation of detailed information for the specialist.

Review articles for the individual volumes are invited by the volume editors. Single contributions can be specially commissioned.

Readership: Polymer scientists, or scientists in related fields interested in polymer and biopolymer science, at universities or in industry, graduate students.

Special offer:

For all clients with a standing order we offer the electronic form of *Advances in Polymer Science* free of charge.

More information about this series at <http://www.springer.com/series/12>

Maria Laura Di Lorenzo • René Androsch
Editors

Industrial Applications of Poly(lactic acid)

With contributions by

D. Bezuidenhout · A. Bouzouita · H. Brünig · A. Cain ·
X. Chen · J. Ding · P. Dubois · G. G. Ferrer · T. Groth ·
W. Hadasha · I. Kühnert · F. Lauro · J. Li · A. Liedmann ·
J. F. Liu · T. Liu · Z.-M. Liu · M. Malinconico · M. S. Niepel ·
D. Notta-Cuvier · J.-M. Raquez · N. Rudolph · Y. Spörer ·
Y. Tajitsu · N. H. A. Tran · M. Van den Eynde ·
P. Van Puyvelde · E. T. H. Vink · L. Yan

 Springer

Editors

Maria Laura Di Lorenzo
National Research Council
Institute of Polymers, Composites and
Biomaterials
Pozzuoli, Italy

René Androsch
Interdisciplinary Center for Transfer-Oriented
Research in Natural Sciences
Martin Luther University Halle-Wittenberg
Halle/Saale, Germany

ISSN 0065-3195

Advances in Polymer Science

ISBN 978-3-319-75458-1

<https://doi.org/10.1007/978-3-319-75459-8>

ISSN 1436-5030 (electronic)

ISBN 978-3-319-75459-8 (eBook)

Library of Congress Control Number: 2018941238

© Springer International Publishing AG, part of Springer Nature 2018

This work is subject to copyright. All rights are reserved by the Publisher, whether the whole or part of the material is concerned, specifically the rights of translation, reprinting, reuse of illustrations, recitation, broadcasting, reproduction on microfilms or in any other physical way, and transmission or information storage and retrieval, electronic adaptation, computer software, or by similar or dissimilar methodology now known or hereafter developed.

The use of general descriptive names, registered names, trademarks, service marks, etc. in this publication does not imply, even in the absence of a specific statement, that such names are exempt from the relevant protective laws and regulations and therefore free for general use.

The publisher, the authors and the editors are safe to assume that the advice and information in this book are believed to be true and accurate at the date of publication. Neither the publisher nor the authors or the editors give a warranty, express or implied, with respect to the material contained herein or for any errors or omissions that may have been made. The publisher remains neutral with regard to jurisdictional claims in published maps and institutional affiliations.

Printed on acid-free paper

This Springer imprint is published by the registered company Springer Nature Switzerland AG
The registered company address is: Gewerbestrasse 11, 6330 Cham, Switzerland

Preface

Poly(L-lactic acid) (PLLA) industrial production has been rapidly increasing because it can fulfil the dream of having cost-efficient and non-petroleum-based plastics with numerous advantageous properties. The huge benefits of PLLA as a renewable and environment-friendly polymer are its versatility and biodegradation after discarding in natural conditions. For example, a PLLA bottle left in the ocean typically degrades within 2 years, whereas conventional plastics may survive several hundred to a thousand years before degrading in the same environment. Accordingly, there is a high potential for PLLA to be useful in short-lifespan applications where biodegradability is highly beneficial. Of note, despite its ability to degrade after disposal, PLLA is extremely robust when used for applications like food packaging, parts in electronic industry, automotive, or in the biomedical sector.

Synthesis, structure and properties of PLLA were covered in a preceding volume of *Advances in Polymer Science*. The present volume completes our collection of research topics on this highly promising biopolymer, with an overview of the state-of-art of the main industrial applications.

The volume starts with a description of processing challenges of PLLA compared to commodity petroleum-based polymers, with details on processing conditions in extrusion, melt spinning, injection molding and additive manufacturing. This is followed by an overview of applications of PLLA in commodities and specialties, focusing on food packaging and agriculture, where compostability and biodegradation of PLLA represent an added value.

The three next chapters describe biomedical applications of PLLA, as it is biocompatible, safe for direct contact with biological tissues, and bioresorbable. PLLA is now widely accepted as biomaterial in cardiovascular devices and skeletal tissue engineering, as well as for controlled drug release. These chapters are followed by details on one of the main processing methods of PLLA used in the biomedical field to produce scaffolds for tissue engineering: additive manufacturing technologies, commonly called 3D printing.

Besides being compostable, biodegradable, biocompatible, and bioresorbable, PLLA has also piezoelectric characteristics, which permits its application in sensor devices, being discussed in a separate chapter. Brand new applications of PLLA appeared in the automotive industry, as the more and more stringent environmental regulations lead to huge research efforts devoted to ecofriendly alternative solutions in the automotive market, summarized in the final chapter of this volume.

As Editors, we would like to express our sincere gratitude to all our friends and colleagues that contributed to this volume, including all the authors that provided excellent contributions on the various aspects of industrial production and applications of PLLA, as well as to all who actively participated in the review process, investing time and efforts to revise and comment each chapter.

We hope that this volume promotes further development of PLLA to widen its range of applications as a bio-sourced and biodegradable polymer, thus limiting the waste of natural resources for plastic production and decreasing plastic production, all to preserve a sustainable environment for our future generations.

Pozzuoli, Italy
Halle/Saale, Germany

Maria Laura Di Lorenzo
René Androsch

Contents

Processing of Poly(lactic Acid)	1
Ines Kühnert, Yvonne Spörer, Harald Brünig, Nguyen Hoai An Tran, and Natalie Rudolph	
Applications of Poly(lactic Acid) in Commodities and Specialties	35
Mario Malinconico, Erwin T.H. Vink, and Andrea Cain	
Poly(lactic acid) as Biomaterial for Cardiovascular Devices and Tissue Engineering Applications	51
Waled Hadasha and Deon Bezuidenhout	
Tailoring Bulk and Surface Composition of Polylactides for Application in Engineering of Skeletal Tissues	79
Gloria Gallego Ferrer, Andrea Liedmann, Marcus S. Niepel, Zhen-Mei Liu, and Thomas Groth	
Poly(lactic acid) Controlled Drug Delivery	109
Jiannan Li, Jianxun Ding, Tongjun Liu, Jessica F. Liu, Lesan Yan, and Xuesi Chen	
3D Printing of Poly(lactic acid)	139
Michael Van den Eynde and Peter Van Puyvelde	
Poly(lactic acid) for Sensing Applications	159
Yoshiro Tajitsu	
Poly(lactic acid)-Based Materials for Automotive Applications	177
Amani Bouzouita, Delphine Notta-Cuvier, Jean-Marie Raquez, Franck Lauro, and Philippe Dubois	
Index	221

Processing of Poly(lactic Acid)



**Ines Kühnert, Yvonne Spörer, Harald Brüning, Nguyen Hoai An Tran,
and Natalie Rudolph**

Abstract Polymer applications range from biomedical devices and structures, packaging, or toys to automotive and industrial items. So far, biopolymers could replace commodity polymers in a variety of products, especially for biomedical applications or food packaging. One of the most used and widely studied biopolymers is poly(lactic acid) (PLA). To generate new application fields and provide a broader application of PLA, research on processing behavior is still required. This chapter covers the processing relevant behavior of PLA and processing conditions for extrusion melt spinning, injection molding, and additive manufacturing. The processing-related behavior is compared to that of commodity polymers. The aim is to provide an overview of the state of the art and some recent new developments in this research field.

Keywords 3D printing • Additive manufacturing • Crystallization • Injection molding • Interface • Interphase • Mechanical properties • Melt spinning • Morphology • Poly(lactic acid) • Processing • Rheological behavior • Skin-core morphology • Thermal properties • Weld line

I. Kühnert (✉), Y. Spörer, and H. Brüning
Leibniz-Institut für Polymerforschung Dresden e. V., Hohe Straße 6, 01069 Dresden, Germany
e-mail: kuehnert@ipfdd.de

N.H.A. Tran
Institute of Textile Machinery and High Performance Material Technology, Technische
Universität Dresden, 01062 Dresden, Germany

N. Rudolph
Polymer Engineering Center, Department of Mechanical Engineering, University of
Wisconsin-Madison, 1513 University Avenue, Madison, WI 53706, USA

Contents

1	Poly(lactic Acid) and Its Processing-Related Behavior	2
1.1	Introduction	2
1.2	Poly(lactic Acid)	2
1.3	Processing-Related Behavior of PLA	3
2	Insights into the Processing of PLA	8
2.1	Extrusion	8
2.2	Melt Spinning	10
2.3	Injection Molding	17
2.4	Additive Manufacturing	25
3	Summary	29
	References	29

1 Poly(lactic Acid) and Its Processing-Related Behavior

1.1 Introduction

Biopolymers (bio-based and/or biodegradable) such as poly(lactic acid) (PLA) are processed and used in the same way as petrochemical-derived polymer materials [1–3]. Morphology development during processing and its correlation with final product properties, together with sketchy long-term behavior, keeps these materials from accelerated market growth [3]. PLA is one of the best known and best understood bio-based materials. Its biocompatibility, biodegradation, and non-toxic behavior makes this material attractive for use as structural parts and also as a functional polymer, for example as an additive in paper materials, adhesives, coatings, thickening agent, flocculants, and concrete agent [1, 2]. In this chapter the processes for manufacturing structural parts and several specific strategies to improve the “structure-process-property” relationship are described.

1.2 Poly(lactic Acid)

The lactic acid monomer for PLA exists in two optically active configurations, namely L-lactic acid and D-lactic acid. Depending on the monomers used and the synthesis reaction conditions, it is possible to control the L-to-D ratio of the final polymer. Therefore, different grades of PLA are available on the market, such as pure poly-L-lactic acid (PLLA), poly-D-lactic acid (PDLA), or PLA with variation of the D content. There are three possible paths for polymerization of lactic acid: direct condensation polymerization, direct poly-condensation in an azeotropic solution, and polymerization through lactic acid formation [4]. As with conventional polymers, a high degree of polymerization and increasing crystallinity lead to an increase in strength, elastic modulus, glass transition temperature (T_g), and melt temperature [5]. According to process parameters, a recrystallization step for the

PLA is set to improve stability against water absorption. In crystalline form, PLA has better chemical stability, and the water resistance and speed of biodegradability are less than for amorphous PLA [5].

Neat PLA shows the following technical properties:

- High Young's modulus
- High scratch resistance
- High transparency
- Certified compostability
- Good printability
- Heat sealability
- High hydrophilicity
- Brittle, low impact strength
- Low heat resistance

To improve the properties and processing behavior of PLA, it is usually compounded and/or blended by the use of different additive packages and fillers. Polymer blends are in general classified into thermodynamically miscible or immiscible blends. Immiscible blends show phase separation and form multiphase structures. Depending on the degree of phase separation of two immiscible polymers, the morphology shows (1) discrete phase-like droplets in the matrix or (2) a bi-continuous phase (co-continuous, matrix-fibrillar structures). From the viewpoint of polymer composites, these structures are in situ reinforced polymer-polymer composites or micro-/nanofibrillar composites [6]. Under certain conditions, the micro- and nanofibrillar structures can be formed during melt processing. Because of the highly hydrophilic behavior of PLA it is recommended that the material be dried before processing. The value of moisture should be less than 0.01 wt% of the total weight to minimize the risk of molecular degradation during processing. For this, PLA resins are packed using moisture-resistant foil liners. The drying condition depends on temperature, time, air flow rate, and dew point. A range of 80–100°C for 4–2 h is recommended for crystalline types. Drying conditions are given in the data sheets of the materials from the manufacturer [4, 7–9].

Some studies of the processing of biomaterials have already been summarized [1–3]. Many academic results exist, and some knowledge has been transferred into industrial applications. Nevertheless, the market growth rate will dynamically increase further in the light of new technology developments (such as in additive manufacturing [AM], melt spinning, and injection molding). A strong driving force is the possibility of controlling structure, especially morphology design, within the product [2, 5, 10–15].

1.3 Processing-Related Behavior of PLA

To understand processing behavior, knowledge of the rheological, thermal, and thermodynamic (pressure-volume-temperature [pvT]) properties of PLA is important [1]. The crystallization behavior of PLA was studied in several investigations

[16–22]. Consequently, the thermal behavior, melting, and crystallization under processing conditions are discussed in detail in the following section. Only a few studies are available regarding rheology and pVT behavior [12, 23, 24], and these are discussed later in Sects. 1.3.2 and 1.3.3.

1.3.1 Thermal Behavior

A typical method to determine thermal properties of polymer materials is differential scanning calorimetry (DSC) [25, 26]. During measurement the sample and a reference are heated and cooled with defined heating and cooling rates, respectively. The differential heat flow is measured, which is proportional to the thermodynamic transformation during melting or crystallization. In contrast to semi-crystalline polymers, for amorphous polymers only T_g can be established. Semi-crystalline polymers show characteristic melting and crystallization behaviors, which, depending on their molecular structure, result in the formation of a detectable heat flow peak. From these peaks the melt and crystallization temperature can be determined. The results can be used to calculate the degree of crystallinity depending on the cooling rate, the crystallization growth rate, and the crystallization temperature. Altogether, these data are important for choosing the right process parameters.

Investigations by Iannace et al. [17] on the isothermal crystallization behavior of PLA have shown that the crystallization growth rate has a maximum which depends on the isothermal crystallization temperature. During these studies, PLA was melted at 200°C for 2 min, cooled down to defined temperatures (90, 110, and 130°C), and then crystallized for 30 min at these temperatures. Following the crystallization, the samples were heated again to 200°C at 10°C/min and the heat flow was measured simultaneously. The influence of cooling condition (cooling rate) was not given. They [17] concluded that the crystallization rate shows a maximum around 105°C and that high undercooling leads to incomplete crystallization. Upon reheating, exothermic crystallization behavior occurs close to the melting point. The presence of amorphous fractions, which do not relax at T_g , was observed. Below 110°C the number of amorphous regions was higher than above 110°C, which means that a regime transition occurs. Similar conclusions were also made in [19, 20]. The crystallization behavior of PLLA using DSC measurements to determine isothermal and non-isothermal thermodynamic behavior was investigated. They reported a discontinuity in crystallization growth at around 116–118°C, resulting in a bell-shaped curve for crystallization growth rate as a function of crystallization temperature. This is shown in Fig. 1, where T_b is the boundary temperature between the low- and high-temperature ranges [20]. The results indicate a difference in the crystallization mechanism between the high and the low temperature values caused by different crystal modifications, which have been reported in various studies [18, 27–29]. Investigations by Miyata [18] have also shown that the crystallization growth rate increases with decreasing average molar mass, M_w [30].

Figure 2 shows the heating curves of PLLA with varying processing history. PLLA was injection molded into a cold mold, which promotes fast cooling

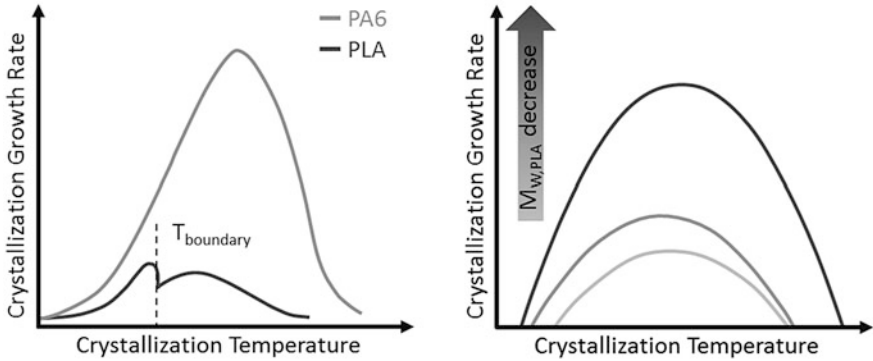


Fig. 1 Bell-shaped crystallization growth curves as a function of isothermal crystallization temperature: (left) PLA [according to 20] compared to PA6 [according to 31]; (right) PLA varying in the molecular mass [according to 18] (modified with permission of Elsevier and AIP)

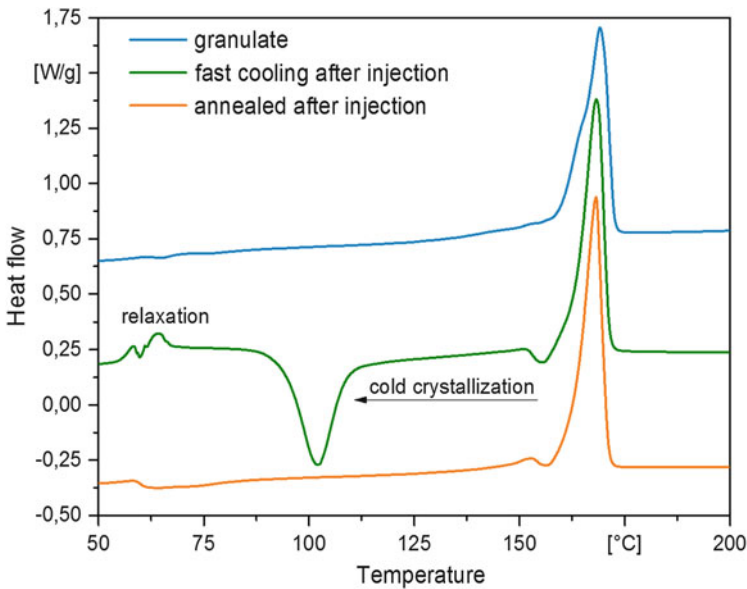


Fig. 2 Heating curves from PLLA after processing. Heating rate 10°C/min and using normal DSC. (Data source: Leibniz-Institut für Polymerforschung Dresden e. V.)

especially on the surface of the molded part. After ejection, the molded parts were optically amorphous and some parts were annealed at 100°C for 24 h. From all injection molded samples, DSC measurements were carried out using a heating and cooling rate of 10°C/min. A cold crystallization peak around 100°C was observed during heating, indicating that macromolecular chains are frozen in their orientation because of the rapid cooling during injection molding. These frozen molecular chains are able to relax and crystallize at temperatures higher than T_g ($T_g = 60^\circ\text{C}$).

Annealing after injection molding occurs with the disappearance of the cold crystallization peak, indicating that the formation of crystallites takes place during this annealing time.

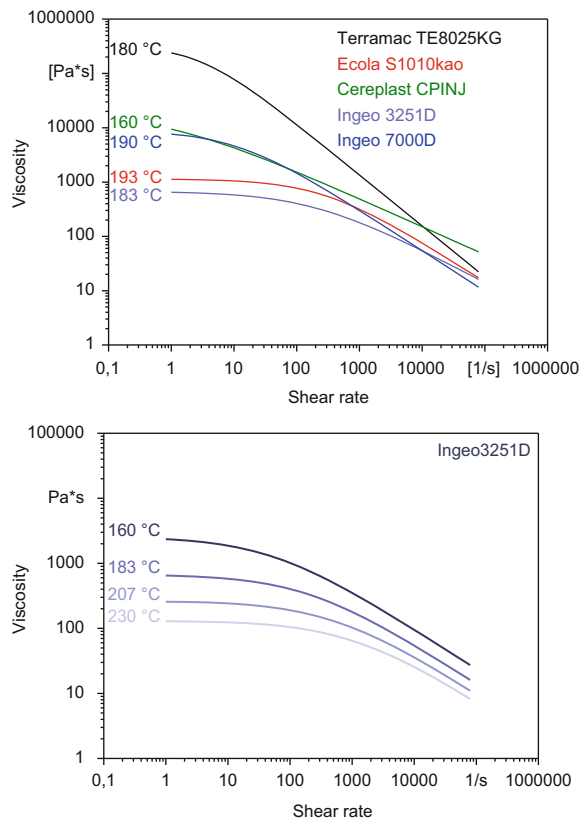
During injection molding, cooling rates of more than $1,000^{\circ}\text{C/s}$ at the polymer/mold interface can occur. To simulate these high cooling rates, fast scanning calorimetry could be used, as is shown in literature for PLLA [32, 33], as well as for other polymers [34, 35].

1.3.2 Flow Behavior

To determine the flow behavior of polymers, the relationship between shear stress and shear rate can be established using rheometers, such as rotational and capillary rheometers [36]. During these measurements, shear strain is induced to determine the viscosity at different temperatures.

Figure 3 shows the influence of shear rate on the viscosity of different PLA types at their average processing temperature (left image) and of PLA 3251D as a function

Fig. 3 Comparison of Moldflow data of viscosity vs shear rate: (*left*) different types of PLA at processing temperature; (*right*) PLA3251D at different temperatures. (Database: Moldflow™, Cadmould, Leibniz-Institut für Polymerforschung Dresden e. V.)



of the temperature (right image). As can be seen, the different types of PLA show different rheological behavior because of their molecular structure. With an increase in temperature (right), the free volume between the molecular chains increases and the intra-molecular friction decreases. This behavior results in the lowering of the viscosity. It is also known that an increase in molecular weight occurs in a shift of the shear rate independent plateau to higher viscosity values [37].

1.3.3 pvT Behavior

pvT measurements are used to describe the thermodynamic behavior of the specific volume, v , as a function of pressure, p , and temperature, T . The data are used to evaluate the processing parameters, especially for injection molding. However, the measurements are carried out using slow heating, and cooling rates are therefore far from real processing conditions.

Amorphous and semi-crystalline polymers show different thermodynamic behavior as shown in Fig. 4. The pvT diagrams show the thermal expansion and specific thermal transitions of polymers [23, 24]. Amorphous polymers such as polycarbonate or polymethylmethacrylate show primary glass transition, T_g , behavior, where T_g is clearly the temperature where the polymer changes from solid to molten state. For semi-crystalline polymers the behavior is different and the pvT diagrams show a transition area in which the polymers maintain structural continuity up to the temperature where the crystals melt. As can be seen in Fig. 4, for PLLA this transition area only occurs at low pressure. However, it is important to note that the cooling rates during these measurements are very slow ($1^\circ\text{C}/\text{min}$). During cooling at high pressure the curve shape assumes a more and more amorphous character, which means that the material becomes solid before crystallization takes place.

To visualize the process-material relation, the pvT diagram can be used. In this diagram the thermodynamic changes of the thermoplastic material and the process data of average part temperature together with the pressure development taken from in-mold pressure measurements during the injection process can be correlated. Finally, all previously discussed material data are basically necessary to reach the optimal process window for the required product properties.

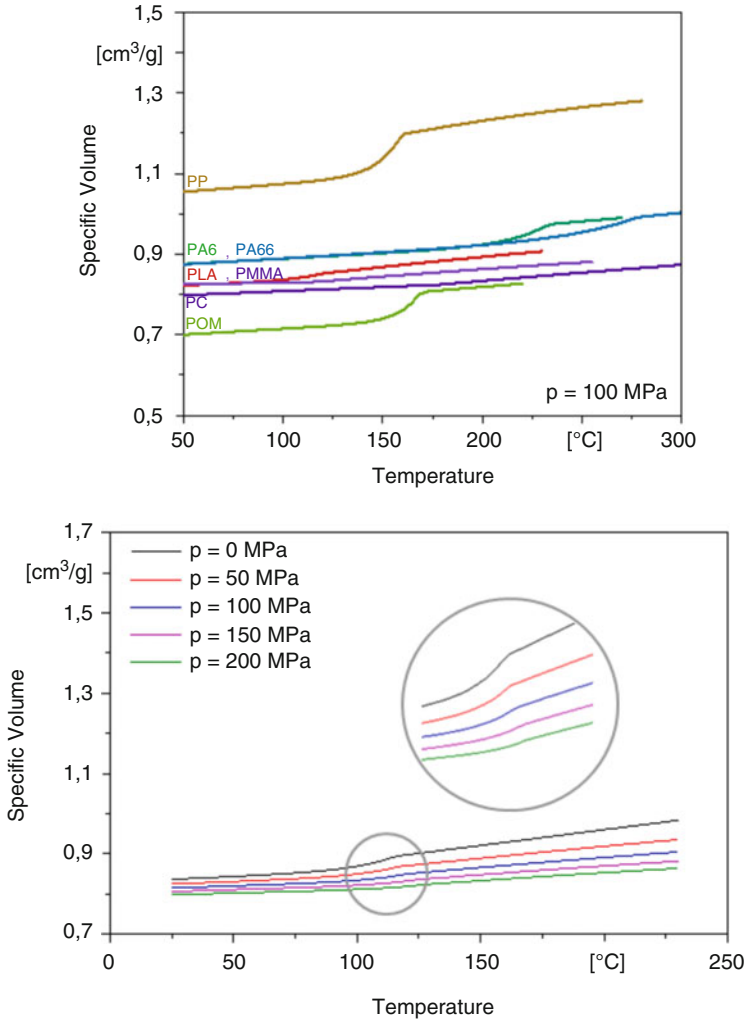


Fig. 4 Comparison of Moldflow data of pVT behavior with specific volume vs temperature and pressure: (*left*) PLA in comparison to other semi-crystalline and amorphous polymers; (*right*) PLA under variation of pressure conditions. (Database: Moldflow™, Cadmould)

2 Insights into the Processing of PLA

2.1 Extrusion

The extrusion process is characterized by the continuous melting, conveying, and discharge of plastic materials through a die. Therefore the typical single screw is divided into feed, transition, and metering sections as shown in Fig. 5. Process

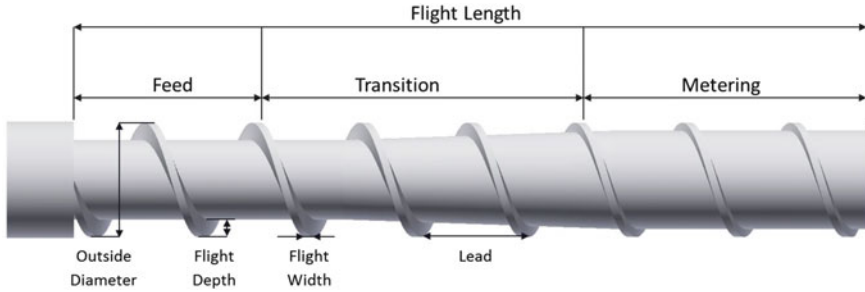


Fig. 5 Extrusion single screw plasticizing unit scheme. (Data source: Leibniz-Institut für Polymerforschung Dresden e. V.)

relevant screw parameters are the L/D ratio and the compression ratio. The L/D ratio is the ratio of flight length to the outer diameter of the screw. The compression ratio is defined as the ratio between the flight depth in the feed section and in the metering section. For PLA, L/D ratios of 24–30 and compression ratios of 2–3 are recommended [38–40].

The plasticizing of PLA starts at the conveying zone with movement of the polymer pellets or powders from the hopper to the screw channel. Inside the channel the rotating screw transports the compacted material down the channel, and the material is sheared and pushed against the barrel wall. Because of the friction during transport through the transition zone, the material melts. Heat bands are wrapped around the outside of the barrel. The thermal energy from the heater combined with frictional heat from the material transport leads to temperatures above the melting point of the PLA ($T_M = 170\text{--}180^\circ\text{C}$) [1]. The temperature of the heater is usually set to $200\text{--}210^\circ\text{C}$ [1] to ensure the deletion of thermal history of the material and that no crystalline structures remain. The size of the solid bed shrinks during the melting of material and a melt pool is formed. After the transition zone, the melt passes into the metering zone, where sufficient pressure is generated to pump the material through the die [1, 41].

Extrusion is used as a shaping process in blow molding and film blowing processes, in which the melt is discharged through a special shaped die. For these processes, a high melt stiffness is required to ensure film stability and a continuous process cycle. In the case of PLA, the melt strength is low and needs to be improved to enlarge the processing window and application field. Therefore, during the last few years, several possibilities have been reported to enhance the melt properties of PLA, dealing primarily with chain modification of PLA [42–48]. Furthermore, the extrusion process plays an important role as plasticizing unit for melt spinning [49–54] and injection molding [5, 55–61].

2.2 Melt Spinning

2.2.1 Introduction

Melt spun PLA fibers from renewable sources are in many cases an alternative for replacement of petroleum-based synthetic fibers, although the requirements regarding thermal stability and rheological flow behavior for the polymeric materials used for melt spinning are high. Two important advantages of the melt spinning process are: (1) the process is environmentally friendly because there are no solvents needed and (2) melt spinning can be done with high productivity, especially by using the high speed spinning process.

The majority of publications focus on melt spinning of PLA and the best results were found using PLA with low D content (lower than 2%) [45].

It is known from injection molding dogbone specimens that PLA parts typically show high brittleness and low elongation at break. However, material processed by a melt spinning process is quite different. Because of the high deformation rate and tensile stress within the spinning line, orientation of the polymeric chains occurs and their crystallization into fibrillary structures is possible. Orientation and crystallization mechanisms allow the producer to adjust significantly the mechanical properties of melt spun PLA fibers. Depending on the spinning conditions, the fibers show elongation at break between 20% (high oriented at maximum possible draw ratio) to 300% (for low speed spinning without drawing), maximum tenacity (tensile strength) up to 35–40 cN/tex¹ (~450–500 MPa), and elastic tensile modulus 2–6 GPa. On account of similarities between PLA fiber properties and their processing behavior with polyethylene terephthalate (PET), the PLA can be processed on existing spinning equipment (filament yarns, staple fibers, spun-bonded nonwovens) [49].

The first laboratory investigations into PLA fiber spinning were carried out with low take-up velocities (lower than 10 m/min). Later, high speed spinning and drawing process conditions were investigated using close to industrial scale extruder spinning equipment [50]. Today, the global production capacity of PLA is ~700,000 tons/year [62] and PLA fiber spinning is now a well-established industrial process.

2.2.2 Properties of PLA Fiber-Grade Pellets

Melt spinning (especially high speed spinning) requires high purity and homogeneity in the primary material. PLA materials differ with respect to their D/L-lactic content, their molecular weight M_w , and their molecular weight/number ratio (M_w/M_n). Typical values for easily spinnable PLA grades are small content of D-lactic (<5%), a molecular weight in the range of $M_w = 250,000$ – $450,000$ g/mol

¹tex is the measure of fineness in textiles (linear density), a fiber has the fineness 1 tex when 1,000 m of fiber length weight 1 g: 1 tex = 1 g/1,000 m.

and a narrow molecular weight distribution ($M_w/M_n = 2-2.5$). Table 1 shows some further properties in comparison with other fiber-forming polymers.

To prevent viscosity/molecular weight degradation during melt spinning, a moisture content of less than 0.005% is recommended. Most drying systems operate using nitrogen or under vacuum.

2.2.3 Melt Spinning of PLA: Process Parameters

Multifilament yarns can be manufactured using melt spinning equipment as shown schematically in Fig. 6. The dried PLA pellets (dried, for example, at 120°C under

Table 1 Comparison of properties of PLA resins with other fiber-forming melt-processable polymers [51]

Property	PLA	Polypropylene	PET	Polyamide
Density (g/cm ³)	1.26	0.92	1.38	1.14
T_g (°C)	55–60	(12–20)	90–100	40–45
Melting temperature (°C)	165–180	175	265	214
Moisture content (%)	0.5	–	0.4	4.5
Heat value (kJ/kg)	19,000	40,000	23,000	31,000

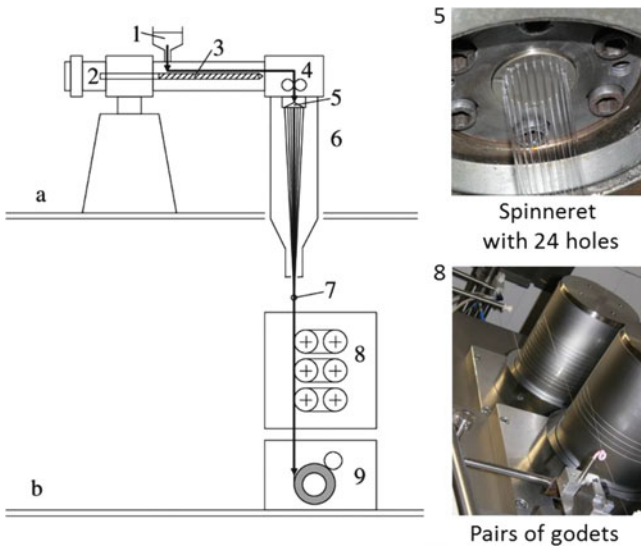


Fig. 6 Melt spinning equipment (schematic): (a) spinning floor; (b) winding floor. (1) Container with polymer pellets, (2) electric motor and drive train, (3) extruder assembly with screw, (4) spinning head with metering pump (gear pump), (5) spinneret with capillary holes, (6) spinning chamber with quenching air, (7) spin finish applicator, (8) pairs of (heatable) godets for online drawing, (9) (high speed) winder. From [52]; corresponds to the melt spinning equipment at Leibniz-Institut für Polymerforschung Dresden e. V.

vacuum for 16 h using a drum dryer) are fed under nitrogen atmosphere into the container (1). Typical dimensions of the extruder screw (3) are 20–40 L/D ratio. The use of a mixing tip and/or a static mixer can be advantageous for creating a uniform melt temperature.

Typical conditions and parameters for the melt spinning of multifilament PLA yarn at Leibniz-Institut für Polymerforschung Dresden e. V. are described below (see Table 2). The extruder zone temperatures and the temperature of the spinning head have to be adapted to the melting temperature of PLA and to its rheological flow behavior. To support a stable spinning process, the viscosity of the melt in the spinneret should be in the range of 100–500 Pas, and the melt pressure should not exceed 50–80 bar.

It is possible to realize the melt spinning procedure with or without an *online* drawing step by godets (as seen in Fig. 6) or with an additional *offline* drawing step after winding the yarn on bobbins at a separate drawing machine.

2.2.4 Mechanical Properties of Fiber Yarns

Figure 7 shows typical results of the mechanical property, tensile strength, as a function of elongation, for three different variants of PLA melt spinning with moderate online drawing. All samples are wound at 3,000 m/min. The values for elongation at break, maximum tensile strength, and Young's modulus are in the ranges of 45–65%, 23–25 cN/tex, and 300–400 MPa, respectively.

An additional offline drawing procedure can be used to improve the yarn's mechanical properties. These external drawing steps increase the orientation as well as the crystallinity of the PLA fiber material, resulting in a reduction of fineness and higher maximum tensile strength (tenacity), higher elastic modulus (Young's modulus), and lower elongation at break. Figure 8 shows the force-elongation behavior of a PLA filament yarn (125 dtex f6) after an offline drawing process with different DR. In this case, a maximum tensile strength of ~30 cN/tex

Table 2 Parameters of melt spinning of PLA. (Data source: Leibniz-Institut für Polymerforschung Dresden e. V.)

Polymer	PLA 6002D (NatureWorks® LLC)
Pellets preparation	Drying at 80°C, 16 h, vacuum
Extruder screw diameter, L/D-ratio	18 mm, 25
Extruder zone temperatures	25, 180, 200, 230, 235, 235°C
Melt temperature	235°C
Spinning pump, mass throughput	18 g/min
Spinneret, number of holes	12
Capillary diameter, L/D ratio	0.3 mm, 2
Quenching chamber, length	1.5 m
Cooling air: temperature, profile	16°C, 0.25 m/s
Take-up velocity, 1st godet	1,500, 2,000, 3,000 m/min
Draw ratio (online)	1.0–3.0
Temperature of drawing godets	80–120°C
Winding speed	3,000–4,500 m/min

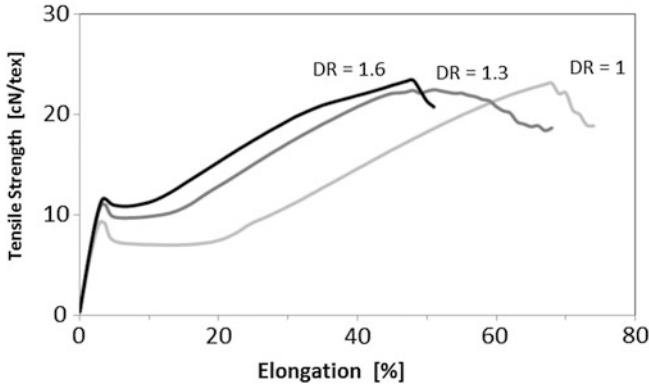


Fig. 7 Tensile strength vs elongation for three different variants of PLA melt spun and online drawn fiber yarns. Online draw ratios (DR) = 1.6, 1.3 and 1.0 (no drawing, for comparison), winding speed: 3,000 m/min, yarn fineness 60 dtex f12. (Data source: Leibniz-Institut für Polymerforschung Dresden e. V. [63])

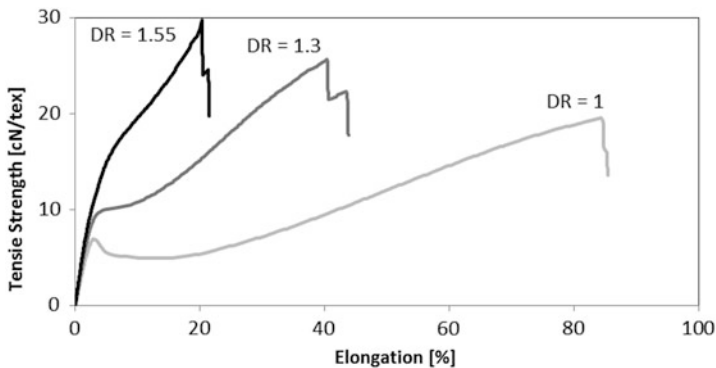


Fig. 8 Tensile strength vs elongation for three different variants of PLA melt spun and offline drawn fiber yarns. Basic yarn fineness: 125 dtex f6, offline DR = 1.55, 1.3, and 1.0 (no drawing, for comparison), fineness after drawing: 97 and 80 dtex f6. (Data source: Leibniz-Institut für Polymerforschung Dresden e. V. [63])

(ca. 375 MPa), an elongation to break of 20%, and an elastic modulus of ~600 MPa was reached for the highest DR = 1.55.

The applied tensile stress is one of the most essential variables for the fiber formation process during the spinning and drawing procedure. The higher the stress the higher the orientation of the polymer chains, which leads to a higher degree of crystallization. This in turn normally leads to improved mechanical properties. However, frozen-in tensions typically cause the thermal shrinkage of the fiber yarns, which is in most cases unwanted. To optimize yarn properties and to reduce internal tensile stress, the producers balance the relaxation by thermal treatment. Figure 9 shows, for example, the shrinkage behavior of a highly

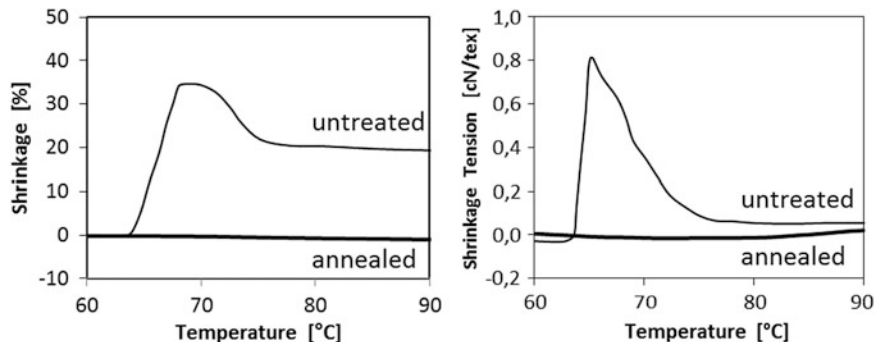


Fig. 9 Shrinkage tension (*left*) and shrinkage (*right*) vs temperature of different thermal treated PLA fiber yarns. The shrinkage of the untreated yarn (*upper curves*) starts at 65°C; the tempered yarn (*lower curves*) shows practically no shrinkage. (Fineness: 480 dtex f48, pre-tension: 0.2 cN/tex, heating rate: 20 K/min). (Data source: Leibniz-Institut für Polymerforschung Dresden e. V. [64])

oriented PLA fiber yarn before and after an additional thermal treatment (annealing at 80°C for 1 h).

2.2.5 Filament and Fiber Yarns

Besides mechanical and thermal properties, the number of single filaments and their fineness are also important for the textile performance of the fibers. Another essential aspect for properties such as tactility, grip, comfort, pilling propensity, etc., is the cross-sectional shape of the single filaments. The most common are fibers of circular cross sections because spinnerets with circular capillary holes are easier to manufacture. Figure 10 schematically shows the cross section areas of melt spun PLA fiber yarns with similar total fineness. Although these yarns are similar in their total fineness and force-elongation characteristics, their tactility and bending is quite different.

For melt spinning of non-circular, profiled, or hollow fibers, custom-built spinnerets with capillary holes corresponding to the desired geometry have to be used. Figure 11 shows examples of profiled capillary holes and Fig. 12 shows the melt spun PLA fiber yarns from these spinnerets with different cross-sectional shapes. All single filaments in Fig. 11 have the same fineness of 5 dtex.

The cross-sectional area of the single filaments in Fig. 12 is equal for each sample; the perimeter and therefore also the fiber surface area increases from left to right. Another criterion for the deviation of the cross section of profiled fibers from circular fibers is the so-called “circularity”, $C = 4 \pi A/P^2$, with A = cross-sectional area and P = perimeter. Table 3 shows the values for perimeter and circularity for the different fiber shapes.

It can be seen that the perimeter and therefore the surface area of the cruciform fibers is about twice as large as those of the circular fibers. Designing the surface area is an interesting aspect for biomedical applications, for example, for wound covering or absorbing applications. Besides the mechanical properties, the

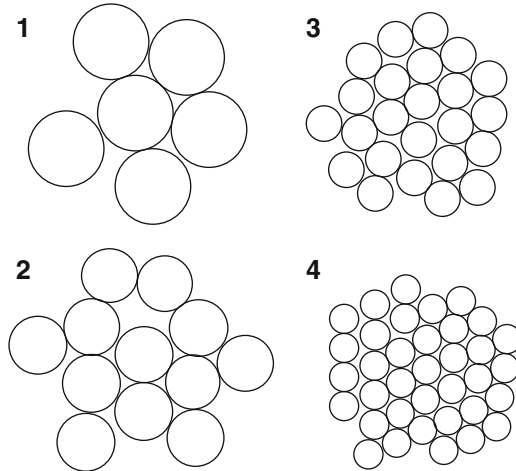


Fig. 10 Comparison of the cross section area of melt spun PLA filament yarns with different numbers of single filaments and different filament diameters (schematic). (1) 150 dtex f6 (single filament diameter 48 μm), (2) 160 dtex f12 (diameter 36 μm), (3) 120 dtex f24 (diameter 22 μm), (4) 120 dtex f36 (diameter 18 μm). (Data source: Leibniz-Institut für Polymerforschung Dresden e. V.)



Fig. 11 Three different cross-sectional shapes of the capillary holes of the spinneret (trilobal short, trilobal long, cruciform); bar 200 μm . (Data source: Leibniz-Institut für Polymerforschung Dresden e. V.)

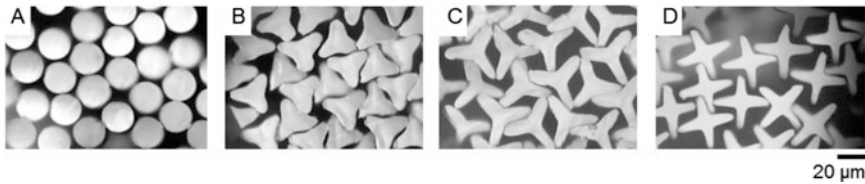


Fig. 12 Cross-sectional shapes of PLA fiber yarns spun with spinneret holes from Fig. 10. Total yarn fineness: 60 dtex f12, single filament fineness: 5 dtex. (a) Circular (for comparison); (b) trilobal short; (c) trilobal long; (d) cruciform; bar 20 μm . (Data source: Leibniz-Institut für Polymerforschung Dresden e. V.)

Table 3 Perimeter P and circularity C of profiled fibers (see Fig. 11)

Shape of fiber	Perimeter (μm)	Circularity C (-)
A – circular	71	1.0
B – trilobal small	92	0.61
C – trilobal long	126	0.33
D – cruciform	139	0.26

biocompatible and biodegradable behavior also plays an important role for medical applications. Tissue engineering based on biocompatible materials is considered as one alternative approach for cell-seeded, three-dimensional scaffold structures. Herewith, textile manufacturing allows the fabrication of structures with adapted mechanical properties based on resorbable and biocompatible PLA fiber materials with a defined degradation behavior. PLA fibers have therefore been investigated for several tissue engineering applications, for example, the anterior cruciate ligament [53, 65, 66]. The challenge is to realize the specific mechanical requirements for the ligament structure together with biocompatibility and a guarantee of high medical standards (e.g., sterilization).

2.2.6 Melt Spinning of PLA Blends, Microfibrillar and Nanofibrillar Structures

A novel and simple fabrication process for producing biodegradable and biocompatible nanofibrillar PLA structures from blends of PLA and poly(vinyl alcohol) (PVLA) has been developed using the conventional melt spinning method [54, 67, 68]. It was found that the as-spun and drawn PLA/PVLA filaments have sufficient strength for further processing in various textile processes such as weaving or knitting. After textile processing, the water soluble PVLA matrix component can be dissolved and the nanofibrillar PLA structures remain (see Figs. 13 and 14).

To sum up, melt spinning of PLA results in fiber yarns with excellent textile and environmental properties. There is a wide spectrum for medical applications, packaging, hygiene products, textile clothing, and houseware. The production processes of high speed spinning and drawing, staple fiber spinning, and spun-bonded nonwovens are well established. Composite materials and/or micro- and nanofibrillar structures can also be produced. However, PLA fibers, so far, have played a limited role in the textile market with respect to market volume and in comparison to oil-based materials.

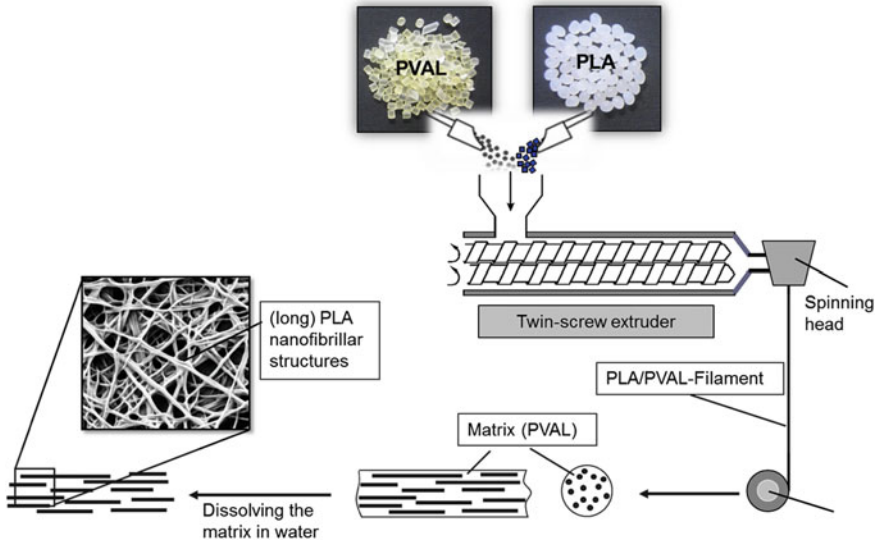


Fig. 13 Melt spinning of nanofibrillar PLA structures from PLA/PVLA blends (schematic)

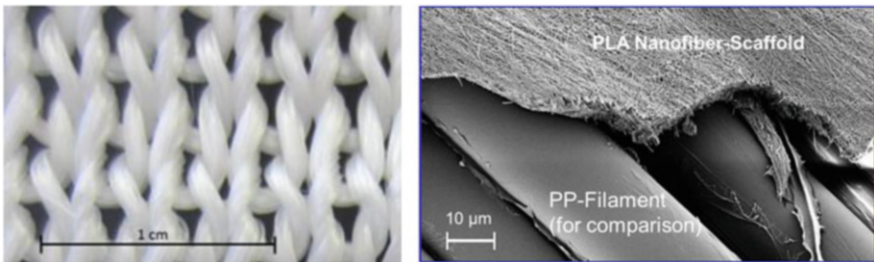


Fig. 14 Knitted fabric from PLA/PVLA 30/70 blend (*left*) and PLA nanofiber scaffold after removing PVLA matrix (*right*). (Data source: Leibniz-Institut für Polymerforschung Dresden e. V. [68])

2.3 Injection Molding

2.3.1 Introduction

Injection molding is one of the most used processing methods for polymers, and also for PLA [1–3, 55]. This economic technology plays an important role in the fabrication of complex parts and mass-produced articles. The main advantages of injection molding are: (1) the direct route from the raw material to the finished part, (2) no or minor post-processing, (3) the possibility of fully automated processing, and (4) high reproducibility and precision. There is no extra injection molding machine configuration for PLA. A common plasticizing unit with a three zone screw to melt the material mainly by friction heating is used. In the same way as for all usual thermoplastics, the thermal management of injection molds works on the assumption that the cycle has to be as short and effective

as possible. Therefore, the mold is tempered at a low temperature to transfer the heat away from the cavity and cool the part down rapidly. Cooling rates are controlled by the ratio between melt and mold temperature, whereby a high cooling rate leads to more characteristic skin-core-like morphology, as is well known from semi-crystalline materials. The skin has a small crystalline morphology that seems amorphous viewed under an optical microscope. In the core the morphology is formed with larger crystalline structures such as spherulites because of the longer remaining time under heat [69].

2.3.2 Influence of Processing Conditions on Structure-Properties Behavior

Injection Molding Process

The injection molding process is divided mainly into eight steps as shown in Fig. 15 [41, 69]. An injection cycle starts with the closing of the mold. In the next step the thermoplastic polymer melt is injected into the mold cavity that is tempered far below the solidification temperature of the polymer. To achieve the filling of the cavity, the screw moves forward until it has moved the required volume of material. During injection the molecular chains are oriented in the flow field by elongational and shear stresses, which lead to specific structure-property effects. After the filling procedure, a holding pressure is maintained to compensate for material shrinkage until the material in the gate solidifies and no additional melt can be pushed into the cavity. The shrinkage is enhanced by the

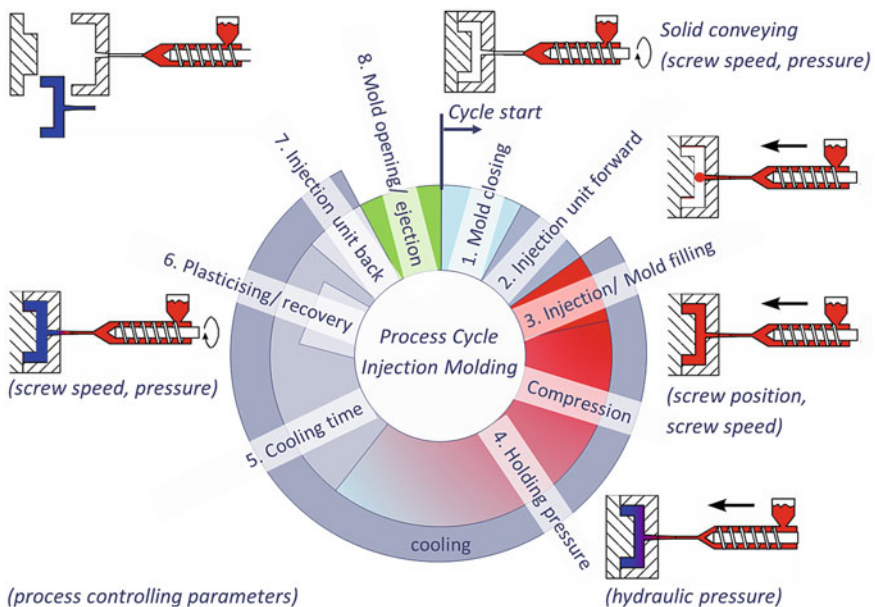


Fig. 15 Scheme of the injection molding process cycle. (Data source: Leibniz-Institut für Polymerforschung Dresden e. V.)

cooling process of polymer materials, in particular when crystallization occurs and the density increases rapidly. After the holding pressure is applied, the part further cools down in the mold and the screw turns back, conveying and melting the material for the following shot. When the injection molded part is sufficiently cooled, the mold opens and the molded part can be ejected. The whole cycle time is calculated from the mold closing until the ejection of the mold part, with the cooling step taking up most of the cycle time.

Crystalline Morphology and Properties

During the injection molding process, the morphology and the thermal and mechanical properties of PLA are influenced by the processing parameters. Important processing parameters are melt temperature (T_m), mold temperature (T_W), injection flow rate (Q_{inj}), holding pressure (P_h), and resulting parameters such as maximum shear rate ($\dot{\gamma}$) and shear stress (τ_W).

The influence of different parameter settings has already been investigated for PLA amongst others [3, 13, 14, 55–57]. In these studies, morphological characterization techniques such as the hot recoverable strain test (HR) to determine the initial level of molecular orientation in molded samples, and differential scanning calorimetry (DSC) to determine the crystallinity degree X_C in injection molded parts were used. The HR describes the difference between the sample dimension before and after thermal treatment. Figure 16 gives an overview of the results and the processing-

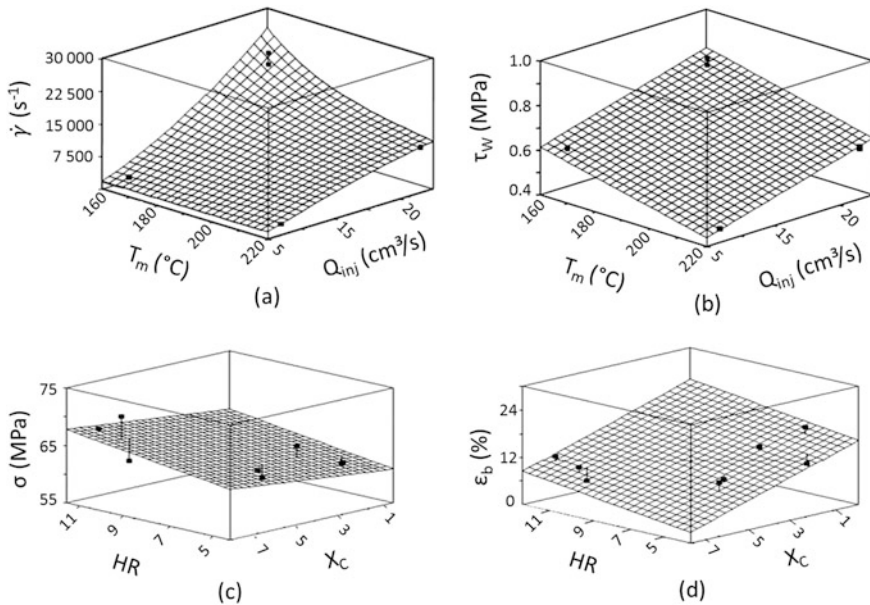


Fig. 16 Overview of processing-property relationships in injection molded PLLA [55]. (a) Maximum shear rate $\dot{\gamma}$ as function of the injection flow rate Q_{inj} and processing melt temperature T_m . (b) Maximum shear stress τ_W as function of the injection flow rate Q_{inj} and processing melt temperature T_m . (c) Maximum yield stress σ as function of the hot recoverable strain HR and the crystallinity X_C . (d) Elongation at break ϵ_b as function of the hot recoverable strain HR and the crystallinity X_C . (With permission of Wiley)

property relationship of injection molded PLLA [55]. In [55] the injection parameters (melt-, mold temperature, holding pressure) were systematically changed and the thermomechanical environment for the mold filling phase was simulated. From the received data the shear stress and shear rate were calculated. The melt temperature T_m and the injection speed Q_{Inj} control the shear rate $\dot{\gamma}$ and shear stress τ_w during filling of the cavity, which respectively influence the hot recoverable strain HR and the crystallinity X_C . Low T_m values and high Q_{Inj} facilitate a high level of $\dot{\gamma}$ and τ_w (Fig. 16a, b) occurring in molecular orientation and high crystallinity degree. Both the orientation and crystallinity influence the tensile strength σ and elongation at break ϵ_b (Fig. 16c, d). An increase in molecular orientation and crystallinity occurs in a maximum σ , whereas an increase in orientation and decrease in crystallinity occur in a high ϵ_b .

Recent optical investigations on thin sections of injection molded tensile bars using polarized light have also shown large amorphous regions in which crystallites in the form of single spherulites are found, as can be seen in Fig. 17. In this case, semi-crystalline PLA could be produced without further additives. The sample was prepared using a slow cooling condition at a mold temperature of 100°C for 10 min. Samples prepared at normal processing conditions (high cooling rate, fast cycle time) stayed amorphous. From the first heating curve of DSC measurements from the molded parts, a crystallization degree of 26% could be observed; see Fig. 18.

Process Influence on Crystallinity

In [55, 56] it is described how the crystallinity in injection molded parts can be improved by chain orientation achieved because of the shear stress during the injection process or by the addition of nucleating agents. Typical nucleating agents are fillers such as talc and PDLA to form stereo-complex crystals [13, 14, 70, 71]. Another study from [56] also focused on the influence of an alternative injection technique, shear controlled orientation in injection molding (SCORIM) on molecular orientation and mechanical properties of PLLA. SCORIM is used to improve molecular orientation compared to the conventional injection molding process and also to improve weld lines in parts. Using the SCORIM technique, the melt inside the cavity is pushed and pulled until the melt is solidified. During this process the molecules are oriented in the flow direction layer by layer. By using the push and pull effect the melt state, in-mold

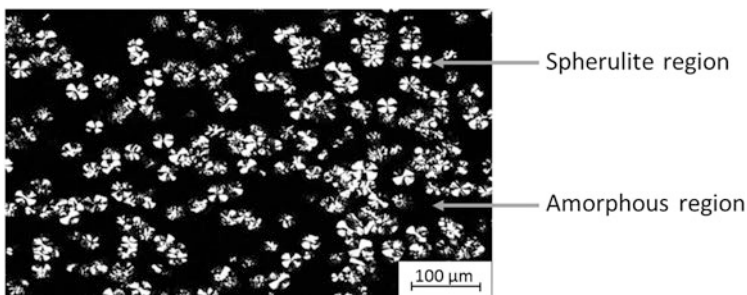


Fig. 17 Observed single spherulites after injection molding process using polarized light microscopy. (Data source: Leibniz-Institut für Polymerforschung Dresden e. V.)

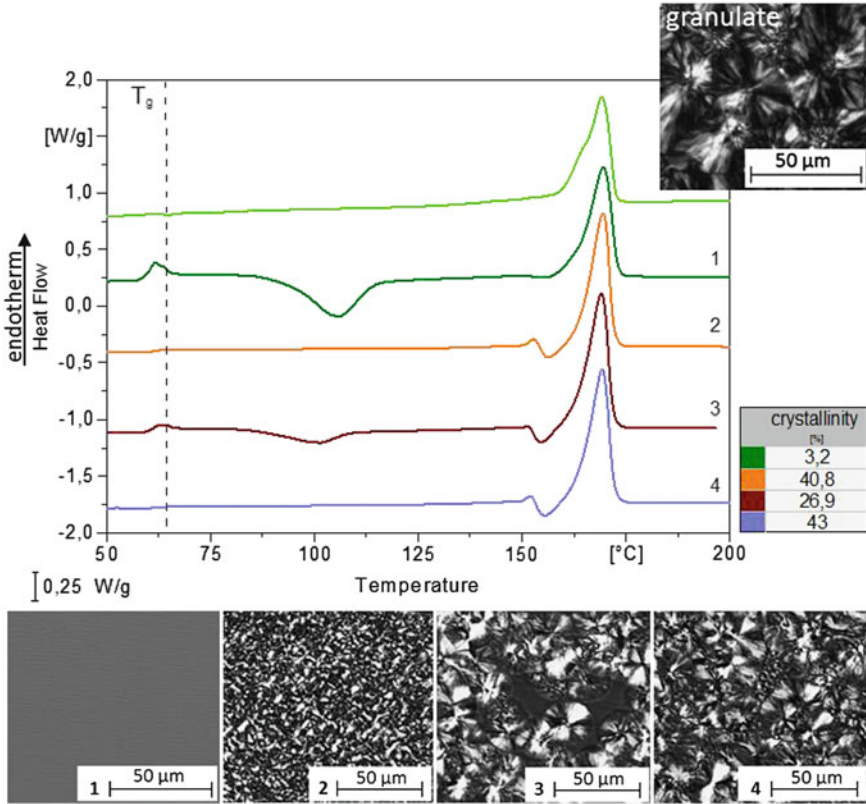


Fig. 18 DSC-first heating curves made from thin cuts of injection molded samples under various process conditions. (1) Amorphous after injection into a cold mold cavity, (2) crystalline after annealing the sample of 1 at a temperature over the T_g for 24 h, (3) crystalline after injection into a hot mold cavity, (4) crystalline after annealing the sample 3 at a temperature over the T_g for 10 min. (Data source: Leibniz-Institut für Polymerforschung Dresden e. V.)

shearing, and cooling can be controlled and thereby the morphology and mechanical behavior, in particular the toughness and maximum stress, can be improved.

Another promising way to improve the crystallinity of PLA is to build PLLA/PDLA stereo-complexes [14]. Common methods are solution casting and melt blending, which are environmentally damaging because of the usage of organic solvents and the degradation of homopolymers at the required blending temperature, respectively. Srithep et al. [14] show the possibility of hand mixing PLLA/PDLA and the effect of molding temperatures on thermal and mechanical properties in injection molded PLLA/PDLA parts compared to pure PLLA. The blend was compounded with 50 wt% PLLA and 50 wt% PDLA. The authors concluded that stereo-complexation improved the elongation at break and storage modulus as well as the crystallization rate, in comparison to pure PLLA. Other investigations have proved the influence of PDLAs varying in their structure [72] and the addition of modifiers by chemical

crosslinking [12] on the rheological and thermal behavior of PLA. The PLLA/PDLA blends showed solid-like viscoelastic behavior at low temperature and the crosslinking density follows a specific order attributed to the stereo-complex crystallites. Investigations on the crystallization behavior [72] have shown that the nucleation mechanism and crystal growth dimension are directly affected by PDLA structure, crystallization temperature, and thermal treatment. Yamoum et al. [12] followed another way and concluded that crosslinking structures can be introduced into PLA by initiation of dicumyl peroxide (DCP) and the presence of crosslinking agents such as bisphenol A ethoxylate dimethacrylate (BIS-EMA). Crosslinked PLAs reveal an improvement in storage modulus and viscosity, and showed a decrease in thermal properties with increasing content of BIS-EMA.

As well as the shear stress during injection molding, crystallinity can also be influenced by tensile strain. The effect of nucleating agents on strain-induced crystallization of PLLA was investigated by Yin et al. [71]. Injection molded specimens were stretched under isothermal conditions (75°C) using a hot stage and the molecular orientation was measured in situ via X-ray scattering. It could be concluded that the crystallinity of nucleated PLLA after uniaxial stretching can be enhanced in the following sequence:

$$\text{talc} < \text{PDLA} < \text{PDLA/talc}$$

The PDLA blends have existing physical crosslinks that are formed by stereo-complex crystals which are a possible reason for faster strain hardening. To eliminate the effect of plastic deformation of formed crystallites, isothermal crystallization after step strain at high stretching speed was performed [71].

2.3.3 Formation of Interfaces

Because of the usual complexity of injection molded parts, multiple gates are often required or the melt flow has to go around mold inserts (flow obstacles). Such design is unavoidable to form those parts. During the injection molding processes, different types of interfaces can occur, such as weld lines [58, 61, 73–75]. Weld lines are well known in any thermoplastic material through optical and/or mechanical weaknesses [61, 73, 74, 76]. The reasons are mainly based on the insufficient structural orientation of the polymer chains in the weld line region [61, 74, 75, 77, 78]. In the last few years, technologies for injection molding have been developed to change the molecular or fiber orientation in the weld line area and therefore reduce weakness, especially of filled polymer systems. The most effective technologies are push-pull and sequential injection molding [79–81].

Regarding the bonding of PLA to other thermoplastic materials or thermoplastic elastomers in soft-hard combinations, the assembly injection molding (overmolding) has been used in some studies [3]. In this case, the interface occurs by overmolding a hot melt on a cooled surface of a previous injection molded part. The influence of injection molding-induced interfaces on the mechanical behavior

and the specific crystalline structure of PLLA at interfaces were recently investigated at Leibniz-Institut für Polymerforschung Dresden e. V. [59–61, 76]. Depending on the cooling conditions during the process, specific structural gradients are developed at those interfaces, for example, frozen boundary layers.

To gain fundamental information on the bonding behavior of PLA and to compare the different kinds of interfaces, some tensile bars with and without interface were manufactured. In addition to the variation of interface development, the process was performed to induce amorphous or semi-crystalline PLA parts as well as to combine the different structured parts by joining through injection molding (overmolding). For amorphous PLA samples the melt was injected into a cold mold. The semi-crystalline samples were made by molding into a hot mold. The results in Fig. 19 show the comparison of reference samples without interfaces, where the tensile strength is strongly dependent on the crystallinity. Amorphous values are higher than the crystalline ones. In the middle of the diagram (Fig. 19), results for weld line samples are seen with lower values compared to amorphous samples without any interface. Interestingly, the weld line strength is the same for amorphous and semi-crystalline samples, and the average value for crystalline samples with weld lines is slightly higher than in samples without interfaces. It seems that the crystalline structure varies a lot, which is also indicated by a higher standard deviation. Finally, for the overmolding-induced interfaces the tensile strength values drop down to lower values, which is related to the thermal conditions during the bonding development on the cold interface of the overmolded part. Indeed, the crystalline combination has reached a rather high level compared to the drastically reduced strength of amorphous samples with that ‘cold’ interface.

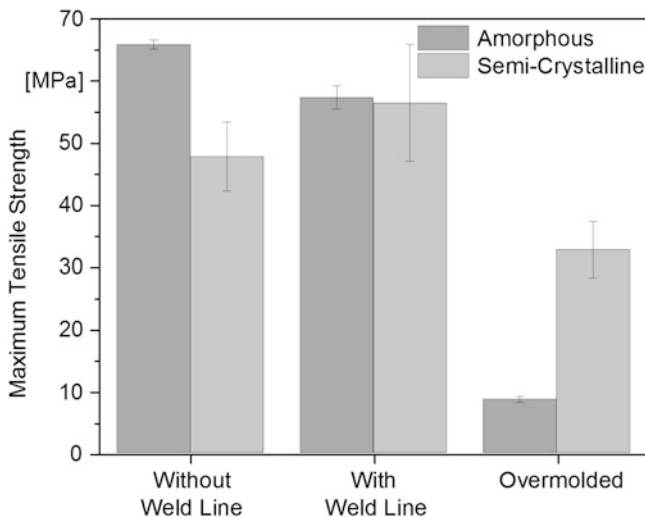


Fig. 19 Maximum tensile strength of injection molded PLA tensile bars without interface, with weld line, and overmolded. (Data source: Leibniz-Institut für Polymerforschung Dresden e. V.)

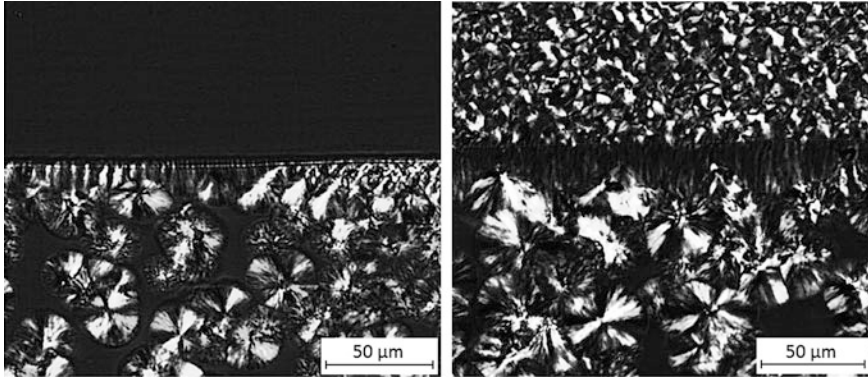


Fig. 20 Polarized light microscopy from overmolded parts: (*left*) overmolded in a cold mold; (*right*) overmolded in a hot mold. (Data source: Leibniz-Institut für Polymerforschung Dresden e. V.)

In Fig. 20 an insight into two different cases of overmolded interfaces with their morphology is given. In the case of the overmolding of amorphous PLA-samples with a hot PLA-melt, the surface is heated and somehow a cold crystallization could take place first. The newly grown crystallites need even more heat to be re-melted. Therefore, the heat flow volume needs to be sufficient for melting and also for initiating bonding mechanisms such as, for example, chain entanglement. In the right micrograph an interface between two crystalline-like PLA moldings was investigated. The second injected part shows a larger spherulite size than the first, which was first injected into a hot mold. Indeed, the second part still remains longer under higher temperature than the first part, which was formed at the mold surface with higher heat conduction coefficient than the PLA and continuously tempered. Figure 21 shows finally a comparison of tensile strength behavior of different semi-crystalline polymers regarding different interfaces through injection molding.

However, the mechanical and thermal properties of injection molded PLA parts are driven by the enormous morphology gradient of the cross section. Common processing conditions (fast cooling, short cycle time) lead to completely amorphous-like molded parts because of the slow crystallization kinetics of PLA. Under processing conditions with high mold temperature, a long residence time in the mold determines the crystallization degree. In turn, this leads to inefficient production. Semi-crystalline parts are only possible to obtain during standard processing cycles if the material contains nucleating agents or blends [1, 2, 14, 55–57].

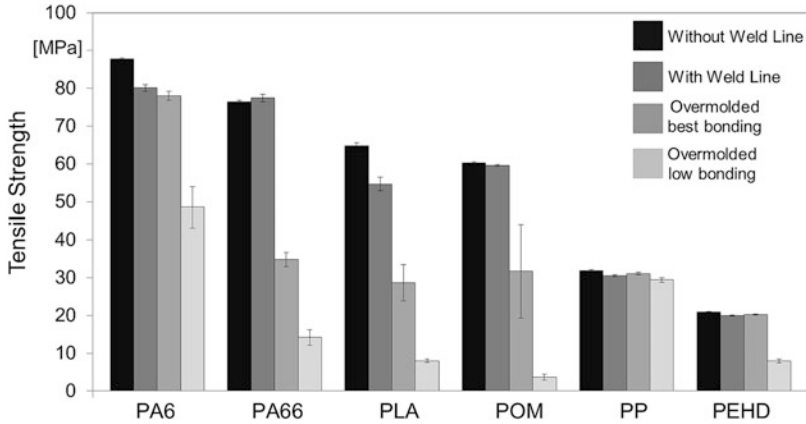


Fig. 21 Tensile strength behavior of semi-crystalline polymers depending on interface formation. (Data source: Leibniz-Institut für Polymerforschung Dresden e. V.)

2.4 Additive Manufacturing

2.4.1 Introduction

In contrast to injection molding or other conventional polymer processing technologies, additive manufacturing (AM) is a relatively new technology and the market for AM is the fastest growing ever seen in the history of industrialization. In 2012 a glorious future for AM was predicted with a value of \$4 billion in 2015 and \$10.8 billion in 2021 [82]. However, in 2014 the value had already reached \$4.1 billion (compound annual growth rate: 35.2%) and is now predicted to reach a value of \$21.2 billion by 2020 [83].

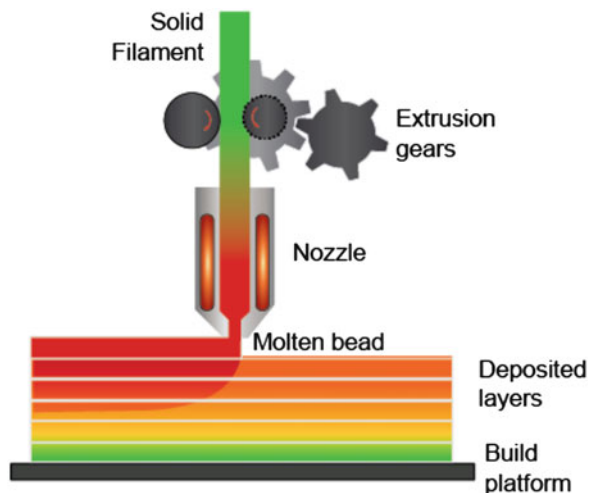
AM, formerly known as rapid prototyping and often synonymously described as 3D (three-dimensional) printing, categorizes processes which join materials to make objects from 3D model data, usually layer upon layer [84]. Among all polymer AM processes that utilize thermoplastics, PLA is mostly used in the material extrusion process. The reason is the applicability of the feedstock manufacturing technologies. All powder-based processes, such as binder jetting and powder bed fusion, require completely spherical particles of defined size (<200 μm) and narrow or bi-modal size distribution. So far, no process has been found that generates PLA powder with these characteristics. However, the feedstock for material extrusion technologies is produced by conventional extrusion, where special care needs to be taken to ensure a tight diameter tolerance and circularity of the produced filament with the downstream extrusion equipment. A typically used configuration is an open bath, laser gauge, belt puller, and winder to control these characteristics. However, the use of a vacuum water tank makes the circularity easier to achieve.

2.4.2 Fused Filament Fabrication

In the last few years, material extrusion has become one of the most common AM technologies. It is often referred to as 3D printing, fused deposition modeling (FDM[®]), fused filament fabrication (FFF), or fused layer manufacturing (FLM). The use of the terminology varies by industry and region. Invented by Stratasys Inc. and commercially available since 1993, FFF is now among the fastest growing AM technologies because of the ease of use, the vast variety of materials, and the range of printers from desktop versions to industrial machines [85]. In most cases the process starts with the creation of a 3D model using computer aided design software. For medical applications and patient-specific models, the 3D data is generated by magnetic resonance imaging or computed tomography scanners where the resulting point cloud is converted to a 3D model. These models are then exported into the STL (STereoLithography) file format, which represents the surface geometry of the part with a mesh of small triangles. This simplified data is then transmitted to the print software and horizontally sliced into different layers depending on the basic print settings. Then the software generates the tool path, which the print head follows. The actual printing process starts by feeding a solid filament through the movement of extrusion gears into a heated nozzle, as shown in Fig. 22. Through heat conduction from the nozzle walls, the material temperature is raised above the melting temperature. The solid filament works as a piston and pushes the molten material out of the tip of the nozzle. These molten beads are then laid down alongside each other, after which they solidify to form a thin horizontal 2D (two-dimensional) layer of polymer. Now either the print head can be raised or the platform can be lowered to print subsequent layers on top of the deposited layer. Hence, complex parts with hollow sections and various surface structures can be easily manufactured. Depending on the part size, the print usually takes several hours.

Two important criteria for FFF printing are the viscosity and heat transfer. The viscosity of the material needs to become low at moderate shear rates to flow out of the

Fig. 22 Schematic of the FFF print process. (Data source: N. Rudolph, Polymer Engineering Center, University of Wisconsin, Madison)



nozzle and rise rapidly upon cooling to avoid sagging of the deposited beads. At the same time, the temperature at the interface still needs to be high enough to allow fusion between beads and layers to occur. Because of the complexity of typical FFF parts, a support structure is needed during printing to prevent overhangs from sagging and to allow for the bridging of long spans. The support structure can either be a break-away support printed with the same material and print head, which is done with most desktop printers, or a water- or detergent-soluble material that is washed out after the print is finished. The latter approach is commonly used for commercial machines with two print heads, and creates smoother surfaces.

PLA is the most commonly used material for desktop or home-user printers. This is because of its low melting temperature in comparison to other filament materials as well as its good adhesion to the build platform and low degree of warpage and delamination. Typical FFF process parameters for PLA are nozzle temperatures of 190–220°C, platform temperatures of RT (room temperature) up to 60°C and print speeds up to 100 mm/s. Another reason for its widespread use in college and community-maker spaces is its low volatile emissions [86].

In commercial printers it is used for applications in the medical and bio-medical industries because of its biocompatibility rather than its mechanical performance. AM in these areas is focused on patient-specific anatomical models and surgery aids, implants containing living cells (bioprinting), scaffolds for tissue engineering, diagnostic platforms, and drug delivery systems [87]. Figure 23 shows a variety of examples.

The requirements range from the macro- to the micro- and nano-levels. For example, the macro-architecture of a scaffold is the overall shape with patient- and organ-specific anatomical features. The microstructure is related to the porosity-like size, shape, and spatial distribution. Finally, the nano-architecture refers to surface modifications that enhance biomolecule adhesion, proliferation, and differentiation. Where the latter is controlled during post-processing, the macro- and micro-



Fig. 23 Ear, nose, and bone scaffolds printed at the Wake Forest Institute for Regenerative Medicine; the PLA scaffolds can be coated with cells to grow body parts [88]. (With permission of Laurie Rubin Photography + Film)

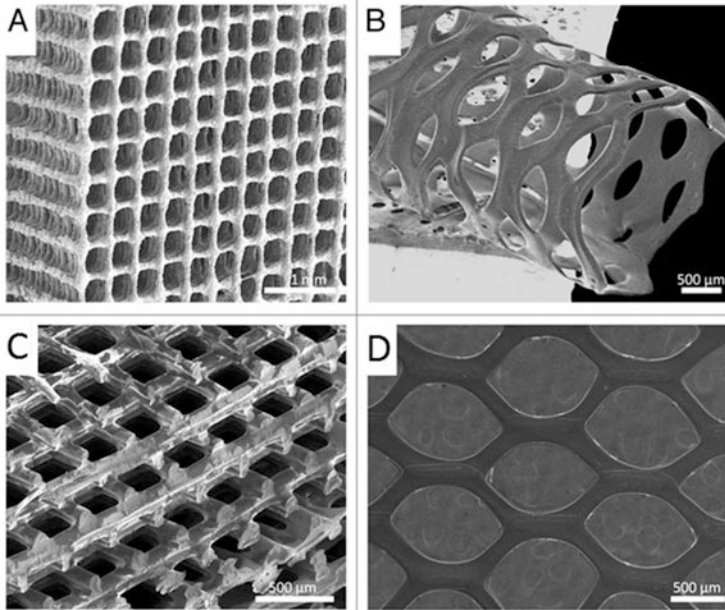


Fig. 24 SEM images of biodegradable 3D structures with PLA and blends: (a) PLA/glass composite orthogonal structure; (b) PLA tubular hexagonal mesh; (c) PLA orthogonal-displaced structure; (d) PLA hexagonal mesh [89] (with permission from Taylor and Francis)

architecture is controlled during design and printing. By using fine nozzles of down to 200 μm , the desired microstructure can be obtained. Studies have been carried out using homogeneous PLA polymers [89, 90] as well as blends. In Fig. 24, examples of scaffold microstructures are shown. Blends are used to improve printability and, more importantly, to increase bioactivity. Common blends are PLA/glass composites to improve the mechanical strength and surface roughness. Poly(lactic-*co*-glycolic acid) (PLGA) is used because of its biodegradability and biocompatibility [91]. It is also used as blends: PLGA-TCP [92], PCL-PLGA-TCP [93], and PLGA-PCL [94].

2.4.3 Vat Photopolymerization

Vat photopolymerization (VP), also known as stereolithography, is another AM technology that was only recently used to print with photo-curable poly(D,L-lactide) resin to create scaffold structures [95]. The necessary photo-crosslinking capability is achieved by modification of the end groups to acrylate or methacrylate. The VP process utilizes a vat of liquid photopolymer resin cured by ultraviolet (UV) laser to solidify the pattern layer by layer to create the solid 3D model. The laser beam traces the boundaries and fills in a 2D cross section of the model, solidifying the resin wherever it passes. Each successive layer is applied by submersion of the build platform into the resin. Once the model is complete, the platform rises out of

the vat and the excess resin is drained out of hollow sections. The model is then removed from the platform, excess resin is washed off, and it is then placed in a UV oven for the final curing process. VP parts have excellent surface properties and the highest attainable resolutions. However, the mechanical properties of most parts printed with photo-curable resins degrade over time because of continued exposure to light. However, this potential downfall is not a problem with patient-specific models, which normally have a service life of a couple of hours to a few weeks.

3 Summary

This chapter gives an overview of the processing-related behavior of PLA and the scientific insights of the last few years are reviewed. Common process methods are extrusion, melt spinning, injection molding, and AM. For these methods an overview of the recommended process conditions is given. Because of the similarities in the processing methods of PLA and petroleum-based materials, no extra equipment is necessary to process PLA. PLA is therefore suitable to replace petroleum-based materials. In the last few years, particularly the structural behavior during and after processing of PLA materials has been investigated. The aim is to generate new application fields for PLA materials. Especially in the areas of melt spinning, injection molding, and AM, the advancement in processing technology and the better understanding of the processes themselves have enhanced the application of PLA. For example, the ability to design the surface structure of melt spinning fibers plays an important role in medical applications. Furthermore, the better understanding of the process-structure-properties behavior makes it possible to influence the crystallinity formation, especially at the interface design in injection molded and fused filament fabricated parts. This knowledge makes PLA useful in technical and 3D designed applications.

Acknowledgments The authors thank the Institute of Textile Machinery and High Performance Material Technology (ITM) and the Technical University in Dresden (TUD) for cooperation and support, especially in the melt spinning process.

References

1. Lim LT, Auras R, Rubino M (2008) Processing technologies for poly(lactic acid). *Prog Polym Sci* 33(8):820–852
2. Ren J (2010) Processing of PLA in biodegradable poly(lactic acid): synthesis, modification, processing and applications. Springer, Berlin
3. Fachagentur Nachwachsender Rohstoffe (FNR) (2016) Processing of bioplastics – a guideline. Report
4. Jamshidian M, Tehrani EA, Imran M, Jacquot M, Desobry S (2010) Poly-lactic acid: production, applications, nanocomposites, and release studies. *Compr Rev Food Sci Food Saf* 9 (5):552–571

5. Endres H-J, Siebert-Raths A (2011) Engineering biopolymers :markets, manufacturing, properties and applications. Hanser, Munich
6. Fakirov S (2012) In: Bhattacharyya D, Fakirov S (eds) Synthetic polymer-polymer composites. Hanser, Munich
7. Jiménez A, Peltzer MA, Ruseckaite RA (2015) Poly(lactic acid) science and technology - processing, additives and applications. RSC, Cambridge
8. Garlotta D (2001) A literature review of poly(lactic acid). *J Polym Environ* 9(2):63–84
9. Saba N, Jawaid M, Al-Othman O (2017) An overview on polylactic acid, its cellulosic composites and applications. *Curr Org Synth* 14(2):156–170
10. Goebel L, Bonten C (2014) Influence of the phase morphology on the weldability of PLA/PBAT-blends by using butt-welding. In: Alstadt V, Keller JH, Fathi A (eds) Proceedings of PPS-29: The 29th International Conference of the Polymer Processing Society PPS 2014, AIP Conference Proceedings, vol 1593. pp 312–315. <https://doi.org/10.1063/1.4873789>
11. Gottermann S, Weinmann S, Bonten C, Standau T, Alstadt V (2016) Modified standard polylactic acid (PLA) for extrusion foaming. In: Holzer CH, Payer M (eds) Proceedings of the Regional Conference Graz 2015, Polymer Processing Society PPS, AIP Conference Proceedings, vol 1779. p 060001. <https://doi.org/10.1063/1.4965522>
12. Yamoum C, Maia J, Magaraphan R (2017) Rheological and thermal behavior of PLA modified by chemical crosslinking in the presence of ethoxylated bisphenol A dimethacrylates. *Polym Adv Technol* 28(1):102–112
13. Harris AM, Lee EC (2008) Improving mechanical performance of injection molded PLA by controlling crystallinity. *J Appl Polym Sci* 107(4):2246–2255
14. Srihthep Y, Pholham D, Turng LS, Veang-in O (2015) Injection molding and characterization of polylactide stereocomplex. *Polym Degrad Stab* 120:290–299
15. Al-Itry R, Lamnawar K, Maazouz A (2012) Improvement of thermal stability, rheological and mechanical properties of PLA, PBAT and their blends by reactive extrusion with functionalized epoxy. *Polym Degrad Stab* 97(10):1898–1914
16. Kolstad JJ (1996) Crystallization kinetics of poly(L-lactide-co-meso-lactide). *J Appl Polym Sci* 62(7):1079–1091
17. Iannace S, Nicolais L (1997) Isothermal crystallization and chain mobility of poly(L-lactide). *J Appl Polym Sci* 64(5):911–919
18. Miyata T, Masuko T (1998) Crystallization behaviour of poly(L-lactide). *Polymer* 39(22):5515–5521
19. Di Lorenzo ML (2005) Crystallization behavior of poly(L-lactic acid). *Eur Polym J* 41(3):569–575
20. Yasuniwa M, Tsubakihara S, Iura K, Ono Y, Dan Y, Takahashi K (2006) Crystallization behavior of poly(L-lactic acid). *Polymer* 47(21):7554–7563
21. Androsch R, Schick C (2016) Interplay between the relaxation of the glass of random L/D-lactide copolymers and homogeneous crystal nucleation: evidence for segregation of chain defects. *J Phys Chem B* 120:4522–4528
22. Di Lorenzo ML, Androsch R (2016) Stability and reorganization of alpha-crystals in random L/D-lactide copolymers. *Macromol Chem Phys* 217(13):1534–1538
23. Sato Y, Inohara K, Takishima S, Masuoka H, Imaizumi M, Yamamoto H, Takasugi M (2000) Pressure-volume-temperature behavior of polylactide, poly(butylene succinate), and poly(butylene succinate-co-adipate). *Polym Eng Sci* 40(12):2602–2609
24. Pantani R, De Santis F, Sorrentino A, De Maio F, Titomanlio G (2010) Crystallization kinetics of virgin and processed poly(lactic acid). *Polym Degrad Stab* 95(7):1148–1159
25. Ehrenstein G, Riedel G, Trawiel P (2004) Thermal analysis of plastics - theory and practice. Carl Hanser, Munich
26. Wunderlich B (2005) Thermal analysis of polymeric materials. Springer, Berlin
27. Desantis P, Kovacs AJ (1968) Molecular conformation of poly(S-lactic acid). *Biopolymers* 6(3):299–306
28. Kalb B, Pennings AJ (1980) General crystallization behavior of poly(L-lactic acid). *Polymer* 21(6):607–612

29. Ohtani Y, Okumura K, Kawaguchi A (2003) Crystallization behavior of amorphous poly (L-lactide). *J Macromol Sci B*42(3–4):875–888
30. Di Lorenzo ML, Rubino P, Immirzi B, Luijkx R, Hérou M, Androsch R (2015) Influence of chain structure on crystal polymorphism 5 of poly(lactic acid). Part 2. Effect of molecular mass on the crystal growth rate and semicrystalline morphology. *Colloid Polym Sci* 293:2459–2467
31. Burnett BB, McDevit WF (1957) Kinetics of spherulite growth in high polymers. *J Appl Phys* 28(10):1101–1105
32. Androsch R, Iqbal HMN, Schick C (2015) Non-isothermal crystal nucleation of poly (L-lactic acid). *Polymer* 81:151–158
33. Androsch R, Schick C, Di Lorenzo ML (2017) Kinetics of nucleation and growth of crystals of poly(L-lactic acid). *Adv Polym Sci*. Springer, Berlin, pp 1–38
34. Kolesov I, Mileva D, Androsch R, Schick C (2011) Structure formation of polyamide 6 from the glassy state by fast scanning chip calorimetry. *Polymer* 52(22):5156–5165
35. Rhoades AM, Williams JL, Androsch R (2015) Crystallization kinetics of polyamide 66 at processing-relevant cooling conditions and high supercooling. *Thermochim Acta* 603:103–109
36. Grellmann W, Altstädt V (2007) Polymer testing. Hanser, Munich
37. Osswald TA, Rudolph N (2015) Polymer rheology :fundamentals and applications. Hanser, Munich
38. Auras R, Harte B, Selke S (2004) An overview of polylactides as packaging materials. *Macromol Biosci* 4(9):835–864
39. Datta R, Henry M (2006) Lactic acid: recent advances in products, processes and technologies - a review. *J Chem Technol Biotechnol* 81(7):1119–1129
40. Naturworks (2015) Sheet extrusion processing guide. Brochure of Naturworks LLC, Minnetonka
41. Osswald TA, Hernández-Ortiz JP (2006) Polymer processing :modeling and simulation. Hanser Gardner, Munich
42. Corre YM, Duchet J, Reignier J, Maazouz A (2011) Melt strengthening of poly (lactic acid) through reactive extrusion with epoxy-functionalized chains. *Rheol Acta* 50(7–8):613–629
43. Ljungberg N, Andersson T, Wesslen B (2003) Film extrusion and film weldability of poly(lactic acid) plasticized with triacetine and tributyl citrate. *J Appl Polym Sci* 88(14):3239–3247
44. Zhou ZF, Huang GQ, Xu WB, Ren FM (2007) Chain extension and branching of poly(L-lactic acid) produced by reaction with a DGEBA-based epoxy resin. *Express Polym Lett* 1(11):734–739
45. Anderson KS, Hillmyer MA (2004) The influence of block copolymer microstructure on the toughness of compatibilized polylactide/polyethylene blends. *Polymer* 45(26):8809–8823
46. Ljungberg N, Wesslen B (2002) The effects of plasticizers on the dynamic mechanical and thermal properties of poly(lactic acid). *J Appl Polym Sci* 86(5):1227–1234
47. Kulinski Z, Piorkowska E (2005) Crystallization, structure and properties of plasticized poly (L-lactide). *Polymer* 46(23):10290–10300
48. Martin O, Averous L (2001) Poly(lactic acid): plasticization and properties of biodegradable multiphase systems. *Polymer* 42(14):6209–6219
49. Hagen R (2013) The potential of PLA for the fiber market. *Bioplast Mag* 8:12ff
50. Schmack G, Tandler B, Optiz G, Vogel R, Kornber H, Haussler L, Voigt D, Weinmann S, Heinemann M, Fritz HG (2004) High-speed melt spinning of various grades of polylactides. *J Appl Polym Sci* 91(2):800–806
51. Perepelkin K (2002) Chemistry and technology of chemical fibres – polylactid fibers: fabrication, properties, use, prospects. *Fiber Chem* 34(2):85–100
52. Beyreuther R, Brüning H (2007) Dynamics of fibre formation and processing :modelling and application in fibre and textile industry. Springer, Berlin
53. Hahn J, Breier A, Brüning H, Heinrich G (2016) Mechanical adapted embroidered scaffolds based on poly(lactic acid) melt spun multifilaments for ligament tissue engineering. Annual report of Leibniz-Institut für Polymerforschung Dresden e. V., Dresden. chapter: Biology-inspired interface and material design. pp. 42–44. <http://www.ipfdd.de/en/publications/annual-reports/>. Comment: The source is from the Leibniz-Institut für Polymerforschung Dresden e.V.

54. Tran NHA, Brünig H, Hinüber C, Heinrich G (2014) Melt spinning of biodegradable nanofibrillary structures from poly(lactic acid) and poly(vinyl alcohol) blends. *Macromol Mater Eng* 299(2):219–227
55. Ghosh S, Viana JC, Reis RL, Mano JF (2007) Effect of processing conditions on morphology and mechanical properties of injection-molded poly(L-lactic acid). *Polym Eng Sci* 47(7):1141–1147
56. Ghosh S, Viana JC, Reis RL, Mano JF (2008) Oriented morphology and enhanced mechanical properties of poly(L-lactic acid) from shear controlled orientation in injection molding. *Mater Sci Eng A* 490(1–2):81–89
57. Siebert-Raths A (2012) Modifizierung von polylactid (PLA) für technische Anwendungen, Verfahrenstechnische Optimierung der Verarbeitungs- und Gebrauchseigenschaften. Dissertation, Hannover
58. Kuehnert I (2009) Cold and hot interfaces during injection molding. In: PPS-25 Polymer Processing Society. Goa, Indien
59. Kuehnert I, Pomsch I (2011) Morphology and strength of injection molded parts with interfaces. In: Proceedings of SPE Antec 2011, Society of Plastics Engineers, Boston
60. Kuehnert I, Schoenfeldt A, Auf der Landwehr M (2013) New insights into interfaces in injection molded parts. In: Proceedings of SPE Antec 2013, Society of Plastics Engineers, Cincinnati
61. Kuehnert I, Spoerer Y, Zimmermann M (2016) Weld lines in injection molded parts: strength, morphology and improvement. In: Proceedings of SPE Antec 2016, Society of Plastics Engineers, Indianapolis
62. Market study and Database on Bio-based Polymers in the World – Capacity, Production and Applications: Status Quo and Trends towards 2020. 2013–7; Nova-Institut GmbH, Chemiepark Knapsack, Industriestraße 300, 50354 Huerth Germany
63. Sundar V (2012) Manufacture and characterization of filament yarns with structured and collagen-coated surfaces for medical purposes. TU-Dresden and Leibniz-Institut für Polymerforschung Dresden e.V
64. Akram W (2015) Manufacturing and characterization of high-oriented, low-shrinkage and biodegradable filament yarns for medical applications. TU-Dresden and Leibniz-Institut für Polymerforschung Dresden e.V
65. Hahner J, Hinüber C, Breier A, Siebert T, Brunig H, Heinrich G (2015) Adjusting the mechanical behavior of embroidered scaffolds to lapin anterior cruciate ligaments by varying the thread materials. *Text Res J* 85(14):1431–1444
66. Hahn J, Breier A, Brünig H, Heinrich G (2017) Long-term hydrolytic degradation study on polymer-based embroidered scaffolds for ligament tissue engineering. *J Ind Text* 804:1–16
67. Tran NHA, Brunig H, Auf der Landwehr M, Heinrich G (2016) Controlling micro- and nanofibrillar morphology of polymer blends in low-speed melt spinning process. Part III: Fibrillation mechanism of PLA/PVA blends along the spinline. *J Appl Polym Sci* 133(48):16
68. Tran N (2016) Melt spinning and characterization of biodegradable micro- and nanofibrillar structures from poly(lactic acid) and poly(vinyl alcohol) blends. PhD-Thesis. TU-Dresden and Leibniz-Institut für Polymerforschung Dresden e.V. TUD Press. ISBN: 978-3-95908-051-4
69. Kamal M, Isayev I, Liu SJ (2009) Injection molding-technology and fundamentals. Hanser, Munich
70. Battagazzore D, Bocchini S, Frache A (2011) Crystallization kinetics of poly(lactic acid)-talc composites. *Express Polym Lett* 5(10):849–858
71. Yin YG, Zhang XQ, Song Y, de Vos S, Wang RY, Joziassé CAP, Liu GM, Wang DJ (2015) Effect of nucleating agents on the strain-induced crystallization of poly(L-lactide). *Polymer* 65:223–232
72. Jing ZX, Shi XT, Zhang GC (2016) Rheology and crystallization behavior of asymmetric PLLA/PDLA blends based on linear PLLA and PDLA with different structures. *Polym Adv Technol* 27(8):1108–1120
73. Malguarnera SC (1982) Weld lines in polymer processing. *Polym-Plast Technol Eng* 18(1):1–45

74. Mennig G (1995) Knit-line behaviour of polypropylene and polypropylene-blends. Polypropylene: structure, blends and composites, vol 1. Chapman & Hall, London, pp 205–226
75. Nguyen-Chung T, Plichta C, Mennig G (1998) Flow disturbance in polymer melt behind an obstacle. *Rheol Acta* 37(3):299–305
76. Fischer M, Ausias G, Kuehnert I (2016) Investigation of interfacial fracture behavior on injection molded parts. In: Rhee B (ed) Proceedings of PPS-31: The 31st International Conference of the Polymer Processing Society PPS 2015, AIP Conference Proceedings. vol 1713. pp 040011. <https://doi.org/10.1063/1.4942276>
77. Haufe A, Kuehnert I, Mennig G (1999) Zum Einfluss strömungsinduzierter Fehlerstellen auf das Versagensverhalten in spritzgegossenen Kunststoffbauteilen. *GAK* 4:354–358
78. Kuehnert I (2005) Grenzflächen beim Mehrkunststoff-Spritzgießen. Dissertation, Fakultät Maschinenbau. TU-Chemnitz, Hanser: Munich. http://archiv.tu-chemnitz.de/pub/2005/0166/data/Diss_Kuehnert.pdf or <https://kunststoffe.de/fachinformationen/dissertationen/artikel/grenzflächen-beim-mehrkunststoffspritzgießen-640067.html>
79. Gutjahr L, Becker H (1989) Herstellen technischer Formteile mit dem Gegendaktspritzgießverfahren. *Kunststoffe* 79(11):1108–1112
80. Malloy RA (2011) Plastic part design for injection molding: an introduction, 2 edn. Hanser, Munich
81. Kuehnert I, Vetter K (2008) Sequential injection moulding as a method for eliminating weld lines - praxis and simulation. *RFP* 3(5):256–261
82. Wohlers T (2013) Wohlers report 2013: additive manufacturing and 3D printing: state of the industry: annual worldwide progress report
83. Wohlers T (2015) Wohlers report 2015: additive manufacturing and 3D printing: state of the industry: annual worldwide progress report
84. ASTM F2792-12a Standard Terminology for Additive Manufacturing Technologies (Withdrawn 2015) (2012) ASTM International West Conshohocken PA
85. Gebhardt A (2011) Understanding additive manufacturing :rapid prototyping, rapid tooling, rapid manufacturing. Hanser, Munich
86. McDonnell B, Guzman X, Doblack M, Simpson T, and Cimbala J Cimbala JM (2016) 3D printing in the wild, a preliminary, investigation of air quality in college maker spaces. In: 27th Annual International Solid Freeform Fabrication Symposium. Austin, TX, USA
87. Chia HN, Wu BM (2015) Recent advances in 3D printing of biomaterials. *J Biol Eng* 9:14
88. Royte E (2013) What lies ahead for 3-D printing? The new technology promises a factory in every home – and a whole lot more. *Smithsonian Magazine*. <http://www.smithsonianmag.com/science-nature/what-lies-ahead-for-3-d-printing-37498558/?all>
89. Serra T, Mateos-Timoneda MA, Planell JA, Navarro M (2013) 3D printed PLA-based scaffolds A versatile tool in regenerative medicine. *Organogenesis* 9(4):239–244
90. Korpela J, Kokkari A, Korhonen H, Malin M, Narhi T, Seppala J (2013) Biodegradable and bioactive porous scaffold structures prepared using fused deposition modeling. *J Biomed Mater Res B Appl Biomater* 101B(4):610–619
91. Yen HJ, Tseng CS, Hsu SH, Tsai CL (2009) Evaluation of chondrocyte growth in the highly porous scaffolds made by fused deposition manufacturing (FDM) filled with type II collagen. *Biomed Microdevices* 11(3):615–624
92. Kim J, McBride S, Tellis B, Alvarez-Urena P, Song YH, Dean D (2012) Rapid-prototyped PLGA/β-TCP/hydroxyapatite nanocomposite scaffolds in a rabbit femoral defect model. *Biofabrication* 4:025003
93. Shim JH, Moon TS, Yun MJ, Jeon YC, Jeong CM, Cho DW, Huh JB (2012) Stimulation of healing within a rabbit calvarial defect by a PCL/PLGA scaffold blended with TCP using solid freeform fabrication technology. *J Mater Sci Mater Med* 23(12):2993–3002
94. Kim JY, Cho DW (2009) Blended PCL/PLGA scaffold fabrication using multi-head deposition system. *Microelectron Eng* 86(4-6):1447–1450
95. Melchels FPW, Feijen J, Grijpma DW (2009) A poly(D,L-lactide) resin for the preparation of tissue engineering scaffolds by stereolithography. *Biomaterials* 30(23–24):3801–3809

Applications of Poly(lactic Acid) in Commodities and Specialties



Mario Malinconico, Erwin T.H. Vink, and Andrea Cain

Abstract The use of oil-derived polymers has been of great benefit to mankind, but it is evident that it causes considerable damage to the ecosystem. Public concern about the environmental impact of wastes is growing day by day and waste management methods are limited as are petroleum resources, so it is very important to find substitutes, particularly in those applications where a relatively short life-time can be forecast, such as packaging and agriculture. This has led to research work to find new biodegradable polymers as an alternative to conventional non-degradable ones. Among bio-based totally biodegradable polymers, poly(lactic acid) (PLA) has been studied for use in different fields because of its compostability and renewability. In this chapter, information on the present situation and trends regarding the applications of PLA is offered. The use of life cycle assessment principles helps to quantify the environmental benefits of PLA polymers. Most recent developments with PLA in the field of packaging show how this plastic material is moving from commodity to specialty applications, facing competition from polyolefins, particularly as barrier polymers for shelf-life enhancement.

Keywords Applications • Commodities • Environmental characteristics • Poly(lactic acid) • Specialties

M. Malinconico (✉)
Istituto per i Polimeri, Compositi e Biomateriali, Consiglio Nazionale delle Ricerche, Via
Campi Flegrei, 34, 80078 Pozzuoli, NA, Italy
e-mail: mario.malinconico@ipcbr.cnr.it

E.T.H. Vink and A. Cain
NatureWorks B.V., P.O. Box 5528, 1410EA Naarden, The Netherlands

Contents

1	Characteristics of Poly(lactic Acid)	36
1.1	General Considerations on PLA Properties	36
1.2	Properties of PLA	37
1.3	Biodegradation of PLA	38
2	Environmental Characteristics of PLA	39
2.1	General Considerations on PLA Environmental Characteristics	39
2.2	Carbon Footprint of PLA INGEO: A Case Study	39
3	Applications of PLA	43
3.1	World Request for Poly(lactic acid)	43
3.2	Textile Industry	46
3.3	Medical and Pharmaceutical Industry	46
3.4	Agriculture	47
3.5	Packaging	47
4	The Future of PLA-Based Materials	48
	References	48

1 Characteristics of Poly(lactic Acid)

1.1 General Considerations on PLA Properties

The polymerization of lactic acid leads to a family of poly(lactic acid) (PLA) polymers that, together with other natural polymers, enables biodegradable and bioresorbable polymers to be obtained. Among biodegradable plastics, PLA is one of the most promising to replace conventional plastics because of its excellent physical and mechanical properties and because it can be processed using existing plants with only minor adjustments. PLA is also a highly versatile material that can be adapted with various formulations to meet most product specifications [1]. When blended with other natural polymers it enables materials with better water resistance properties to be developed [2]. Products made in PLA are totally compostable in existing installations. With the proper equipment PLA can also be reverted to monomer (via hydrolysis) and again to polymer. PLA is a stable, odorless polymer. It is clear and shiny, similar to polystyrene (used to make cups, batteries and toys), and is resistant to moisture and grease. It has flavor and odor barrier characteristics similar to polyethylene terephthalate plastics, and can be used for non-alcoholic beverages and for other non-food products. The tensile strength and modulus of elasticity of PLA are also comparable to those of polyethylene. However, it is more hydrophilic than polyethylene, which has a lower density. It is stable in ultraviolet light, resulting in fabrics that do not fade. Its flammability is low [3].

PLA can be formulated to be rigid or flexible and can be copolymerized with other materials. It can be made with various mechanical characteristics depending on the manufacturing process followed.

1.2 Properties of PLA

In addition to its ability to biodegrade, PLA has properties that compare favorably with plastics commonly used, for example, for packaging. This is an important factor because it allows PLA to replace petrochemical polymers without redesigning products or investing heavily in new processing equipment [1].

PLA may be formulated to be both rigid and flexible and copolymerized with other monomers; it can also be prepared using appropriate specific manufacturing processes such as injection molding, sheet extrusion, blow molding, thermoforming, film formation, and spinning, using most conventional techniques and equipment. PLA is classified as generally recognized as safe by the US Food and Drug Administration [4].

The hydroxy acid precursor of PLA, lactic acid, with an asymmetric carbon atom, has four stereoisomeric forms: L, D, meso, and racemic mixture. It is made from corn, sugar beet, wheat, and other starchy grains from amorphous to crystalline by manipulation of mixtures of isomer D (–) and L (+).

The physical, mechanical, biological and, physiological properties of PLA depend on the composition of the polymer, its molecular weight, and its crystallinity. The crystallinity can be adjusted from a value of 0–40% in the form of linear or branched homopolymers and copolymers such as random or block [5].

As an example, in biomedical applications a crystalline form (mostly composed of L-lactide) of high molecular weight (>100,000 Da) ensures long resorption (approximately 1–2 years), and different formulations and the addition of side chains enable the resorption rate to be controlled. Using 100% L-PLA, a material with high melting point and high crystallinity is obtained. If a mixture of D and L is used, an amorphous polymer with a glass transition temperature of 60°C is obtained. With a mixture of 90% D and 10% L, a copolymer material which can be polymerized in an oriented manner with temperatures above its glass transition temperature is obtained. The processing temperature is between 60 and 125°C and depends on the proportion of D- or L-lactic acid in the polymer. However, the PLA can be plasticized with monomeric or alternatively oligomeric lactic acid and this allows a decrease in the glass transition temperature [6].

Södergard [7] indicates that the PLA has mechanical properties in the same range as those of petrochemical polymers, except for low elongation. However, this property can be tuned during the polymerization (copolymerization) or post-modifications (for example by plasticizers). Table 1 shows a comparison of some mechanical properties of plastics of petrochemical origin with those of PLA. One of the limitations of PLA, compared with other plastic packaging, is the low distortion temperature (HDT); this can be a problem in applications where the packing material is exposed to heating peaks during filling, transport, or storage, and can eventually deform [7]. This limitation can be partly solved by blending PLA with other compatible polyesters, such as polybutylene succinate [8].

PLA can be as hard as acrylic, soft as polyethylene or polystyrene, or rigid as flexible elastomer. It can also be formulated to provide a variety of resistances. PLA resins can be subjected to sterilization with gamma rays and are stable when exposed to ultraviolet rays. PLA formulations may impart properties of interest such as softness, scratch resistance, and wear resistance [10].

Table 1 Comparison of typical biodegradable polymer properties [9]

	T_g (°C)	T_m (°C)	Tensile strength (MPa)	Tensile modulus (MPa)	Elongation at break (%)
LDPE	-100	98-115	8-20	300-500	100-1,000
PCL	-60	59-64	4-28	390-470	700-1,000
Starch	-	110-115	35-80	600-850	580-820
PBAT	-30	110-115	34-40	-	500-800
PTMAT	-30	108-110	22	100	700
PS	70-115	100	34-50	2,300-3,300	1.2-2.5
Cellulose	-	-	55-120	3,000-5,000	18-55
PLA	40-70	130-180	48-53	3,500	30-240
PHB	0	140-180	25-40	3,500	5-8
PHA	-30 to 10	70-170	18-24	700-1,800	3-25
PHB-PHV	0-30	100-190	25-30	600-1,000	7-15
PVA	58-85	180-230	28-46	380-530	-
Cellulose acetate	-	115	10	460	13-15
PET	73-80	245-265	48-72	200-4,100	30-300
PGA	35-40	225-230	890	7,000-8,400	30
PEA	-20	125-190	25	180-220	400

PET polyethylene terephthalate, PGA poly(glutamic acid), PEA poly(ester amide)

1.3 Biodegradation of PLA

With PLA, microorganisms (fungi and bacteria) can colonize the polymer surface and are capable of secreting enzymes that break the polymer into small fragments. Colonization depends on factors such as surface tension, porosity, surface texture, and accessibility to the polymer chains. The hydrophilic groups of enzymes (-COOH, -OH, -NH) attack the ester groups of the polymer chains by hydrolysis followed by oxidation reactions, thus reducing the polymer molecular weight to fragments less than 500 g/mol, which can be digested by microorganisms. In living tissue, PLA is completely depolymerized by chemical hydrolysis. Polymer degradation begins by a loss of molecular weight (no mass loss) and is terminated by a loss of mass, decomposition of the polymer in monomers, and phagocytosis by macrophages [11]. The fact that it is an enzymatic process, reabsorption of the polymer leads to a weak reaction of the tissue, which is limited to a foreign body reaction. After solubilization, lactic acid is degraded via lactates and pyruvate, and is then removed as carbon dioxide (CO₂), essentially via a respiratory process [12]. Current research focuses on lowering production costs of precursor (through the use of agro-industrial wastes as fermentation substrates, in the search for strongly producing microorganisms and the application of new technologies for extraction processes), on improving the physical and mechanical properties of the polymer, on improving methods for assessing the microbial stability of packaging based on PLA, and on studies of laws and norms for food contact packaging [13].

2 Environmental Characteristics of PLA

2.1 General Considerations on PLA Environmental Characteristics

Many recent reports indicate that PLA appears to be a useful and environmental friendly product. It is biodegradable, so PLA objects, having completed their life cycle, can be efficiently composted in an industrial composting plant. It also comes from renewable resources, so the raw material is always available. A major point of criticism of the polymer occurs during its biological disruption. PLA degradation under anaerobic conditions releases CO₂ and methane, substances involved in the greenhouse effect. Actually, the net balance is zero CO₂ because the CO₂ released into the atmosphere is the same CO₂ that was absorbed during photosynthesis of the plant [14]. Another criticism is that fossil fuels are still needed to produce PLA. Although fossil fuels are not used in the polymer itself, they are necessary in the processes of collecting the crop and in the chemical production. PLA producers recognize that fossil fuels are used to produce plastic, but indicate that their manufacture requires 20–50% less fossil resources than plastics derived from oil. They also make use of abundant fossil resources such as coal and natural gas and ongoing research on the use of biomass [15].

Lactic acid, and therefore PLA, may also be derived from corn, beet, and other crops, allowing its production to adapt to the specific climates of each region. Importantly, PLA manufacturing technology is new, just 10 years old, compared with almost 100 years manufacture of petrochemical plastics, during which technology has been improving. A frequently reported criticism of the use of crops for production of lactic acid rather than food is less relevant than claimed. Actually, it is estimated that less than 0.02% of arable land is used for the production of bioplastics, including PLA. However, such criticism is pushing research toward the exploitation of different sources for lactic acid production, such as cellulosic biomass, organic waste, and algal biomass, so-called third generation biorefinery.

Finally, PLA needs to be composted to degrade correctly and is usually mixed with organic waste which is then used as fertilizer.

2.2 Carbon Footprint of PLA INGENEO: A Case Study

Figure 1 illustrates the major flows in the global carbon cycle.

In the atmosphere, carbon is present primarily as CO₂, which is fixed as biomass during photosynthesis. This process has been going on for hundreds of millions of years and has led to the vast resources of oil, gas, and coal that our society relies on at present. From the beginning of the industrial revolution, these resources have been used at an increasing rate to produce materials, chemicals, and fuels. As a result, much of the carbon stored millions of years ago is now being released into the atmosphere in

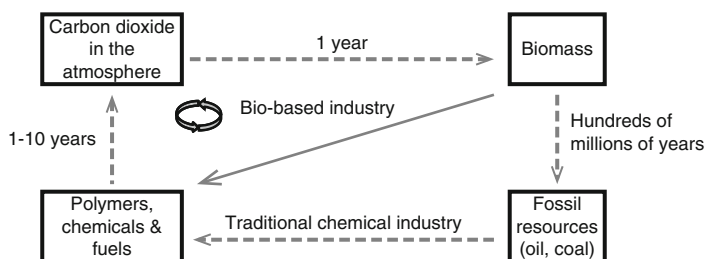


Fig. 1 Global carbon cycles. The fossil carbon cycle vs the biological carbon cycle

a very short period of time, geologically speaking. The result is that there is a net translocation of vast quantities of carbon from the earth into the atmosphere, leading to the above-mentioned increase in CO_2 level, which recently passed 400 ppm and continues to rise [16]. The increasing levels of CO_2 and other greenhouse gases such as methane and nitrous oxide trap more of the sun's heat, thereby raising the average temperature of the atmosphere – including both land and ocean – and leading to global climate change. This process will dramatically affect life on this planet. The use of fossil resources can, from a carbon point of view, be considered as a simple, linear process. The biobased industry offers an alternative and more sustainable route in terms of material carbon, with biobased resources utilized in a more circular process. The carbon harnessed during photosynthesis is used to produce biomaterials and, depending on the application, is released back into the atmosphere within a period of 1–10 years. Each year, plants repeatedly harness this CO_2 to produce biomass, closing the material carbon loop. The key value proposition of biobased materials such as PLA is their intrinsic zero material carbon footprint, assuming that after use the carbon in the polymer flows back to the atmosphere by composting or incineration. In other words, the fundamental intrinsic material carbon footprint value proposition for PLA is CO_2 removal from the environment and incorporation into the polymer molecule in harmony with nature's biological carbon cycles. Specifically, the value for PLA is 1.83 kg of CO_2 /kg PLA. Plastics made from fossil resources cannot be credited with any CO_2 removal [17]. With each fossil-based item used and incinerated at the end of its useful lifecycle, the material carbon released to the atmosphere increases by an amount equivalent to the quantity of fossil carbon present in the product, whereas the material carbon released in the case of the biobased product remains zero as the biobased carbon is again taken up from the atmosphere for the next product cycle. Recycling of fossil-based materials has been considered as a long-term solution, but from a material carbon point of view it is just a minimal delay in the process of translocating fossil carbon from the earth into the atmosphere.

In 2003, NatureWorks published the first cradle-(corn production)-to-polymer factory-to-exit gate life cycle inventory data, also often referred to as an ecoprofile, for Ingeo polylactide production [18], with updated ecoprofiles presented in 2007 and 2010 [19, 20].

The data provided in the underlying 2014 report are specific to the corn feedstock currently in use by NatureWorks [21], and are only valid for Ingeo and not for

polylactide production in general. The ecoprofile data for polylactides produced elsewhere are different because of the use of different feedstocks (i.e., sugarcane, sugar beet) and local production practices, different logistics, different technologies for processing sugars for fermentation, different fermentation and polymerization technologies, and different data for electricity and fuels used at all stages. For these reasons, the specific nomenclature “Ingeo” is used below to delineate clearly wherever NatureWorks’ polylactide biopolymer is being referenced.

Up-to-date life cycle inventory data are needed by research institutes, universities, retailers, brand owners, and authorities to provide better insights into the environmental performance of the products they use and to investigate and make meaningful comparisons between products. It should be noted, however, that the production and use of PLA and products made from PLA are still in their infancy compared with traditional petroleum-based polymers and products. Therefore, there is significant potential for further reduction in the environmental footprint of PLA and products made from it over their complete life cycles. This chapter reports on the life cycle performance/impacts of the 2014 Ingeo polylactide manufacturing system from cradle-to-polymer factory exit gate for a 150,000-ton production facility.

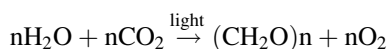
The study was conducted according to the requirements of ISO14040 and 14044. The simplified process flow diagram for the production of Ingeo is given in Fig. 3. The production system is divided into five steps:

- Corn production and transport of corn to the corn wet mill
- Corn processing and the conversion of the corn starch into dextrose
- Conversion of dextrose into lactic acid
- Conversion of lactic acid into lactide
- Polymerization of lactide into Ingeo polymer pellets

The primary inputs to these five steps are listed on the right and left sides of the flow diagram. In the final ecoprofile, all primary inputs are traced back to the extraction of the raw materials from the earth. All the processes included in the calculation of the Ingeo ecoprofile are given within the black lined box in Fig. 2.

The box surrounding all the processes represents the system boundary; the ecoprofile is the inventory of all the flows (inputs and outputs) passing this system boundary, including the raw materials from the earth, CO₂, water, and the emissions to air, water, and soil. Here only aggregated data are provided to protect the proprietary information of Cargill and NatureWorks.

The life cycle of Ingeo starts with corn production; all free energy consumed by the corn plant comes from solar energy captured by photosynthesis. The basic stoichiometric equation for photosynthesis is



In this equation, (CH₂O)_n represents simple sugars that are the basic building blocks for all substances present in the corn plant, such as starch, sugar, and cellulose. Therefore, all the carbon, hydrogen, and oxygen found in the starch

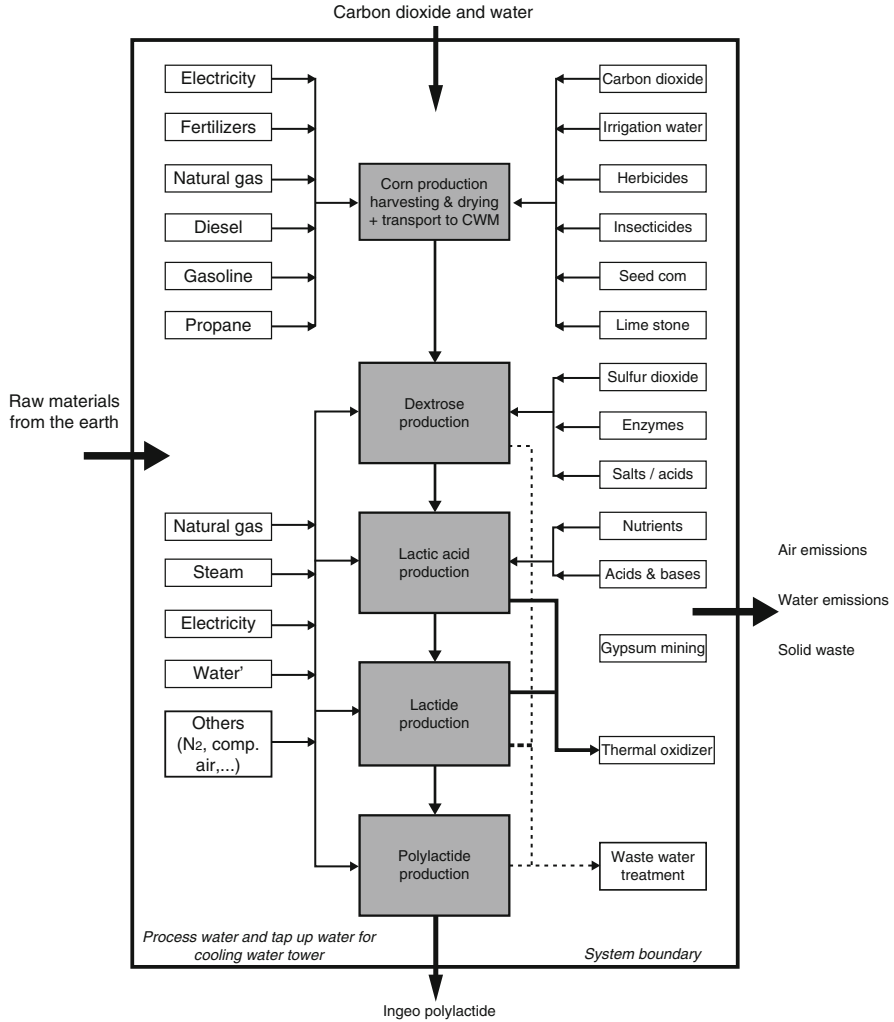


Fig. 2 Flow diagram for the manufacture of Ingeo PLA biopolymers

molecule and the final Ingeo polymer originates from water and CO₂. The data include all the relevant inputs for corn production, including production of corn seed, fertilizers, limestone, electricity, and fuels (natural gas, diesel, propane, and gasoline) used on the farm. the atmospheric CO₂ used through photosynthesis, the irrigation water applied to the corn field, and the production of the herbicides and insecticides used to protect the corn. On the output side, emissions including dinitrogen oxide, nitrogen oxides, nitrates, and phosphates are taken into account. The production of the farm equipment (tractors and harvest combines) employed was investigated, but their contributions are negligible.

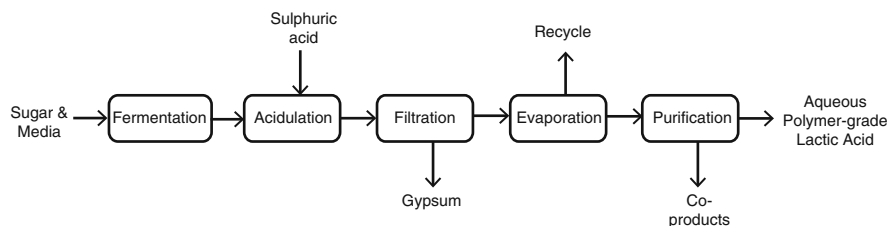


Fig. 3 Lactic acid production process

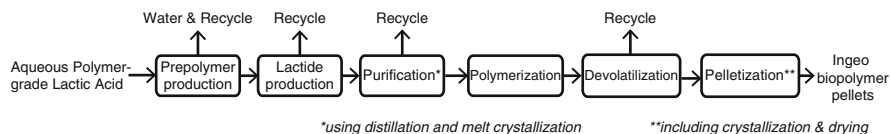


Fig. 4 NatureWorks' lactide formation and polylactide polymerization process

Lactic acid is produced by fermentation of the dextrose sugar. The process, illustrated in Fig. 3, combines dextrose and other media, adds a microbial inoculum, and produces crude lactic acid.

Figures 4 and 5 illustrate the process and the steps, respectively, of the polymerization process.

Figure 6a presents the latest available data for the primary energy of non-renewable resources in MJ Higher Heating Value (HHV)/kg polymer for a selection of polymers produced in the US and EU and Fig. 6b provides the global warming potential expressed as CO₂ equiv/kg polymer for the same polymers. These are net GWP (global warming potential) values from cradle-to-polymer factory-to-exit gate. For Ingeo, the uptake of CO₂ from the atmosphere is included, as this takes place during corn production, a process within the system boundary.

3 Applications of PLA

3.1 World Request for Poly(lactic acid)

Global demand for poly(lactic acid) and lactate esters for 2015 was 200,000 tons, a sector dominated by the food, beverage, and personal care industries (<https://www.gminsights.com/industry-analysis/lactic-acid-and-polylactic-acid-market>). PURAC BIOCHEM (Netherlands) is the worldwide leader in biotechnological production of lactic acid. A survey of lactic acid producers (the precursor of PLA) revealed that production capacity could even rise to roughly 950,000 tons/year to meet concrete requests.

At 30 sites worldwide, 25 companies developed a production capacity of more than 180,000 tons/year of PLA in 2012.

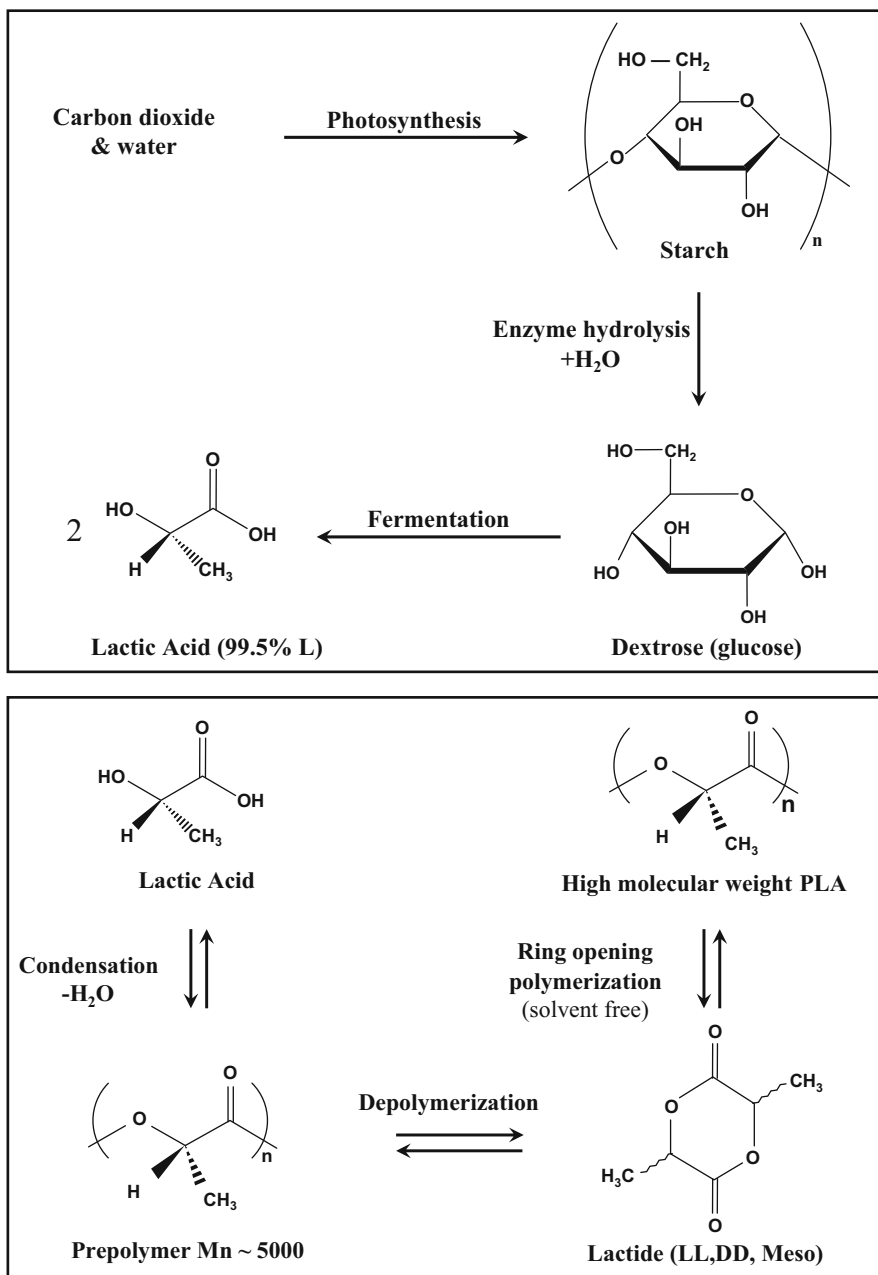


Fig. 5 Steps to Ingeo production

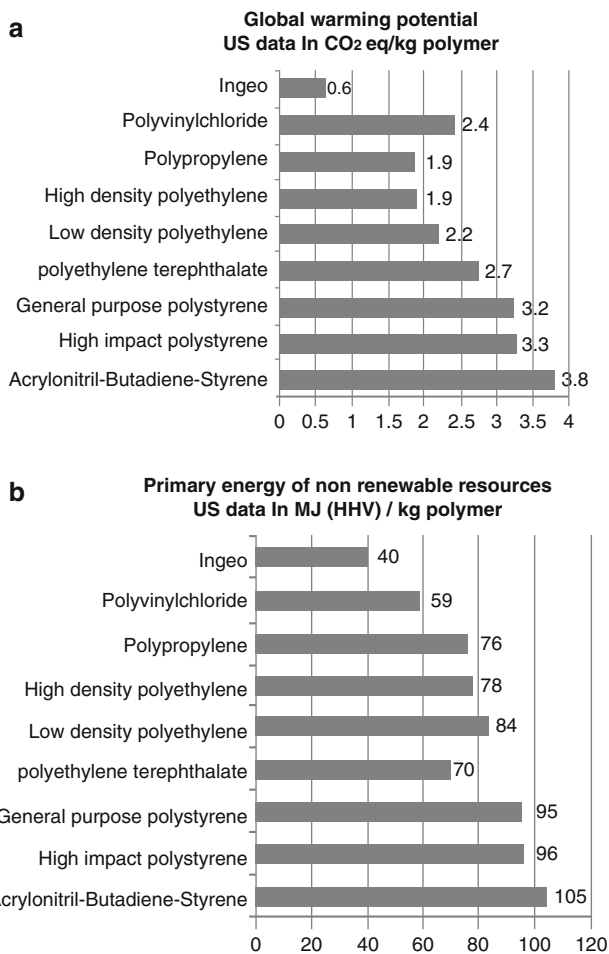


Fig. 6 (a) Primary energy of non-renewable resources. (b) GWP-cradle-to-polymer factory-gate

The largest producer, NatureWorks, had a capacity of 140,000 tons/year in 2011. The other producers have current capacity of between 1,500 and 10,000 tons/year. According to their own forecasts, existing PLA producers are planning to expand considerably their capacity of over 50,000 tons/year by that time. Current (2015) world production of PLA is 200,000 tons/year and it is used in the food, chemical, and pharmaceutical industries. In 2004 the NEC Corporation developed a plant-based plastic PLA with high fire resistance and no toxic halogens or phosphorus derivatives, and in the same year the Japanese company Sanyo[®] introduced a compact disc made of PLA, incorporating plastic packaging foams formed from mixtures of starch with PLA, protecting from damp and against shock and vibration during transport.

3.2 *Textile Industry*

PLA polymers also have many potential applications in fiber technology. They present very attractive features for many traditional uses. PLA polymers are more hydrophilic than polyethylene terephthalate, have a lower density, and exhibit high bending and stretching strengths [22].

The degree and temperature of shrinkage of PLA materials are readily controllable. These polymers tend to be stable to UV light, resulting in fabrics with little discoloration. It is a fire retardant and low smoke material.

Its applications include clothing, upholstery of certain furniture, diapers, feminine hygiene products, and fabrics resistant to UV radiation for outdoor uses [23].

3.3 *Medical and Pharmaceutical Industry*

The selection criteria for PLAs depend on the applications, so higher mechanical strength is obtained by selection of the amorphous (DL-PLA) or long-term biodegradability by selection of the semi-crystalline form (L-PLA). Copolymers of L/DL-PLA are used to preserve the mechanical properties and speed of biodegradability [24].

In the field of surgery, L-PLA finds great applications as material for absorbable sutures (ophthalmological surgery, conjunctival, thoracoabdominal, neurological anastomosis), and in orthopedic surgery (resorbable implants, screws, pins, plates, staples), reconstructive surgery, and craniofacial and maxillofacial surgery involving bone and soft tissues [13, 24, 25].

PLA is used in the creation of matrices for guided tissue regeneration as skin, cartilage, bone, cardiovascular structures, intestine, and urinary tissue among others [26].

It is also used to microencapsulate and nanoencapsulate slow release drugs such as insulin, cisplatin, taxol, somatostatin, anti-inflammatory drugs, ganciclovir, angiogenesis inhibitors, etc. The drug is absorbed in the center of a matrix of PLA polymer microspheres, which is capable of protecting the drug or organism. As the matrix is hydrolyzed, the drug is released. It is also used in the application of cancer chemotherapy or contraception [27, 28].

The following are the worldwide applications:

- Biodegradable scaffolds for tissue engineering
- Reconstructive and bioabsorbable implants
- Equipment and instrumentation for surgeons
- Implants for fracture fixation
- Treating facial lipoatrophy
- Absorbable internal fixation plates face fractures, orthognathic and craniofacial surgery
- Preparation of biodegradable microspheres
- Bioresorbable fixation devices in orbital reconstructions
- Intravitreal administration of antivirals

3.4 Agriculture

The main effect of crop mulching is to promote soil warming, thereby allowing root development of the plant, and mulching is also often complemented by a tunnel microclimate [29]. The use of mulching for horticultural crops can advance harvesting, reduce water consumption, avoid the use of herbicides, and enhance the quality of production, fostering integrated and organic production.

Traditional mulching materials are linear low density polyethylenes, opaque or transparent, depending on the crop cycle in which it is used and the effect it is intended to have. These plastic materials have mechanical properties and exceptional optics, often being directly responsible for the success of planting. Other purposes are reducing soil evapotranspiration, combatting weed flora, reducing the loss of minerals, and, by black coloration, stopping the growth of infesting plants. The problems arising from their use, on the other hand, arise because of their excellent mechanical properties, which gives them a long life. End-of-life management, although illegal, often involves soil burial or incineration or superficial abandonment with climate agents such as wind taking the residues to various locations and ecosystems, in all cases leading to soil contamination [30–33]. This, together with their great development that has allowed them to be used anywhere, their repeated use, their small thicknesses and poor agricultural practices, has prompted the search for alternatives in those places where they cannot be recovered after use [34, 35].

The alternative of biodegradable mulching could be the solution to the problem, provided that the degradation of the mulching material occurs in a fast and reliable way [36–38]. For those mulching materials whose base polymer is composed of or derived from PLA, there are two factors, among others, related to soil condition which have a direct influence on degradation processes, the degree of humidity and the microbiota existing in the areas where the pieces of mulched films are buried, that assure complete degradation of the residual films prior to the beginning of the next crop [39, 40]. The activity of the bacterial flora is responsible for the disappearance of the sheets of films when feeding them, and their presence and multiplication is possible provided there is some degree of moisture in the soil.

3.5 Packaging

The most successful application of PLA is in containers and food packaging. However, the higher affinity to water and, consequently, the higher potential for fungal growth in biodegradable materials compared to non-biodegradable oil-derived polymers may be a negative characteristic for use in some food sectors [41, 42]. Therefore bio-packages are more suitable for foods with high breathing and short storage life such as vegetables, and for the packaging of some bakery products.

In the food industry, PLA has been the subject of a detailed study by the FDA in which it was found that the migration of lactic acid, lactide, and lactoyllactic acid was limited and it was therefore concluded that PLA is a substance recognized as safe and can be used as a packaging material for food [7].

Materials consisting of 10% PLA plus 90% copolyester, 10% PLA plus 90% copolyamide, 10% PLA plus 90% starch, and 10% PLA plus 90% polycaprolactone have been used as packing material for yogurt, butter, margarine, and cheese spread. These materials have fulfilled functions such as mechanical protection and a barrier to moisture, light, grease, and gases. They have also been used as “windows” in packaging for dry goods such as bread, which play a role as a moisture barrier, and in the preparation of coated paper PLA containers for packaging beverages, also playing a role as a moisture barrier [43].

Södergard [7] says that the most promising application of PLA in packaging materials is for products that must remain cold and have limited lifetimes, such as dairy products. However, in a study conducted at the Technical University of Denmark, where the convenience of using biobased packaging materials for foods was assessed, they concluded that the high fungal growth on materials obtained from biodegradable bases is a negative factor for use in foods and claim that biopackagings are more suitable for foods with high breathing and short storage life such as vegetables, and for the packaging of some bakery products [43].

4 The Future of PLA-Based Materials

Although the values of global installed capacity for the production of biodegradable plastics do not reach 1% of the total world demand for plastic resins, progress is vigorous in the packaging market. The growth and acceptance of biodegradable resins is related to the high price of oil, consumer awareness of environment protection, technological achievements in the new generation of biodegradable resins, and governmental laws. Some companies predict market growth in Europe at a rate of 20% annually, and the Association of Biodegradable Polymers (IBAW) estimates that, with existing quality and price, a possible potential for about 10% of the plastics market share, which in Europe is 40 million tons/year is forecastable.

It appears that in the food industry, in food packaging, packaging for toys, candy wrappers and flowers, in making boxes, milk cartons, soda bottles, oil bottles, home curtains, sheets, pillows, tablecloths, upholstery, and textile fibers, products of PLA will increase significantly in the coming years.

References

1. Galactic Laboratories (2017). <https://www.lactic.com/en-us/applications/industry/bioplastics.aspx>

2. Biresaw G (2004) Compatibility in polymer blends comprising biodegradable polyesters. In: Proceedings of International Conference on Polymers for Advanced Technologies, December 15–17, 2004, Thiruvananthapuram, India
3. Dugan JS (2001) Novel properties of PLA fibers. *Int Nonwovens J* 10(3):31
4. Balkcom M et al (2002) Notes from the packaging laboratory: polylactic acid an exciting new packaging material. <http://ufdcimages.uflib.ufl.edu/IR/00/00/15/27/00001/AE21000.pdf>
5. Garlotta D (2001) A literature review of poly(lactic acid). *J Polym Environ* 9(2):63–84
6. Weber C (2000) [http://www.biodeg.net/fichiers/Book%20on%20biopolymers%20\(Eng\).pdf](http://www.biodeg.net/fichiers/Book%20on%20biopolymers%20(Eng).pdf)
7. Södergard A (2000) Lactic acid based polymers for packaging materials for the food industry. Conference Proceedings. The Food Biopack Conference. Copenhagen, Denmark, pp 19–22
8. Nobile MR, Lucia G, Santella M, Malinconico M, Cerruti P, Pantani R (2016) Biodegradable compounds: rheological, mechanical and thermal properties. *AIP Conf Proc* 1695:020058. <https://doi.org/10.1063/1.4937336>
9. Clarinval AM, Halleux J (2005) Classification of biodegradable polymers. In: Smith R (ed) *Biodegradable polymers for industrial applications* 1st edn. CRC Press, Boca Raton, pp 3–31
10. Naitove MH (1995) Push is on to commercialize biodegradable lactide polymers. *Plast Technol* 41(3):15–17
11. Kimura H, Ogura Y, Moritera T, Honda Y, Tabata Y, Ikada Y (1994) In vitro phagocytosis of polylactide microspheres by retinal pigment epithelial cells and intracellular drug release. *Curr Eye Res* 13:353–360
12. Zhang X, Wyss UP, Pichora D, Goosen MFA (1994) An Investigation of Poly(lactic acid) Degradation. *Journal of Bioactive and Compatible Polymers* 9:80–100
13. Serra T, Mateos-Timoneda MA, Planell JA, Navarro M (2013) 3D printed PLA-based scaffolds. A versatile tool in regenerative medicine. *Organogenesis* 9:239–244
14. Hottle TA, Bilec MM, Landis AE (2013) Sustainability assessments of bio-based polymers. *Polym Degrad Stab* 98:1898–1907
15. Landis AE (2010) Cradle to gate environmental footprint and life cycle assessment of poly(lactic acid). In: Auras R, Lim LT, Selke SEM, Tsuji H (eds) *Poly(lactic acid) synthesis, structures, properties, processing, and application*. Wiley, Hoboken, p 431
16. National Oceanic & Atmospheric Administration. Earth System Research Laboratory, Global Monitoring Division. <http://esrl.noaa.gov/gmd/ccgg/trends>
17. Narayan R (2014) Why bio-based? What are the compelling reasons to increase the proportion of biobased products in your inventory? Presentation at Bioproducts World, October 7, 2014, Columbus, OH (available on request from narayan@msu.edu)
18. Vink ETH, Rabago KR, Glassner DA, Gruber PR (2003) Applications of life cycle assessment to NatureWorks™ polylactide (PLA) production. *Polym Degrad Stab* 80:403–419
19. Vink ETH, Glassner DA, Kolstad JJ et al (2007) The eco-profiles for current and near future NatureWorks polylactide (PLA) production. *Ind Biotechnol* 3:58–81
20. Vink ETH, Davies S, Kolstad JJ (2010) The eco-profile for current Ingeo polylactide production. *Ind Biotechnol* 6:212–224
21. Vink ETH, Davies S (2015) Life cycle inventory and impact assessment data for 2014 Ingeo™ polylactide production. *Ind Biotechnol* 11:167–180
22. Avinc O, Khoddami A (2010) Overview of poly(lactic acid) (PLA) fibre. *Fibre Chem* 42(1):68
23. Shafer A (2002) Polylactic acid polymers from corn: potential applications in the textiles industry. *J Ind Text* 29:3
24. Hamad K, Kaseem M, Yang HW, Deri F, Ko YG (2015) Properties and medical applications of polylactic acid: a review. *eXPRESS Polym Lett* 9:435–455
25. Liu A, Xue G, Miao S, Shao H, Ma C, Qing G, Gou Z, Yan S, Liu Y, He Y (2016) 3D printing surgical implants at the clinic: a experimental study on anterior cruciate ligament reconstruction. *Nat Sci Rep* 6:21704
26. Marler J (1998) Transplantation of cells in matrices for tissue regeneration. *Adv Drug Deliv Rev* 33:165–182

27. Hyon SH (2000) Biodegradable poly (lactic acid) microspheres for drug delivery systems. *Yonsei Med J* 41:720–734
28. Pavot V, Berthet M, Rességuier J, Legaz S, Handké N, Gilbert SC, Paul S, Verrier B (2014) Poly(lactic acid) and poly(lactic-co-glycolic acid) particles as versatile carrier platforms for vaccine delivery. *Nanomedicine* 9:2703–2718
29. Tarara J (2000) Microclimate modification with plastic mulch. *Hortscience* 35:169–180
30. Catalina F, Peinado C, Allen NS, Corrales T (2002) Chemiluminescence of polyethylene: the comparative antioxidant effectiveness of phenolic stabilisers in LDPE. *J Polym Sci Pt A Polym Chem* 40:3312–3326
31. Corrales T, Catalina F, Peinado C, Allen NS, Montan E (2002) Photooxidative and thermal degradation on polyethylenes: interrelationship by chemiluminescence, thermal gravimetric analysis and FTIR data. *J Photochem Photobiol* 147:213–224
32. Shogren R, Hochmuth R (2004) Field evaluation of watermelon grown on paper polymerized vegetable oil mulches. *Hortscience* 39:1588–1591
33. Liu EK, He WQ, Yan CR (2014) ‘White revolution’ to ‘white pollution’—agricultural plastic film mulch in China. *Environ Res Lett* 9:091001. <https://doi.org/10.1088/1748-9326/9/9/091001>
34. Briassoulis D, Babou E, Hiskakis M, Scarascia G, Picuno P, Guardie D, Dejean C (2013) Review, mapping and analysis of the agricultural plastic waste generation and consolidation in Europe. *Waste Manag Res* 31(12):1262–1278
35. Briassoulis D, Hiskakis M, Babou E (2013) Technical specifications for mechanical recycling of agricultural plastic waste. *Waste Manag* 33:1516–1530
36. López J, González A, Bañón S, Franco JA, Contreras F (2005) Materiales de acolchado biodegradables como alternativa al polietileno lineal de baja densidad. *Actas Portuguesas Hortic* 7(3):346–351
37. López J, González A, Fernández JA, Bañón S (2007) Behaviour of biodegradable films used for mulching in melon cultivation. *Acta Hort* 747:125–130
38. Briassoulis D, Dejean C (2010) Critical review of norms and standards for biodegradable agricultural plastics, part I. Biodegradation in soil. *J Polym Environ* 18(3):384–400
39. Dharmalingam S, Hayes DG, Wadsworth LC, Dunlap RN (2016) Analysis of the time course of degradation for fully biobased nonwoven agricultural mulches in compost-enriched soil. *Text Res J* 86(13):1343–1355
40. Guerrini S, Borreani G, Voojis H (2017) Biodegradable materials in agriculture: case histories and perspectives. In: Malinconico M (ed) *Soil degradable bioplastics for a sustainable modern agriculture*. Springer, New York, p 35. ISBN 978-3-662-54130-235
41. Siracusa V, Rocculi P, Romani S, Dalla Rosa M (2008) Biodegradable polymer for food packaging: a review. *Trends Food Sci Technol* 19:634–643
42. Petersen K, Nielsen P (2000) Potential biologically based food packaging. Proceedings. The Food Biopack Conference. Copenhagen, Denmark, p 76
43. Haugaard V, Udsen A, Mortensen G, et al (2000) Potential food applications of biobased materials: an EU-concerted action project. Conference Proceedings: The Food Biopack Conference. Copenhagen, Denmark, pp 59–68

Poly(lactic acid) as Biomaterial for Cardiovascular Devices and Tissue Engineering Applications



Waled Hadasha and Deon Bezuidenhout

Abstract Synthetic bioabsorbable polymers, such as poly-lactic acid (PLA) and its copolymers (PLA-based polymers), have attracted a lot of attention in the medical field. With their excellent biocompatibility, mechanical properties, and tunable biodegradability, PLA-based polymers have found uses in various clinical applications, including sutures and orthopedic fixation devices (e.g. pins, plates, and screws). PLA-based polymers have also been the materials of choice for various cardiovascular applications. For example, they are extensively used as coatings for metallic drug-eluting coronary stents and in the development of the new generation of fully bioresorbable vascular scaffolds. In addition, the emergence of tissue engineering and regenerative medicine (TERM) has further extended the applications of PLA. In this chapter, we discuss the importance of PLA-based polymers as biomaterials and review the applications of this family of materials in cardiovascular applications, specifically in coronary stenting and TERM approaches to vascular grafts, heart valves, and cardiac patches. A brief insight is also given into the current market value and growth potential of PLA-based biomaterials.

Keywords Biomaterial • Cardiac patches • Heart valves • PLA • Stents • Tissue engineering • Vascular grafts

Dedication This paper is dedicated to the late Prof. Ronald D. Sanderson, founder of the Institute for Polymer Science (now incorporated into the Department of Chemistry and Polymer Science) at the University of Stellenbosch.

W. Hadasha and D. Bezuidenhout (✉)
Cardiovascular Research Unit, Christiaan Barnard Division of Cardiothoracic Surgery, Faculty of Health Sciences, University of Cape Town, Cape Town, South Africa
e-mail: Deon.Bezuidenhout@uct.ac.za

Contents

1	Introduction	52
2	Poly(lactic acid) as Biomaterial	53
3	Cardiovascular Applications	55
	3.1 Coronary Stents	55
	3.2 Tissue Engineering	58
4	Market Status	68
5	Conclusions	69
	References	70

1 Introduction

In the latter half of the twentieth century, the focus on inertness and stability of biomaterials led to the development of many medical devices that were intended to have minimal interaction with the host tissue. Although these devices have saved, and improved, the quality of many lives, no material is completely inert in the body and long-term negative host responses eventually lead to device failure [1].

This is illustrated by the following examples in the field of cardiovascular implants: (1) mechanical heart valves (introduced in 1952) are extremely durable but require lifelong anticoagulation because of inherent thrombogenicity of the metals and polymers/pyrolytic carbon from which they are made [1]; (2) crosslinked bioprosthetic (BP) heart valves (1972) do not require anticoagulation but have a limited lifespan as a result of calcific degeneration, especially in younger patients [2]; (3) polyethylene terephthalate (PET; 1954) and expanded polytetrafluoroethylene (ePTFE; 1975) small-diameter vascular grafts have high failure rates due to mid-graft stenosis and anastomotic intimal hyperplasia associated with thrombogenicity and mechanical mismatch (respectively) [3]; and (4) a high percentage of bare metal coronary stents fail because of restenosis after implantation [4].

Although there have been improvements in these outcomes by more controlled anticoagulation for mechanical heart valve recipients, improved crosslinking and anticalcification treatment of BP tissues [2], heparinization of ePTFE grafts [5], and the development of drug-eluting stents [4], these implants persist in the body and eventually may lead, respectively, to thromboembolic or bleeding events, degeneration to a point of failure, depletion of eluted drugs, or occlusion due to thrombosis [6].

The generation of living structures and organs through recent advances in tissue engineering (TE) and regenerative medicine (RM) promises not only long-term function, but also the potential for growth when used in young individuals [7, 8]. Because these technologies often rely on the use of temporary scaffolds to guide and optimize tissue growth, there is a great need for suitable biocompatible and resorbable materials. In addition to natural materials employed in some applications, a range of synthetic degradable polymers has been developed for this purpose

[9, 10]. Of these, poly(lactic acid) (PLA) and its copolymers, including poly(glycolic acid) (PGA), polycaprolactone (PCL), poly(lactide-*co*-caprolactone) (PLA-PCL) and poly(lactic-*co*-glycolic acid) (PLGA) have probably been the most extensively investigated. They are therefore included in discussion in this chapter [8].

2 Poly(lactic acid) as Biomaterial

PLA is biocompatible, considered safe for direct contact with biological tissue, and is one of the few degradable materials approved by the US Food and Drug Administration (FDA) and many other regulatory agencies [11]. PLA is usually produced by two methods: direct polycondensation reaction of 2-hydroxy propionic acid (lactic acid) and ring-opening polymerization of lactide (a cyclic dimer of lactic acid). Lactic acid exists in two isomeric forms, L-lactic acid and D-lactic acid, which can produce four distinct materials: poly(D-lactic acid) (PDLA), a crystalline material with a regular chain structure; poly(L-lactic acid) (PLLA), which is semicrystalline, and likewise with a regular chain structure; poly(D,L-lactic acid) (PDLLA) which is amorphous; and meso-PLA, obtained by polymerization of meso-lactide. The meso-isomer is rarely used in biomedical applications and amorphous PDLLA is generally selected for drug-eluting applications. The semicrystalline PLLA is preferred for uses where mechanical strength is required and is also preferred over PDLA, as the former degrades to the naturally occurring L(+) lactic acid [12–14].

PLA production is a multistep process that includes the production of lactic acid through either fermentation of carbohydrates by a bacterial or a synthetic approach. Approximately 90% of all lactic acid produced is made by bacterial fermentation because it has the lowest energy consumption and provides high product specificity (i.e., L-lactic acid or D-lactic acid) [1, 2]. PLLA of variable molecular weight is produced by polycondensation or ring-opening polymerization. Whereas polycondensation usually produces relatively low molecular weight PLLA, high molecular weight PLLA can be obtained through ring-opening polymerization. Production of medical grade PLLA-based polymers requires the use of reagents of high purity and nontoxic catalyst systems, such as stannous octoate. The latter has been approved by the FDA as biologically safe for use in medical and food applications, including the production of PLLA. PLLA usually passes through extensive purification processes, which may significantly increase its production costs and market price [15, 16].

These polymers, however, do have disadvantages that may limit their applications as homopolymers, including slow degradation, poor mechanical ductility, and lack of biological interaction [17]. To overcome these limitations and tailor PLA properties to suit applications, PLA has been modified using the following approaches [17–20]:

- *Copolymerization* with glycolic acid or polyethylene glycol (PEG) to impart hydrophilicity and modulate the degradation rate
- *Crosslinking* with gamma irradiation in the presence of crosslinking agents to improve thermal and mechanical properties
- *Blending* with other degradable or nondegradable polymers to tailor mechanical and degradation properties, or to alter processability without sacrificing degradability and biocompatibility
- *Plasticization* with oligomeric lactic acid, PEG, etc. to improve elongation at break
- *Reinforcement* with fillers or fibers
- *Chemical or physical surface modification* to improve biocompatibility and cellular interaction
- *Chemical modification* of the backbone by cleavage of some ester groups and appending biomolecules, such as adhesive peptides.

In vivo degradation times for PLA depend on the application and circumstances. It typically varies from 50% in 1–2 years to 100% in 12–16 months, whereas PLGA (75:25) is typically fully degraded in 50–100 days [21]. The hydrolytic degradation of PLA and PLGA is characterized by hydration, loss of mechanical strength caused by breakdown of the backbone and formation of acidic oligomers, mass loss, further water absorption as a result of diffusion of oligomers and water, and finally polymer dissolution/phagocytosis [22]. The hydrolysis may involve enzymatic action [21, 22]. The lactic and glycolic acids formed are further metabolized to carbon dioxide and water in the Krebs cycle [23, 24]. The acidic breakdown products of PLA can lead to a local decrease in pH of the tissue surrounding the implant, which may result in cell necrosis and inflammation [25].

The general characteristics of biocompatibility, biodegradability, thermoplastic processability, and tunable chemical and physical properties of PLA and its copolymers lend themselves to a variety of biomedical applications. The polymers' high mechanical strength makes them especially suitable for applications such as orthopedic screws, rods/pins, and plates (many of which are now in clinical use), and PLGA (Vicryl[®]) resorbable sutures (introduced in the 1970s) [26, 27]. The use of PLA in drug delivery systems and TE is, however, with a few noted exceptions, still in the experimental and preclinical phases. In addition to the clinical application of drug-eluting stents (discussed in detail in the Sect. 3.1), PLA has been extensively used to develop carriers (nanoparticles, microparticles, and microcapsules) for the controlled release of drugs, peptides/proteins, polysaccharides, and genetic material (DNA, RNA) [12, 21, 22].

PLA-based materials have also been widely used to fabricate 3D TE scaffolds for orthopedic [28], nerve [29] and cardiovascular [30–32] applications, in which not only the actual material but also the scaffold design, architecture, microstructure, and physical strength play important roles.

This chapter focuses on the use of PLA and its copolymers in cardiovascular applications, specifically in drug-eluting and degradable stents, and in TE approaches to heart valves, vascular grafts, and cardiac patches for treatment of myocardial infarction.

3 Cardiovascular Applications

3.1 Coronary Stents

Coronary artery disease (CAD), the narrowing of coronary arteries by fatty deposits that leads to inadequate blood flow and eventually stenosis (blockage), is a major cause of morbidity and mortality worldwide. Left untreated, CAD leads to angina (chest pain) and myocardial infarction (heart attack). In advanced pathologies, coronary artery bypass grafting, in which the obstruction is bypassed with healthy autologous vessels (from the patient's own body) during open-heart surgery, is the best recourse. For less severe cases, percutaneous transluminal coronary angioplasty, which involves widening the vessel with a balloon through minimally invasive percutaneous catheterization techniques, is used. This technique was introduced in the late 1970s by Andreas Gruentzig [33]. Acute occlusive dissection (4–8%) and a high incidence of restenosis (30–50%) of the vessel after angioplasty led to the development of the vascular stent (an artificial tubular mesh), by Palmaz in 1985, as an alternative treatment procedure to reopen narrowed vessels and provide continued mechanical support to the healing vessels. Stainless steel was initially the preferred metal for balloon expandable stents, with cobalt alloys (Co-Cr and Co-Pt) gaining increasing favor because of their superior mechanical properties. In many cases, however, (16–44% [33]), these bare metals stents led to persistent local inflammation [34] of the vessel wall, which led to excessive neointimal proliferation and (in 16–44% of cases) to in-stent restenosis (ISR) (narrowing of more than 50% in the stented area of the vessel) [35].

To overcome these complications, drug-eluting stents (DESs) were introduced in 2002/2003 [36]. DESs consist of a metallic structure coated with a thin polymer layer that elutes a drug to reduce the proliferation and thus prevent ISR. First generation DESs used durable polymers (e.g., poly(styrene-*b*-isobutylene-*b*-styrene) or poly-*n*-butyl methacrylate) to elute drugs with anti-inflammatory and antiproliferative action, such as dexamethasone, rapamycin, and paclitaxel. Lincoff et al. was one of the first to use a PLLA/dexamethasone-coated titanium stent as a sustainable site-specific drug delivery system [37]. Short-term in vivo results showed that the DES was an effective drug delivery approach that caused minimal thrombosis and inflammatory response.

Although ISR was reduced to approximately 10% with drug elution, the presence of a foreign body long after the drug was completely released could potentially lead to delayed healing and local chronic inflammation, and potentially to late and very late stent thrombosis (ST; 3% at 4 years) [33].

Second generation DESs saw the use of more biocompatible durable coatings (fluorinated polymers and phosphoryl choline-containing polymers) as well as the introduction of absorbable materials (e.g., PLA), resulting in improvements in outcomes to ISR of 6–8% and ST of 1% at 3 years [33, 38]. Several companies have since developed various DESs using PLA-based polymers as coatings with various drugs, as summarized in Table 1.

Table 1 Various PLA-based drug-eluting stents, adapted from [38, 39]

Stent	Mesh material	Drug	Polymer coating	Manufacturer
BioMime	Co-Cr	Sirolimus	PLLA/PLGA	Meril Life Sciences (India)
DESyne BD	Co-Cr	Novolimus	PLLA	Elixir Medical (USA)
Synergy	Pt-Cr	Everolimus	PLGA	Boston Scientific (USA)
BioMatrix	SS	Biolimus A9	PDLLA	Biosensors (Switzerland)
Nobori	SS	Biolimus A9	PDLLA	Terumo (Japan)
Yukon Choice PC	SS	Sirolimus	PDLLA	Translumina (Germany)
Orsiro	Co-Cr	Sirolimus	PLLA	Biotronik (Germany)
Ultimaster	Co-Cr	Sirolimus	PDLLA/PCL	Terumo (Japan)

SS stainless steel, Co-Cr cobalt chromium, Pt-Cr platinum chromium

In addition to these delayed complications, persistent metallic stents have drawbacks related to the need for removal/replacement if repeat procedures are required, due to restenosis of previously stented vessels. Furthermore, the lack of a permanent foreign object would reduce the risk of late ISR and thrombosis, and thus the development of bioresorbable vascular scaffolds (BVSs) is inevitable.

Third generation vascular stents are made from biodegradable/bioresorbable materials (metals such as magnesium or iron, or various synthetic polymers) as their structural elements. Because of their strong mechanical properties and tunable degradation rate, semicrystalline PLA-based polymers have been widely employed in either drug-free or drug-eluting BVSs [39–42]. The degradation rate of BVSs is an important parameter that can affect vessel remodeling and healing, as premature degradation can lead to acute vessel recoil and prolonged degradation can result in chronic inflammation and, hence, delayed healing [43, 44].

The concept of a BVS was introduced in 1988 by Stack et al., who created a knitted PLA stent design that could withstand a crush pressure up to 1,000 mmHg and maintain its radial strength for 1 month [45]. The stent was successfully implanted in an animal model and showed significant improvement in reducing inflammatory response; however, neointimal growth was observed because of vessel wall injury. These results inspired others to investigate BVSs as an alternative to permanent metal-based stents. To reduce vessel wall injury, the original knitted design of BVSs was changed to a coil design, which significantly reduced the risk of blood vessel wall injury and, hence, reduced neointimal hyperplasia.

The first human trial of a BVS was conducted using the Igaki-Tamai stent (Igaki Medical Planning Company, Kyoto, Japan), fabricated from drug-free high molecular weight (HMW) PLLA in a zig-zag helical configuration (see Fig. 1c and Table 2) [46]. The stent design significantly reduced vascular injury at the implantation site, leading to a reduction in initial thrombus deposition and blood clots, and presented no major cardiac complications, with only 10.5% restenosis at 6-month follow-up. The 4- and 10-year follow-up results demonstrated the feasibility and safety of PLLA-based bioresorbable stents.

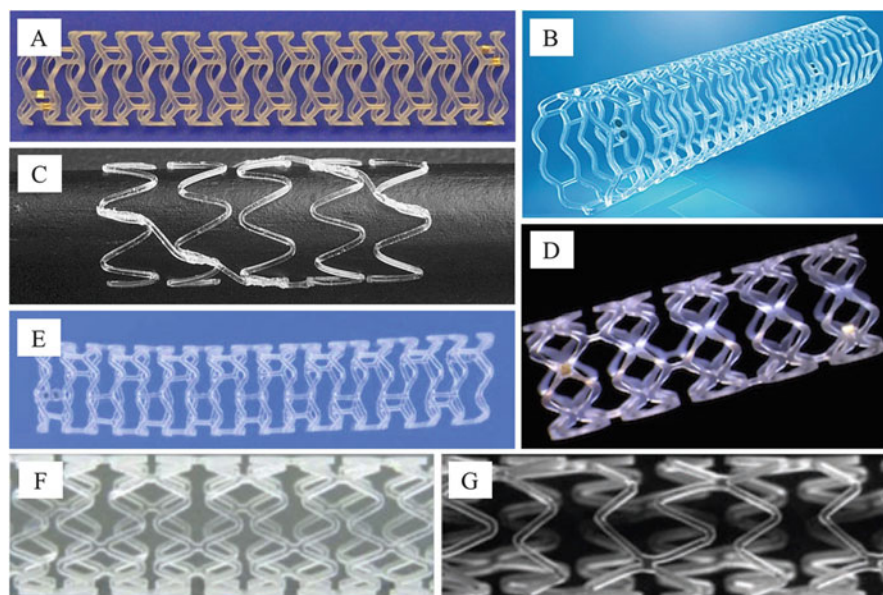


Fig. 1 Various BVSs in clinical or preclinical use. (a) Fortitude (Amaranth Medical, USA), (b) DESolve 100 (Elixir Medical, USA), (c) Igaki-Tamai (Kyoto Medical, Japan), (d) ART18Z BRS (Arterial Remodeling Technologies, France), (e) Absorb BVS 1.1 (Abbott Vascular, USA), (f) Xinsorb (Huaan Biotech, China), and (g) Acute BRS (OrbusNeich Medical, USA). Images adapted from [46, 47]

Table 2 Summary of various bioresorbable vascular scaffolds. Adapted from [39, 41]

Stent	Mesh material	Drug	Polymer coating	Manufacture	Current status
Igaki-Tamai	PLLA	–	–	Kyoto Medical	CE mark
Fortitude	PLLA	–	–	Amaranth	Clinical trails
Mirage BRMS	PLLA	Sirolimus	–	Mirage BRMS	Clinical trails
Absorb BVS	PLLA	Everolimus	PDLLA	Abbott Vascular	CE mark
Xinsorb	PLLA	Sirolimus	PLA	Huaan Biotech	Clinical trails
Acute	PLLA–PCL	Sirolimus	PLA	OrbusNeich Medical	–
DESolve	PLLA	Myolimus	–	Elixir Medical	EC mark
DESolve 100	PLLA	Novolimus	PLLA	Elixir Medical	EC mark
MeRes	PLLA	Paclitaxel	PLGA	Meril Life Sciences	Clinical trails
ART18Z BRS	PDLLA	Sirolimus	PLLA	Arterial Remodeling Remodeling Tech	Clinical trails
FADES	PLGA/Mg	–	–	Zorion Medical	–

BVSs may of course also serve as a drug delivery system, as demonstrated by Yamakawi et al., who incorporated an antiproliferative agent (tyrosine kinase inhibitor) in PLLA-based stents. The results obtained suggested that the stent was able to suppress neointima hyperplasia caused by balloon injury [48]. Analogous to regular DESs, drug-eluting BVSs generally consist of a platform made of biodegradable materials, such as PLA or Mg with a thin layer of drug-loaded biodegradable polymer such as amorphous PDLLA or other PLA-based polymers [42, 49, 50]. The stent platform usually has a slow degradation rate to provide mechanical support of suitable duration, whereas the degradation of the outer thin layer is usually tuned to allow uniform dispersion and controlled drug release.

Various PLA-based drug-eluting BVSs either have received the CE mark or are currently undergoing clinical trials. Abbott Vascular produced the first drug-eluting BVSs, Absorb BVS (Fig. 1e and Table 2) (PLLA with everolimus/PDLLA coating). It is now widely available, including in the USA and Europe, with more than 150,000 having been implanted [51]. In a preclinic in vivo study, the stent showed similar drug release profiles to those obtained from previously approved DESs, and the stent exhibited positive vessel remodeling and full absorption of platform in a 2-year clinical trial. Table 2 summarizes a number of BVSs currently under development and/or in clinical use.

3.2 *Tissue Engineering*

The term “tissue engineering” was introduced by Dr Fung of California University in 1987. Since then, TE has been widely used and has emerged as a potential alternative to organ transplantation or as a treatment method for repair of damaged tissues and organs. Ultimately, the purpose of TE is to generate compatible, healthy, and functional tissue and organs that are readily available for implant. Accordingly, this should contribute to overcoming the shortage of tissue donors, as well as minimizing the use of artificial implants and the need for prolonged medication and/or additional procedures to remove the implants.

TE is a multidisciplinary field that combines various aspects of materials science, biology, engineering, and medicine, with the aim of fabricating biological substitutes that are able to repair, maintain, or replace damaged tissues and organs. The generation of new tissue can either be in vitro, usually known as “tissue engineering”, or in vivo, usually referred to as “regenerative medicine” [52–54]. In the TE approach, the new tissue is generated in vitro by seeding isolated cells (same cell types as the native tissue cells) onto a 3D scaffold and culturing in a dish or bioreactor prior to implantation. However, in the RM approach, the tissue is fabricated in vivo by implanting an acellular 3D scaffold that guides and directs the migration of native cells to regenerate new tissue, using the host as bioreactor. As the new tissue is formed, the 3D scaffold degrades into metabolically removable materials, leaving behind fully functional and compatible new tissue or a new organ [52, 54]. For the

sake of simplicity, the “TE” will be used throughout this chapter to describe both approaches.

In natural tissue, cells are surrounded by a connective network of extracellular matrix (ECM) that provides an essential physical framework, and crucial biochemical and biomechanical cues required for cellular constituents during tissue development and maturation. TE scaffolds mimic the development of growth and generation of tissue to produce a functional organ. Therefore, developing a successful and effective TE approach relies on the appropriate combination of three important components that exist in natural tissue: (1) a 3D scaffold, (i.e., organ-specific composition and shape), (2) isolated cells (i.e., cell population, culture) and (3) cell signaling cues (i.e., chemical and physical cues).

One of the key elements in TE strategies that determines the function and shape of the engineered tissue is the 3D scaffold. Mimicking ECMs, the scaffold serves as a temporary artificial template that supports and regulates cells’ activities, from attachment to differentiation. To fulfill the ECM function, the scaffold should exhibit organ-specific composition, and mechanical and architectural characteristic features. Therefore, the scaffold should (1) comprise a biocompatible, bioactive, and degradable material; (2) exhibit suitable mechanical and physical properties, compatible with the mechanical function of engineered tissue; and (3) have an appropriate macro- and microstructure design.

The scaffold material should be compatible with the tissue and be able to degrade biologically at a suitable rate, specifically, a rate that matches the formation rate of new ECM, and with predictable degradation kinetics, byproducts, and rates.

The resorption of scaffold materials is a critical parameter in tissue regeneration. In order to generate healthy new tissue, the scaffold should maintain sufficient physical and mechanical features until the formation of adequate new ECM. Therefore, as mentioned, the scaffold degradation rate should match the rate of new ECM formation. Whereas fast degradation can result in mechanical instability and poor tissue formation, slow degradation leads to excessive chronic inflammation and the formation of unhealthy tissue.

Ideally, the scaffold should display physical and mechanical properties similar to those of the targeted tissue in its native state. For example, scaffolds intended for blood vessel engineering should have resistance, elasticity, or resilience compatible with the dynamic nature of the cardiovascular system. This is particularly important in TE of cardiovascular and cardiac tissue, where tissue undergoes continuous and variable mechanical stresses that can influence the behavior of seeded cells. For example, mesenchymal stem cells (MSCs) have been found to differentiate into neural, myogenic, or osteogenic tissue according to scaffold stiffness. Scaffolds intended for heart valve (HV) replacement should have a stiffness of approximately 0.5 MPa.

Other important characteristic features of a scaffold in TE that significantly influence cell behavior and function are the scaffold morphology and the macro- and microstructure. During tissue formation, the various activities that cells perform require highly porous structures to ensure a constant supply of nutrients and oxygen. Without a scaffold, most cells tend to aggregate to a certain thickness

(ca. 1–2 mm) before apoptosis arises because of the lack of an adequate supply and exchange of nutrients, oxygen, and waste metabolites [55–57]. Thus, growing large organized cell aggregates capable of tissue regeneration demands scaffolds of appropriate design that are able to provide the necessary environments for cellular activities. These activities typically require scaffolds with microstructures of interconnected pores to permit sufficient flow of gases, nutrients, and other signaling molecules that regulate cell behavior. Such microstructure features are also important for angiogenesis (i.e., formation of new blood vessels) as well as cell proliferation, differentiation, and motility. The average pore size, volume, and shape, as well as the overall morphology, are all important parameters that depend on the type of cell and tissue. The scaffold design, therefore, must be tailored and optimized to resemble the *in vivo* cellular macro- and microenvironments in native tissues.

The design of an effective scaffold with optimum structural features typically depends on the material used and the scaffold fabrication method. The selected method should be efficient and capable of producing scaffolds with complex architectures that mimic the macro-, micro-, and nanostructure of natural ECMs. Several fabrication techniques have been developed and optimized for fabricating highly porous scaffolds, for example, electrospinning, 3D printing, emulsion freeze-drying, and salt leaching [56, 58–61]. These methods have enabled the fabrication of scaffolds of various shapes and morphologies. For example, electrospinning has been widely used to fabricate fibrous scaffolds with tunable microstructure, thickness, and composition from a wide range of polymeric materials. The high surface area-to-volume ratio and interconnected porous microstructure of nanofiber-based scaffolds offers highly attractive features for many TE applications. Detailed descriptions of various scaffold fabrication techniques are reported in many excellent reviews [10, 60–63].

As a conceptual creation in TE, the scaffold that is used should be temporary and biologically degradable. Therefore, consideration of the biodegradability of the material is of great importance when designing implantable scaffolds. Various biodegradable polymeric scaffolds have been used in many TE applications, including polymers of natural [64, 65] or synthetic [28, 66–68] origin, as well as decellularized tissue [69–72].

Natural polymers (e.g., chitosan, collagen, and cellulose) generally have better interactions with cells and better bioactivity compared with synthetic polymers; however, poor mechanical performance, and high risk of immunogenic response and infection have limited their application [53]. In recent years, various biodegradable synthetic polymers such as PLA, PGA, and PCL have been used to overcome the limitations associated with natural polymers [73]. PLA-based polymers have received significant attention in many TE applications. Their use in cardiovascular applications is described in the following sections.

3.2.1 Tissue-Engineered Heart Valves

The human heart consists of four heart valves that synchronically open and close to maintain unidirectional, unhindered blood flow during a person's lifetime. If one of the valves malfunctions (a condition commonly known as valvular heart dysfunction) and is left untreated, it could lead to heart failure and even death. The best available treatment for such a condition is surgical valve replacement with artificial valves. Artificial heart valves, such as mechanical and biological valves, are clinically used. However, the success of this approach requires the use of postoperative medication for a prolonged period as well as routine follow-ups, or even the need for reoperation (especially in young patients). TE represents a potential alternative treatment that can provide suitable valve replacements that are capable of growth and self-remodeling *in vivo*. Hence, the complications associated with traditional approaches can be avoided.

The generation of fully functional valve substitutes through TE strongly depends on the design and materials of the scaffold, as well as the selection of suitable cell types [74]. In addition to the general scaffold requirements of biocompatibility and biodegradability, the materials should mimic the mechanical and physical properties of native valvular ECMs [75]. The scaffold design should be nonobstructive, with the ability to adapt to change in physiological conditions and to withstand the mechanical loading during opening/closing of cyclic beating.

The concept of the tissue-engineered heart valve (TEHV) was introduced by Shinoka et al. in 1995 [76]. It involves the use of artificial scaffolds to direct the proliferation and growth of cells into a fully functioning valve, as schematically shown in Fig. 2. Thereafter, many other research groups investigated the concept further, using different types of cells and scaffolds, including decellularized [78, 79], biologically based [80, 81], and synthetic-based polymers, including PLA-based polymers [82–85].

PLA-based polymers have been used as synthetic materials to fabricate scaffolds for TEHVs [86]. For example, Mayer et al. [87, 88] investigated an *in vitro* TEHV using PGA and PGLA scaffolds. In this study, HV-shaped scaffolds consisted of a woven PLA mesh sandwiched between two nonwoven PGA fibrous scaffolds and seeded with endothelial cells (ECs) and myofibroblast cells. Histological examinations revealed the formation of cellular architecture and ECMs similar to those of native valves [89].

In a similar study, Sutherland et al. utilized PGA/PLLA (50:50 blend) scaffolds seeded with bone-marrow-derived MSCs to fabricate autologous semilunar TEHVs *in vitro*. The obtained valves were implanted into the pulmonary position of sheep on cardiopulmonary bypass. Histology analysis showed the deposition of ECM and distribution of cell phenotypes in the engineered valves similar to that displayed in native pulmonary valves. The obtained TEHVs functioned well *in vitro* for 4 months and underwent extensive remodeling *in vivo* [74].

Hinderer et al. [90] used different scaffolds consisting of electrospun PEG dimethacrylate–PLA, which showed biomechanical properties similar to those of

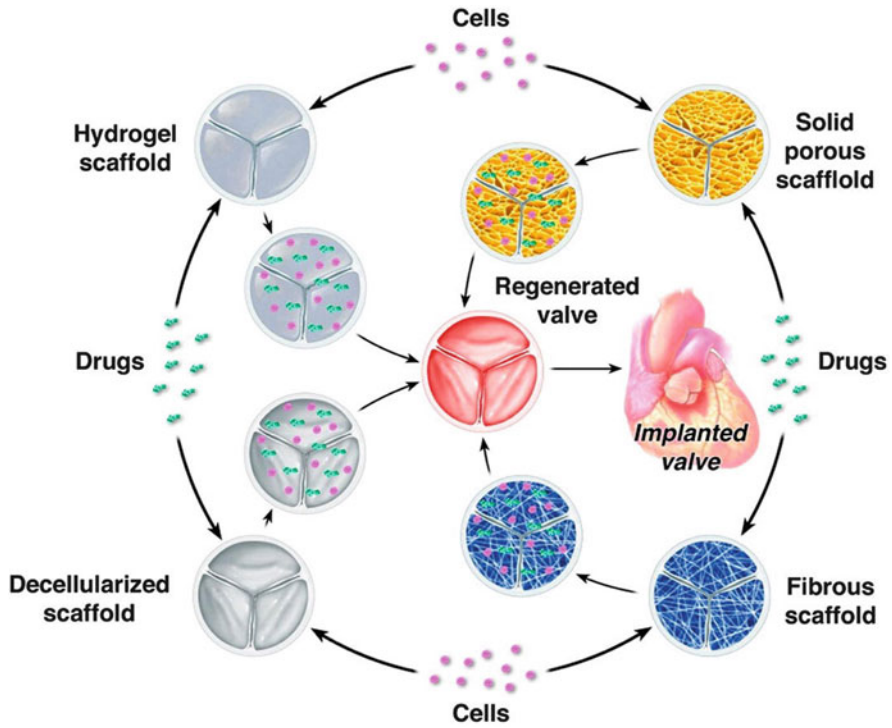


Fig. 2 Diagrams of aortic heart valve tissue engineering. Living cells are grown onto a supporting three-dimensional biocompatible structure to proliferate, differentiate, and ultimately grow into a functional tissue construct [77]

natural valve leaflets. The scaffolds were UV crosslinked before being seeded with valvular ECs and valvular interstitial cells and cultured in a bioreactor under physiological conditions [90, 91]. Three-dimensional (3D) printing is a versatile technique for producing many types of medical implants. It was used by Lueders et al. [92] to fabricate scaffolds suitable for TEHV from PGA/PLA copolymers.

TEHVs have also been fabricated using a combination of PLA-based polymers and natural materials. For example, Novakovic et al. [93] fabricated highly porous scaffolds using a composite of PDLA–PCL or PLGA and type I collagen. The scaffolds were then seeded with neonatal heart cells and cultured for 8 days. Compared with controls made of individual materials, the composite scaffolds showed higher cell densities with higher cardiac marker expression and contractile properties. The results were attributed to the suitable porosity, mechanical properties, and degradability of the scaffolds.

PLA-based hydrogels have also been developed and used as scaffolds for TEHVs. Anseth et al. investigated the attachment of valvular interstitial cells on biodegradable hydrogel scaffolds prepared from a photo-crosslinkable PLA–poly

(vinyl alcohol) multifunctional macromere and found improved cell attachment by increasing the PLA segments [94].

The limited use of PLA-based polymers to produce scaffolds for TEHVs can be attributed to its low flexibility and long degradation times. As a result, other degradable polymers (poly-4-hydroxybutyrate, PCL and copolymers with PGA) are now preferred.

3.2.2 Tissue-Engineered Vascular Grafts

Cardiovascular disease, including stenosis/occlusion and damage of blood vessels, is one of the leading causes of death worldwide. One of the available treatments for vascular pathologies is surgery utilizing either natural autologous (from the patient's own body) or synthetic vascular grafts [e.g., ePTFE (Teflon), polyurethane, and PET (Dacron[®])] for replacement or bypass grafting. However, this approach is usually limited either by the availability of healthy and suitable autologous vessel replacements or by hyperplastic stenosis and/or thrombus formation [31, 95, 96]. To overcome such limitations, TE techniques were proposed by Weinberg and Bell for fabrication of native-like vascular prostheses [97]. TE of vascular grafts is currently a very active research area in which PLA-based polymers have been widely used to fabricate scaffolds for tissue-engineered vascular grafts (TEVG).

The scaffold material plays a key role in TE applications because it should have appropriate mechanical properties to match the native vessels, especially as they are under cyclic stress. Various PLA-based polymers, such as PLLA, PLA-PCL, PLGA copolymers/blends, and PLA combined with other natural polymers, have been used to fabricate scaffolds for TEVG applications, with the advantage that mechanical properties of these polymers can be tuned by varying the concentrations of the constituents [98–103].

Several research groups have used these polymers to fabricate highly porous scaffolds suitable for VGTE through different fabrication methods, such as freeze-drying (Fig. 3) and electrospinning (Fig. 4).

Many studies have employed electrospinning techniques to fabricate tubular fibrous scaffolds of PLA-based materials, as it provides an efficient and effective

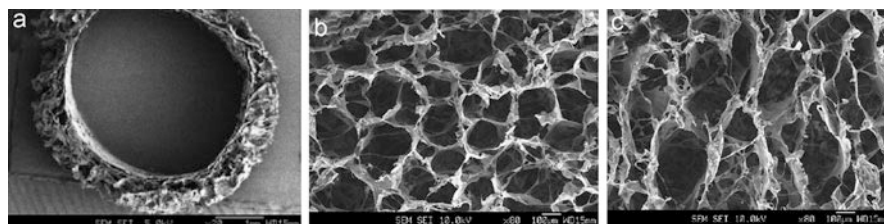


Fig. 3 SEM images of freeze-dry fabricated PLGA/collagen scaffolds: (a) cross-section of tubular collagen scaffolds, (b) inner surface of collagen scaffolds, and (c) outer surface of collagen scaffolds [98]. Scale bars 1 mm for (a) and 100 μm for (b) and (c)

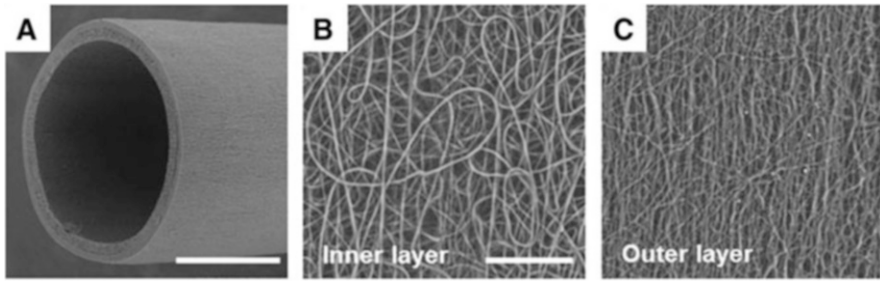


Fig. 4 (a) SEM image of bilayered electrospun vascular graft; *scale bar* = 500 μm . (b) PLLA microfibrils on the inner surface and (c) PLCG + PCL nanofibers on the outer surface of the graft; *scale bar* = 50 μm . Picture obtained from [104]

approach to the fabrication of tubular scaffolds of any diameter required for vascular conduit specification [105]. The fibrous scaffolds obtained generally have highly porous structures and good mechanical properties, suitable for vascular applications. In efforts to produce blood vessels by means of TE, PLGA has been electrospun into tubular scaffolds. A blend of PLGA, PCL, and elastin, in addition to heparin and vascular endothelial growth factor, was used to fabricate a scaffold by electrospinning. In vivo results showed that the scaffolds promoted the recovery of damaged vessels and enhanced cell attachment and proliferation [106].

Li et al. [104, 107, 108] seeded bone marrow MSCs onto modified nanofibrous PLLA scaffolds (see Fig. 4). The scaffolds showed reduced in vivo thrombotic response as compared to unseeded scaffolds. Kurobe et al. [109] fabricated small diameter TEVGs (<6 mm) using electrospun PLA scaffolds for implantation in mice. Significant increase in expressions of smooth muscle cell (SMC) markers, collagen I, and collagen III with excellent overall patency rate and tissue remodeling with autologous cells were seen after 12 months. Mooney et al. [110] fabricated TEVGs by seeding SMCs onto PLLA- and PGLA-coated PGA tubular scaffolds. The PLLA-coated tubular scaffolds were implanted in rats the scaffolds maintained their tubular structures during fibrovascular tissue ingrowth.

PLA–PCL copolymers have also been extensively used by several research groups [30, 111, 112]. Patterson et al. [112] fabricated TEVG utilizing bone-marrow mononuclear cells (BM-MNCs) seeded onto PLA–PCL copolymers [102, 113]. Initially, they seeded mixed cells obtained from femoral veins onto tube-shaped biodegradable scaffolds composed of 50:50 copolymer of PLA–PCL, reinforced with nonwoven PGA (PLA–PCL/PGA) to fabricate inferior vena cava (IVC) [114]. They subsequently investigated the use of scaffolds consisting of poly (chitosan-*g*-PLA)/PGA and BM-MNCs as a cell source for TEVGs [115]. The BM-MNCs were seeded onto the scaffold and cultured before implantation as interposition grafts replacing the intrathoracic IVC in an adult beagle model, with harvesting over a 2-year period. The TEVGs showed no evidence of thrombosis, stenosis, or aneurysm formation.

Following these results, the investigators adapted this approach to fabricate TEVGs for clinical use, employing slower degrading scaffolds than the original PGA scaffolds. In these studies, PLA–PCL/PLA scaffolds were seeded with BM-MNCs and cultured *in vitro* before being implanted in young patients aged between 1 and 24 years [115–117]. Late-term follow-up analysis showed that the implanted TEVGs remained patent with no evidence of rupture, aneurysm dilatation, or calcification. These studies illustrate the importance and advantage of PLA-based polymers in the field of TEVG.

Niklason et al. [32, 118] prepared tissue-engineered small-diameter vascular grafts using a bioreactor system that applies mechanical stimulation. PLGA/PGA scaffolds were seeded with bovine SMCs and ECs in the bioreactor system under physiologically relevant strain and pulsatile flow. Grafts showed the formation of an ECM with architecture and compliance comparable to the natural vasculature. Mechanical analysis of these grafts showed that the vessel strength increased when mechanical stimulation was applied compared with vessels produced under static culture. *In vivo* investigations revealed that one of these engineered vessels remained patent, without detectable stenosis or dilation, for up to a month when implanted in Yucatan minipig as saphenous vein grafts [119].

Traditional TE approaches involve long production times and a risk of infection or mismatch, which are disadvantages compared with the production of off-the-shelf vascular grafts. The utilization of acellular scaffolds that are patient-specific offers an alternative and faster approach to the production of vascular grafts in which cell-free scaffolds are implanted into the affected area, allowing *in vivo* tissue regeneration. This approach is particularly important in tissue replacement or repair of defective tissue in children, as these treatments require multiple interventions to replace the implanted device/tissue as the child matures. In regenerative tissue, the newly formed tissue matures spontaneously, similar to natural tissue.

The use of PLA-based scaffolds in a regenerative medicine approach to TEVGs, where TEVGs were produced by implanting acellular scaffolds, has also been followed [120]. In an *in vivo* study [103], scaffolds consisting of either PGA, PLA–PCL, or PGA–PCL implanted in dogs as a pulmonary artery replacement exhibited patency for up to 12 months. Examination of the explants revealed the formation of SMC and EC layers with ECM content similar to that found in natural tissues.

The use of PLA-based polymers to fabricate scaffolds suitable for TEVG has been explored with some positive results, including encouraging clinical application. The lack of cell recognition sites as well as scaffold hydrophobicity, limit the success of the approach. However, these initial positive results indicate promising findings that could lead to more success in this field.

3.2.3 Tissue-Engineered Cardiac Patches

Myocardial infarction (heart attack) is caused by ischemia (lack of blood flow) that results in irreversible damage to the heart muscle and fibrous scar formation that can eventually lead to heart failure. Ideally, a heart transplant is the treatment of choice to replace the damaged heart; however, due to low organ-donor availability,

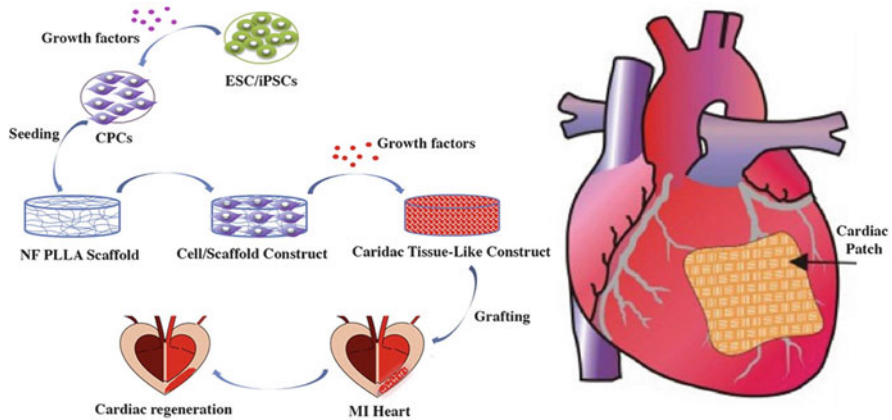


Fig. 5 Illustration of tissue engineered heart patch. Adapted from [121, 122]

high costs of surgery, and the risk of rejection complications, alternative treatments are required. Two approaches have been used in the treatment of heart failure, cell therapy and tissue-engineered heart constructs. In the cell therapy approach, isolated cell types are implanted at the affected area to regenerate the damaged tissue. In the TE approach, a cell-seeded scaffold (prepared in vitro) is implanted at the affected area to replace the damaged tissue, as illustrated in Fig. 5 [121–123].

One of the major challenges in tissue-engineered heart patches, and TE in general, is the design and fabrication of tissue-like scaffolds capable of supporting cell activities. The scaffolds should display mechanical and functional properties similar to native cardiac tissues, such as coherent contractility and low diastolic tension. Fabricating such scaffolds requires biocompatible materials with suitable and tunable mechanical properties. PLA-based scaffolds have been used in several studies to fabricate a construct with mechanical properties suitable for cardiac TE [124, 125].

PLGA scaffolds with different PLLA contents have been used to investigate rat cardiomyocyte (CM) cell attachment and proliferation behavior. In vitro studies revealed that CM cells had higher activity on scaffolds with high PLLA content than on the other scaffolds considered. This was attributed to the hydrophobicity of PLLA [126]. These studies also demonstrated that CM cells seeded on electrospun PLLA scaffolds developed mature contractile machinery (sarcomeres, as indicated by optical imaging using voltage-sensitive dye) [126]. Furthermore, Simon-Yarza et al. [127] implanted PLGA-based scaffolds containing a cardiovascular growth factor, neuregulin-1, into a rat model of myocardial ischemia. Histological analysis revealed the presence of an inflammatory response and an increase in the M2:M1 macrophage ratio, indicating the induction of constructive tissue remodeling.

Several other studies have explored the use of PLGA scaffolds to fabricate TE cardiac tissue [128–132]. Yu et al. utilized the electrospinning technique to fabricate peptide-loaded PLGA scaffolds to investigate the in vitro behavior of rat CM cells [130]. Two adhesive peptides, *N*-acetyl-GRGDSPGYG (RGD) and *N*-acetyl-GYIGSRGYG (YIGSR), covalently conjugated to poly-L-lysine, were incorporated

into fibrous PLGA scaffolds through solution mixing before electrospinning. The results suggested that YIGSR-incorporated PLGA scaffolds were better candidates for the formation of cardiac patches because cells cultured on these scaffolds showed physiological-like morphology.

PLA-based scaffolds have also been used in TE of cardiac patches to stimulate revascularization and preserve the left ventricular (LV) function [133]. In a study carried out by Kellar et al., knitted vicrylic meshes (PGA-to-PLA ratio of 90:10) were used to fabricate heart patches via seeding with human dermal fibroblast cells. Following cell culture, the patches were implanted in mice with induced heart infarction. Results showed that the use of engineered patches improved the LV function and attenuated further loss [134]. Ramakrishna and coworkers [135] investigated the differentiation behavior of pluripotent embryonic stem cells (ESCs) seeded on electrospun PLGA and PLGA/collagen scaffolds. Results showed that ESCs and PLGA/collagen were comparable with the PLGA scaffolds.

In another study, Prabhakaran et al. [136] used electrospun scaffolds consisting of poly(1,8-octanediol-*co*-citrate) (POC) and PLLA-PCL to fabricate scaffolds suitable for cardiac TE. They found that scaffolds of POC and PLLA-PCL (40:60) have mechanical properties similar to native cardiac tissue. The proliferation in vitro experiments also showed, with increasing POC content in the scaffolds, an increase in the proliferation of cardiac rat myoblast cells from days 2 to 8. Bhaarithy et al. [137] fabricated PLA-PCL-based scaffolds through electrospinning with silk fibroin and aloe vera to improve cell functionality. These scaffolds exhibited elasticity and mechanical properties comparable to myocardium, which enhanced cell activities (e.g., adhesion, proliferation, and morphology).

Ozawa et al. [138] carried out a study in which PLA-reinforced PCL-PLA sponges were seeded with SMCs and cultured to generate patches. These patches were then implanted in rats to replace a surgically induced defect in the right ventricular outflow tract. Histological examination showed that the PCL-PLA scaffolds were replaced by more SMCs and more elastin-rich ECMs compared with patches made of gelatin gel or PGA. Results of the study indicated that the use of these PLA-based scaffolds permits the construction of autologous patches to repair congenital heart defects.

The beating action of the heart is a result of synchronous contractile activity of the cardiomyocytes through continuous electrical signals. One of the major challenges in cardiac TE using biological or synthetic scaffolds is achieving synchronous contractility of the engineered patches. In an attempt to overcome these challenges, researchers have used various techniques, including the addition of inorganic materials such as carbon nanotubes (CNTs) [139], gold, and electroactive polymers (e.g., polypyrrole; PPy) [140, 141], among other techniques [139, 142–146]. In this regard, Webster et al. [147, 148] investigated the viability of cardiac tissue cell functions, including cardiomyocytes and neurons, seeded on conductive scaffolds made of PLGA with embedded CNTs. Results showed that the conductivity of these scaffolds increased with increasing CNT content. Scaffolds of PLGA and CNTs (50:50) exhibited significantly higher adsorption of specific proteins (fibronectin and vitronectin), which promotes the adhesion and proliferation of CM

cells, compared to pure PLGA scaffolds. Mooney et al. [149] also used PLA/CNT scaffolds to investigate MSC differentiation. It was found that these scaffolds provide a cardiomimetic cue that directs MSC differentiation into cardiomyocyte cells. In addition, the cells also adopted elongated morphology and reoriented perpendicularly to the direction of the current after stimulation using an electrophysiological bioreactor.

Another commonly used method to enhance conductivity is the incorporation of conductive polymers such as PPy or polyaniline (PANI) [150–152]. Hsiao et al. [153] used PLGA/PANI fibrous scaffolds to enhance the attachment of CM cells. Hydrochloric acid was used to dope PANi to induce positive charges on the scaffolds, which attract the negatively charged adhesive proteins fibronectin and laminin, and hence improve CM cell attachment on the scaffolds. Jin et al. [154] used PPy to enhance CM cell proliferation through surface modification of PLLA fibrous scaffolds. In this study, pyrrole was polymerized on the surface of electrospun PPLA fibers, resulting in scaffolds with a 3D interconnected pore structure. In vitro investigations using CM cells showed that these scaffolds provided suitable 3D micro-environments for the proliferation of CM cells, as indicated by the increase in cell proliferation rate. Results were better than with PPy mesh scaffolds.

Although further investigations into the use of such scaffolds is required, there are already indications that PLA-based polymers provide promising scaffolds that can stimulate the growth and activity of cardiomyocytes and potentially imitate the contraction of normal heart tissue [147, 148, 155].

4 Market Status

Economic and technological developments and growing environmental concerns have driven considerable scientific and engineering efforts into the utilization of biosourced polymers to replace petroleum-based polymers [156–158]. With increasing worldwide consciousness of environmental protection, the use of biobased and ecofriendly polymers, such as PLA and starch, has become more desirable over the last two decades. The growing interest in biobased polymers can be seen by the steadily growing production capacity of these polymers; global production is expected to increase from ~0.7 million tons in 2014 to 1.2 million tons in 2019 [159]. Of the biobased polymers, PLA represents an ideal biosourced polymer, with its low energy consumption production and excellent properties that have attracted great attention in applications such as packaging, textiles, construction, and low volume/high value medical applications [158].

In 2014, the global PLA market, by application, was valued at ~\$300 million, which is projected to reach \$850 million at a compound annual growth rate of 22.8%

over the period 2014–2019. Although the packaging application is still the largest market segment of PLA, ongoing extensive research in the biomedical field is expected to increase the demand for PLA-based polymers [158]. Biomedical application of PLA-based polymers is still a relatively new targeted industry; it requires high value and low volume medical grade PLA. Although the application of PLA-based polymers represents a small fraction of the overall PLA raw materials market, the real contribution of PLA is seen in its high value products. Generally, medical grade PLA polymers command prices that are orders of magnitude higher than polymers used in other consumer devices because of the extensive synthetic and purification processes involved. In other words, the small amounts of PLA used as biomaterials do not accurately reflect the impact that PLA has in medical and, specifically, cardiovascular applications. An example of a high value/low volume PLA application are BVS coronary stents; DES/BVS stents, which contain a very small amount of PLA-based polymer, can sell for thousands of US dollars [160]. The current value of the BVS market, with only a few approved products, was valued at \$18 million in 2015. However, due to the efficiency and advantages of BVSs, with the addition of almost-approved products, the market is expected to grow and reach \$1.7 billion by 2024 as the market progresses at a CAGR of 30.1% [161].

5 Conclusions

Poly(lactic acid) is an ideal example of a biocompatible and biodegradable polymer with excellent properties, indicating a promising future for applications. The use of PLA in the medical field is rapidly expanding because of its biocompatibility, availability, processability and, most importantly, regulatory approval by the FDA. The ability to modify PLA through copolymerizing or blending represents another advantage that extends PLA application. PLA has already made a significant contribution to the development of therapeutic procedures to overcome various diseases. In the cardiovascular field, for example, PLA-based polymers have made the most clinical impact in the treatment of coronary diseases through drug-eluting and bioresorbable vascular stents, for which it is well suited. Other exciting cardiovascular applications of PLA-based polymers include vascular grafts and heart patches. Furthermore, there is large growth potential for the use of this family of polymers in the myriad of tissue engineering applications currently under development.

Acknowledgements The authors wish to thank the National Research Foundation of South Africa Incentive Program for Rated Researchers (CPRR) and the University of Cape Town Faculty of Health Sciences Postdoctoral Fellowship for funding and support.

Potential Conflict of Interest None.

References

1. Williams D (1999) Bioinertness: an outdated principle. In: Zilla P, Greisler HP (eds) *Tissue engineering of vascular prosthetic grafts*. RG Landes, Austin, pp 459–462
2. Zilla P, Brink J, Human P, Bezuidenhout D (2008) Prosthetic heart valves: catering for the few. *Biomaterials* 29(4):385–406
3. Zilla P, Bezuidenhout D, Human P (2007) Prosthetic vascular grafts: wrong models, wrong questions and no healing. *Biomaterials* 28(34):5009–5027
4. van der Sijde JN, Regar E (2015) Stent platforms anno 2015: is there still a place for bare metal stents at the front line? *Neth Hear J* 23(2):122–123
5. Samson RH, Morales R, Showalter DP, Lepore Jr MR, Nair DG (2016) Heparin-bonded expanded polytetrafluoroethylene femoropopliteal bypass grafts outperform expanded polytetrafluoroethylene grafts without heparin in a long-term comparison. *J Vasc Surg* 64(3):638–647
6. Reinthaler M, Jung F, Landmesser U, Lendlein A (2016) Trend to move from permanent metals to degradable, multifunctional polymer or metallic implants in the example of coronary stents. *Expert Rev Med Devices* 13(11):1001–1003
7. Frey BM, Zeisberger SM, Hoerstrup SP (2016) Tissue engineering and regenerative medicine – new initiatives for individual treatment offers. *Transfus Med Hemother* 43(5):318–319
8. Asti A, Gioglio L (2014) Natural and synthetic biodegradable polymers: different scaffolds for cell expansion and tissue formation. *Int J Artif Organs* 37:187–274
9. Amoabediny G, Salehi-Nik N, Heli B (2011) The role of biodegradable engineered scaffold in tissue engineering. In: Pignatello R (ed) *Biomaterials science and engineering*. InTech, Shanghai, pp 153–172
10. Dhandayuthapani B, Yoshida Y, Maekawa T, Sakthi Kumar D (2011) Polymeric scaffolds in tissue engineering application: a review. *International Journal of Polymer Science* 2011:290602
11. Treiser M, Abramson S, Langer R, Kohn J (2013) Degradable and resorbable biomaterials. In: Ratner ASH BD, Schoen FJ, Lemons JE (eds) *Biomaterials science* 3rd edn. Elsevier, London
12. Ulery BD, Nair LS, Laurencin CT (2011) Biomedical applications of biodegradable polymers. *J Polym Sci B Polym Phys* 49(12):832–864
13. Lim LT, Auras R, Rubino M (2008) Processing technologies for poly(lactic acid). *Prog Polym Sci* 33(8):820–852
14. Datta R, Henry M (2006) Lactic acid: recent advances in products, processes and technologies – a review. *J Chem Technol Biotechnol* 81(7):1119–1129
15. Puaux J-P, Banu I, Nagy I, Bozga G (2007) A study of L-lactide ring-opening polymerization kinetics. *Macromol Symp* 259(1):318–326
16. Masutani K, Kimura Y (2015) PLA synthesis. From the monomer to the polymer. *Poly(lactic acid) science and technology: processing, properties, additives and applications*. Royal Society of Chemistry, Cambridge, pp 1–36
17. Xiao L, Wang B, Yang G, Gauthier M (2012) Poly (lactic acid)-based biomaterials: synthesis, modification and applications. InTech
18. Tian H, Tang Z, Zhuang X, Chen X, Jing X (2012) Biodegradable synthetic polymers: preparation, functionalization and biomedical application. *Prog Polym Sci* 37(2):237–280
19. Deng C, Tian H, Zhang P, Sun J, Chen X, Jing X (2006) Synthesis and characterization of RGD peptide grafted poly(ethylene glycol)-b-poly(l-lactide)-b-poly(l-glutamic acid) triblock copolymer. *Biomacromolecules* 7(2):590–596
20. Wang S, Cui W, Bei J (2005) Bulk and surface modifications of polylactide. *Anal Bioanal Chem* 381(3):547–556
21. Manavitehrani I, Fathi A, Badr H, Daly S, Negahi Shirazi A, Dehghani F (2016) Biomedical applications of biodegradable polyesters. *Polymers* 8(1):20

22. Makadia HK, Siegel SJ (2011) Poly lactic-co-glycolic acid (PLGA) as biodegradable controlled drug delivery carrier. *Polymers* 3(3):1377–1397
23. D'Souza S, Faraj J, Dorati R, DeLuca P (2016) Enhanced degradation of lactide-co-glycolide polymer with basic nucleophilic drugs. *Adv Pharm* 2015:10
24. Dänmark S, Finne-Wistrand A, Schander K, Hakkarainen M, Arvidson K, Mustafa K, et al. (2011) In vitro and in vivo degradation profile of aliphatic polyesters subjected to electron beam sterilization. *Acta Biomater* 7(5):2035–2046
25. Ramot Y, Haim-Zada M, Domb AJ, Nyska A (2016) Biocompatibility and safety of PLA and its copolymers. *Adv Drug Deliv Rev* 107:153–162
26. Saini P, Arora M, Kumar MNVR (2016) Poly(lactic acid) blends in biomedical applications. *Adv Drug Deliv Rev* 107:47–59
27. Ratner BD, Hoffman AS, Schoen FJ, Lemons JE (1996) *Biomaterial Science* 3rd edn. Academic Press, Boston
28. Lopes MS, Jardini AL, Filho RM (2012) Poly (lactic acid) production for tissue engineering applications. *Proc Eng* 42:1402–1413
29. Subramanian A, Krishnan UM, Sethuraman S (2009) Development of biomaterial scaffold for nerve tissue engineering: biomaterial mediated neural regeneration. *J Biomed Sci* 16 (1):108–108
30. Chung S, Ingle NP, Montero GA, Kim SH, King MW (2010) Bioresorbable elastomeric vascular tissue engineering scaffolds via melt spinning and electrospinning. *Acta Biomater* 6 (6):1958–1967
31. Ravi S, Chaikof EL (2010) Biomaterials for vascular tissue engineering. *Regen Med* 5(1):107
32. Niklason LE, Langer RS (1997) Advances in tissue engineering of blood vessels and other tissues. *Transpl Immunol* 5(4):303–306
33. Azzalini L, L'Allier PL, Tanguay J-F (2016) Bioresorbable scaffolds: the revolution in coronary stenting? *Aims Med Sci* 3(1):126–146
34. Baine KR, Norris CM, Graham MM, Ghali WA, Knudtson ML, Welsh RC (2008) Clinical in-stent restenosis with bare metal stents: is it truly a benign phenomenon? *Int J Cardiol* 128 (3):378–382
35. Mani G, Feldman MD, Patel D, Agrawal CM (2007) Coronary stents: a materials perspective. *Biomaterials* 28(9):1689–1710
36. Serruys PW, Kutryk MJB, Ong ATL (2006) Coronary-artery stents. *N Engl J Med* 354 (5):483–495
37. Lincoff AM, Furst JG, Ellis SG, Tuch RJ, Topol EJ (1997) Sustained local delivery of dexamethasone by a novel intravascular eluting stent to prevent restenosis in the porcine coronary injury model. *J Am Coll Cardiol* 29(4):808–816
38. Ernst A, Bulum J (2014) New generations of drug-eluting stents – a brief review. *EMJ Int Cardiol* 1:100–106
39. Ho M-Y, Chen C-C, Wang C-Y, Chang S-H, Hsieh M-J, Lee C-H, et al. (2016) The development of coronary artery stents: from bare-metal to bio-resorbable types. *Metals* 6 (7):168
40. Tenekecioglu E, Farooq V, Bourantas CV, Silva RC, Onuma Y, Yilmaz M, et al. (2016) Bioresorbable scaffolds: a new paradigm in percutaneous coronary intervention. *BMC Cardiovasc Disord* 16(1):38
41. Iqbal J, Onuma Y, Ormiston J, Abizaid A, Waksman R, Serruys P (2014) Bioresorbable scaffolds: rationale, current status, challenges, and future. *Eur Heart J* 35(12):765–776
42. Onuma Y, Ormiston J, Serruys PW (2011) Bioresorbable scaffold technologies. *Circ J* 75 (3):509–520
43. Campos CM, Ishibashi Y, Eggermont J, Nakatani S, Cho YK, Dijkstra J, et al. (2015) Echogenicity as a surrogate for bioresorbable everolimus-eluting scaffold degradation: analysis at 1-, 3-, 6-, 12- 18-, 24-, 30-, 36- and 42-month follow-up in a porcine model. *Int J Cardiovasc Imaging* 31(3):471–482

44. Vorpahl M, Nakano M, Perkins LEL, Otsuka F, Jones RL, Acampado E, et al. (2014) Vascular healing and integration of a fully bioresorbable everolimus-eluting scaffold in a rabbit iliac arterial model. *EuroIntervention* 10(7):833–841
45. Stack RS, Califf RM, Phillips HR, Pryor DB, Quigley PJ, Bauman RP, et al. (1988) Interventional cardiac catheterization at Duke Medical Center. *Am J Cardiol* 62(10 Pt 2):3f–24f
46. Tamai H, Igaki K, Kyo E, Kosuga K, Kawashima A, Matsui S, et al. (2000) Initial and 6-month results of biodegradable poly-l-lactic acid coronary stents in humans. *Circulation* 102(4):399
47. Muramatsu T, Onuma Y, Zhang Y-J, Bourantas CV, Kharlamov A, Diletti R, et al. (2013) Progress in treatment by percutaneous coronary intervention: the stent of the future. *Rev Esp Cardiol* 66(06):483–496. English Edition
48. Yamawaki T, Shimokawa H, Kozai T, Miyata K, Higo T, Tanaka E, et al. (1998) Intramural delivery of a specific tyrosine kinase inhibitor with biodegradable stent suppresses the restenotic changes of the coronary artery in pigs in vivo. *J Am Coll Cardiol* 32(3):780–786
49. Wittchow E, Adden N, Riedmüller J, Savard C, Waksman R, Braune M (2013) Bioresorbable drug-eluting magnesium-alloy scaffold: design and feasibility in a porcine coronary model. *EuroIntervention* 8(12):1441–1450
50. Ferdous J, Kolachalama VB, Shazly T (2013) Impact of polymer structure and composition on fully resorbable endovascular scaffold performance. *Acta Biomater* 9(4):6052–6061
51. Abbott (2016) Abbott's Absorb™ bioresorbable stent approved as the first fully dissolving heart stent in Japan. <http://www.abbott.com/>
52. Chen G, Ushida T, Tateishi T (2002) Scaffold design for tissue engineering. *Macromol Biosci* 2(2):67–77
53. Nair LS, Laurencin CT (2007) Biodegradable polymers as biomaterials. *Prog Polym Sci* 32(8–9):762–798
54. Peter SJ, Miller MJ, Yasko AW, Yaszemski MJ, Mikos AG (1998) Polymer concepts in tissue engineering. *J Biomed Mater Res* 43(4):422–427
55. Loh QL, Choong C (2013) Three-dimensional scaffolds for tissue engineering applications: role of porosity and pore size. *Tissue Eng Part B Rev* 19(6):485–502
56. Chen G, Ushida T, Tateishi T (2001) Development of biodegradable porous scaffolds for tissue engineering. *Mater Sci Eng C* 17(1–2):63–69
57. Pan Z, Ding J (2012) Poly(lactide-co-glycolide) porous scaffolds for tissue engineering and regenerative medicine. *Interface Focus* 2(3):366–377
58. Villarreal-Gomez LJ, Cornejo-Bravo JM, Vera-Graziano R, Grande D (2016) Electrospinning as a powerful technique for biomedical applications: a critically selected survey. *J Biomater Sci Polym Ed* 27(2):157–176
59. An J, Teoh JEM, Suntornmond R, Chua CK (2015) Design and 3D printing of scaffolds and tissues. *Engineering* 1(2):261–268
60. Do A-V, Khorsand B, Geary SM, Salem AK (2015) 3D printing of scaffolds for tissue regeneration applications. *Adv Healthc Mater* 4(12):1742–1762
61. Sultana N, Hassan MI, Lim MM (2015) Scaffold fabrication protocols. *Composite synthetic scaffolds for tissue engineering and regenerative medicine*. Springer, Cham, pp 13–24
62. Aishwarya V, D S (2016) A review on scaffolds used in tissue engineering and various fabrication techniques. *Int J Res Biosci* 5:1–9
63. Chan BP, Leong KW (2008) Scaffolding in tissue engineering: general approaches and tissue-specific considerations. *Eur Spine J* 17(Suppl 4):467–479
64. Malafaya PB, Silva GA, Reis RL (2007) Natural-origin polymers as carriers and scaffolds for biomolecules and cell delivery in tissue engineering applications. *Adv Drug Deliv Rev* 59(4–5):207–233
65. Ivanova EP, Bazaka K, Crawford RJ (2014) Natural polymer biomaterials: advanced applications. In: Ivanova EP, Bazaka K, Crawford RJ (eds) *New functional biomaterials for medicine and healthcare* 1st edn. Woodhead Publishing, Oxford

66. Place ES, George JH, Williams CK, Stevens MM (2009) Synthetic polymer scaffolds for tissue engineering. *Chem Soc Rev* 38(4):1139–1151
67. O'Brien FJ (2011) Biomaterials & scaffolds for tissue engineering. *Mater Today* 14(3):88–95
68. Guo B, Ma PX (2014) Synthetic biodegradable functional polymers for tissue engineering: a brief review. *SCIENCE CHINA Chem* 57(4):490–500
69. Gilbert TW, Sellaro TL, Badylak SF (2006) Decellularization of tissues and organs. *Biomaterials* 27(19):3675–3683
70. Badylak SF, Taylor D, Uygun K (2011) Whole-organ tissue engineering: decellularization and recellularization of three-dimensional matrix scaffolds. *Annu Rev Biomed Eng* 13(1):27–53
71. Kim K, Evans G (2005) Tissue engineering: the future of stem cells. *Top Tissue Eng* 2:1–21
72. Perán M, García M, Lopez-Ruiz E, Jiménez G, Marchal J (2013) How can nanotechnology help to repair the body? Advances in cardiac, skin, bone, cartilage and nerve tissue regeneration. *Materials* 6(4):1333
73. Demirbag B, Huri PY, Kose GT, Buyuksungur A, Hasirci V (2011) Advanced cell therapies with and without scaffolds. *Biotechnol J* 6(12):1437–1453
74. Sutherland FWH, Perry TE, Yu Y, Sherwood MC, Rabkin E, Masuda Y, et al. (2005) From stem cells to viable autologous semilunar heart valve. *Circulation* 111(21):2783–2791
75. Cheung DY, Duan B, Butcher JT (2015) Current progress in tissue engineering of heart valves: multiscale problems, multiscale solutions. *Expert Opin Biol Ther* 15(8):1155–1172
76. Shinoka T, Breuer CK, Tanel RE, Zund G, Miura T, Ma PX, et al. (1995) Tissue engineering heart valves: valve leaflet replacement study in a lamb model. *Ann Thorac Surg* 60(6 Suppl):S513–S516
77. Jana S, Tefft BJ, Spoon DB, Simari RD (2014) Scaffolds for tissue engineering of cardiac valves. *Acta Biomater* 10(7):2877–2893
78. Fang NT, Xie SZ, Wang SM, Gao HY, Wu CG, Pan LF (2007) Construction of tissue-engineered heart valves by using decellularized scaffolds and endothelial progenitor cells. *Chin Med J* 120(8):696–702
79. Bechtel JF, Stierle U, Sievers HH (2008) Fifty-two months' mean follow up of decellularized SynerGraft-treated pulmonary valve allografts. *J Heart Valve Dis* 17(1):98–104. Discussion 104
80. Rothamel D, Schwarz F, Sager M, Herten M, Sculean A, Becker J (2005) Biodegradation of differently cross-linked collagen membranes: an experimental study in the rat. *Clin Oral Implants Res* 16(3):369–378
81. Taylor PM, Allen SP, Dreger SA, Yacoub MH (2002) Human cardiac valve interstitial cells in collagen sponge: a biological three-dimensional matrix for tissue engineering. *J Heart Valve Dis* 11(3):298–306. Discussion 306–297
82. Sodian R, Hoerstrup SP, Sperling JS, Daebritz S, Martin DP, Moran AM, et al. (2000) Early in vivo experience with tissue-engineered trileaflet heart valves. *Circulation* 102(Suppl 3):Iii-22–Iii-29
83. Fong P, Shin'oka T, Lopez-Soler RI, Breuer C (2006) The use of polymer based scaffolds in tissue-engineered heart valves. *Prog Pediatr Cardiol* 21(2):193–199
84. Morsi YS (2014) Bioengineering strategies for polymeric scaffold for tissue engineering an aortic heart valve: an update. *Int J Artif Organs* 37(9):651
85. Liu C, Xia Z, Czernuszka JT (2007) Design and development of three-dimensional scaffolds for tissue engineering. *Chem Eng Res Des* 85(7):1051–1064
86. Stock UA, Mayer Jr JE (2001) Tissue engineering of cardiac valves on the basis of PGA/PLA co-polymers. *J Long-Term Eff Med Implants* 11(3–4):249–260
87. Zund G, Breuer CK, Shinoka T, Ma PX, Langer R, Mayer JE, et al. (1997) The in vitro construction of a tissue engineered bioprosthetic heart valve. *Eur J Cardiothorac Surg* 11(3):493–497

88. Sodian R, Sperling JS, Martin DP, Stock U, Mayer Jr JE, Vacanti JP (1999) Tissue engineering of a trileaflet heart valve-early in vitro experiences with a combined polymer. *Tissue Eng* 5(5):489–494
89. Gottlieb D, Kunal T, Emani S, Aikawa E, Brown DW, Powell AJ, et al. (2010) In vivo monitoring of function of autologous engineered pulmonary valve. *J Thorac Cardiovasc Surg* 139(3):723–731
90. Hinderer S, Seifert J, Votteler M, Shen N, Rheinlaender J, Schäffer TE, et al. (2014) Engineering of a bio-functionalized hybrid off-the-shelf heart valve. *Biomaterials* 35(7):2130–2139
91. Svenja H, Nian S, Léa-Jeanne R, Jan H, Dieter PR, Sara YB, et al. (2015) In vitro elastogenesis: instructing human vascular smooth muscle cells to generate an elastic fiber-containing extracellular matrix scaffold. *Biomed Mater* 10(3):034102
92. Lueders C, Jastram B, Hetzer R, Schwandt H (2014) Rapid manufacturing techniques for the tissue engineering of human heart valves. *Eur J Cardiothorac Surg* 46(4):593–601
93. Park H, Radisic M, Lim JO, Chang BH, Vunjak-Novakovic G (2005) A novel composite scaffold for cardiac tissue engineering. *In Vitro Cell Dev Biol Anim* 41(7):188–196
94. Nuttelman CR, Henry SM, Anseth KS (2002) Synthesis and characterization of photocrosslinkable, degradable poly(vinyl alcohol)-based tissue engineering scaffolds. *Biomaterials* 23(17):3617–3626
95. Verma S, Szmítko PE, Weisel RD, Bonneau D, Latter D, Errett L, et al. (2004) Should radial arteries be used routinely for coronary artery bypass grafting? *Circulation* 110(5):e40–e46
96. Kannan RY, Salacinski HJ, Butler PE, Hamilton G, Seifalian AM (2005) Current status of prosthetic bypass grafts: a review. *J Biomed Mater Res B Appl Biomater* 74B(1):570–581
97. Weinberg C, Bell E (1986) A blood vessel model constructed from collagen and cultured vascular cells. *Science* 231(4736):397–400
98. In Jeong S, Kim SY, Cho SK, Chong MS, Kim KS, Kim H, et al. (2007) Tissue-engineered vascular grafts composed of marine collagen and PLGA fibers using pulsatile perfusion bioreactors. *Biomaterials* 28(6):1115–1122
99. Stegemann JP, Kaszuba SN, Rowe SL (2007) Review: advances in vascular tissue engineering using protein-based biomaterials. *Tissue Eng* 13(11):2601–2613
100. Kim MJ, Kim J-H, Yi G, Lim S-H, Hong YS, Chung DJ (2008) In vitro and in vivo application of PLGA nanofiber for artificial blood vessel. *Macromol Res* 16(4):345–352
101. Koch S, Flanagan TC, Sachweh JS, Tanius F, Schnoering H, Deichmann T, et al. (2010) Fibrin-poly(lactide)-based tissue-engineered vascular graft in the arterial circulation. *Biomaterials* 31(17):4731–4739
102. Roh JD, Nelson GN, Brennan MP, Mirensky TL, Yi T, Hazlett TF, et al. (2008) Small-diameter biodegradable scaffolds for functional vascular tissue engineering in the mouse model. *Biomaterials* 29(10):1454–1463
103. Yokota T, Ichikawa H, Matsumiya G, Kuratani T, Sakaguchi T, Iwai S, et al. (2008) In situ tissue regeneration using a novel tissue-engineered, small-caliber vascular graft without cell seeding. *J Thorac Cardiovasc Surg* 136(4):900–907
104. Janairo RRR, Zhu Y, Chen T, Li S (2014) Mucin covalently bonded to microfibers improves the patency of vascular grafts. *Tissue Eng Part A* 20(1–2):285–293
105. Zhao W, Li J, Jin K, Liu W, Qiu X, Li C (2016) Fabrication of functional PLGA-based electrospun scaffolds and their applications in biomedical engineering. *Mater Sci Eng C* 59:1181–1194
106. Yeon CJ, Young JK, Ki CS, Ok LJ, Hoon JS (2010) Fabrication and in vivo evaluation of the electrospun small diameter vascular grafts composed of elastin/PLGA/PCL and heparin-VEGF. *J Tissue Eng Regen Med* 7:149–154
107. Hashi CK, Zhu Y, Yang G-Y, Young WL, Hsiao BS, Wang K, et al. (2007) Antithrombotic property of bone marrow mesenchymal stem cells in nanofibrous vascular grafts. *Proc Natl Acad Sci* 104(29):11915–11920

108. Hashi CK, Derugin N, Janairo RRR, Lee R, Schultz D, Lotz J, et al. (2010) Antithrombogenic modification of small-diameter microfibrillar vascular grafts. *Arterioscler Thromb Vasc Biol* 30(8):1621–1627
109. Kurobe H, Maxfield MW, Tara S, Rocco KA, Bagi PS, Yi T, et al. (2015) Development of small diameter nanofiber tissue engineered arterial grafts. *PLoS One* 10(4):e0120328
110. Mooney DJ, Mazzoni CL, Breuer C, McNamara K, Hern D, Vacanti JP, et al. (1996) Stabilized polyglycolic acid fibre-based tubes for tissue engineering. *Biomaterials* 17 (2):115–124
111. Udelsman BV, Khosravi R, Miller KS, Dean EW, Bersi MR, Rocco K, et al. (2014) Characterization of evolving biomechanical properties of tissue engineered vascular grafts in the arterial circulation. *J Biomech* 47(9):2070–2079
112. Patterson JT, Gilliland T, Maxfield MW, Church S, Naito Y, Shinoka T, et al. (2012) Tissue-engineered vascular grafts for use in the treatment of congenital heart disease: from the bench to the clinic and back again. *Regen Med* 7(3):409–419
113. Shin'oka T, Matsumura G, Hibino N, Naito Y, Watanabe M, Konuma T, et al. (2005) Midterm clinical result of tissue-engineered vascular autografts seeded with autologous bone marrow cells. *J Thorac Cardiovasc Surg* 129(6):1330–1338
114. Watanabe M, Shin'oka T, Tohyama S, Hibino N, Konuma T, Matsumura G, et al. (2001) Tissue-engineered vascular autograft: inferior vena cava replacement in a dog model. *Tissue Eng* 7(4):429–439
115. Matsumura G, Miyagawa-Tomita S, Shin'oka T, Ikada Y, Kurosawa H (2003) First evidence that bone marrow cells contribute to the construction of tissue-engineered vascular autografts in vivo. *Circulation* 108(14):1729–1734
116. Shin'oka T, Imai Y, Ikada Y (2001) Transplantation of a tissue-engineered pulmonary artery. *N Engl J Med* 344(7):532–533
117. Naito Y, Imai Y, Shin'oka T, Kashiwagi J, Aoki M, Watanabe M, et al. (2003) Successful clinical application of tissue-engineered graft for extracardiac Fontan operation. *J Thorac Cardiovasc Surg* 125(2):419–420
118. Niklason LE, Gao J, Abbott WM, Hirschi KK, Houser S, Marini R, et al. (1999) Functional arteries grown in vitro. *Science* 284(5413):489–493
119. Niklason LE, Abbott W, Gao J, Klagges B, Hirschi KK, Ulubayram K, et al. (2001) Morphologic and mechanical characteristics of engineered bovine arteries. *J Vasc Surg* 33 (3):628–638
120. Matsumura G, Nitta N, Matsuda S, Sakamoto Y, Isayama N, Yamazaki K, et al. (2012) Long-term results of cell-free biodegradable scaffolds for in situ tissue-engineering vasculature: in a canine inferior vena cava model. *PLoS One* 7(4):e35760
121. Arnal-Pastor M, Chachques JC, Pradas MM, Vallés-Lluch A (2013) Biomaterials for cardiac tissue engineering. In: Andrades JA (ed) *Regenerative medicine and tissue engineering*. InTech, Rijeka
122. Liu Q, Tian S, Zhao C, Chen X, Lei I, Wang Z, et al. (2015) Porous nanofibrous poly(l-lactic acid) scaffolds supporting cardiovascular progenitor cells for cardiac tissue engineering. *Acta Biomater* 26:105–114
123. Amezcua R, Shirolkar A, Frazee C, Stout AD (2016) Nanomaterials for cardiac myocyte tissue engineering. *Nanomaterials* 6(7). doi:10.3390/nano6070133
124. Badrossamay MR, McIlwee HA, Goss JA, Parker KK (2010) Nanofiber assembly by rotary jet-spinning. *Nano Lett* 10(6):2257–2261
125. Kenar H, Kose GT, Toner M, Kaplan DL, Hasirci V (2011) A 3D aligned microfibrillar myocardial tissue construct cultured under transient perfusion. *Biomaterials* 32 (23):5320–5329
126. Zong X, Bien H, Chung C-Y, Yin L, Fang D, Hsiao BS, et al. (2005) Electrospun fine-textured scaffolds for heart tissue constructs. *Biomaterials* 26(26):5330–5338

127. Simon-Yarza T, Rossi A, Heffels KH, Prosper F, Groll J, Blanco-Prieto MJ (2015) Polymeric electrospun scaffolds: neuregulin encapsulation and biocompatibility studies in a model of myocardial ischemia. *Tissue Eng Part A* 21(9–10):1654–1661
128. Khan M, Xu Y, Hua S, Johnson J, Belevych A, Janssen PML, et al. (2015) Evaluation of changes in morphology and function of human induced pluripotent stem cell derived cardiomyocytes (HiPSC-CMs) cultured on an aligned-nanofiber cardiac patch. *PLoS One* 10(5):e0126338
129. Prabhakaran MP, Mobarakeh LG, Kai D, Karbalaie K, Nasr-Esfahani MH, Ramakrishna S (2014) Differentiation of embryonic stem cells to cardiomyocytes on electrospun nanofibrous substrates. *J Biomed Mater Res B Appl Biomater* 102(3):447–454
130. Yu J, Lee A-R, Lin W-H, Lin C-W, Wu Y-K, Tsai W-B (2014) Electrospun PLGA fibers incorporated with functionalized biomolecules for cardiac tissue engineering. *Tissue Eng Part A* 20(13–14):1896–1907
131. Senel-Ayaz HG, Perets A, Govindaraj M, Brookstein D, Lelkes PI (2010) Textile-templated electrospun anisotropic scaffolds for tissue engineering and regenerative medicine. *Conf Proc IEEE Eng Med Biol Soc* 2010: 255–258, doi: 10.1109/IEMBS.2010.5627466
132. Bursac N, Loo Y, Leong K, Tung L (2007) Novel anisotropic engineered cardiac tissues: studies of electrical propagation. *Biochem Biophys Res Commun* 361(4):847–853
133. Kellar RS, Landeen LK, Shepherd BR, Naughton GK, Ratcliffe A, Williams SK (2001) Scaffold-based three-dimensional human fibroblast culture provides a structural matrix that supports angiogenesis in infarcted heart tissue. *Circulation* 104(17):2063–2068
134. Kellar RS, Shepherd BR, Larson DF, Naughton GK, Williams SK (2005) Cardiac patch constructed from human fibroblasts attenuates reduction in cardiac function after acute infarct. *Tissue Eng* 11(11–12):1678–1687
135. Molamma PP, Dan K, Laleh G-M, Seeram R (2011) Electrospun biocomposite nanofibrous patch for cardiac tissue engineering. *Biomed Mater* 6(5):055001
136. Prabhakaran MP, Nair AS, Kai D, Ramakrishna S (2012) Electrospun composite scaffolds containing poly(octanediol-co-citrate) for cardiac tissue engineering. *Biopolymers* 97(7):529–538
137. Bhaarathy V, Venugopal J, Gandhimathi C, Ponpandian N, Mangalaraj D, Ramakrishna S (2014) Biologically improved nanofibrous scaffolds for cardiac tissue engineering. *Mater Sci Eng C* 44:268–277
138. Ozawa T, Mickle DAG, Weisel RD, Koyama N, Ozawa S, Li R-K (2002) Optimal biomaterial for creation of autologous cardiac grafts. *Circulation* 106(12 Suppl 1):I-176–I-182
139. Stout DA, Basu B, Webster TJ (2011) Poly(lactic-co-glycolic acid): carbon nanofiber composites for myocardial tissue engineering applications. *Acta Biomater* 7(8):3101–3112
140. Gelmi A, Zhang J, Cieslar-Pobuda A, Ljunggren MK, Los MJ, Rafat M et al (2015) Electroactive 3D materials for cardiac tissue engineering. *Proc SPIE* 9430:94301T doi:10.1117/12.2084165
141. Gelmi A, Cieslar-Pobuda A, de Muinck E, Los M, Rafat M, Jager EWH (2016) Direct mechanical stimulation of stem cells: a beating electromechanically active scaffold for cardiac tissue engineering. *Adv Healthc Mater* 5(12):1471–1480
142. Dvir T, Timko BP, Brigham MD, Naik SR, Karajanagi SS, Levy O, et al. (2011) Nanowired three-dimensional cardiac patches. *Nat Nanotechnol* 6(11):720–725
143. Stout DA, Yoo J, Santiago-Miranda AN, Webster TJ (2012) Mechanisms of greater cardiomyocyte functions on conductive nanoengineered composites for cardiovascular application. *Int J Nanomedicine* 7:5653–5669
144. Tian B, Liu J, Dvir T, Jin L, Tsui JH, Qing Q, et al. (2012) Macroporous nanowire nanoelectronic scaffolds for synthetic tissues. *Nat Mater* 11(11):986–994
145. Engelmayr GC, Cheng M, Bettinger CJ, Borenstein JT, Langer R, Freed LE (2008) Accordion-like honeycombs for tissue engineering of cardiac anisotropy. *Nat Mater* 7(12):1003–1010

146. Sapir Y, Kryukov O, Cohen S (2011) Integration of multiple cell-matrix interactions into alginate scaffolds for promoting cardiac tissue regeneration. *Biomaterials* 32(7):1838–1847
147. Asiri AM, Marwani HM, Khan SB, Webster TJ (2014) Greater cardiomyocyte density on aligned compared with random carbon nanofibers in polymer composites. *Int J Nanomedicine* 9:5533–5539
148. Asiri AM, Marwani HM, Khan SB, Webster TJ (2015) Understanding greater cardiomyocyte functions on aligned compared to random carbon nanofibers in PLGA. *Int J Nanomedicine* 10:89–96
149. Mooney E, Mackle JN, Blond DJP, O’Cearbhaill E, Shaw G, Blau WJ, et al. (2012) The electrical stimulation of carbon nanotubes to provide a cardiomimetic cue to MSCs. *Biomaterials* 33(26):6132–6139
150. Borriello A, Guarino V, Schiavo L, Alvarez-Perez MA, Ambrosio L (2011) Optimizing PANi doped electroactive substrates as patches for the regeneration of cardiac muscle. *J Mater Sci Mater Med* 22(4):1053–1062
151. Humpolicek P, Kasparkova V, Saha P, Stejskal J (2012) Biocompatibility of polyaniline. *Synth Met* 162(7–8):722–727
152. Kai D, Prabhakaran MP, Jin G, Ramakrishna S (2011) Guided orientation of cardiomyocytes on electrospun aligned nanofibers for cardiac tissue engineering. *J Biomed Mater Res B Appl Biomater* 98B(2):379–386
153. Hsiao C-W, Bai M-Y, Chang Y, Chung M-F, Lee T-Y, Wu C-T, et al. (2013) Electrical coupling of isolated cardiomyocyte clusters grown on aligned conductive nanofibrous meshes for their synchronized beating. *Biomaterials* 34(4):1063–1072
154. Jin L, Wang T, Feng Z-Q, Zhu M, Leach MK, Naim YI, et al. (2012) Fabrication and characterization of a novel fluffy polypyrrole fibrous scaffold designed for 3D cell culture. *J Mater Chem* 22(35):18321–18326
155. Stout DA, Raimondo E, Marostica G, Webster TJ (2014) Growth characteristics of different heart cells on novel nanopatch substrate during electrical stimulation. *Biomed Mater Eng* 24(6):2101–2107
156. Babu RP, O’Connor K, Seeram R (2013) Current progress on bio-based polymers and their future trends. *Prog Biomater* 2(1):8
157. Sangeetha VH, Deka H, Varghese TO, Nayak SK (2016) State of the art and future perspectives of poly(lactic acid) based blends and composites. *Polym Comp* doi:10.1002/pc.23906
158. Jamshidian M, Tehrani EA, Imran M, Jacquot M, Desobry S (2010) Poly-lactic acid: production, applications, nanocomposites, and release studies. *Compr Rev Food Sci Food Saf* 9(5):552–571
159. Prasad E. (2016) Polylactic acid market by application (packaging, agriculture, electronics, textiles, bio-medical). Global opportunity analysis and industry forecast 2014–2020. Allied Market Research, Portland
160. NICE (2016) Absorb bioresorbable vascular scaffold for coronary artery disease. National Institute for Health and Care Excellence (NICE), London [nice.org.uk/guidance/mib84](https://www.nice.org.uk/guidance/mib84)
161. Transparency Market Research (2017) Biodegradable stents market (stent type – coronary artery stent and peripheral artery stents, material – polymer based and metal based, end users – hospitals, cardiac catheterization laboratories, and ambulatory surgery centers) – Global industry analysis, size, share, growth, trends and forecast 2016–2024. Transparency Market Research, Albany

Tailoring Bulk and Surface Composition of Polylactides for Application in Engineering of Skeletal Tissues



Gloria Gallego Ferrer, Andrea Liedmann, Marcus S. Niepel, Zhen-Mei Liu, and Thomas Groth

Abstract Synthetic biodegradable polylactides have been used extensively to fabricate scaffolds for engineering skeletal tissues such as bone and cartilage. This chapter summarizes the application of polylactides in tissue engineering and shows strategies for tailoring its bulk and surface composition for optimized degradation rates, mechanical properties, and bioactivities that cannot be achieved with pure polylactide polymers. Hence, block copolymers and the use of blending as a cost-effective strategy are described here. Furthermore, polymeric networks are shown that are advantageous in porogen-leaching manufacture of scaffolds, in preventing crystallization during degradation, and in allowing the incorporation of hydrophilic chains. In addition, mechanical reinforcement of the polymer is achieved when organic–inorganic composites of polylactides are formed. The last

G.G. Ferrer

Centre for Biomaterials and Tissue Engineering (CBIT), Universitat Politècnica de València, Camino de Vera s/n, 46022 Valencia, Spain

Biomedical Research Networking Center in Bioengineering, Biomaterials and Nanomedicine (CIBER-BBN), Zaragoza, Spain

A. Liedmann

Biomedical Materials Group, Institute of Pharmacy, Martin Luther University Halle-Wittenberg, Heinrich-Damerow-Strasse 4, 06120 Halle (Saale), Germany

M.S. Niepel and T. Groth (✉)

Biomedical Materials Group, Institute of Pharmacy, Martin Luther University Halle-Wittenberg, Heinrich-Damerow-Strasse 4, 06120 Halle (Saale), Germany

Interdisciplinary Center of Materials Science, Martin Luther University Halle-Wittenberg, 06099 Halle (Saale), Germany

e-mail: thomas.groth@pharmazie.uni-halle.de

Z.-M. Liu

Faculty of Dentistry, University of Toronto, Toronto, ON, Canada

part of this chapter focusses on the modification of the surface to tailor the biocompatibility of polylactides only, without changing the bulk properties of the material. Surface modification by wet chemical processes and adsorption of biogenic multilayers of glycosaminoglycans is described that not only significantly improves biocompatibility but may also help to drive differentiation of stem cells into the desired lineage.

Keywords Blending • Bone • Cartilage • Composites • Copolymer • Crosslinking • Polyelectrolyte multilayers • Polylactides • Polymeric networks • Surface modification

Contents

1	Tissue Engineering of Skeletal Tissues	80
2	Advantages and Disadvantages of Using Polylactides in Tissue Engineering	82
3	Tailoring the Bulk Composition of Polylactides	86
3.1	Block Copolymers	87
3.2	Blends	88
3.3	Polymeric Networks	89
3.4	Organic–Inorganic Composites	91
3.5	Commercially Available Products for Skeletal Tissue Engineering	94
4	Surface Modification of Polylactides by Chemical and Physical Methods	95
4.1	Surface Modification of Polylactides	95
4.2	Covalent Activation versus Adsorptive Binding of Polyamines	95
4.3	Physical Surface Modification of PLLA with Polyelectrolyte Multilayers	98
5	Summary and Outlook	100
	References	102

1 Tissue Engineering of Skeletal Tissues

Tissue engineering is an interdisciplinary field that applies the principles of engineering and biomedical sciences to the development of biological substitutes that can restore, maintain, or improve tissue or organ functions that are defective or have been lost as a result of trauma or disease [1]. The rapidly developing field of regenerative medicine requires rational molecular and supramolecular design of temporary scaffold materials for cells in order to control their bioactivity and physical properties [2–4].

The ideal scaffold material is biocompatible, nontoxic to cells or the surrounding tissue, biodegradable, chemically and mechanically stable, and has low immunogenicity [5, 6]. Most biomaterials should be structurally stable for long enough to allow repaired or regenerated tissue to organize into a desired three-dimensional (3D) structure [7, 8]. The material should ideally degrade without any toxic residues remaining [9]. Furthermore, the microstructure and porosity of the material should be controllable, so that biomaterials provide structural support to the surrounding tissue or encourage cell proliferation, spreading, and differentiation [5, 10, 11]. This can be accomplished with techniques that include modifying the material's wetting

properties, charge, pore structure, surface topography, or functionalization of the material surface with extracellular matrix (ECM)-like molecules or therapeutic proteins [12–15]. Ideally, a given biomaterial can be formed or processed into a variety of shapes such as tubes, sheets, meshes, sponges, and foams. In cases in which local delivery of potentially therapeutic molecules is desired, the materials should permit a controlled and sustained delivery of those molecules for the required duration [5, 16].

Tissue engineering of skeletal tissues reveals several challenges, in spite of their relatively simple structures. Skeletal tissues consist of highly organized 3D networks of cells and matrix, giving rise to tissue structures with remarkable mechanical properties. The cells continually remodel the tissue and respond to changes in the physical and mechanical environment of the body. The building of functional tissue addresses very complex biological problems, especially creation of higher order skeletal structures such as the zonal organization of articular cartilage or a complete joint with integrated cartilage and bone tissue. For roles that purely nonbiological prosthetics are incapable of fulfilling, the engineering designs may require control of the spatial organization of multiple cell types in a 3D system that encourages the production of the correct types and amounts of matrix molecules in the appropriate structural framework [17]. Therefore, the next generation of engineered musculoskeletal tissues needs to be more complex and structurally organized to mimic normal tissue structure and function more fully.

For example, slow degradation is required for tissue engineering of the skeletal system, whereas for skin the scaffold does not need to stay in place for longer than 1 month. Different requirements for a scaffold depend on the different biological properties of normal articular tissue. Bone is a self-repairing structural material, but adult articular cartilage contains no blood supply, neural network, or lymphatic drainage and rarely heals, even with continuous passive motion. Therefore, tissue engineering strategies for cartilage attempt to introduce cells to the injury site, with or without a scaffold, to take over the role of ECM production and remodeling. Bone tissue engineering efforts, on the other hand, focus on implantation of biomaterials and factors that augment the natural repair process in larger defects [17]. A considerable challenge in skeletal tissue repair is the fact that the scaffold must be able to withstand physiologic loading until sufficient tissue regeneration occurs. Most soft porous biomaterials such as collagen (COL) are not able to endure fixation with sutures because of their low tearing strength. In such cases, reinforcement (e.g., with resorbable fibers) is required [18].

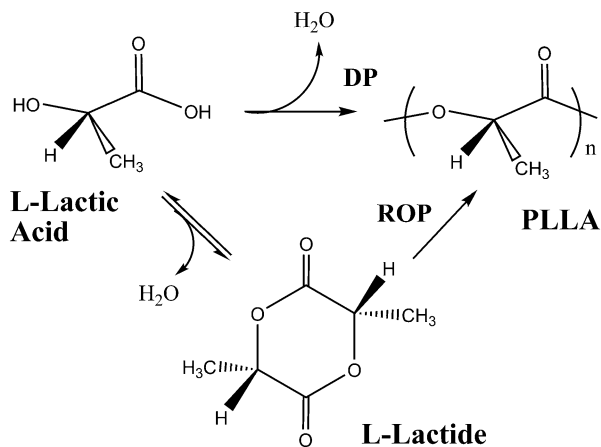
Synthetic biodegradable poly(α -hydroxy ester)s or their copolymers, such as poly(lactic acid) (PLA) have been used extensively to fabricate scaffolds for engineering skeletal tissues such as bone [19] and cartilage [11, 20–22]. They enable relatively good mechanical and manufacturing properties, moderate biocompatibility, and precise control over physiochemical properties such as degradation rate, porosity, and microstructure and over mechanical properties [23]. Nevertheless, the vast majority of biodegradable polymers appear to have obvious drawbacks that hinder their broader application.

In the next section, the advantages and disadvantages of the biodegradable polymer PLA will be discussed. Subsequent sections deal with the possibilities of modifying PLA to overcome its negative properties or adapting it to a particular application. Section 3 focusses on strategies for tailoring its bulk composition to develop functional scaffolds. Implants and tissue engineering scaffolds interact with the biological environment via their surface. Bulk and surface properties of biomaterials used for implants have been shown to directly influence and, in some cases, control the dynamic interactions that take place at the tissue–implant interface [13]. Modification of the outermost part of materials may be sufficient to tailor their biocompatibility, which extensively affects the cell response if the materials are exposed to a biosystem [24]. Based on this, the strategies for biomaterial surface modification have been adapted over the years to improve the surfaces for desired applications. Surface modification is a feasible approach for making hydrophobic biomaterials more wettable or introducing biospecific cues to promote adhesion of cells [4, 25, 26]. Section 4 describes selected strategies for surface modification of polylactides by chemical and physical modification, which can be used to increase cell adhesion and mesenchymal stem cell (MSC) differentiation.

2 Advantages and Disadvantages of Using Poly lactides in Tissue Engineering

The vast majority of biodegradable polymers studied belong to the polyester family, which includes polyglycolides and polylactides. PLA belongs to a family of linear aliphatic polyesters of α -hydroxy acid derivatives. In general, PLA can be obtained either by direct condensation of lactic acid or by the ring-opening polymerization of the cyclic lactide dimer [27] (Fig. 1).

Fig. 1 Polymerization routes to obtain PLLA (*DP* direct polymerization, *ROP* ring-opening polymerization)



Because lactide has two asymmetric carbons, three optically active isomers are possible, L- and D-stereoisomers and the racemic D,L-form. These different isomers give rise to a range of different poly lactides, including poly(L-lactide) (PLLA), poly(D,L-lactide) (PDLA), and poly(L-lactide-co-D,L-lactide) (PDLLA). The chirality of lactide unit provides the means to adjust the degradation rate as well as the physical and mechanical properties. PLLA and PDLA are semicrystalline solids with similar hydrolytic degradation rates as poly(glycolic acid) (PGA). However, PLLA is more hydrophobic and also more resistant to hydrolytic attack than PGA. For most applications, the L-isomer of lactic acid is usually preferred because PLLA offers the best compromise in terms of mechanical stability and degradation rate [9]. These properties favor its use for most clinical applications, as does its more optimal metabolism in vivo.

The degradation of PLLA and its copolymers generally involves random hydrolysis of their ester bonds. Hydrolysis begins with diffusion of water into the amorphous regions, and proceeds by hydrolytic cleavage, which occurs from the edge toward the center of crystalline domains. This process results in a decrease in molecular weight (MW) followed by a reduction in mechanical properties and loss of mass. PLLA degrades to lactic acid, which is generally present in the metabolic pathways of mammals. The natural pathways (metabolism, excretion) of all animals and microorganisms eliminate the final degradation products [28]. Eventually, PLLA enters the tricarboxylic acid cycle and is digested into water and carbon dioxide [29]. Administration of carbon-13 (C^{13})-labeled PLA results in little radioactivity in feces or urine, indicating that most of the degradation products are released through respiration [30, 31]. Because PLLA is more hydrophobic and less crystalline than PGA, it degrades at a slower rate [7]. The degradation rate of the amorphous copolymer can be easily controlled by altering the ratio of PLA to PGA in the formulation when blends or copolymers are produced.

In addition to biodegradability, an advantage of polyesters is their simple and scalable manufacture into a variety of different shapes. Polyesters such as PGA and PLA can be easily formed into desired forms by molding, protrusion, and solvent processing [32], which makes them ideal candidates for making scaffolds for tissue engineering applications. For formation of PGA- and PLA-derived scaffolds, the solvent-casting method is applied when a polymer mesh is required, which is precipitated from viscous solutions into a low toxicity laminar film. Macroporous PLA scaffolds with microporous trabeculae can be prepared by freeze-extraction and particle leaching processes using dioxane as solvent (and also microporogen) and spherical polymeric particles as macroporogen. Applying this technique, we performed a systematic variation of polymer/dioxane and polymer/porogen ratios to manufacture PLLA scaffolds with a broad range of physical properties [33]. The dioxane proportion was varied until the limit of processability. Experimental results of different uniaxial compression tests, permeability studies, porosity, and pore size distribution function were properly correlated with the synthesis parameters to quantify solvent and mass weight of porogen. The obtained structures were observed with scanning electron microscopy (SEM), as depicted in Fig. 2.

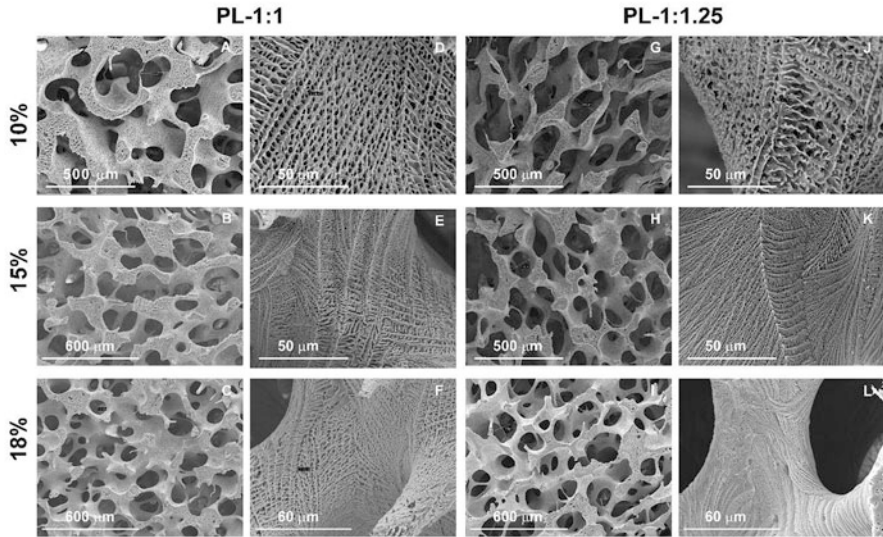


Fig. 2 Scanning electron micrographs of PLLA scaffolds prepared from different PLLA/dioxane solutions (10, 15, and 18 wt% of PLLA). (a–c, g–i) Low magnification images showing the macroporous structure for two series (1:1 and 1:1.25 PLLA solution/porogen weight ratio). (d–f, j–l) High magnification images showing the microporosity and trabecular structure of the scaffolds. Reprinted with permission from [33]

Macropores ranged from approximately 108–164 μm , whereas micropores were 1.3–13.7 μm . The micrographs showed a clear decrease in micropore size with a reduction in the amount of dioxane. A higher quantity of porogen spheres produced a closer connection between them, leaving bigger pores after their removal. However, increasing the porogen concentration (from 1:1 to 1:1.25) had a slight influence on macropore size (Fig. 2).

These polymers offer distinct advantages. To date, PLLA has been used for the regeneration of different tissues and organs, such as liver [34], bone [35], cartilage [20, 22], and skin [36]. Furthermore, it is a suitable substrate for osteoblast culture and exhibits bone fracture healing capabilities, with results comparable to those obtained with metallic implants [37]. In addition, chondrocyte differentiation is significantly improved in the presence of PLLA [38]. Furthermore, the *in vivo* degradation rates of PLLA are similar to those exhibited *in vitro* [21].

On the other hand, many studies have shown that the aforementioned polymers and their copolymers do have some limitations in tissue engineering applications. Some disadvantages of these polymers are their lack of cell adhesion motives, hydrophobicity, self-acceleration of degradation (autocatalysis), release of acidic degradation products, high melting points that influence processability, and early decline of mechanical properties during degradation. These properties are serious drawbacks to their medical application [8].

PLLA is a relatively hydrophobic polymer, whose biocompatibility depends on its molecular weight and crystallinity [19]. Crystallization kinetics of PLLA from the melt is slow and depends remarkably on the cooling rate [39, 40]. Amorphous PLLA is usually obtained by cooling it from the melt at a broad range of rates. Amorphous samples can then be placed at the cold crystallization temperature for different times to produce materials with different crystallinities [41]. Crystallinity and crystal size are parameters that regulate PLLA biocompatibility and its interaction with cells [42]. However, the main importance of these parameters is that they modulate the degradation kinetics of the polymer. Poly lactides undergo degradation mainly through hydrolysis, which is initiated in the amorphous phase of the polymer [43] and its rate strongly depends on the initial crystallinity of the polymer [44, 45]. Tailor-made scaffolds with desired degradation rates can be produced from amorphous PLLA scaffolds by allowing them to crystallize at the cold crystallization temperature.

The degradation products of poly lactides are acidic and can be toxic to implanted cells if released in large quantities [46]. Some studies have shown systemic or local reactions caused by acidic degradation products [28]. Concerns about the biocompatibility of PLLA were heightened following the demonstration that PLLA produced toxic solutions, probably as a result of acidic degradation, usually in cases where the implant used was of considerable size [47]. Another concern is the release of small particles during degradation *in vivo*, which can cause an inflammatory response through phagocytosis by macrophages and multinucleated giant cells [48]. It has also been noted that no adverse biological responses occur in cases where the volume of the material used is relatively small [9]. However, the biocompatibility of poly lactide-based scaffolds is not high for all type of cells due to the hydrophobic nature of the polymer [49], which may result in impaired adhesion of human mesenchymal stem cells (hMSCs). The low wettability is related to these findings [50]. It has been shown in a number of studies that hydrophobic biomaterial surfaces hamper attachment of cells and/or impair their subsequent growth and function [51]. The underlying reasons for this phenomenon are the altered adsorption and conformation of adhesive proteins such as fibronectin (FN), which may lead to impaired interaction with cellular adhesion receptors, namely integrins [52, 53]. Furthermore, the adsorption of blood cells on porous poly lactide scaffolds indicates that these scaffolds are highly thrombogenic [54]. Additionally, the absence of reactive functional sites on their chains is a further limitation to their application as scaffolds. Because of these obvious drawbacks regarding control of degradation and corresponding mechanical properties, generation of acidic by-products, and limited support for cell adhesion, the modification of bulk composition and surface of poly lactides has been introduced for applications in tissue engineering [55]. These modifications are described in more detail in Sects. 3 and 4.

3 Tailoring the Bulk Composition of Polylactides

Despite the benefits of pure PLLA in cartilage and bone tissue engineering [23, 42, 56, 57], there is extensive literature on tailoring its bulk composition to develop scaffolds with properties that best fit the properties of these tissues. The most common modifications are aimed at regulating the degradation rate to align it with the real production of new ECM and at achieving mechanical properties more similar to those of the specific tissue. One problem is that polylactides have long degradation rates of about 1 year or more. Even if hydrolysis first affects the amorphous phase, completely amorphous samples have longer degradation rates than semicrystalline samples, because degraded chains, instead of being released from the polymer, remain in the samples and start to crystallize [44]. This means that there is a limit to the degradation rate, which cannot be overcome by modulating the crystallinity of the sample. Faster degradation rates can be obtained by combining polylactides with other hydrophobic polymers with faster hydrolysis rates or with hydrophilic polymers that speed up water absorption. Regarding the mechanical properties, the same modifications that accelerate the degradation rate can give rise to softer materials that are desirable, for instance, in cartilage regeneration [58]. When reinforcement is needed (e.g., in bone), organic–inorganic composites can be effective for increasing the elastic modulus, which in turn improves bioactivity [59, 60]. The ECM of cartilage is highly hydrated and, consequently, hydrophilic materials such as hydrogels are preferred as a synthetic matrix to replace this tissue [58]. However, hydrogels are extremely soft and polylactides that can provide mechanical stability seem to be a better alternative. However, the cell adhesive pore walls of PLA-based scaffolds are not adequate for chondrocytes because they lose their phenotype when adhering to the pore surface [61]. Hence, polylactides can be combined with hydrophilic polymers to reduce cell adhesiveness, such as cylindrical osteochondral scaffolds based on PLA [62, 63]. Devices less invasive to the subchondral bone have been proposed for regenerating the articulation as a whole [64].

We summarize here the main strategies described in the literature for optimizing bulk materials in the search for optimized degradation rates, mechanical properties, and bioactivities that cannot be achieved with pure PLA polymers. We start by reviewing block copolymers, because the resulting morphologies are more predictable than those obtained by blending. Then, we summarize the main blends and discuss the use of blending as a cost-effective strategy. Polymeric networks are systems that are not soluble in good solvents of the polymer, but are advantageous in porogen-leaching manufacture of scaffolds, in preventing crystallization during degradation, and in allowing incorporation of hydrophilic chains. Because of their importance in regeneration of bone, we also review organic–inorganic composites as bioactive systems with good mechanical properties.

3.1 Block Copolymers

Three kinds of copolymers are usually synthesized: AB diblock, ABA triblock, and multi-arm block copolymers. Because the blocks in the copolymers are usually immiscible, they have phase-separated morphologies with ordered domains, forming a variety of nanostructures, which can also be crystalline [65]. Despite phase separation, because the blocks correspond to the same chain, the obtained domains are normally smaller than found in blends and the resulting properties are different. PLA is usually copolymerized with PGA to obtain poly(lactide-*co*-glycolic acid) (PLGA) copolymers, with degradation rates regulated by the ratio of their respective monomers [66, 67]. In contrast to PLA and PGA, PLGA copolymers are amorphous with glass transition temperatures (T_g s) in the general range of 45–55°C, depending on the lactide and glycolide ratio [68]. Glycolic acid units are more hydrophilic than lactic acid units, meaning that copolymers rich in the former present faster degradation than copolymers rich in lactic acid, with the exception of the 50:50 copolymer that presents the highest degradation rate [69]. The most commercialized compositions for medical products are 50:50, 65:35, 75:25, 85:15, and 90:10 [70]. Despite the advantages of these copolymers, their toughness is too high for certain biomedical applications, and copolymerization with more flexible chains is recommended. This is the case for L-lactide and ϵ -caprolactone copolymers (PLCL) that are more flexible than PLA and PLGA thanks to the low T_g of poly(ϵ -caprolactone) (PCL) (–60°C) and consequently higher mobility of caprolactone blocks at body temperature [71]. For lactic acid contents higher than 30 wt%, copolymers are amorphous with T_g values increasing with lactide content, which also affects the mechanical properties [72]. Degradation rates of these copolymers are usually faster than those of the homopolymers and can be varied over a wide time range [73]. Such elastic, biodegradable PLCL scaffolds are able to deliver effective mechanical stimulation to cells and could be useful for cartilage regeneration [74].

Amphiphilic copolymers of PLA are very interesting because they are able to reduce PLA brittleness and increase surface hydrophilicity, with controlled degradation rates. Poly(ethylene glycol) (PEG) block copolymers with PLA have been proposed for making scaffolds due to the good biocompatibility and nontoxicity of PEG. ABA triblock copolymers of PLLA-*b*-PEG-*b*-PLLA (PELA) exhibit a good balance between degradation rate and hydrophilicity [75]. The T_g depends on several factors, but is usually lower than that of pure PLA. As described [76], the T_g ranges between 15 and 35°C. The melting peak is also shifted to lower temperatures and lies in the range of 60–120°C. These copolymers form a microphase-separated structure with hard domains alternating with soft domains, forming a thermoplastic physical hydrogel [76, 77].

The combination of PLA with polysaccharides is also an interesting strategy for increasing the hydrophilicity and modulating the degradation rate of polyesters, although the main application of these copolymers is focused on drug delivery systems. For instance, amphiphilic brush-like copolymers of PLA and dextran have

been proposed as compatibilizers of PLA/dextran blends, giving rise to blends with improved mechanical properties [78]. In-situ forming microgels of hyaluronic acid (HA) grafted with PLA find application in intraarticular administration of anti-inflammatory drugs [79].

3.2 Blends

Polymer blending is perhaps the most economic solution for modifying the properties of PLA. However, as most polymers are immiscible, polymer blending gives rise to phase-separated materials with domains that are usually larger than those obtained in copolymers. Furthermore, the properties of the resulting blend can be poorer than those of pure polymers if the microstructure is not adequate [80]. As recently reviewed, compatibilization strategies can effectively enhance PLA properties in blends, but care has to be taken to maintain the material's biocompatibility for biomedical applications [81].

PLLA and PDLA of average molecular weights below $1 \times 10^5 \text{ g mol}^{-1}$ form miscible blends because of their ability to form stereocomplexed crystallites that melt at about 230°C, which is 50°C above the melting temperature of PLLA or PDLA homocrystals [82, 83]. Stereocomplexation provides higher mechanical and thermal stability to blends and extends the range of application of polylactides in medicine [84]. As a consequence of stereocomplexation, PLLA/PDLA blends show slower degradation rates than PLLA, which results in milder inflammatory reactions in vivo [85].

Literature referring to PLA/PGA blends is rare, probably because phase separation gives rise to systems with properties that are not advantageous compared with the copolymers. On the other hand, the resulting morphology of these blends allows preparation of very interesting porous fibers by selectively solubilizing the PLA phase of electrospun membranes [86]. PLLA blended with PLGA is more common and can lead to materials with tailored degradation rates and mechanical properties that depend on the molecular weight of the pristine polymers, lactide-to-glycolide ratio in PLGA, and the blending ratio of both components [83]. A systematic study on a range of compositions of PLLA and PLGA demonstrated that for a certain composition (PLA/PGA 3:1), the blend is partially miscible and presents a Young's modulus higher than that predicted by the additive rule of phases [87]. This partial miscibility also accelerates the degradation of the PLLA matrix, which can be advantageous in tissue engineering.

Blending of PCL with PLLA increases ductility and improves the ultimate strength of PLLA [83]. Although both polymers are immiscible, dispersing PCL domains in the PLLA matrix increased elongation at break, toughness, and thermal stability of PLLA as a result of the plasticizing effect of the mixed amorphous phase and reduction in PLLA crystallinity [88]. Block copolymers of PLA and PCL can be added to blends to increase their compatibility [89], giving reduced PCL domain size when the copolymers are present.

In a similar way as for copolymers, PEG blending with PLA leads to more ductile materials with an accelerated degradation rate [83]. Blending avoids the use of toxic catalysts employed in copolymer synthesis (e.g., stannous octoate) [90]. More importantly, PEG chains in the blends act as plasticizer, facilitating PLA extrusion [91] and direct 3D printing [92].

Attempts have been made to mix PLA with other hydrophilic biomaterials of natural origin such as chitosan (CHI), starch, or gelatine (GEL) by the use of a common solvent [62, 93–95]. However, in these cases, immiscibility is more marked than when two hydrophobic polymers are mixed and processing processes need to be modified to prevent large phase-separated domains that could compromise the properties of the blends. For instance, a PLA/CHI solution was precipitated in acetone [93], which is a very fast way to eliminate the solvent, preventing phase separation to some extent. Dimethyl sulfoxide (DMSO) is a common solvent of PLA and GEL and, although phase-separated blends were obtained [95], the GEL-dispersed domains in the blends with a content below 5% were of several hundred nanometers, without reaching the micrometer scale. Furthermore, the mechanical properties did not decrease much with respect to pure PLA. GEL provided hydrophilicity and prevented PLA crystallization, and the low content GEL mixtures were better than pure materials in terms of degradation profile. As a result, hydrogel blends of PLA had increased hydrophilicity, improved biocompatibility, and did not necessarily compromise the mechanical properties of PLLA if present in a low percentage [25, 96]. A good example of this combination is an osteochondral scaffold [62] made of a blend of starch and PLLA on the cartilage side, which was found to possess adequate hydration capability. For the bone region, where more stiffness and strength is required, PLLA reinforced with hydroxyapatite (HAp) was used. PLLA elasticity was also regulated by mixing with the microbial polyester poly(3-hydroxybutyrate-*co*-3-hydroxyvalerate) (PHBV) [97], which enhanced cell biocompatibility, particularly for the 60:40 and 50:50 composition ratios [98].

3.3 Polymeric Networks

A polymer network is formed when a polymer is chemically crosslinked. If the crosslinker has two or more functionalities, it is able to bind to two or more polymer chains at the same time, forming a network that swells in the presence of a proper solvent but does not dissolve in it. The interest on polymeric networks of PLA in tissue engineering is dual. On the one hand, PLA allows the preparation of scaffolds using porogen particles that need to be removed with organic solvents that are also good solvents of PLA. For instance, porogens are present in templates formed by sintered polymeric particles [99]. The precursor solution of the polymer is injected in the voids of the template, polymerized and/or crosslinked, and the porogen is then removed by dissolution with an organic solvent that must not dissolve the polymer; this process generates a porous structure [99]. It is difficult to find a combination of solvents for this technique because the porogen solvent also usually

dissolves the PLA. The problem can be avoided by crosslinking PLA in the presence of the porogen to avoid its dissolution when removing the porogen.

On the other hand, polymer network formation can prevent PLA crystallization, giving rise to more ductile materials. It also permits the combination of PLA with other polymers in the network, which can regulate PLA hydrophilicity, crystallinity, and degradation rate.

Methacrylate end-capped PLA macromers were successfully synthesized through condensation of PLA diol with methacrylic anhydride [100]. When a solution of this macromer is exposed to UV light in the presence of an initiator, the double bonds at the end of the chains are opened and radicals react with each other, giving rise to PLA networks. The hydrophilicity of PLA in these systems can be tuned by adding different amounts of an acrylic, hydrophilic monomer, which accelerates hydrolytic and enzymatic degradation of PLA and promotes MSC differentiation to the osteogenic phenotype [26, 100]. PLA crystallization is prevented by network formation and the T_g of the polyester domains shifts from 45°C in the pure network to 40°C or less in the hydrophilic networks.

In a similar way, polymeric networks combining PLA and PCL can be prepared by crosslinking solutions of methacrylate-terminated PLA and PCL macromers at different proportions [101]. This strategy produces quasi-compatibilized networks with a single T_g in the differential scanning calorimetry (DSC) thermograms that is lower than for the pure PLA network and splits into two relaxations in the differential mobility spectrometry (DMS) spectra, indicating segregation into small domains of pure PCL. Combined networks are amorphous, except for a 70 wt% of PCL. Network formation from macromer solutions in the voids of a polymeric template allowed synthesis of interconnected macroporous scaffolds with different hydrophilicities that promoted osteogenic differentiation of MSCs [102] and chondrogenic differentiation of de-differentiated chondrocytes [103].

PLA/CHI networks with short degradation times regulated by the amount of PLA were successfully obtained by grafting PLA chains onto CHI in the presence of stannous octoate and trimethylamine, subsequent methacrylation of the end group of grafted PLA chains, and final exposure to UV light [104]. Because PLA chains acted as crosslinker in these networks, the swelling capacity of CHI increased with the addition of PLA, thus reducing the compressive modulus. This system demonstrated injectability into the body and is a proper hydrogel scaffold for tissue engineering of bone because it efficiently released BMP-2 growth factor and induced osteoblastic differentiation and mineralization.

Hydrogel networks formed from multifunctional macromers of PLA-*b*-PEG-*b*-PLA end-capped with dimethacrylate (DM) groups (PEG-LA-DM) are also injectable hydrogels that find application in tissue engineering [105]. Their combination with a slowly degrading macromer such as PEGDM leads to networks with different degradation rates that can induce osteogenesis and mineralization, both of which increase with degradation time.

3.4 Organic–Inorganic Composites

Hard tissues such as bone require scaffolds able to sustain the load applied *in vivo*. Ceramic materials are brittle and stiff, and therefore macroporous materials made with them are fragile. By contrast, most polymeric materials are unable to sustain the applied loads in bone [106]. Of the biodegradable polymers, PLA offers good mechanical properties and has been proposed for tissue engineering of bone. However, in macroporous scaffolds, the mechanical properties are affected by the porosity and reinforcement is a recurrent issue in bone replacement. Nanocomposites of a PLA matrix reinforced with HAp or other ceramic material such as tricalciumphosphate (TCP), silica, or bioactive glass have been developed with the aim of enhancing the mechanical properties of PLA and designing porous materials for tissue engineering of bone [107]. The popularity of these composites lies not only in the mechanical reinforcement; the inorganic filler also acts as a buffer for the decrease in local pH caused by PLA degradation products. Hence, the filler modulates degradation rate and enhances cell adhesion, osteoconductivity, and bioactivity of the PLA scaffold [107, 108]. Bioactivity has been defined as the ability of a biomaterial to bind bone directly without forming any surrounding connective tissue. Of the bioactive inorganic fillers, HAp is preferred because it has the same formulation as mineral bone [$\text{Ca}_{10}(\text{PO}_4)_6(\text{OH})_2$] and, from the crystallographic point of view, is the most similar to natural bone [108].

Finding the adequate amount of inorganic filler, properly dispersing it in the polymeric matrix, and enhancing the interfacial bond strength with the matrix are probably the most discussed challenges in obtaining the required bioactivity and reinforcement for these composites [109]. Sonication of a solution of PLA in dioxane containing HAp particles and subsequent freeze-extraction leads to proper dispersion of HAp in membranes [110] and scaffolds [111]. As an example, Fig. 3 shows the SEM image of a PLLA membrane containing 10 wt% of HAp prepared by freeze-extraction, together with the corresponding energy dispersive spectroscopy (EDS) scan that confirms the effective incorporation of HAp (Ca and P peaks) [110]. The scan shows that HAp particles are homogeneously dispersed in the walls of the pores.

To improve bioactivity, these composite scaffolds can be mineralized *in vitro* by immersion in simulated body fluid (SBF) prior to implantation. Their integration in the host bone and the bone regenerative potential is superior to that of nonmineralized composites or bare PLA scaffolds, as described previously [111]. In that study, we demonstrated that PLLA scaffolds, PLLA/HAp composite scaffolds with 5 wt% of HAp, and PLLA/HAp scaffolds coated with biomimetic apatite (by immersion in SBF) (PLLA/HAp/SBF) respond differently when implanted into the bone of sheep [111]. Masson's trichrome staining histologies of implanted scaffolds and surrounding tissue are seen in Fig. 4a, and the detail of the interface between the scaffolds and the host bone in Fig. 4b, demonstrating good integration of the three scaffolds with the host tissue and no fibrous capsule formation. The microscopic aspect of the regenerated tissue varied strongly with scaffold composition (Fig. 4c). PLLA with and without HAp was invaded by a

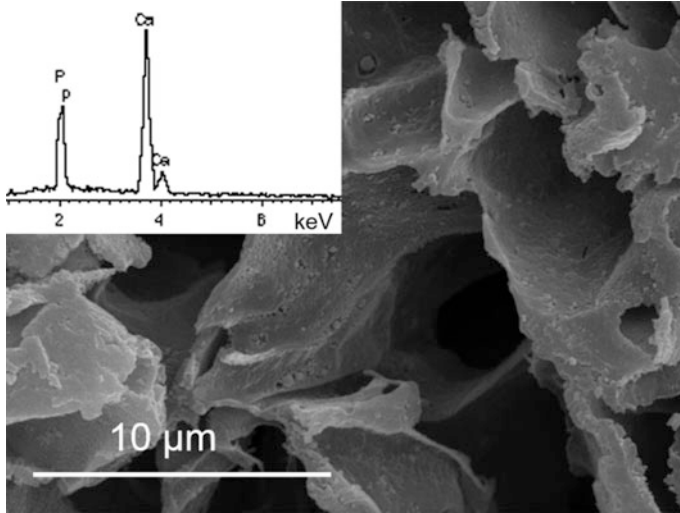


Fig. 3 Scanning electron micrograph (SEM) and energy dispersive spectroscopy (EDS) analysis (*inset*) of a membrane of PLLA/HAP nanocomposite with 10 wt% of HAp and a surface plasma treatment to increase its hydrophilicity. The membrane was manufactured by freeze-extraction from a 15 wt% of PLLA solution in dioxane. Reprinted with permission from [110]

fibrous-like tissue with an abundance of COL fibers surrounding the PLLA pores. The scaffold implanted with a layer of HAp covering its pores was invaded by tissue that showed zones with an aspect very similar to osteoids (Fig. 4c, asterisks), suggesting regenerated tissue more mature than in the other scaffolds. Quantification of the area occupied by these osteoid structures is shown in Fig. 4d and the extent of the COL type I expression (see [111]) confirmed these observations.

Despite the fact that organic–inorganic composites of PLA are beneficial for bone regeneration in terms of bioactivity, the use of hydrophilic inorganic fillers such as HAp or SiO₂ has certain drawbacks because of poor interaction with the hydrophobic PLA matrix. Even if these fillers are well dispersed within the matrix, the mechanical properties of the composite scaffolds tend to be equal or inferior to those of pure PLA. Filler particle surface modification by grafting prior to combination with PLA has been proposed as a way to overcome these drawbacks [112, 113]. Chemical grafting is tedious and expensive, but there are cheaper strategies that are also easier to apply and convenient. A mixture of the hydrophilic fillers HAp and SiO₂ was more effective in enhancing the mechanical properties of PLLA scaffolds than either filler alone [114]. This ability was a result of the hydrophilic interaction between particles that were oriented such that their hydrophobic part faced the PLLA matrix, causing a stronger hydrophobic interaction with the polymeric matrix [114]. Consequently, the Young's modulus of the scaffold containing a mixture of HAp and SiO₂ was 30% greater than for the pure PLLA and reached a value of ~7 MPa (Fig. 5), which is considerably higher than the usual values obtained in polymeric scaffolds based on PLA. As expected, compression moduli decreased after some time in SBF as a result of polymer degradation.

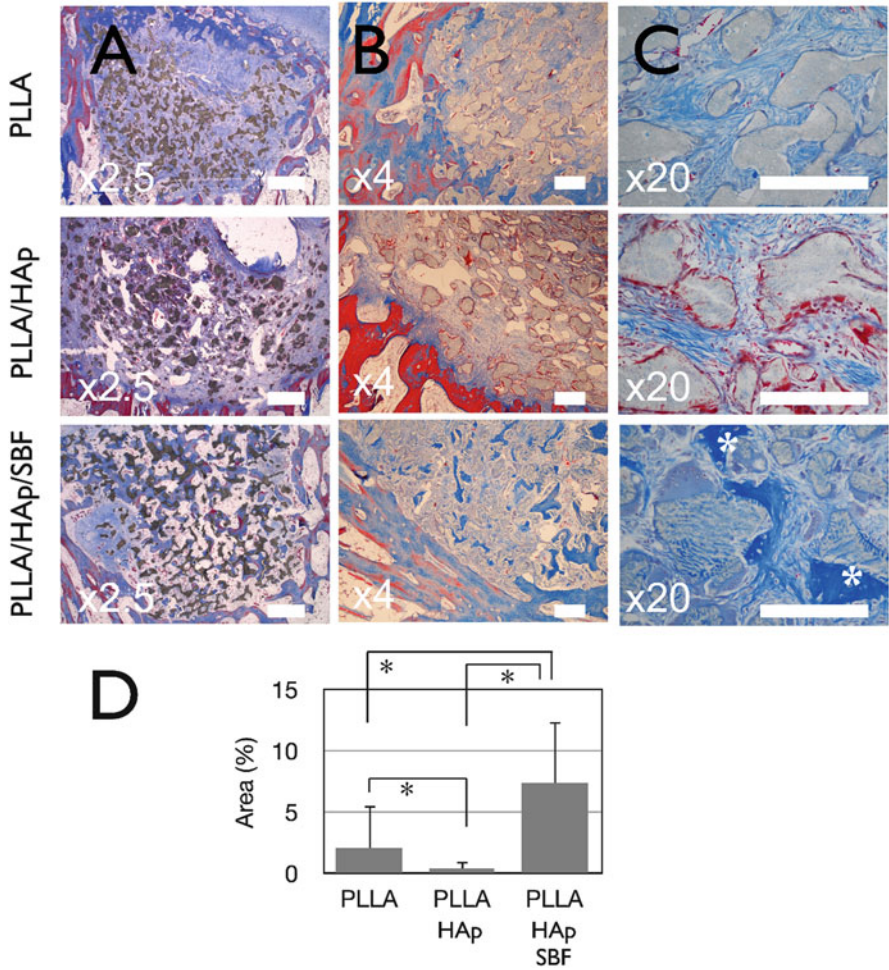


Fig. 4 Masson's trichrome staining of the histological sections of tissue regenerated by PLLA, PLLA/HAp, and PLLA/HAp/SBF scaffolds 6 weeks after implantation: (a) View of the PLLA implant inside the structure of the subchondral bone. (b) Detail of the edge between the implant and host bone tissue. (c) Detail of the scaffolds and tissue regenerated inside their pores. (D) Percentage area occupied by osteoids inside the scaffolds, as determined by ImageJ software (10 fields per sample were used for the quantification). For the analysis, $p < 0.05$ was considered as significant. Implants were placed in lesions performed in the femoral condyle of 3-month-old healthy sheep. Tissue filling the pores of the scaffolds can be observed, but osteoids (asterisk) are only present in the PLLA/HAp/SBF scaffold. Scale bars: 200 μm (a), 100 μm (b, c). Reprinted with permission from [111]

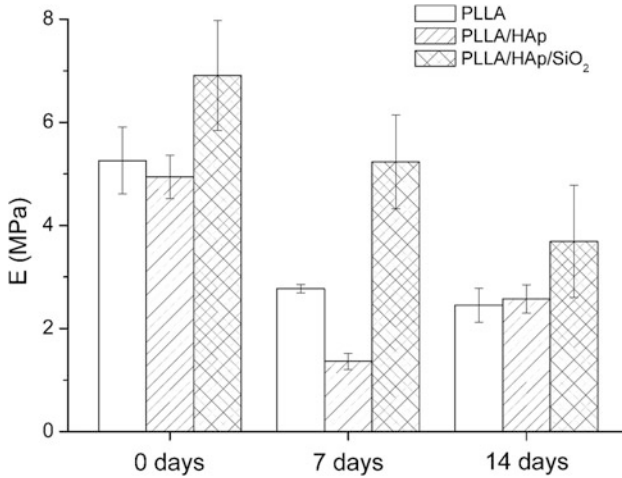


Fig. 5 Apparent Young's moduli at compression of PLLA, PLLA/HAp 90:10, and PLLA/HAp/SiO₂ 90:9.5:0.5 scaffolds after various times of immersion in simulated body fluid. Reprinted with permission from [114]

3.5 Commercially Available Products for Skeletal Tissue Engineering

Despite the abundance of literature related to the use of PLA and its combinations in tissue engineering, very few products reach the market or clinical trials. In tissue engineering of cartilage, most of the matrices are composed of COL or hyaluronic acid (HA) [58]. BioSeed[®]-C (BioTissue AG, Zürich, Switzerland) is the only matrix material for autologous chondrocyte implantation based on PLA that is on the market. It is a PGA/PLA/poly-*p*-dioxanone supportive matrix (derived from one of the materials of biodegradable sutures, polyglactin 910) that is combined with culture-expanded autologous chondrocytes suspended in fibrin glue and used for the regeneration of cartilage lesions [115, 116]. The radiological outcome of the clinical implantation of BioSeed[®]-C in knee lesions seems to be better than the traditional therapy of autologous chondrocyte implantation, which is a proof of the benefits of using scaffolds in cartilage defects [115].

Alvelac[™] is a porous, osteoconductive, biocompatible, and biodegradable synthetic scaffold synthesized from PLGA and polyvinyl alcohol (PVA) produced via 3D printing by Bio Scaffold International Pte Ltd. Its proposed application is for regeneration of alveolar bone after teeth extraction [117], although other orthopaedic uses are being explored. As it is produced by 3D printing, the advantage of this product is that scaffolds with the shape of the defect in the patient can be produced. Soft Tissue Regeneration Inc. is currently involved in a clinical trial study of their product L-C Ligament[®], based on a PLLA scaffold designed to facilitate re-growth of a patient's anterior cruciate ligament (ACL) within the knee [118].

4 Surface Modification of Polylactides by Chemical and Physical Methods

4.1 Surface Modification of Polylactides

Certain disadvantages of polylactide polymers in several tissue engineering applications have been briefly discussed, such as the lack of cell adhesion motives and their relative hydrophobicity, which can lead to undesired effects on protein adsorption and subsequent interaction with cells [8, 9]. Surface modification of polymers can be achieved by physical or chemical methods and has been reviewed in detail in a number of publications [40, 119]. Physical modification of PLA by adsorption of ECM proteins such as COL and FN has been suggested by some authors, although the process is not well defined and lacks strategies for sterilization because of the negative effects on proteins, making this method less suitable [71]. Other methods of adsorption such as the layer-by-layer (LbL) technique can be used to apply more stable molecules such as glycosaminoglycans (GAG) that can mimic the natural environment of cells, but can be sterilized by UV radiation or other techniques [120, 121]. A wide variety of chemical treatments for polymers have been described in more detail in other reviews (e.g., [122]). Treatment of polymers for the introduction of functional groups such as amino groups has been carried out using nitrogen plasma or allylamine [123, 124]. Plasma treatment is useful for polylactides, and its copolymers and blends, because the treatment does not involve any organic solvents that can migrate into the polymer or water that can induce hydrolysis. On the other hand, previous work has successfully shown the use of wet chemistry for modification of PLA with bioactive molecules such as heparin (HEP) or hirudin for applications in contact with blood [125, 126]. Extensive reviews on the surface modifications of PLA can be found elsewhere [71, 127]. Briefly, we describe ways to modify PLA by simple adsorption techniques or chemical modification to introduce amino groups that promote cell adhesion [53] and adsorption of bioactive GAG, which promotes not only cell adhesion and spreading, but also differentiation of hMSCs.

4.2 Covalent Activation versus Adsorptive Binding of Polyamines

Poly(ethylene imine) (PEI) is widely used as an agent to support transfection of cells and has been immobilized on polymers such as polyimides, showing promoting effects on the adhesion of keratinocytes [128]. Hence, surface modification of PLLA cast films with different PEIs of either high (750 kDa) or low (25 kDa) MW (either by adsorptive or covalent immobilization) was carried out to study the effect on the activity of bone cells. The samples obtained after adsorption of PEI were designated as AH (PEI MW 750 kDa) or AL (PEI MW 25 kDa), where A stands for adsorption and H and L for high and low MW PEI, respectively. Covalent binding

Table 1 Surface properties of PLLA films after immobilization of poly(ethylene imine)

Sample	Surface elemental composition (mol%)			Amino group density ($\times 10^{16}$ cm $^{-2}$)	Water contact angle ($^{\circ}$)
	C	N	O		
PLLA	61.6	–	38.4	–	72.4 \pm 0.3
AL	64.2	0.5	35.3	2.51 \pm 0.19	60.5 \pm 0.9
CL	63.7	0.5	35.8	9.36 \pm 0.62	59.4 \pm 0.6
AH	65.1	1.0	33.9	12.14 \pm 0.40	56.8 \pm 2.7
CH	63.3	3.7	33.0	12.79 \pm 0.36	56.2 \pm 1.9

AL adsorptive binding of low molecular weight PEI, *CL* covalent binding of low molecular weight PEI, *AH* adsorptive binding of high molecular weight PEI, *CH* covalent binding of high molecular weight PEI.

Surface elemental composition was obtained by XPS, amino group density of PLLA surfaces measured by acid orange assay, and water contact angle with the sessile drop method (Modified from [129])

of PEI to terminal carboxylic groups of PLLA was achieved using *N*-(3-dimethylaminopropyl)-*N'*-ethylcarbodiimide hydrochloride (EDC) and *N*-hydroxysuccinimide (NHS). Details of the procedure can be found elsewhere [129]. The samples were designated as CH (PEI MW 750 kDa) or CL (PEI MW 25 kDa), where C stands for chemical binding of PEI.

Because the surface composition and properties of biomaterials dictate the adsorption of proteins and adhesion of cells [16], surface characterization of substrata using X-ray photoelectron spectroscopy (XPS) was carried out to quantify the chemical composition after immobilization of PEI (as shown in Table 1). PLLA contained 61.6% carbon and 38.4% oxygen. After PEI modification, the ratio of C to O increased because carbon from PEI was bound to the surface. In addition, Table 1 shows that nitrogen was found after deposition of PEI and increased for samples modified with high MW (HMW) PEI, especially for sample CH with 3.7 mol% nitrogen, indicating that the covalent immobilization was most efficient. The amino group density on PEI-modified PLLA films was quantified by acid orange assay [128] and showed consistency with XPS studies regarding the higher amount of amino groups when HMW PEI was used (Table 1). Water contact angle (WCA) measurements using the sessile drop method confirmed these findings, showing a decrease in WCA from about 72 $^{\circ}$ for relatively hydrophobic PLLA to about 57 $^{\circ}$ for HMW PEI, irrespective of the modification method. The results were in line with previous studies on PEI immobilization using other types of polymers [128].

The promoting effect on biocompatibility and osteogenic activity of PLLA modification with PEI of different MWs by either adsorption or covalent binding was further studied with the osteoblast-like cell line MG-63 [130]. This cell line has a controlled growth behavior and expresses osteogenic features such as alkaline phosphatase (ALP) activity [131]. Studies of adhesion and proliferation of MG-63 cells on different sample surfaces revealed that adhesion and cell growth were similar for all surface modifications with PEI but showed significantly lower cell

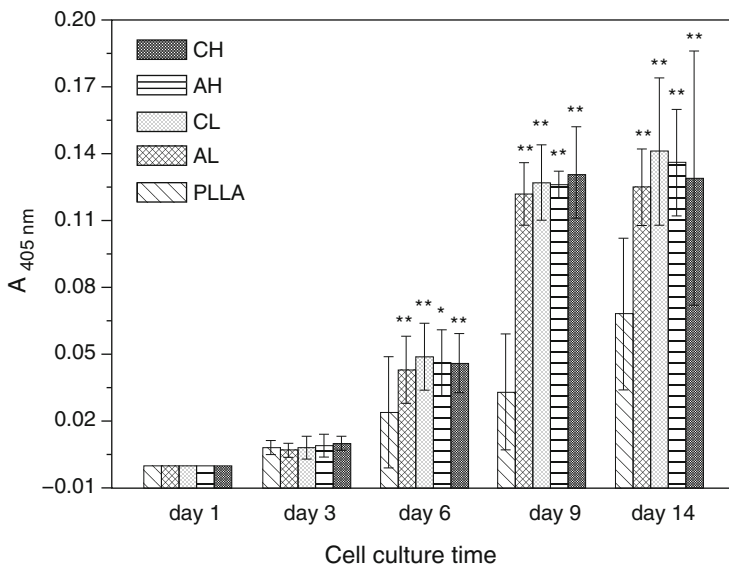


Fig. 6 Alkaline phosphatase (ALP) assay for differentiation of MG-63 cells measured as absorbance ($A_{405 \text{ nm}}$) versus culture time. *PLLA* plain *PLLA*; *AL* or *AH* *PLLA* modified with low (L) or high (H) molecular weight PEI by adsorption (A); *CL* or *CH* *PLLA* modified with low (L) or high (H) molecular weight PEI by covalent binding (C). Asterisks indicate a significant difference between PEI-treated samples and *PLLA*, with $p \leq 0.05$. Reprinted with permission from [129]

growth on plain *PLLA*, which corresponds to cell behavior on more hydrophobic materials [53].

The osteogenic activity of cells was quantified by the expression of ALP, an enzyme involved in the calcification of bone [131]. As shown in Fig. 6, no ALP activity of MG-63 cells was detected on the tested surfaces at day 1, which reflects the fact that ALP activity is upregulated at later stages of culture [132]. After 6 days, the ALP activity of MG-63 cells increased significantly and continued to rise until day 9. Cells cultured on PEI-modified samples expressed significantly higher ALP activity ($p < 0.05$) than those grown on plain *PLLA*. However, no remarkable differences were observed between the different PEI-modified surfaces.

The results indicate that PEI is useful for covalent and noncovalent modification of polymer surfaces such as *PLLA* films. The inherent cytotoxicity of HMW PEI found in other studies [133, 134] was not observed here, which suggests that it is a suitable candidate for making hydrophobic polymer surfaces more biocompatible. The choice of immobilization method (adsorptive or covalent) and the MW of PEI (low or high) depends on the desired application, such as the preparation of polyelectrolyte multilayers (PEM) on implant materials.

4.3 *Physical Surface Modification of PLLA with Polyelectrolyte Multilayers*

Of the possible physical surface modification techniques, LbL assembly of polyelectrolytes (PEL) is a simple method for generating multilayers on charged material surfaces [120, 135]. The LbL technique is based on electrostatic interaction between charged substrata and PEL in aqueous solution, followed by ion pairing during their complexation on the surface [135]. In addition, hydrogen bonding and hydrophobic, host–guest, and other interactions are useful for complexation of macromolecules, particulate material, and cells on surfaces in an LbL approach [120]. The inner structure and surface properties of PEM strongly depend on PEL characteristics such as MW and presence of basic or acidic functionalities (strong or weak). Solution temperature and composition in terms of PEL concentration, ionic strength, and pH are also important [136, 137]. The LbL technique can also be applied to prepare multilayers that partly resemble the composition of the ECM by using matrix proteins and GAG. Here, we present an example using CHI as polycation and GEL, HA, and HEP as polyanions for formation of multilayer films on PLLA films. The experimental details can be found elsewhere [14]. The PLLA films were pre-activated with HMW PEI by covalent binding to maximize the content of amino groups that acquire a positive surface charge at acidic pH values used during PEL adsorption [129]. Multilayer formation was carried out until 10 or 11 single layers were obtained. Layer growth was studied by surface plasmon resonance (SPR), which quantified the adsorption of PEL by changes in the angle shift. Figure 7 shows the results of SPR measurements for GEL/CHI, HA/CHI, and HEP/CHI multilayer formation and represents the SPR angle shifts during formation of PEM on the sensor surface with a total of 11 PEL layers.

The SPR curves revealed different increases in layer mass for the three PEL pairs studied. Combination of the strong PEL HEP with the weak PEL CHI resulted in the largest angle shifts, indicating highest layer mass. Multilayer growth was exponential compared with the rather linear growth of HA/CHI multilayers. Furthermore, growth of the HA/CHI system was low, and almost insignificant for the GEL/CHI system. In addition, WCA measurements indicated whether the differences in growth regimes resulted in a specific surface wettability that depended on the PEL pair as well as the terminal layer. As seen in Fig. 8, plain PLLA films were rather hydrophobic, with a WCA value of 72°. Modification with PEI led to a decrease in WCA to 60°, which was in accordance with previous investigations [24, 129]. When this surface was exposed to the polyanions, a slight increase in WCA was observed, especially for the PEL pair HA/CHI (71°) and GEL/CHI (65°). The terminal layer of CHI/HEP had a lower WCA of about 50°. The results of these studies showed that both chemical and physical surface modification of PLLA can change the overall physical properties such as wettability, but also the chemical composition of the surface without a change in bulk properties of the material.

Human MSCs, isolated from bone marrow and other tissues, possess multipotent differentiation capacities that are stimulated by appropriate signals [138, 139]. The induction of MSC differentiation is a highly programmed, lineage-specific process

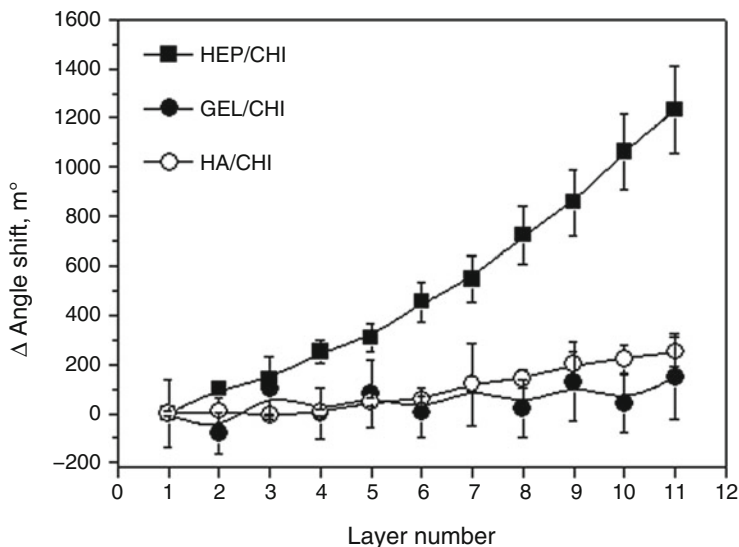


Fig. 7 Changes in SPR angle as a function of number of layers of gelatine/chitosan (GEL/CHI, filled circles), hyaluronan/chitosan (HA/CHI, open circles) and heparin/chitosan (HEP/CHI, filled squares) formed from 2 mg mL^{-1} PEL solutions in 0.14 M NaCl . Layer 1 represents PEI as primary layer; even layers polyanions (GEL, HA, HEP); odd layers CHI. Reprinted with permission from [14]

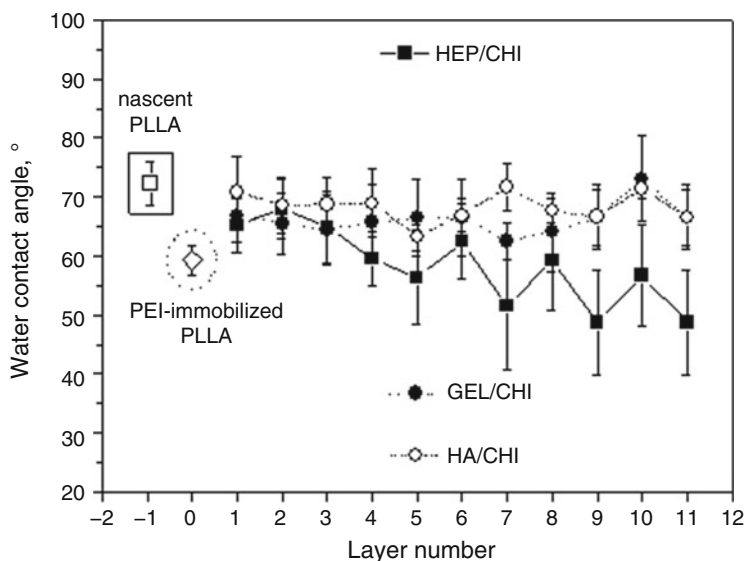


Fig. 8 Water contact angles (WCA) measured after each adsorption step during multilayer formation for PEL pairs of gelatine/chitosan (GEL/CHI, filled circles), hyaluronan/chitosan (HA/CHI, open circles) and heparin/chitosan (HEP/CHI, filled squares). Reprinted with permission from [14]

at the molecular level controlled by hormones, cytokines, and growth factors [140] and by the nature and topography of scaffolds [141]. We studied whether the modification of PLLA with PEM, which leads to a change in the microenvironment because of the different surface composition, can have a synergistic effect in the presence of osteogenic stimuli on the osteogenic differentiation of MSCs. Because long-term culture in normal medium revealed strong differences in cell morphology and growth of large nodules on HA and HEP layers, alterations in osteogenic differentiation were expected [129, 142]. Here, osteogenic differentiation of hMSCs was visualized by staining calcified areas with Alizarin Red, as shown in Fig. 9.

The strongest staining in cells cultured in normal medium was found in cultures on CHI/GEL multilayers (Fig. 9, left column), where large areas with strong red color were visible, indicating the formation of calcified areas. Previous reports have indicated that strong spreading of hMSCs resulted in upregulation of genes related to osteogenic differentiation [143]. The results in this study are consistent with previous reports [143], because both cell adhesion and proliferation studies have demonstrated strong spreading of hMSCs on CHI/GEL multilayers [144]. In contrast to this, hMSCs cultured on CHI/HEP grew in aggregates, but did not show significant staining. Weak staining was also observed in cultures on plain PLLA and CHI/HA, indicating limited formation of calcified areas. Interestingly, some weak staining was only found there in nodules formed during long-term culture of hMSCs.

Striking differences were found when hMSCs were cultured on PEM-coated PLLA in osteogenic medium (Fig. 9, right column). Generally, it is anticipated that nodule formation is a consequence of osteogenic differentiation, which seemed to be supported by the more hydrophilic nature of the polyanions HA and HEP. These studies on MSC differentiation demonstrate that the simple coating of PLLA with PEM made of ECM components can lead to a change in the microenvironment of cells, thus promoting the desired differentiation of MSCs into osteoblasts.

5 Summary and Outlook

We summarize here the benefits of using PLA in engineering of skeletal tissues. Bimodal pore architectures can be obtained from freeze-extraction and particle leaching with micro- and macroporosity that enable modulation of permeability and mechanical properties by changing the solvent content and porogen amount. Furthermore, several bulk modifications of PLA (copolymerization, blending, network formation, and composite design) allow the properties of scaffolds to be adapted for different requirements in engineering of bone and cartilage. Although the feasibility of PLLA scaffolds for the culture and differentiation of MSCs into chondrocyte-like cells has been demonstrated [57], combination of PLA with hydrogels seems to be a more powerful strategy for articular cartilage regeneration [103]. Organic–inorganic composite scaffolds of PLA can be optimized as structures for bone replacement, where the filler acts as mechanical reinforcement, confers bioactivity, and neutralizes acidic degradation products of PLA.

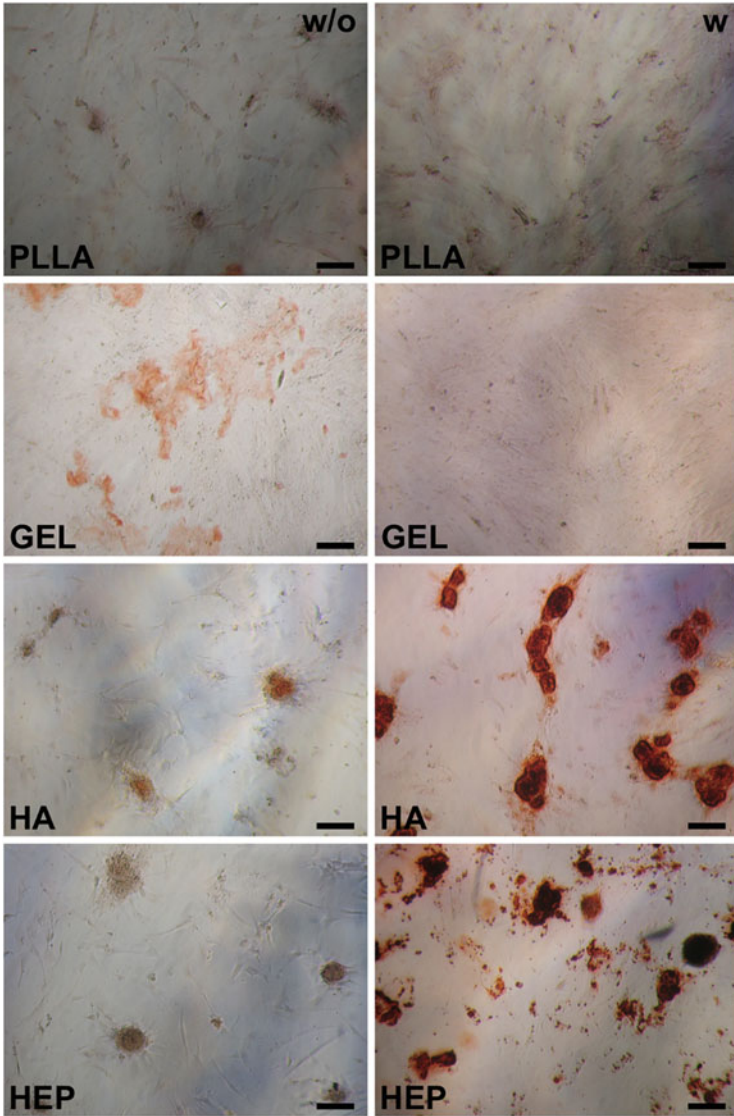


Fig. 9 Alizarin Red staining of human mesenchymal stem cells (hMSCs) cultured on multilayers from gelatine/chitosan (*GEL*), hyaluronan/chitosan (*HA*) and heparin/chitosan (*HEP*) in normal medium (DMEM with 10% FBS, *left*) or osteogenic medium (DMEM, 10% FBS and osteogenic inducer, *right*) after 3 weeks. Note that cells were cultured on the terminal polyanion layers (Scale bar = 100 μ m). Reprinted with permission from [14]

In addition to changing the bulk properties of PLA, different surface modification techniques can be applied to tailor the surfaces for specific applications in tissue engineering. We present simple physical (adsorptive) and chemical modifications that could allow improved adhesion and growth of bone and other cells. In addition, ECM components such as proteins and GAG can be used to change the microenvironment of cells, fostering their differentiation into the desired lineage, such as described here for osteogenic differentiation of hMSCs.

Acknowledgments This work was supported by Marie Curie Industry-Academia Partnerships and Pathways (FP7-PEOPLE-2012-IAPP, with grant agreement PIAP-GA-2012-324386) and IOF-Marie Curie fellowship program (Protodel 331655) as well as the German Research Society (DFG) through Grant GR 1290/10-1 and the Spanish Ministry of Economy and Competitiveness through the MAT2016-76039-C4-1-R Project (including Feder funds).

References

1. Ratner BD, Bryant SJ (2004) Biomaterials: where we have been and where we are going. *Annu Rev Biomed Eng* 6:41–75
2. Fields GB et al. (1998) Proteinlike molecular architecture: biomaterial applications for inducing cellular receptor binding and signal transduction. *Biopolymers* 47(2):143–151
3. Green D et al. (2002) The potential of biomimesis in bone tissue engineering: lessons from the design and synthesis of invertebrate skeletons. *Bone* 30(6):810–815
4. Liu JC, Heilshorn SC, Tirrell DA (2004) Comparative cell response to artificial extracellular matrix proteins containing the RGD and CS5 cell-binding domains. *Biomacromolecules* 5(2):497–504
5. Orive G et al. (2009) Biomaterials for promoting brain protection, repair and regeneration. *Nat Rev Neurosci* 10(9):682–692
6. Williams DF (1999) *The Williams dictionary of biomaterials*. Liverpool University Press, Liverpool
7. Thomson R et al. (1995) Biodegradable polymer scaffolds to regenerate organs. In: Peppas NA, Langer RS (eds) *Biopolymers II*. Springer, Berlin Heidelberg, pp 245–274
8. Jagur-Grodzinski J (2006) Polymers for tissue engineering, medical devices, and regenerative medicine. Concise general review of recent studies. *Polym Adv Technol* 17(6):395–418
9. Gunatillake PA, Adhikari R (2003) Biodegradable synthetic polymers for tissue engineering. *Eur Cell Mater* 5(1):1–16. Discussion 16
10. Shin YM et al. (2008) Modulation of spreading, proliferation, and differentiation of human mesenchymal stem cells on gelatin-immobilized poly(l-lactide-co- ϵ -caprolactone) substrates. *Biomacromolecules* 9(7):1772–1781
11. Akdemir ZS et al. (2008) Photopolymerized injectable RGD-modified fumarated poly(ethylene glycol) diglycidyl ether hydrogels for cell growth. *Macromol Biosci* 8(9):852–862
12. Webb K, Hlady V, Tresco PA (1998) Relative importance of surface wettability and charged functional groups on NIH 3T3 fibroblast attachment, spreading, and cytoskeletal organization. *J Biomed Mater Res* 41(3):422–430
13. Bauer S et al. (2013) Engineering biocompatible implant surfaces: Part I: Materials and surfaces. *Prog Mater Sci* 58(3):261–326
14. Liu Z-M et al. (2010) Synergistic effect of polyelectrolyte multilayers and osteogenic growth medium on differentiation of human mesenchymal stem cells. *Macromol Biosci* 10(9):1043–1054

15. Mikos AG, Temenoff JS (2000) Formation of highly porous biodegradable scaffolds for tissue engineering. *Electron J Biotechnol* 3:114–119
16. Roach P et al. (2007) Modern biomaterials: a review – bulk properties and implications of surface modifications. *J Mater Sci Mater Med* 18(7):1263–1277
17. Sharma B, Elisseff JH (2004) Engineering structurally organized cartilage and bone tissues. *Ann Biomed Eng* 32(1):148–159
18. Ikada Y (2006) Challenges in tissue engineering. *J R Soc Interface* 3(10):589–601
19. Salgado AJ et al. (2006) Influence of molecular weight and crystallinity of poly(L-lactic acid) on the adhesion and proliferation of human osteoblast like cells. *Mater Sci Forum* 514–516: 1020–1024
20. Chen R et al. (2006) The use of poly(L-lactide) and RGD modified microspheres as cell carriers in a flow intermittency bioreactor for tissue engineering cartilage. *Biomaterials* 27(25):4453–4460
21. Richardson SM et al. (2006) The differentiation of bone marrow mesenchymal stem cells into chondrocyte-like cells on poly-L-lactic acid (PLLA) scaffolds. *Biomaterials* 27(22): 4069–4078
22. Yan H, Yu C (2007) Repair of full-thickness cartilage defects with cells of different origin in a rabbit model. *Arthroscopy* 23(2):178–187
23. Farah S, Anderson DG, Langer R (2016) Physical and mechanical properties of PLA, and their functions in widespread applications – a comprehensive review. *Adv Drug Deliv Rev* 107:367–392
24. Liu ZM et al. (2010) Biocompatibility of poly(L-lactide) films modified with poly(ethylene imine) and polyelectrolyte multilayers. *J Biomater Sci Polym Ed* 21(6):893–912
25. Moffa M et al. (2013) Microvascular endothelial cell spreading and proliferation on nano-fibrous scaffolds by polymer blends with enhanced wettability. *Soft Matter* 9(23): 5529–5539
26. Fernández JM et al. (2016) Biodegradable polyester networks including hydrophilic groups favor BMSCs differentiation and can be eroded by macrophage action. *Polym Degrad Stab* 130:38–46
27. Drumright RE, Gruber PR, Henton DE (2000) Polylactic acid technology. *Adv Mater* 12(23): 1841–1846
28. Middleton JC, Tipton AJ (2000) Synthetic biodegradable polymers as orthopedic devices. *Biomaterials* 21(23):2335–2346
29. Hakkarainen M (2002) Aliphatic polyesters: abiotic and biotic degradation and degradation products. *Adv Polym Sci* 157:113–138
30. Williams DF, Mort E (1977) Enzyme-accelerated hydrolysis of polyglycolic acid. *J Bioeng* 1(3):231–238
31. Vert M et al. (1984) Bioresorbable plastic materials for bone surgery. In: Hastings G, Ducheyne P (eds) *Macromolecular biomaterials*. CRC series in structure-property relationship of biomaterials. CRC, Boca Raton, pp 119–142
32. Hubbell JA (1995) Biomaterials in tissue engineering. *Biotechnology (N Y)* 13(6):565–576
33. Santamaria VA et al. (2012) Influence of the macro and micro-porous structure on the mechanical behavior of poly(L-lactic acid) scaffolds. *J Non-Cryst Solids* 358(23):3141–3149
34. Kojima N, Matsuo T, Sakai Y (2006) Rapid hepatic cell attachment onto biodegradable polymer surfaces without toxicity using an avidin-biotin binding system. *Biomaterials* 27(28):4904–4910
35. Yu GH, Fan YB (2008) Preparation of poly(D,L-lactic acid) scaffolds using alginate particles. *J Biomater Sci Polym Ed* 19(1):87–98
36. Garric X et al. (2005) Human skin cell cultures onto PLA50 (PDLLA) bioresorbable polymers: influence of chemical and morphological surface modifications. *J Biomed Mater Res A* 72(2):180–189
37. Pihlajamaki H et al. (1994) Tissue-implant interface at an absorbable fracture fixation plug made of polylactide in cancellous bone of distal rabbit femur. *Arch Orthop Trauma Surg* 113(2):101–105

38. Rahman MS, Tsuchiya T (2001) Enhancement of chondrogenic differentiation of human articular chondrocytes by biodegradable polymers. *Tissue Eng* 7(6):781–790
39. Miyata T, Masuko T (1998) Crystallization behaviour of poly(L-lactide). *Polymer* 39(22):5515–5521
40. Wang Y et al. (2005) Morphological contributions to glass transition in poly(l-lactic acid). *Macromolecules* 38(11):4712–4718
41. Salmerón Sánchez M et al. (2007) Effect of the cooling rate on the nucleation kinetics of poly(l-lactic acid) and its influence on morphology. *Macromolecules* 40(22):7989–7997
42. Costa Martínez E et al. (2007) Effect of poly(L-lactide) surface topography on the morphology of in vitro cultured human articular chondrocytes. *J Mater Sci Mater Med* 18(8):1627–1632
43. Li S, Garreau H, Vert M (1990) Structure-property relationships in the case of the degradation of massive poly(α -hydroxy acids) in aqueous media. *J Mater Sci Mater Med* 1(4):198–206
44. Tsuji H, Mizuno A, Ikada Y (2000) Properties and morphology of poly(L-lactide). III. Effects of initial crystallinity on long-term in vitro hydrolysis of high molecular weight poly(L-lactide) film in phosphate-buffered solution. *J Appl Polym Sci* 77(7):1452–1464
45. Deplaine H et al. (2014) Evolution of the properties of a poly(l-lactic acid) scaffold with double porosity during in vitro degradation in a phosphate-buffered saline solution. *J Appl Polym Sci* 131(20):40956
46. Tan W, Krishnaraj R, Desai TA (2001) Evaluation of nanostructured composite collagen–chitosan matrices for tissue engineering. *Tissue Eng* 7(2):203–210
47. Taylor MS et al. (1994) Six bioabsorbable polymers: in vitro acute toxicity of accumulated degradation products. *J Appl Biomater* 5(2):151–157
48. Gibbons D (1992) Tissue response to resorbable synthetic polymers. Degradation phenomena on polymeric biomaterials. Springer, Berlin Heidelberg, pp 97–105
49. Hasirci V et al. (2001) Versatility of biodegradable biopolymers: degradability and an in vivo application. *J Biotechnol* 86(2):135–150
50. Nieminen T et al. (2008) Degradative and mechanical properties of a novel resorbable plating system during a 3-year follow-up in vivo and in vitro. *J Mater Sci Mater Med* 19(3):1155–1163
51. Tzoneva R et al. (2002) Remodeling of fibrinogen by endothelial cells in dependence on fibronectin matrix assembly. Effect of substratum wettability. *J Mater Sci Mater Med* 13(12):1235–1244
52. Altankov G, Groth T (1994) Reorganization of substratum-bound fibronectin on hydrophilic and hydrophobic materials is related to biocompatibility. *J Mater Sci Mater Med* 5(9–10):732–737
53. Faucheux N et al. (2004) Self-assembled monolayers with different terminating groups as model substrates for cell adhesion studies. *Biomaterials* 25(14):2721–2730
54. Choi YJ et al. (2005) Evaluations of blood compatibility via protein adsorption treatment of the vascular scaffold surfaces fabricated with polylactide and surface-modified expanded polytetrafluoroethylene for tissue engineering applications. *J Biomed Mater Res A* 75(4):824–831
55. Kim BS, Mooney DJ (1998) Development of biocompatible synthetic extracellular matrices for tissue engineering. *Trends Biotechnol* 16(5):224–230
56. Gamboa-Martínez TC, Ribelles JLG, Ferrer GG (2011) Fibrin coating on poly(L-lactide) scaffolds for tissue engineering. *J Bioact Compat Polym* 26(5):464–477
57. Izal I et al. (2013) Culture of human bone marrow-derived mesenchymal stem cells on poly(L-lactic acid) scaffolds: potential application for the tissue engineering of cartilage. *Knee Surg Sports Traumatol Arthrosc* 21(8):1737–1750
58. Huang BJ, Hu JC, Athanasiou KA (2016) Cell-based tissue engineering strategies used in the clinical repair of articular cartilage. *Biomaterials* 98:1–22
59. Arkudas A et al. (2015) Characterisation of vascularisation of scaffolds for tissue engineering. *Mater Sci Technol* 31(2):180–187

60. Rezwan K et al. (2006) Biodegradable and bioactive porous polymer/inorganic composite scaffolds for bone tissue engineering. *Biomaterials* 27:3413–3431
61. Gamboa-Martínez TC et al. (2013) Chondrocytes cultured in an adhesive macroporous scaffold subjected to stirred flow bioreactor behave like in static culture. *J Biomater Tissue Eng* 3(3):312–319
62. Ghosh S et al. (2008) Bi-layered constructs based on poly(L-lactic acid) and starch for tissue engineering of osteochondral defects. *Mater Sci Eng C Biomim Supramol Syst* 28(1):80–86
63. Verhaegen J et al. (2015) TruFit plug for repair of osteochondral defects-where is the evidence? Systematic review of literature. *Cartilage* 6(1):12–19
64. Vikingsson L et al. (2015) Implantation of a polycaprolactone scaffold with subchondral bone anchoring ameliorates nodules formation and other tissue alterations. *Int J Artif Organs* 38(12):659–666
65. Huang SY, Jiang SC (2014) Structures and morphologies of biocompatible and biodegradable block copolymers. *RSC Adv* 4(47):24566–24583
66. Gentile P et al. (2014) An overview of poly(lactic-co-glycolic) acid (PLGA)-based biomaterials for bone tissue engineering. *Int J Mol Sci* 15(3):3640–3659
67. Makadia HK, Siegel SJ (2011) Poly lactic-co-glycolic acid (PLGA) as biodegradable controlled drug delivery carrier. *Polymers (Basel)* 3(3):1377–1397
68. Park PIP, Jonnalagadda S (2006) Predictors of glass transition in the biodegradable polylactide and poly-lactide-co-glycolide polymers. *J Appl Polym Sci* 100(3):1983–1987
69. Alexis F (2005) Factors affecting the degradation and drug-release mechanism of poly(lactic acid) and poly[(lactic acid)-co-(glycolic acid)]. *Polym Int* 54(1):36–46
70. Singh G et al. (2014) Recent biomedical applications and patents on biodegradable polymer-PLGA. *Int J Pharmacol Pharm Sci* 1:30–42
71. Wang S, Cui W, Bei J (2005) Bulk and surface modifications of polylactide. *Anal Bioanal Chem* 381(3):547–556
72. Pang X et al. (2010) Polylactic acid (PLA): research, development and industrialization. *Biotechnol J* 5(11):1125–1136
73. Cohn D, Salomon AH (2005) Designing biodegradable multiblock PCL/PLA thermoplastic elastomers. *Biomaterials* 26(15):2297–2305
74. Jung Y et al. (2008) Cartilage regeneration with highly-elastic three-dimensional scaffolds prepared from biodegradable poly(L-lactide-co-epsilon-caprolactone). *Biomaterials* 29(35):4630–4636
75. Lins LC et al. (2016) Development of bioresorbable hydrophilic-hydrophobic electrospun scaffolds for neural tissue engineering. *Biomacromolecules* 17(10):3172–3187
76. Huh KM, Bae YH (1999) Synthesis and characterization of poly(ethylene glycol)/poly(L-lactic acid) alternating multiblock copolymers. *Polymer* 40(22):6147–6155
77. Li F, Li S, Vert M (2005) Synthesis and rheological properties of polylactide/poly(ethylene glycol) multiblock copolymers. *Macromol Biosci* 5(11):1125–1131
78. Cai Q et al. (2003) Synthesis and characterization of biodegradable polylactide-grafted dextran and its application as compatilizer. *Biomaterials* 24(20):3555–3562
79. Pitarresi G et al. (2013) Injectable in situ forming microgels of hyaluronic acid-g-polylactic acid for methylprednisolone release. *Eur Polym J* 49(3):718–725
80. Konwar DB, Jacob J, Satapathy BK (2016) A comparative study of poly(l-lactide)-block-poly(E-caprolactone) six-armed star diblock copolymers and polylactide/poly(E-caprolactone) blends. *Polym Int* 65(9):1107–1117
81. Zeng J-B, Li K-A, Du A-K (2015) Compatibilization strategies in poly(lactic acid)-based blends. *RSC Adv* 5(41):32546–32565
82. Ikada Y et al. (1987) Stereocomplex formation between enantiomeric poly(lactides). *Macromolecules* 20(4):904–906
83. Goonoo N, Bhaw-Luximon A, Jhurry D (2015) Biodegradable polymer blends: miscibility, physicochemical properties and biological response of scaffolds. *Polym Int* 64(10):1289–1302

84. Lopez-Rodriguez N et al. (2014) Improvement of toughness by stereocomplex crystal formation in optically pure polylactides of high molecular weight. *J Mech Behav Biomed Mater* 37:219–225
85. Ishii D et al. (2009) In vivo tissue response and degradation behavior of PLLA and stereo-complexed PLA nanofibers. *Biomacromolecules* 10(2):237–242
86. You Y et al. (2006) Preparation of porous ultrafine PGA fibers via selective dissolution of electrospun PGA/PLA blend fibers. *Mater Lett* 60(6):757–760
87. Carmagnola I et al. (2014) Poly(lactic acid)-based blends with tailored physicochemical properties for tissue engineering applications: a case study. *Int J Polym Mater Polym Biomater* 64(2):90–98
88. Vilay V et al. (2009) Characterization of the mechanical and thermal properties and morphological behavior of biodegradable poly(L-lactide)/poly(ϵ -caprolactone) and poly(L-lactide)/poly(butylene succinate-co-L-lactate) polymeric blends. *J Appl Polym Sci* 114: 1784–1792
89. Choi NS et al. (2002) Morphology and hydrolysis of PCL/PLLA blends compatibilized with P(LLA-co- ϵ -CL) or P(LLA-b- ϵ -CL). *J Appl Polym Sci* 86(8):1892–1898
90. Wang BY et al. (2012) Electrospun polylactide/poly(ethylene glycol) hybrid fibrous scaffolds for tissue engineering. *J Biomed Mater Res A* 100(2):441–449
91. Zhang W et al. (2013) Processing and characterization of supercritical CO₂ batch foamed poly(lactic acid)/poly(ethylene glycol) scaffold for tissue engineering application. *J Appl Polym Sci* 130(5):3066–3073
92. Serra T et al. (2014) Relevance of PEG in PLA-based blends for tissue engineering 3D-printed scaffolds. *Mater Sci Eng C Mater Biol Appl* 38:55–62
93. Chen C, Dong L, Cheung MK (2005) Preparation and characterization of biodegradable poly(L-lactide)/chitosan blends. *Eur Polym J* 41(5):958–966
94. Duarte ARC, Mano JF, Reis RL (2009) Preparation of starch-based scaffolds for tissue engineering by supercritical immersion precipitation. *J Supercrit Fluids* 49(2):279–285
95. Zhao X, Liu W, Yao K (2006) Preparation and characterization of biocompatible poly(L-lactic acid)/gelatin blend membrane. *J Appl Polym Sci* 101(1):269–276
96. Kim HW, Yu HS, Lee HH (2008) Nanofibrous matrices of poly(lactic acid) and gelatin polymeric blends for the improvement of cellular responses. *J Biomed Mater Res A* 87(1):25–32
97. Ferreira BMP, Zavaglia CAC, Duek EAR (2002) Films of PLLA/PHBV: thermal, morphological, and mechanical characterization. *J Appl Polym Sci* 86(11):2898–2906
98. Santos Jr AR et al. (2004) Differentiation pattern of Vero cells cultured on poly(L-lactic acid)/poly(hydroxybutyrate-co-hydroxyvalerate) blends. *Artif Organs* 28(4):381–389
99. Diego RB et al. (2005) Acrylic scaffolds with interconnected spherical pores and controlled hydrophilicity for tissue engineering. *J Mater Sci Mater Med* 16(8):693–698
100. Escobar Ivirico JL et al. (2009) Poly(L-lactide) networks with tailored water sorption. *Colloid Polym Sci* 287(6):671–681
101. Ivirico JLE et al. (2011) Biodegradable poly(L-lactide) and polycaprolactone block copolymer networks. *Polym Int* 60(2):264–270
102. Ivirico JL et al. (2009) Proliferation and differentiation of goat bone marrow stromal cells in 3D scaffolds with tunable hydrophilicity. *J Biomed Mater Res B Appl Biomater* 91(1): 277–286
103. Olmedilla MP et al. (2012) In vitro 3D culture of human chondrocytes using modified ϵ -caprolactone scaffolds with varying hydrophilicity and porosity. *J Biomater Appl* 27(3):299–309
104. Kim S et al. (2014) In vitro evaluation of photo-crosslinkable chitosan-lactide hydrogels for bone tissue engineering. *J Biomed Mater Res B Appl Biomater* 102(7):1393–1406
105. Benoit DS, Durney AR, Anseth KS (2006) Manipulations in hydrogel degradation behavior enhance osteoblast function and mineralized tissue formation. *Tissue Eng* 12(6):1663–1673
106. Kang Z et al. (2017) Preparation of polymer/calcium phosphate porous composite as bone tissue scaffolds. *Mater Sci Eng C Mater Biol Appl* 70(Pt 2):1125–1131

107. Stevens MM (2008) Biomaterials for bone tissue engineering. *Mater Today* 11:18–25
108. Tajbaksh S, Hajiali F (2017) A comprehensive study on the fabrication and properties of biocomposites of poly(lactic acid)/ceramics for bone tissue engineering. *Mater Sci Eng C Mater Biol Appl* 70(Pt 1):897–912
109. Supova M (2009) Problem of hydroxyapatite dispersion in polymer matrices: a review. *J Mater Sci Mater Med* 20(6):1201–1213
110. Deplaine H, Ribelles JLG, Ferrer GG (2010) Effect of the content of hydroxyapatite nanoparticles on the properties and bioactivity of poly(L-lactide) – hybrid membranes. *Compos Sci Technol* 70(13):1805–1812
111. Deplaine H et al. (2013) Biomimetic hydroxyapatite coating on pore walls improves osteo-integration of poly(L-lactic acid) scaffolds. *J Biomed Mater Res B Appl Biomater* 101(1): 173–186
112. He JQ et al. (2012) Hydroxyapatite-poly(L-lactide) nanohybrids via surface-initiated ATRP for improving bone-like apatite-formation abilities. *Appl Surf Sci* 258(18):6823–6830
113. Yan S et al. (2011) Apatite-forming ability of bioactive poly(l-lactic acid)/grafted silica nanocomposites in simulated body fluid. *Colloids Surf B Biointerfaces* 86(1):218–224
114. Guerzoni S et al. (2014) Combination of silica nanoparticles with hydroxyapatite reinforces poly(L-lactide acid) scaffolds without loss of bioactivity. *J Bioact Compat Polym* 29(1): 15–31
115. Erggelet C et al. (2010) Autologous chondrocyte implantation versus ACI using 3D-bioresorbable graft for the treatment of large full-thickness cartilage lesions of the knee. *Arch Orthop Trauma Surg* 130(8):957–964
116. Jeuken RM et al. (2016) Polymers in cartilage defect repair of the knee: current status and future prospects. *Polymers* 8:219
117. Serino G et al. (2003) Ridge preservation following tooth extraction using a polylactide and polyglycolide sponge as space filler: a clinical and histological study in humans. *Clin Oral Implants Res* 14(5):651–658
118. Walsh WR et al. (2015) Long-term in-vivo evaluation of a resorbable PLLA scaffold for regeneration of the ACL. *Orthop J Sports Med* 3(7 Suppl 2):2325967115S00033
119. Groth T et al. (2010) Chemical and physical modifications of biomaterial surfaces to control adhesion of cells. In: Shastri VP, Altankov G, Lendlein A (eds) *Advances in regenerative medicine: role of nanotechnology, and engineering principles*. Springer Netherlands, Dordrecht, pp 253–284
120. Silva JM, Reis RL, Mano JF (2016) Biomimetic extracellular environment based on natural origin polyelectrolyte multilayers. *Small* 12(32):4308–4342
121. Zhao M et al. (2014) Improved stability and cell response by intrinsic cross-linking of multilayers from collagen I and oxidized glycosaminoglycans. *Biomacromolecules* 15(11): 4272–4280
122. Hoffman AS (1996) Surface modification of polymers: physical, chemical, mechanical and biological methods. *Macromol Symp* 101(1):443–454
123. Hamerli P et al. (2003) Enhanced tissue-compatibility of polyethyleneterephthalat membranes by plasma aminofunctionalisation. *Surf Coat Technol* 174–175:574–578
124. Hamerli P et al. (2003) Surface properties of and cell adhesion onto allylamine-plasma-coated polyethyleneterephthalat membranes. *Biomaterials* 24(22):3989–3999
125. Seifert B, Romaniuk P, Groth T (1996) Bioresorbable, heparinized polymers for stent coating: in vitro studies on heparinization efficiency, maintenance of anticoagulant properties and improvement of stent haemocompatibility. *J Mater Sci Mater Med* 7(8):465–469
126. Seifert B, Romaniuk P, Groth T (1997) Covalent immobilization of hirudin improves the haemocompatibility of polylactide-polyglycolide in vitro. *Biomaterials* 18(22):1495–1502
127. Cheng Y et al. (2009) Poly(lactic acid) (PLA) synthesis and modifications: a review. *Front Chem Chin* 4(3):259–264
128. Trimper C et al. (2006) Poly(ether imide) membranes modified with poly(ethylene imine) as potential carriers for epidermal substitutes. *Macromol Biosci* 6(4):274–284

129. Liu ZM et al. (2009) Immobilization of poly(ethylene imine) on poly(l-lactide) promotes MG63 cell proliferation and function. *J Mater Sci Mater Med* 20(11):2317–2326
130. Franceschi RT, James WM, Zerlauth G (1985) 1α , 25-Dihydroxyvitamin D3 specific regulation of growth, morphology, and fibronectin in a human osteosarcoma cell line. *J Cell Physiol* 123(3):401–409
131. Farley JR, Baylink DJ (1986) Skeletal alkaline phosphatase activity as a bone formation index in vitro. *Metabolism* 35(6):563–571
132. Zur Nieden NI, Kempka G, Ahr HJ (2003) In vitro differentiation of embryonic stem cells into mineralized osteoblasts. *Differentiation* 71(1):18–27
133. Niepel MS et al. (2009) pH-dependent modulation of fibroblast adhesion on multilayers composed of poly(ethylene imine) and heparin. *Biomaterials* 30(28):4939–4947
134. Brunot C et al. (2007) Cytotoxicity of polyethyleneimine (PEI), precursor base layer of polyelectrolyte multilayer films. *Biomaterials* 28(4):632–640
135. Richardson JJ, Bjornmalm M, Caruso F (2015) Multilayer assembly. Technology-driven layer-by-layer assembly of nanofilms. *Science* 348(6233):aaa2491
136. Hammond PT (2012) Building biomedical materials layer-by-layer. *Mater Today* 15(5):196–206
137. Moehwald H, Brezesinski G (2016) From Langmuir monolayers to multilayer films. *Langmuir* 32(41):10445–10458
138. Muraglia A, Cancedda R, Quarto R (2000) Clonal mesenchymal progenitors from human bone marrow differentiate in vitro according to a hierarchical model. *J Cell Sci* 113(7):1161
139. Friedenstein AJ et al. (1974) Precursors for fibroblasts in different populations of hematopoietic cells as detected by the in vitro colony assay method. *Exp Hematol* 2(2):83–92
140. Liu Z-J, Zhuge Y, Velazquez OC (2009) Trafficking and differentiation of mesenchymal stem cells. *J Cell Biochem* 106(6):984–991
141. Jäger M et al. (2005) Proliferation and osteogenic differentiation of mesenchymal stem cells cultured onto three different polymers in vitro. *Ann Biomed Eng* 33(10):1319–1332
142. McBride SH, Knothe Tate ML (2008) Modulation of stem cell shape and fate a: the role of density and seeding protocol on nucleus shape and gene expression. *Tissue Eng A* 14(9):1561–1572
143. McBeath R et al. (2004) Cell shape, cytoskeletal tension, and RhoA regulate stem cell lineage commitment. *Dev Cell* 6(4):483–495
144. Sun XJ et al. (2008) In vitro proliferation and differentiation of human mesenchymal stem cells cultured in autologous plasma derived from bone marrow. *Tissue Eng A* 14(3):391–400

Poly(lactic acid) Controlled Drug Delivery



Jiannan Li, Jianxun Ding, Tongjun Liu, Jessica F. Liu, Lesan Yan,
and Xuesi Chen

Abstract Various drug delivery systems are being rapidly developed for controlled drug release, improved efficacy, and reduced side effects with the goal of improving quality of life for patients and curing disease. Poly(lactic acid) (PLA) possesses numerous advantages compared with other polymers, including biocompatibility, biodegradability, low cost, environmental friendliness, and easily modified mechanical properties. These properties make PLA a promising polymer for biomedical applications. This review introduces the specific characteristics of PLA that enable its application for controlled drug delivery and describes different forms of PLA used for drug delivery, including nanoparticles, microspheres, hydrogels, electrospun fibers, and scaffolds. Previous work is summarized and future development is discussed.

Keywords Controlled drug release • Electrospun fiber • Hydrogel • Microparticle • Nanoparticle • Poly(lactic acid) • Scaffold

J. Li

Key Laboratory of Polymer Ecomaterials, Changchun Institute of Applied Chemistry, Chinese Academy of Science, Changchun 130022, People's Republic of China

Department of General Surgery, The Second Hospital of Jilin University, Changchun 130041, People's Republic of China

J. Ding (✉) and X. Chen

Key Laboratory of Polymer Ecomaterials, Changchun Institute of Applied Chemistry, Chinese Academy of Science, Changchun 130022, People's Republic of China

e-mail: jxding@ciac.ac.cn

T. Liu

Department of General Surgery, The Second Hospital of Jilin University, Changchun 130041, People's Republic of China

J.F. Liu and L. Yan

Department of Bioengineering, University of Pennsylvania, Philadelphia, PA 19104-6321, USA

Contents

1	Introduction	110
2	PLA-Based Carriers for Drug Delivery	114
2.1	Nanoparticles	114
2.2	Microspheres	119
2.3	Hydrogels	122
2.4	Electrospun Fibers	124
2.5	Scaffolds	126
3	Conclusions and Perspectives	128
	References	129

1 Introduction

There are serious problems associated with the therapeutic use of small molecule drugs (SMDs), including insolubility, instability (e.g., rapid degradation in physiological environments), sequestration within the blood space by endothelial barriers, and poor uptake by tissues and cells [1–3]. A wide variety of drug delivery systems (DDSs) have been designed to overcome these challenges, which are of crucial importance in healthcare and clinical applications [3–7]. Drug delivery is a process, by which specific drugs are delivered to a target area in the organism (i.e., animals or humans) to achieve a therapeutic effect [8]. Controlled DDSs can be specially designed to increase the solubility of SMDs, improve stability by preventing SMD degradation under physiological conditions, reduce side effects by targeting the lesion regions without affecting healthy sites, and maintain sustained drug release at optimal doses [9, 10]. Moreover, the use of DDSs removes the need for frequent administration, which is the primary cause of various degrees of bodily injury. As a result, DDSs have shown significant efficacy in improving quality of life in patients. Packaging an existing clinically approved drug into an effective delivery system as an advanced formulation can also reduce the economic cost and time required for new drug development.

In controlled DDSs, the carriers are as important as the bioactive drugs. Successful delivery of drugs to target tissues requires that the carriers sustain good stability during administration. Additionally, these carriers should be biocompatible. A variety of polymers, including natural and synthetic polymers, can serve as drug carriers, but few can meet the requirements of acceptable biocompatibility, biodegradability, and absorbability [9, 11]. Recently, the field has begun to pay more attention to the use of biodegradable polymers as drug carriers because of their extraordinary performance [9, 12]. Many forms of carriers, including nanoparticles (NPs), microspheres, hydrogels, electrospun fibers, and scaffolds, have been investigated for the delivery of different types of drugs or for adaptation to different situations in *in vivo* microenvironments.

Among the numerous biodegradable polymers that have been used as drug carriers, poly(lactic acid) (PLA) is one of the most promising candidates (Fig. 1).

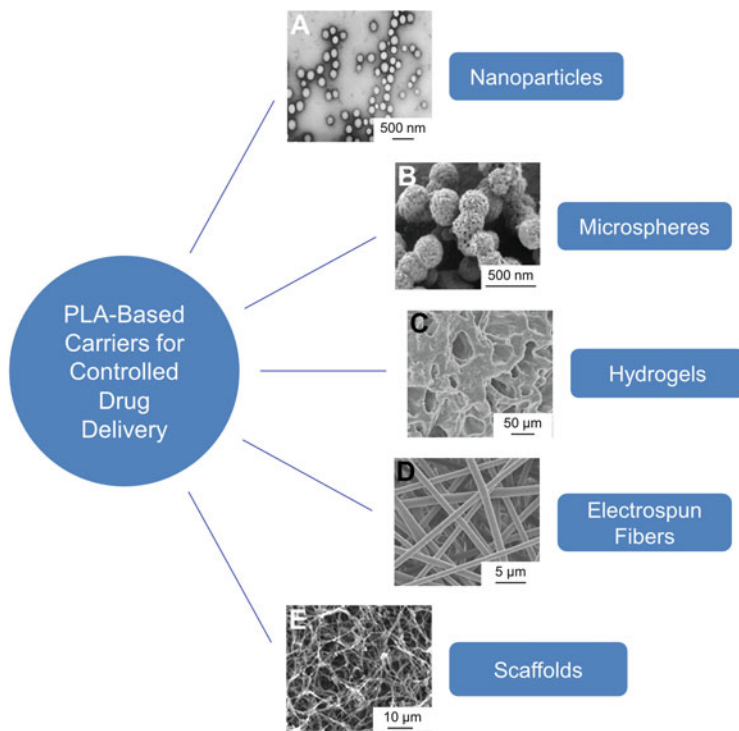


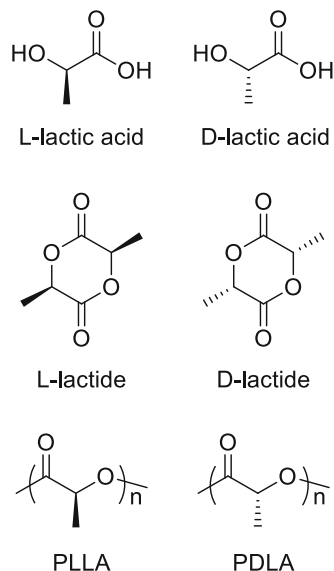
Fig. 1 PLA-based carriers for controlled drug delivery. (a) TEM image of PLA nanoparticles [13]. (b–e) SEM images of (b) microspheres [15], (c) hydrogels [119], (d) electrospun fibers [17], and (e) scaffolds [18]. Reproduced from [13] with permission of Springer, from [15, 119] with permission of Elsevier, from [17] with permission of American Chemical Society, and from [18] with permission of John Wiley and Sons, respectively

PLA can be fabricated into various forms for controlled drug release, including NPs [13, 14], microspheres [15], hydrogels [16], electrospun fibers [17], and scaffolds [18]. Its various advantages include being environmentally friendly, existing in multiple forms, exhibiting good biocompatibility and biodegradability, sustaining long drug retention times, having easily modified mechanical properties, and being low cost [19, 20].

PLA is derived from renewable sources, such as sugar, maize, potato, sugarcane, and beet [21]. It is prepared by different polymerizations of lactic acid, which is in turn typically produced by bacterial fermentation [22] or glycolysis [23], with little environmental pollution. Furthermore, lactic acid, the degradation product of PLA, can be removed completely *in vivo*. Therefore, PLA is a green biomaterial.

Lactic acid is a chiral molecule existing as L and D isomers (Fig. 2). PLA exists primarily in three forms: poly(L-lactic acid) (PLLA), poly(D-lactic acid) (PDLA), and poly(D,L-lactic acid) (PDLLA) [22, 24, 25]. Of these, PLLA has attracted the most attention in DDSs as a result of its favorable mechanical properties. However,

Fig. 2 Chemical structures of L-lactic acid, D-lactic acid, L-lactide, D-lactide, PLLA, and PDLA



because PLLA has a long degradation time and is therefore likely to cause inflammatory responses *in vivo*, it is often used in combination with polymerization of D, L-lactide monomers [22, 26].

Biocompatibility is a highly desirable trait in DDSs and has been the focus of much research. PLA is biodegradable with high biocompatibility and does not circulate *in vivo* for extended periods of time. Although PLA is hydrophobic, it can undergo scission, primarily by hydrolysis, to monomeric units of lactic acid *in vivo* even in the absence of enzymes [21]. This degradation process leaves no foreign or toxic substances because lactic acid is a natural intermediate of carbohydrate metabolism [27, 28]. As a result, PLA is highly biocompatible, biodegradable, and bioresorbable *in vivo*.

Another advantage of biodegradable PLA DDSs is their long retention time. Compared with other polymers, PLA possesses better biodegradability, which is relatively moderate and can be properly controlled. This biodegradability mainly relies on the crystallinity, morphology, and relative molecular mass of the polymer [20]. PLA tends to be crystalline when the PLLA content is higher than 90%, whereas the less optically pure form is amorphous [22]. Auras et al. [29] reported that the densities of solid PLLA, PDLLA, crystalline PLA, and amorphous PLA are 1.36, 1.33, 1.36, and 1.25 g cm⁻³, respectively. PLA of low molecular weight is preferred for use as a drug carrier because it has a shorter degradation time, giving better release properties [30]. For drug carriers composed of nondegradable polymers, the drug release rate slows gradually with a reduction in the amount of encapsulated drug. PLA systems avoid this problem because the structure of PLA gradually loosens with continued degradation *in vivo*. As a result, the resistance to drug diffusion out of the PLA carrier is reduced, and the drug release rate is

upregulated. Because the increased drug release rate counteracts the reduced drug concentration, a long-term constant release of drug from the carrier can be achieved [31].

The chemical and physical properties of PLA, especially its biocompatibility and biodegradability, are easily influenced by adding different surfactants or changing the molecular weight, size, shape, temperature, and moisture [21, 22, 29]. This enables the creation of desired DDSs under specific conditions with different formulations [32–38]. It is also possible to control the distribution and release behavior of drugs in the PLA devices. As a typical example, Fernandez et al. [39] extracted proanthocyanidins from grapes and stabilized them with PDLA using an emulsion-evaporation method. They evaluated three factors in the formulation: sonication time for the emulsion process, loading of grape extracts, and concentration of stabilizing agent. They concluded that the extract load and stabilizer concentration were closely related to the properties of this drug model. Wei et al. [25] loaded oxaliplatin (OXA) into NP and compared the drug delivery characteristics of poly(ethylene glycol) (PEG)–PLA NP with that of PLA-only NP. They found that the OXA concentration in the tumor in the PEG–PLA NP group was higher than that in the PLA NP group. Furthermore, less OXA accumulated in the liver and lungs after PEG–PLA NP was administered. The results indicated that the PEG-modified platform possessed good drug retention ability and could deliver more drugs to the target sites. Many others have demonstrated that PEG can resist nonspecific absorption of proteins in the blood [40–44]. However, PEG has some limitations as a coating for PLA DDSs, particularly in achieving effective PEG surface densities [45, 46]. To combat this problem, Deng et al. [47] applied hyperbranched polyglycerol (HPG) as an alternative coating of PLA NP. They found that the antitumor agent camptothecin (CPT) had a longer blood circulation time, higher stability, less accumulation in the liver, and better therapeutic effectiveness against tumors in the HPG–PLA NP group than that in the PEG–PLA NP group. They concluded that HPG is a better surface coating for NPs than PEG for applications in drug delivery. In a study performed by Yamakawa et al. [48], neurotensin analogue-loaded PDLLA microspheres with different PLA molecular weights were prepared. The authors found that when the molecular weight changed, the rate of initial burst and the length of time, over which the drug was released, varied. Zeng et al. [49] examined the influence of surfactants on the diameter of electrospun PLLA fibers by adding cationic, anionic, and nonionic surfactants, that is, triethyl benzyl ammonium chloride, sodium dodecyl sulfate, and aliphatic PPO–PEO ether, respectively. Rifampin (RIF; a drug for tuberculosis) and paclitaxel (PTX; an anticancer drug) were used as model drugs and loaded into PLLA fibers. It was revealed that the addition of each of the three types of surfactant could reduce the diameter and narrow the distribution of electrospun fibers. Furthermore, RIF contained in these fibrous mats could be released constantly with no burst release behavior.

All the advantages of PLA make it a popular drug carrier matrix, and it has been approved by the Food and Drug Administration (FDA) for in vivo applications in humans [21]. The next section gives details on different forms of PLA for

controlled drug delivery, including NPs, microspheres, hydrogels, electrospun fibers, and scaffolds.

2 PLA-Based Carriers for Drug Delivery

With the assistance of DDSs, it is possible to achieve a much greater therapeutic effect for many clinical applications, including a reduced pain burden and improved quality of life. It is also possible to limit side effects by controlling drug release rate and specifically transporting drugs to target sites [50]. A variety of advanced delivery systems have been developed to achieve high efficiency and safety in drug delivery and overcome the disadvantages of traditional formulations [24, 25]. The biomedical applications of PLA-based drug carriers discussed in this section are summarized in Table 1.

2.1 Nanoparticles

NPs are spherical skeletons composed of polymer matrix, with diameters ranging from 1 to 500 nm.

2.1.1 Properties

Of the various categories of drug carrier systems, NPs have attracted the most attention because of their unique properties [34, 51]. NPs have many advantages compared with other DDS formulations. First, NPs have a high drug retention rate, which can prevent inactivation *in vivo*; second, NPs allow well-controlled drug distribution by delivering drugs to disease sites with few side effects in other areas; and third, NPs allow long-term drug release [52, 53]. A variety of biocompatible and biodegradable biomaterials, especially PLA, have been used as raw materials for NPs, thereby increasing their clinical utility.

2.1.2 Applications

PLA NPs have been the subject of much interest as DDSs to access the central nervous system (CNS) [54]. The blood–brain barrier (BBB) is a significant challenge for drug delivery to the CNS, because it is composed of special endothelial cells that form tight junctions, blocking drug transport into the CNS [34, 52]. Drugs are typically unable to pass through the BBB in free form [34]. However, by varying the molecular weight of PLA and using surfactants or surface modifications, the PLA NPs loaded with different drugs can be successfully delivered to the CNS. For example, Liu et al. [13] prepared the breviscapine (BVP)-loaded PDLLA NPs of different sizes and investigated the distribution of BVP in rats. The mean

Table 1 PLA-based carriers for drug delivery

Category	Polymer	Drug	Application	Reference
NPs	PDLLA	BVP	Penetrating BBB	[13]
	PLLA	Ritonavir (RIT)	Penetrating BBB	[55]
	PLA	MTX	Intranasal delivery	[61]
	PLA	Endostar	Cancer therapy	[63]
	PEG–PDLLA	IFF	Cancer diagnosis	[64]
	PEG–PDLLA	PTX and RAP	Cancer therapy	[65]
	PLA	BF ₂ dbmPLA	Cell imaging	[72]
	PEG–PLA	TNF α	Inflammatory bowel disease	[73]
	PEG–PLA	TNF α	Inflammatory bowel disease	[73]
	PLA	TC	Antibacterial	[74]
	PEG–PLA	Minocycline (MC)	Periodontitis	[44]
	PLA/PLGA	TC	Periodontitis	[76]
	PLA	Bone morphogenic protein 2 (BMP-2)	Bone repair	[77]
	PLA	Betamethasone phosphate (BMS)	Autoimmune uveoretinitis	[79]
	PEG–PLA	Bis-triazole DO870	Chagas disease	[80]
Microspheres	PLLA–PEG–PLLA	MTX	Cancer therapy	[97]
	Dextran/PLGA–PLA	rIL-2	Cancer therapy	[98]
	PDLLA	Epirubicin (EPI)	Cancer therapy	[99]
	PLLA	5-FU	Cancer therapy	[100]
	PDLLA	CDDP	Cancer therapy	[101]
	PLLA	PTX	Cancer therapy	[103]
	PLA	5-FU	Cancer therapy	[104]
	PLA	5-FU	Cancer therapy	[106]
	PEG–PLA	Amphotericin B (AmB)	Local antibiotic delivery	[108]
	PLA	Gentamicin (GEN)	Local antibiotic delivery	[109]
	PLA	Piroxicam (PIR)	Anti-inflammation	[112]
	PLA	IL-1 β	Vaccine	[113]
	PLA	TV and FEP proteins	Vaccine	[114]
	PLA/PLGA	IFN- γ	Vaccine	[116]
	PLLA	HBsAg	Vaccine	[117]
Hydrogels	PEG–PLCPHA	CEF	Antibacterial	[125]
	PLA/PEO/PLA	Bovine serum albumin (BSA) and fibrinogen (Fib)	Drug release	[126]
	PEG–PLA	CDDP	Drug release	[128]
	PLEOF	Stromal derived factor-1 α (SDF-1 α)	Tissue engineering	[127]

(continued)

Table 1 (continued)

Category	Polymer	Drug	Application	Reference
	PLA–L64–PLA	DTX and LL-37 peptide	Colorectal peritoneal carcinomatosis	[129]
	PLA–DX–PEG	siRNA	Bone repair	[130]
	PLA	FGF and IGF-1	Cardiovascular engineering	[131]
Electrospun fibers	PLLA	5-FU	Cancer therapy	[140]
	PLLA	DOX	Cancer therapy	[137]
	PEG–PLA/PLGA	Cefoxitin (CFX)	Adhesion prevention	[142]
	PLLA	Silver NP	Antibacterial and anti-adhesion	[144]
	PLLA	IBU	Anti-inflammation and anti-adhesion	[145]
	PELA	Celecoxib (CEL)	Adhesion prevention	[146]
	PELA	IBU	Adhesion prevention	[147]
	PLLA	bFGF	Adhesion prevention	[148]
	PLLA	Bone marrow MSCs	Vascular tissue engineering	[149]
	PLLA	TGF	Annulus fibrosus repair and regeneration	[152]
	PDLLA	2,3-Dihydroxybenzoic acid (DBC)	Antibacterial	[153]
	PLA	Polybiguanide (PBG)	Antibacterial	[154]
	PLA/PCL	KGF	Wound healing	[158]
PLA/PGA	IBU	Wound healing	[159]	
Scaffolds	PLA	VEGF	Bone repair	[163]
	Chitosan/PLLA	BMP-2-derived peptide	Bone repair	[165]
	PLLA	Tranilast (TRA)	Local drug delivery	[167]
	PLA	EGF	Nerve engineering	[168]
	PLLA	Retinoic acid (RA)	Nerve engineering	[171]
	PLLA	β -Tricalcium phosphate (β -TCP)	Bone repair	[170]
	PLLA	ALK	Wound healing	[172]
	PLA	CUR	Wound healing	[173]
	PLA/PCL	KGF	Wound healing	[158]
	PLA	IBU, ALK, and CUR	Wound healing	[174]

diameters of these NPs were 177 and 319 nm. The BVP-loaded PDLLA NPs could not only avoid capture by the reticuloendothelial system (RES), but also penetrated the BBB and enhanced accumulation of BVP in the brain. Additionally, a larger NP could deliver more BVP to the CNS. In another study, the PLLA NP loaded with ritonavir (a protease inhibitor) was attached to a trans-activating transcriptional activator (TAT) peptide [55]. The results indicated that TAT increased the transport of NPs across the BBB. In addition, the TAT-conjugated NPs were able to maintain a therapeutic drug level in the brain, which could be effective in controlling viral replication in the CNS. In a recent study, Sun et al. [56] demonstrated that the coating was necessary for drug delivery across the BBB. Compared with the modified PLA NP, the unmodified platform was able to deliver only a small amount of drug to the brain [34, 57–59]. However, in all cases, less than 1% of the administered dose reached the CNS, far less than enough to achieve a significant therapeutic effect.

By-passing the BBB is another efficient way of achieving drug delivery for CNS diseases. Intranasal delivery is one such method for circumventing the BBB and not only provides rapid access to the CNS, but also avoids first-pass hepatic clearance and tends to avoid systemic side effects [60]. Unfortunately, the brain concentration of drugs delivered intranasally is often still too low to achieve a desired therapeutic effect. NPs may help to solve this problem: loading drugs into NPs can protect them from degradation in the nasal enzymatic microenvironment. For example, Jain et al. [61] delivered methotrexate (MTX) by designing the thermosensitive PLA NP that exhibited enhanced residence time in the nasal cavity and by-passed the BBB. The results indicated that more NP was detected in the brain than free drug. Xia et al. [62] applied low molecular weight protamine (LMWP) to decorate the surface of methoxy poly(ethylene glycol) (mPEG)–PLA NP and determined the percentage of drug delivered to the brain after intranasal administration. Their results showed that the LMWP-modified mPEG–PLA NP could be more effectively delivered to the CNS than the unmodified one.

PLA NPs are also widely used for the diagnosis and treatment of cancers. Li et al. [63] first fabricated PLA NP encapsulating Endostar, then conjugated the near-infrared (NIR) dye IRDye 800CW and GX1 peptide onto NP (IGPNE). With NIR, fluorescence molecular imaging, and bioluminescence imaging, they were able to use this composite to attain a real-time image of U87MG tumor. Furthermore, IGPNE accumulated in the tumor site and had an antiangiogenic therapeutic effect. Miller et al. [64] incorporated dechloro-4-iodo-fenofibrate (IFF) into the core of PEGylated PDLLA (PEG–PDLLA) micelle and investigated its effect on tumor targeting, as shown in Fig. 3a. The results showed that the separation process of the drug from the carrier was extremely fast and that the drug accumulated more in the tumor than did the carrier (Fig. 3b, c). Mishra et al. [65] investigated the angiogenesis inhibition effect of mPEG-*b*-PDLLA micelle loaded with PTX and rapamycin (RAP). The results indicated that the PTX–RAP dual drug micelle had an enhanced antiangiogenesis effect that was promising for cancer chemotherapy. Other studies have also reported the anticancer effects of PLA DDSs loaded with chemotherapy drugs [66–71].

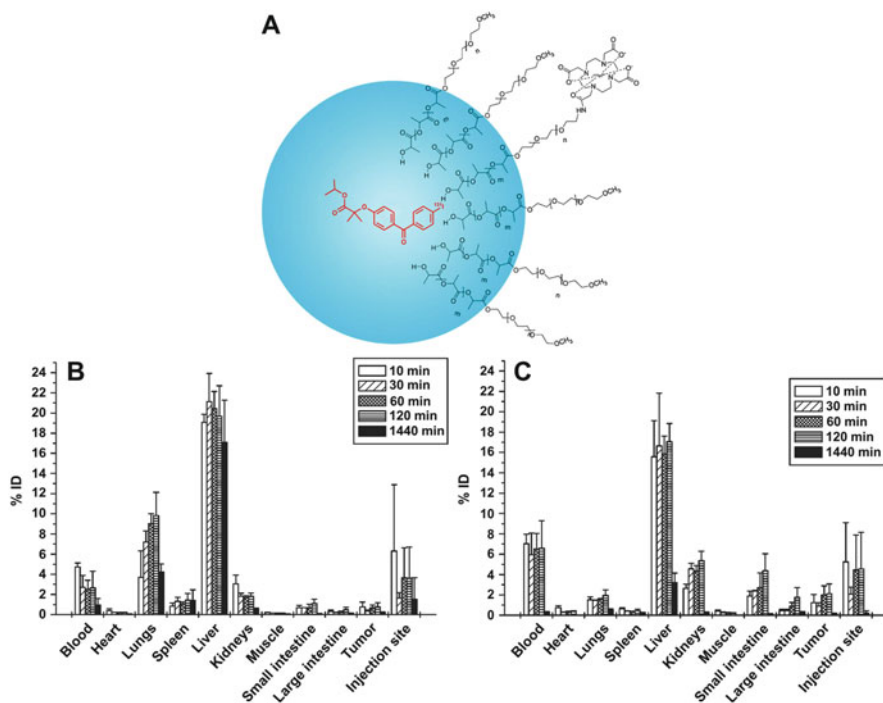


Fig. 3 Micelle composition and metabolism in vivo [64]. (a) The core component consists of PDLLA, which hosts the radioactively labeled drug ^{131}I FF or ^{125}I FF. The particle shell is covered with PEG. The surfaces show a mixture of ^{111}In -DOTA-HN-PEG and H_3CO -PEG. (b) Biodistribution (%ID) of polymer carrier and (c) IFF drug payload (%ID). All statistical data are presented as mean \pm standard deviation (SD; $n = 3$). Reproduced from [64] with permission of Elsevier

PLA NPs also play an important role in other areas, such as live cell imaging and treatment, and diagnosis of various other diseases. For instance, Contreras et al. [72] prepared the PLA NP based on difluoroboron dibenzoylmethane dye (BF_2dbmPLA). They found that the BF_2dbmPLA NP could be internalized into cultured HeLa cells by endocytosis and that the NP retained its fluorescence property, suggesting that the unique optical property of this complex could be harnessed for live cell imaging. In another study, the Fab'-bearing siRNA tumor necrosis factor α ($\text{TNF}\alpha$)-loaded PEG-PLA NP was prepared and studied for use in inflammatory bowel disease [73]. The in vivo experiment indicated that colitis was inhibited efficiently as the $\text{TNF}\alpha$ -siRNA-loaded NP was released to and accumulated in the diseased area. Babak et al. [74] prepared PLA DDSs for long-term antibacterial applications. They designed the composite platforms of poly(ϵ -caprolactone) (PCL) with different concentrations of the triclosan (TC)-loaded PLA NPs and investigated their drug release properties and antibacterial effects. Because of the advantages of PLA, including its higher glass transition temperature (T_g) and lower flexibility,

this biocomposite showed reduced burst release of TC and an antibacterial effect that lasted approximately 2 years.

Various other studies have shown the therapeutic effect of drugs loaded into PLA NPs against many diseases, including hearing loss by cisplatin (CDDP) chemotherapy [75], periodontitis [44, 76], colitis [73], acute hepatic failure [73], bone fracture [77], dermatitis [78], autoimmune uveoretinitis [79], and Chagas disease [80].

2.2 *Microspheres*

Microspheres are another kind of fine particle dispersion system in which drug molecules are dispersed or adsorbed. The diameters of microspheres range from 1 to 250 μm , and the main difference between NPs and microspheres is their size [81]. Because microspheres are larger than NPs in size, they are unlikely to cross biological barriers. Furthermore, microspheres tend to stay in place if injected into certain tissues. Additionally, microspheres can be only taken up by phagocytosis, whereas NPs can be taken up by both phagocytosis and pinocytosis [81]. For these reasons, microspheres are most widely used in cancer treatment as DDSs. However, NPs can be applied in many medical areas, as discussed in Sect. 2.1.

2.2.1 *Properties*

The drug-loaded microspheres can disperse specifically to target tissues *in vivo*, improving local drug concentrations and reducing systemic side effects. As a result of their excellent biocompatibility and biodegradability, PLA and its copolymers are the most frequently used polymers for DDSs. However, discovering which factors affect the rate of microsphere degradation and achieving more appropriate degradation behaviors is extremely important. Previous studies have found that the degradation of microspheres is associated with molecular weight, polymer crystallinity, microsphere size, and the presence of drugs [82]. Li et al. [83] found that a copolymer with 50% lactic acid and 50% glycolic acid (50:50 PLGA) has a shorter half-life period than 75:25 PLGA, and degrades faster than PLA.

The PLA-based microspheres loaded with different drugs are primarily delivered by intravascular injection, subcutaneous injection, *in situ* injection, and oral administration. Various types of drugs have been loaded into microspheres for medical applications, including anticancer drugs, antibiotics, antituberculosis drugs, antiparasitic drugs, asthma drugs, and vaccines. Of these, anticancer therapeutics have been most studied.

The microspheres composed of biocompatible and biodegradable polymers like PLA can also increase the stability and bioavailability of drugs, reduce gastrointestinal irritation, prolong the duration of drug release, and deliver drugs to target sites [84, 85]. Guan et al. [86] formulated the PLA microspheres loaded with

lovastatin (LVT) for oral administration, and evaluated the *in vitro* and *in vivo* characteristics of the microspheres. They concluded that PLA microspheres could significantly prolong the circulation time of LVT *in vivo* and also significantly increase the relative bioavailability of LVT. Ding et al. [15] evaluated the drug loading ability and drug release behavior of amorphous calcium phosphate (ACP) microspheres containing mPEG–PDLLA. The ACP porous hollow microspheres were found to have a high docetaxel (DTX) loading capacity, thus causing more damage to tumor cells. Lu et al. [87] prepared the RIF-loaded PLA microspheres using the electrospray technique and showed that drug release from the microspheres lasted for more than 60 h *in vitro*. In another study, Chen et al. [88] formulated the emodin (ED)-loaded PLA microspheres and studied their lung-targeting effect. Apart from determining the optimal parameters for formulation and sustained drug release, this research also indicated that ED was mainly delivered to lung tissue without causing toxicity to the liver and kidneys. Mirella et al. [89] compared PLLA microspheres with poly(lactide-*co*-glycolide) (PLGA) microspheres prepared by the same technique. They concluded that the PLLA microspheres had the best physical properties, the highest drug loading content, and the most efficient drug release behavior without any burst effect. Other studies have similarly shown that PLA microspheres increase drug release time, stability, and bioactivity, all of which increase their medical applicability [90–96].

2.2.2 Applications

PLA microspheres are primarily used for delivering anticancer drugs to target sites. In a study conducted by Chen et al. [97], the *in vitro* and *in vivo* antitumor efficacy of magnetic composite microspheres of the MTX-loaded Fe₃O₄-PLLA-PEG-PLLA (MMCMs) was investigated. The results from experiments at the cellular, molecular, and integrated level indicated that MMCMs with magnetic induction possess the ability to accumulate MTX in tumor tissue, leading to apoptosis of the tumor cells. Zhao et al. [98] investigated the antitumor efficacy of dextran/PLGA–PLA core/shell microspheres loaded with recombinant interleukin-2 (rIL-2), as depicted in Fig. 4. They injected a single dose of microspheres intratumorally in a subcutaneous colon carcinoma BALB/c mouse model and demonstrated that the antitumor effect of the microspheres was promising. Tumor growth was significantly suppressed in the rIL-2-loaded microsphere group (Fig. 4). Zhou et al. [99] explored the use of epirubicin (EPI)-loaded PDLLA microspheres for treating hepatocellular carcinoma (HCC) in mice. Compared with the blank microsphere group and the normal saline control group, the group treated with the EPI-loaded PDLLA microspheres had the longest survival time, which indicated that the PLA microspheres combined with EPI are highly effective in treating HCC in mice. In another study, the PLLA microspheres containing 5-fluorouracil (5-FU) were prepared [100]. The authors found that the microspheres were primarily located in the liver and were more efficient than free 5-FU in prolonging the survival time of rats with liver tumors. In a study performed by Kuang et al. [101], the PDLLA microspheres

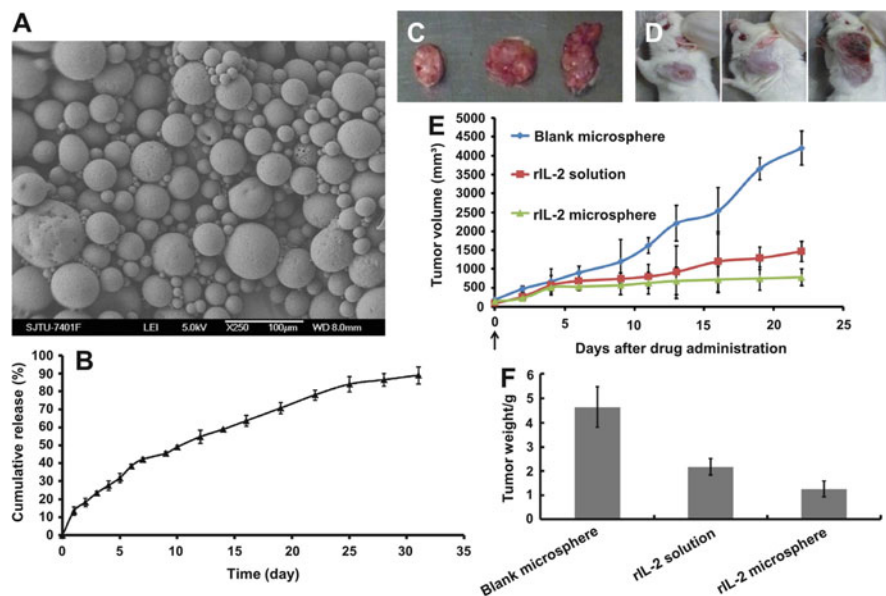


Fig. 4 Properties and antitumor efficacy of rIL-2-loaded dextran/PLGA–PLA core/shell microsphere [98]. (a) SEM image of drug-loaded microsphere. (b) In vitro cumulative rIL-2 release profile of loading microsphere in phosphate-buffered saline (PBS) of pH 7.4 at 37 °C. Error bars represent the SD ($n = 3$). (c–f) In vivo antitumor efficacy of rIL-2-loaded dextran/PLGA–PLA core/shell microsphere toward BALB/c mice bearing colon carcinoma. All mice were euthanized on day 22, and tumors were stripped, weighed, and photographed. (c) Representative photographs of tumors. (d) Representative photographs of BALB/c mice bearing tumors. (e) Tumor volumes in the different groups (blank microsphere, rIL-2 solution, and rIL-2-loaded microsphere) as a function of days post-treatment. Arrow represents the day that each formulation was administered for the first time. (f) Tumor weights after euthanizing on day 22. Data are expressed as mean \pm SD ($n = 4$). Reproduced from [98] with permission of Elsevier

loaded with CDDP were injected into mammary tumors in rats. These microspheres had a similar antitumor effect as aqueous CDDP solution in that the tumor became significantly smaller or disappeared 16 days after treatment. Fascinatingly, the CDDP-loaded PDLLA microspheres showed less nephrotoxicity than the aqueous CDDP solution. Other studies have also revealed the anticancer effects of drug-loaded PLA microspheres and provided an experimental basis for further therapies [102–106].

In addition to anticancer drugs, other kinds of drugs, including antibiotics [107–109], anti-TB drugs [110], asthma drugs [111, 112], and vaccines [113–118] have been loaded into PLA microspheres. Consequently, PLA microspheres are another widely used DDS for medical applications.

2.3 Hydrogels

Hydrogels, a type of three-dimensional (3D) polymer network containing significant amounts of water [119, 120], have received increasing attention in the fields of drug delivery and tissue engineering [121, 122].

2.3.1 Properties

The environmentally sensitive hydrogels are widely studied because of their biocompatibility and resemblance to biological tissues [123]. As a result of its biocompatibility, PLA has gained favor for the construction of hydrogels. The most attractive feature of PLA hydrogels is their thermal sensitivity: the PLA copolymer is soluble at room temperature and changes into a gel at body temperature. In addition, PLA hydrogels have good controlled drug release properties and can maintain drug release for over a month. However, crystallization and subsequent precipitation in solution is a major challenge for PLA use in hydrogel fabrication. To solve this problem, PLGA–PEG systems are often chosen. The PLGA–PEG solution is liquid at room temperature and immediately forms a hydrogel at body temperature. Furthermore, its mechanical properties are superior to those of PLA-only hydrogels [124].

Compared with hydrophobic materials, hydrogels interact less strongly with immobilized biomolecules. Because of the biocompatibility of PLA and the high water content of hydrogels, the use of PLA hydrogels is ideal for sustained drug release. Various studies have demonstrated this idea: for example, Lai et al. [125] developed a thermosensitive methoxy poly(ethylene glycol)-*co*-poly(lactic acid-*co*-aromatic anhydride) (mPEG–PLCPHA) hydrogel for cefazolin (CEF) delivery that exhibited long-term antibacterial effects. Wang et al. [119] studied the safety of a pH-sensitive hydrogel consisting of mPEG, PLA, and itaconic acid, and concluded that it might be used as a safe method for drug delivery. Other studies have also provided convincing evidence that PLA hydrogels can serve as efficient DDSs [126–128].

2.3.2 Applications

PLA hydrogels have already shown great potential as DDSs for medical applications. In one study, researchers dispersed NPs of DTX and LL-37 peptide into a PLA–L64–PLA thermosensitive hydrogel and evaluated the intraperitoneal effect of this composite in a colorectal peritoneal carcinomatosis HCT116 model [129]. They found that the hydrogel showed significant antitumor efficacy both in vitro and in vivo. Manaka et al. [130] evaluated the bone formation effect of a PDLLA–*p*-dioxanone–PEG hydrogel carrier for siRNA delivery. The hydrogel was found to be safe and efficient for siRNA delivery, and could promote new bone

formation (Fig. 5). Devin et al. [131] synthesized a degradable methacrylate PLA hydrogel loaded with bioactive basic fibroblast growth factor (bFGF) and insulin-like growth factor-1 (IGF-1). This hydrogel loaded with growth factors was injected into infarcts in Lewis rats and found to improve cardiac function and geometry compared with the saline control. The results indicated that PLA hydrogel can act as a carrier of growth factors to influence cardiac remodeling. In another study, a diblock hydrogel of mPEG–PLA was studied for adhesion prevention [122]. The

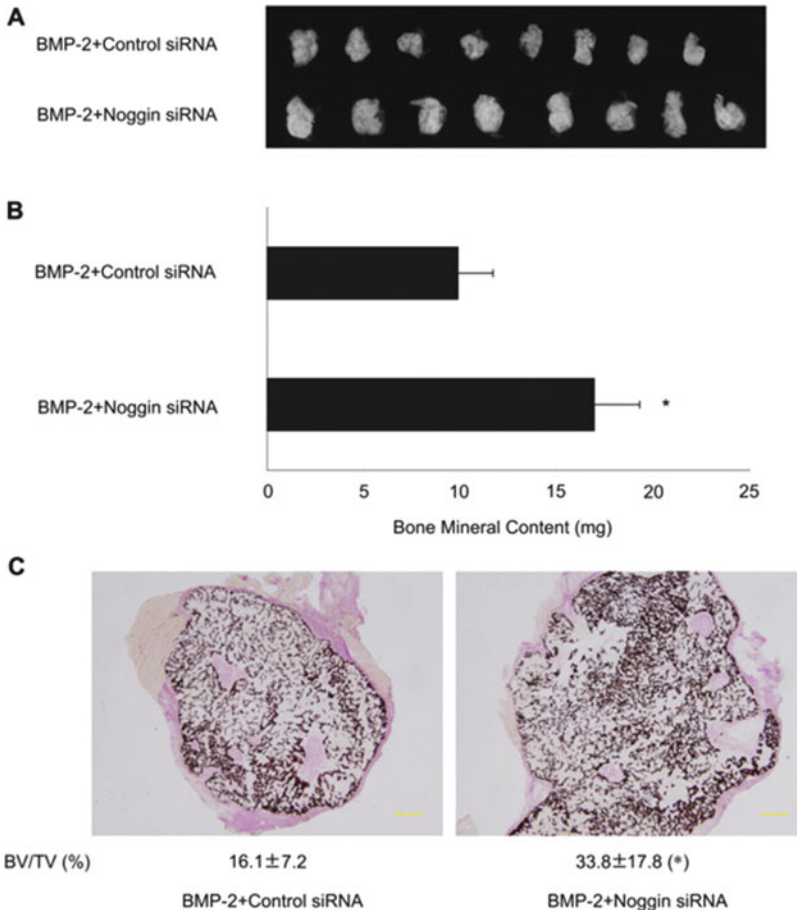


Fig. 5 Characterization of ectopic bone formation [130]. (a) Soft X-ray examination of newly formed ectopic bone induced by hydrogel containing 2.5 mg rhBMP-2 without Noggin siRNA [BMP(+)/siRNA(-)] or with Noggin [BMP(+)/siRNA(+)] for 2 weeks. (b) Bone mineral contents of ossicles measured by dual-energy X-ray absorptiometry (DXA). * $P < 0.05$, compared with control group. (c) Von Kossa and van Gieson staining of sections of undercalcified BMP-induced ectopic bone without or with Noggin siRNA. Bone volume per tissue volume (BV/TV) is expressed as mean. * $P < 0.05$ compared with control group. Reproduced from [130] with permission of Elsevier

results showed that the hydrogel system was equally effective compared with the commercial anti-adhesion product. Furthermore, this hydrogel system could be more promising for adhesion prevention if it were loaded with antifibrosis and anti-inflammatory drugs.

Even though PLA hydrogels are not as widely used as PLA NPs and microspheres, they still play an important role in controlled drug delivery.

2.4 Electrospun Fibers

Electrospinning is a facile and economic technique for producing nanoscale or microscale fibers from different polymers. The fibers can then be used for a variety of biomedical applications [132–137].

2.4.1 Properties

Electrospun fibers have attracted increasing attention as DDSs because of their specific advantages, including a high surface to area ratio, which can lead to high drug loading capacity, variable pore size, and mechanical flexibility [135, 136, 138]. Electrospinning is an efficient and simple method of rapidly and reproducibly manufacturing fiber networks incorporating different kinds of drugs [139]. However, hydrophilic water-soluble drugs cannot be directly mixed into solutions of PLA. Fortunately, the techniques of emulsion electrospinning and coaxial electrospinning can be used to encapsulate hydrophilic drugs in the core of the fibers to mitigate the initial burst release of drug [137]. Furthermore, the characteristics of electrospun fibers as DDSs can be modified by biological, chemical, optical, thermal, magnetic, and electric stimuli [139]. As a result, electrospun fibers can be designed to achieve the desired drug transport properties for medical application. PLA electrospun fibers play a significant role in this area.

2.4.2 Applications

Like other PLA DDSs, electrospun PLA fibers are widely used in cancer therapy. Zhang et al. [140] manufactured the PLLA electrospun fibers loaded with 5-FU and OXA for treatment of colorectal cancer. They found that the PLLA electrospun fiber loaded with chemotherapy drugs significantly suppressed tumor growth and prolonged mouse survival time. In another study (Fig. 6), researchers prepared the electrospun PLLA fibers loaded with multiwalled carbon nanotubes (MWCNTs) and doxorubicin (DOX) [141]. As demonstrated in Fig. 6, the combination of photothermal therapy using MWCNTs and chemotherapy induced with DOX greatly suppressed tumor growth, with less damage to nearby normal tissue.

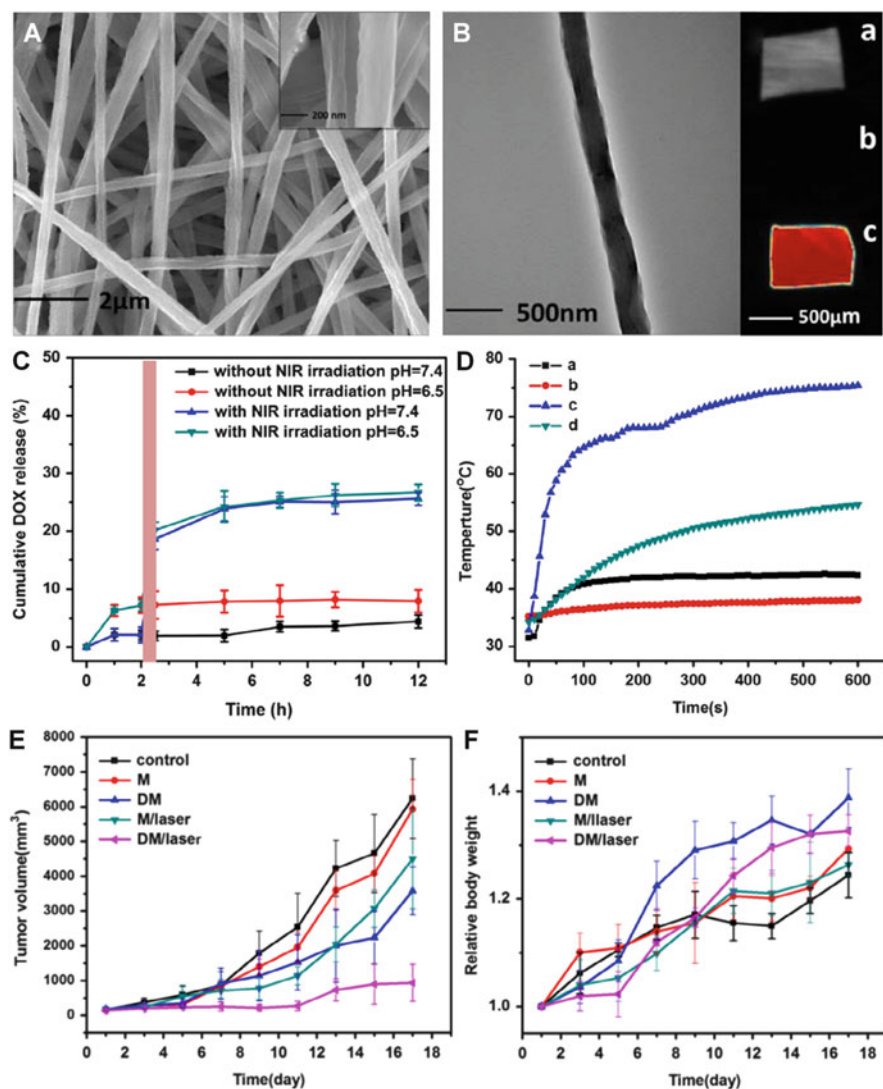


Fig. 6 Fabrication of DOX/MWCNT co-loaded electrospun PLA fibers for treatment of U14 cervical cancer in mice [141]. (A) SEM image of co-loaded fibers. (B) TEM of co-loaded fiber, and fluorescence image of (a) PLA fiber, (b) MWCNT-loaded PLA fiber, and (c) co-loaded PLA fiber. (C) Release profiles of DOX from co-loaded fiber in PBS at 37°C without or with NIR irradiation of 2 W/cm². The column zone indicates when the NIR irradiation was applied. (D) Temperature of tumor region at different time points under NIR irradiation of 1.5 W/cm². Control group: (a) tumor surface, (b) 3 mm inside tumor. Fiber dressing group: (c) tumor surface, (d) 3 mm inside tumor. (E) Evolution of U14 tumor volumes of KM mice as a function of time. (F) Relative body weight changes with time of U14 tumor-bearing mice. All the fibers were implanted only once in the beginning at an equivalent DOX dose of 0.1 mg and MWCNT dose of 0.1 mg. In groups of M/laser and DM/laser, tumor regions were exposed to NIR irradiation (1.5 W/cm²) for 10 min after fiber dressing for 24 h. Reproduced from [141] with permission of Elsevier

The electrospun PLA fibers loaded with various kinds of drugs are also used for adhesion prevention [137]. Tissue adhesion is one of the most common postoperative complications, in most cases requiring a second operation to remove the adhesions [142]. Electrospun PLA membranes not only act as a physical barrier, but can also be loaded with many kinds of drugs to prevent post-surgical adhesions. Because of the excellent biocompatibility and biodegradability of PLA, antibacterial drugs [142–144], anti-inflammatory drugs [145–147], drugs that facilitate healing [148], and synergistic combinations [149] have also been loaded into electrospun PLA fibers.

Electrospun PLA fibers can be applied in many other medical fields, including tissue engineering [150–152], antibiotic therapy [144, 153–155], bone repair [156, 157], and wound healing [158, 159]. For example, Screerekha et al. [150] developed a fibrin-based electrospun composite scaffold that provided a natural environment for cell attachment, migration, and proliferation. The results indicated that the electrospun-based composite was promising for myocardial tissue engineering. In another study, Spasova et al. [155] prepared PLA stereocomplex fibers using an amphiphilic block copolymer and demonstrated good antibacterial properties in experiments on blood cells and pathogenic microorganisms. Ni et al. [156] developed an electrospun PEG/PLA fibrous scaffold to provide an interconnected porous environment for attachment of mesenchymal stem cells (MSCs). The results showed good cell response, excellent osteogenic ability, and outstanding biocompatibility of the electrospun PEG/PLA fibrous composite for bone repair. Kobsa et al. [158] developed a PLA-based electrospun scaffold integrating nucleic acid delivery and studied its effect in the treatment of full thickness wounds. They found that the scaffold could serve as a protective barrier in the early stages of wound healing, as well as induce cell migration and growth.

2.5 Scaffolds

Tissue engineering scaffolds, especially those prepared from biocompatible and biodegradable polymers, are increasingly widely used. The scaffolds loaded with different drugs are crucial for the regeneration of large defects.

2.5.1 Properties

PLA has also become a popular scaffold for tissue engineering, again due to its outstanding biocompatibility and biodegradability. PLA scaffolds can be designed to match the mechanical properties of native tissues [160]. Furthermore, because the concentration of degradation products is reduced with increased porosity, PLA is a favorable material for scaffold fabrication [160].

2.5.2 Applications

PLA is promising for tissue engineering applications, not only as a scaffold material, but also for its drug delivery properties [24, 25, 161]. PLA scaffolds can be implanted at injured sites to support injured tissues and enhance the repair process. By loading drugs into the scaffolds, it is also possible to generate multifunctional PLA scaffolds for various applications [162]. However, release properties are important when scaffolds are also harnessed as DDSs. Many parameters, such as loading method, scaffold properties, and choice of polymer, can all play an important role in the mechanism of drug release, which occurs primarily via desorption, degradation, and diffusion in the electrospun PLA scaffolds [160].

The PLA scaffolds loaded with various agents have been the subject of much research in bone, vascular, and other tissue engineering applications. As a typical example, Zhou et al. [163] exploited a calcium phosphate–PLA composite as a coating for a tantalum porous scaffold (Fig. 7). Vascular endothelial growth factor (VEGF) and transforming growth factor (TGF) were loaded into the scaffold and used for bone defect repair. Their results indicated that the scaffold provided growth factors, physical support, structural guidance, and interfaces for new bone growth, and was therefore useful to guide new bone regeneration. Other studies have also reported the superior effects of various PLA scaffolds for tissue engineering [158, 164–173]. For example, Hu et al. [166] fabricated a nanofibrous PLLA scaffold for blood vessel regeneration. The results showed that the scaffold preferentially supported the reconstruction of tissue-engineered vascular graft. In another study, Niu et al. [165] developed a microencapsulated chitosan (CM), nanohydroxyapatite/collagen (nHAC), and PLLA-based microsphere–scaffold delivery system. Bone morphogenetic protein-2 (BMP-2)-derived synthetic peptide

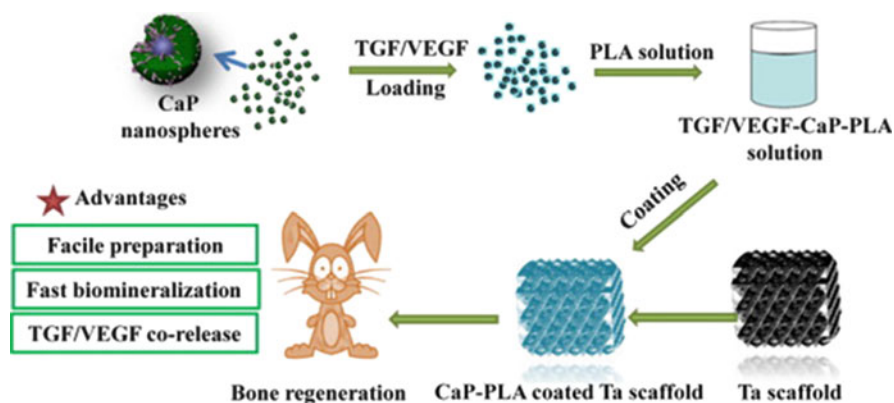


Fig. 7 Strategy for preparation and bone defect repair application of porous tantalum scaffold coated with a composite of calcium phosphate and PLA. Reproduced from [163] with permission of Elsevier

was incorporated into the synthesized composite. The results showed that the CM/nHAC/PLLA composite can accelerate the regeneration of cancellous bone defect with controlled release of the incorporated peptide. Haddad et al. [168] developed a 3D PLA scaffold with polyallylamine to introduce amine groups, followed by grafting of epidermal growth factor (EGF) onto the scaffold. They found that neural stem-like cells were able to proliferate on the EGF-grafted substrates and might be promising for repair of the CNS. The PLA scaffolds loaded with drugs, such as ibuprofen IBU, alkannin ALK, and curcumin (CUR), are also used for promoting cutaneous wound healing [160]. However, a detailed discussion is beyond the scope of this review on DDSs.

3 Conclusions and Perspectives

This review introduces the characteristics of PLA as a promising matrix for DDSs in its five most commonly used forms: NPs, microspheres, hydrogels, electrospun fibers, and scaffolds. The PLA DDSs can effectively deliver drugs to the target sites, reduce drug toxicity, and increase the therapeutic effect. In addition, PLA can be modified to achieve various desired properties in DDSs. As a result, PLA has great potential for DDS development.

The PLA DDSs loaded with different drugs can be used for the treatment of many diseases. For example, the PLA DDSs loaded with anticancer agents like PTX can directly deliver drugs to tumor sites, thereby increasing drug accumulation and retention time in the tumor while reducing systemic side effects. Meanwhile, the PLA DDSs loaded with different cytokines, such as BMP, can control drug release via degradation and play an important role in bone repair. The PLA DDSs loaded with other drugs, including anti-inflammatory agents [107, 108], antihypotensors [174], painkillers [158], and vaccines [113, 114, 118], can also be used for other medical applications.

With the development of biotechnology, peptide and protein drugs have become increasingly prevalent. However, the short retention time of these drugs limits their application, as continuous administration is often impractical. PLA DDSs may be able to improve the application of peptide- and protein-based therapeutics. Furthermore, PLA DDSs can be engineered to be intelligent drug delivery vehicles. For example, a smart PLA glucose monitor may be engineered to be inserted into body tissue and release the proper dose of insulin according to glucose fluctuations.

Although some aspects of PLA DDSs still need to be improved, further research will allow PLA to play an increasingly important role as a matrix promising material for DDSs and provide more efficacious treatment methods for many diseases.

References

1. Datta M, Via LE, Kamoun WS, Liu C, Chen W, Seano G, Weiner DM, Schimel D, England K, Martin JD, Gao X, Xu L, Barry CE, Jain RK (2015) Anti-vascular endothelial growth factor treatment normalizes tuberculosis granuloma vasculature and improves small molecule delivery. *Proc Natl Acad Sci* 112(6):1827–1832
2. Chen J, Ding J, Xiao C, Zhuang X, Chen X (2015) Emerging antitumor applications of extracellularly reengineered polymeric nanocarriers. *Biomater Sci* 3(7):988–1001
3. Gu X, Ding J, Zhang Z, Li Q, Zhuang X, Chen X (2015) Polymeric nanocarriers for drug delivery in osteosarcoma treatment. *Curr Pharm Des* 21(36):5187–5197
4. Pacardo DB, Ligler FS, Gu Z (2015) Programmable nanomedicine: synergistic and sequential drug delivery systems. *Nanoscale* 7(8):3381–3391
5. Ding J, Xiao C, Yan L, Tang Z, Zhuang X, Chen X, Jing X (2011) pH and dual redox responsive nanogel based on poly(L-glutamic acid) as potential intracellular drug carrier. *J Control Release* 152:E11–E13
6. Ding J, Chen J, Li D, Xiao C, Zhang J, He C, Zhuang X, Chen X (2013) Biocompatible reduction-responsive polypeptide micelles as nanocarriers for enhanced chemotherapy efficacy in vitro. *J Mater Chem B* 1(1):69–81
7. Xiao H, Qi R, Liu S, Hu X, Duan T, Zheng Y, Huang Y, Jing X (2011) Biodegradable polymer-cisplatin(IV) conjugate as a pro-drug of cisplatin(II). *Biomaterials* 32(30):7732–7739
8. Tiwari G, Tiwari R, Sriwastawa B, Bhati L, Pandey S, Pandey P, Bannerjee SK (2012) Drug delivery systems: an updated review. *Int J Pharm Investig* 2(1):2–11
9. Zhang Y, Chan HF, Leong KW (2013) Advanced materials and processing for drug delivery: the past and the future. *Adv Drug Deliv Rev* 65(1):104–120
10. Ikada Y, Tsuji H (2000) Biodegradable polyesters for medical and ecological applications. *Macromol Rapid Commun* 21(3):117–132
11. Couvreur P (2013) Nanoparticles in drug delivery: past, present and future. *Adv Drug Deliv Rev* 65(1):21–23
12. Doppalapudi S, Jain A, Domb AJ, Khan W (2016) Biodegradable polymers for targeted delivery of anti-cancer drugs. *Expert Opin Drug Deliv* 13(6):891–909
13. Liu M, Li H, Luo G, Liu Q, Wang Y (2008) Pharmacokinetics and biodistribution of surface modification polymeric nanoparticles. *Arch Pharm Res* 31(4):547–554
14. Feng C, Piao M, Li D (2016) Stereocomplex-reinforced PEGylated polylactide micelle for optimized drug delivery. *Polymers* 8(4):165
15. Ding GJ, Zhu YJ, Qi C, Lu BQ, Wu J, Chen F (2015) Porous microspheres of amorphous calcium phosphate: block copolymer templated microwave-assisted hydrothermal synthesis and application in drug delivery. *J Colloid Interface Sci* 443:72–79
16. Li J, Darabi M, Gu J, Shi J, Xue J, Huang L, Liu Y, Zhang L, Liu N, Zhong W, Zhang L, Xing M, Zhang L (2016) A drug delivery hydrogel system based on activin B for Parkinson's disease. *Biomaterials* 102:72–86
17. Cheng M, Wang H, Zhang Z, Li N, Fang X, Xu S (2014) Gold nanorod-embedded electrospun fibrous membrane as a photothermal therapy platform. *ACS Appl Mater Interfaces* 6(3):1569–1575
18. Duan S, Yang X, Mei F, Tang Y, Li X, Shi Y, Mao J, Zhang H, Cai Q (2015) Enhanced osteogenic differentiation of mesenchymal stem cells on poly(L-lactide) nanofibrous scaffolds containing carbon nanomaterials. *J Biomed Mater Res A* 103(4):1424–1435
19. Pang XA, Zhuang XL, Tang ZH, Chen XS (2010) Polylactic acid (PLA): research, development and industrialization. *Biotechnol J* 5(11):1125–1136
20. Chang FY, Teng PT, Tsai TH (2013) Property measurement and processing parameter optimization for polylactide micro structure fabrication by thermal imprint. *Jpn J Appl Phys* 52(6S):06GJ09

21. Armentano I, Bitinis N, Fortunati E, Mattioli S, Rescignano N, Verdejo R, Lopez-Manchado MA, Kenny JM (2013) Multifunctional nanostructured PLA materials for packaging and tissue engineering. *Prog Polym Sci* 38(10–11):1720–1747
22. Lasprilla AJ, Martinez GA, Lunelli BH, Jardini AL, Filho RM (2012) Poly-lactic acid synthesis for application in biomedical devices – A review. *Biotechnol Adv* 30(1):321–328
23. Manome A, Okada S, Uchimura T, Komagata K (1998) The ratio of L-form to D-form of lactic acid as a criteria for the identification of lactic acid bacteria. *J Gen Appl Microbiol* 44(6):371–374
24. Wang J, Xu W, Ding J, Lu S, Wang X, Wang C, Chen X (2015) Cholesterol-enhanced polylactide-based stereocomplex micelle for effective delivery of doxorubicin. *Materials* 8(1):216–230
25. Wang J, Shen K, Xu W, Ding J, Wang X, Liu T, Wang C, Chen X (2015) Stereocomplex micelle from nonlinear enantiomeric copolymers efficiently transports antineoplastic drug. *Nanoscale Res Lett* 10(1):206
26. Ajiro H, Kuroda A, Kan K, Akashi M (2015) Stereocomplex film using triblock copolymers of polylactide and poly(ethylene glycol) retain paclitaxel on substrates by an aqueous inkjet system. *Langmuir* 31(38):10583–10589
27. Chen C, Lv G, Pan C, Song M, Wu C, Guo D, Wang X, Chen B, Gu Z (2007) Poly(lactic acid) (PLA) based nanocomposites – A novel way of drug-releasing. *Biomed Mater* 2(4):L1–L4
28. Lasprilla AJR, Martinez GAR, Lunelli BH, Jardini AL, Maciel R (2010) Biomaterials for application in bone tissue engineering. *J Biotechnol* 150:S455–S455
29. Auras R, Harte B, Selke S (2004) An overview of polylactides as packaging materials. *Macromol Biosci* 4(9):835–864
30. Gupta AP, Kumar V (2007) New emerging trends in synthetic biodegradable polymers – polylactide: a critique. *Eur Polym J* 43(10):4053–4074
31. Townshend A (1985) *Anal Chim Acta* 177:304
32. Di Martino A, Sedlarik V (2014) Amphiphilic chitosan-grafted-functionalized polylactic acid based nanoparticles as a delivery system for doxorubicin and temozolomide co-therapy. *Int J Pharm* 474(1–2):134–145
33. Hou Z, Li L, Zhan C, Zhu P, Chang D, Jiang Q, Ye S, Yang X, Li Y, Xie L, Zhang Q (2012) Preparation and in vitro evaluation of an ultrasound-triggered drug delivery system: 10-Hydroxycamptothecin loaded PLA microbubbles. *Ultrasonics* 52(7):836–841
34. Li J, Sabliov C (2013) PLA/PLGA nanoparticles for delivery of drugs across the blood-brain barrier. *Nanotechnol Rev* 2(3):241–257
35. Sun D, Ding J, Xiao C, Chen J, Zhuang X, Chen X (2015) Drug delivery: pH-responsive reversible PEGylation improves performance of antineoplastic agent (Adv. Healthcare Mater. 6/2015). *Adv Healthc Mater* 4(6):786–786
36. Wu Y-L, Chen X, Wang W, Loh XJ (2016) Engineering bioresponsive hydrogels toward healthcare applications. *Macromol Chem Phys* 217(2):175–188
37. Zhang J, Wang X, Liu T, Liu S, Jing X (2016) Antitumor activity of electrospun polylactide nanofibers loaded with 5-fluorouracil and oxaliplatin against colorectal cancer. *Drug Deliv* 23(3):794–800
38. Li Z, Zhang FL, Pan LL, Zhu XL, Zhang ZZ (2015) Preparation and characterization of injectable mitoxantrone poly(lactic acid)/fullerene implants for in vivo chemo-photodynamic therapy. *J Photochem Photobiol B Biol* 149:51–57
39. Fernandez K, Aburto J, von Plessing C, Rockel M, Aspe E (2016) Factorial design optimization and characterization of poly-lactic acid (PLA) nanoparticle formation for the delivery of grape extracts. *Food Chem* 207:75–85
40. Feng X, Gao X, Kang T, Jiang D, Yao J, Jing Y, Song Q, Jiang X, Liang J, Chen J (2015) Mammary-derived growth inhibitor targeting peptide-modified PEG-PLA nanoparticles for enhanced targeted glioblastoma therapy. *Bioconjug Chem* 26(8):1850–1861

41. Dou S, Yang XZ, Xiong MH, Sun CY, Yao YD, Zhu YH, Wang J (2014) ScFv-decorated PEG-PLA-based nanoparticles for enhanced siRNA delivery to Her2(+) breast cancer. *Adv Healthc Mater* 3(11):1792–1803
42. Yao L, Song Q, Bai W, Zhang J, Miao D, Jiang M, Wang Y, Shen Z, Hu Q, Gu X, Huang M, Zheng G, Gao X, Hu B, Chen J, Chen H (2014) Facilitated brain delivery of poly(ethylene glycol)-poly(lactic acid) nanoparticles by microbubble-enhanced unfocused ultrasound. *Biomaterials* 35(10):3384–3395
43. Liu B, Han SM, Tang XY, Han L, Li CZ (2014) Cervical cancer gene therapy by gene loaded PEG-PLA nanomedicine. *Asian Pac J Cancer Prev* 15(12):4915–4918
44. Yao W, Xu P, Pang Z, Zhao J, Chai Z, Li X, Li H, Jiang M, Cheng H, Zhang B, Cheng N (2014) Local delivery of minocycline-loaded PEG-PLA nanoparticles for the enhanced treatment of periodontitis in dogs. *Int J Nanomedicine* 9:3963–3970
45. Amoozgar Z, Yeo Y (2012) Recent advances in stealth coating of nanoparticle drug delivery systems. *Wiley Interdiscip Rev Nanomed Nanobiotechnol* 4(2):219–233
46. Yeh P-YJ, Kainthan RK, Zou Y, Chiao M, Kizhakkedathu JN (2008) Self-assembled monothiol-terminated hyperbranched polyglycerols on a gold surface: a comparative study on the structure, morphology, and protein adsorption characteristics with linear poly(ethylene glycol)s. *Langmuir* 24(9):4907–4916
47. Deng Y, Saucier-Sawyer JK, Hoimes CJ, Zhang JW, Seo YE, Andrejcsk JW, Saltzman WM (2014) The effect of hyperbranched polyglycerol coatings on drug delivery using degradable polymer nanoparticles. *Biomaterials* 35(24):6595–6602
48. Yamakawa I, Tsushima Y, Machida R, Watanabe S (1992) In vitro and in vivo release of poly(DL-lactic acid) microspheres containing neurotensin analog prepared by novel oil-in-water solvent evaporation method. *J Pharm Sci* 81(8):808–811
49. Jing Z, Xu XY, Chen XS, Liang QZ, Bian XC, Yang LX, Jing XB (2003) Biodegradable electrospun fibers for drug delivery. *J Control Release* 92(3):227–231
50. Maestrelli F, Bragagni M, Mura P (2016) Advanced formulations for improving therapies with anti-inflammatory or anaesthetic drugs: a review. *J Drug Delivery Sci Technol* 32:192–205
51. Zhu Z (2013) Effects of amphiphilic diblock copolymer on drug nanoparticle formation and stability. *Biomaterials* 34(38):10238–10248
52. Patel T, Zhou JB, Piepmeier JM, Saltzman WM (2012) Polymeric nanoparticles for drug delivery to the central nervous system. *Adv Drug Deliv Rev* 64(7):701–705
53. Ishihara T, Takahashi M, Higaki M, Mizushima Y (2009) Efficient encapsulation of a water-soluble corticosteroid in biodegradable nanoparticles. *Int J Pharm* 365(1–2):200–205
54. Choonara YE, Kumar P, Modi G, Pillay V (2016) Improving drug delivery technology for treating neurodegenerative diseases. *Expert Opin Drug Deliv* 13(7):1029–1043
55. Rao KS, Reddy MK, Horning JL, Labhasetwar V (2008) TAT-conjugated nanoparticles for the CNS delivery of anti-HIV drugs. *Biomaterials* 29(33):4429–4438
56. Sun WQ, Xie CS, Wang HF, Hu Y (2004) Specific role of polysorbate 80 coating on the targeting of nanoparticles to the brain. *Biomaterials* 25(15):3065–3071
57. Kulkarni SA, Feng SS (2011) Effects of surface modification on delivery efficiency of biodegradable nanoparticles across the blood-brain barrier. *Nanomedicine* 6(2):377–394
58. Lu W, Wan J, She ZJ, Jiang XG (2007) Brain delivery property and accelerated blood clearance of cationic albumin conjugated PEGylated nanoparticle. *J Control Release* 118(1):38–53
59. Gan CW, Feng SS (2010) Transferrin-conjugated nanoparticles of poly(lactide)-D-alpha-tocopheryl polyethylene glycol succinate diblock copolymer for targeted drug delivery across the blood-brain barrier. *Biomaterials* 31(30):7748–7757
60. Hashizume R, Gupta N (2010) Telomerase inhibitors for the treatment of brain tumors and the potential of intranasal delivery. *Curr Opin Mol Ther* 12(2):168–175

61. Jain DS, Bajaj AN, Athawale RB, Shikhande SS, Pandey A, Goel PN, Gude RP, Patil S, Raut P (2016) Thermosensitive PLA based nanodispersion for targeting brain tumor via intranasal route. *Mater Sci Eng C* 63:411–421
62. Xia HM, Gao XL, Gu GZ, Liu ZY, Zeng N, Hu QY, Song QX, Yao L, Pang ZQ, Jiang XG, Chen J, Chen HZ (2011) Low molecular weight protamine-functionalized nanoparticles for drug delivery to the brain after intranasal administration. *Biomaterials* 32(36):9888–9898
63. Li Y, Du Y, Liu X, Zhang Q, Jing L, Liang X, Chi C, Dai Z, Tian J (2015) Monitoring tumor targeting and treatment effects of IRDye 800CW and GX1-conjugated polylactic acid nanoparticles encapsulating endostar on glioma by optical molecular imaging. *Mol Imaging* 14:356–365
64. Miller T, Breyer S, van Colen G, Mier W, Haberkorn U, Geissler S, Voss S, Weigandt M, Goepferich A (2013) Premature drug release of polymeric micelles and its effects on tumor targeting. *Int J Pharm* 445(1–2):117–124
65. Mishra GP, Nguyen D, Alani AW (2013) Inhibitory effect of paclitaxel and rapamycin individual and dual drug-loaded polymeric micelles in the angiogenic cascade. *Mol Pharm* 10(5):2071–2078
66. Xu W, Ding J, Li L, Xiao C, Zhuang X, Chen X (2015) Acid-labile boronate-bridged dextran-bortezomib conjugate with up-regulated hypoxic tumor suppression. *Chem Commun* 51(31):6812–6815
67. Liu Y, Wang X, Sun CY, Wang J (2015) Delivery of mitogen-activated protein kinase inhibitor for hepatocellular carcinoma stem cell therapy. *ACS Appl Mater Interfaces* 7(1):1012–1020
68. Zhang X, Yang Y, Liang X, Zeng X, Liu Z, Tao W, Xiao X, Chen H, Huang L, Mei L (2014) Enhancing therapeutic effects of docetaxel-loaded dendritic copolymer nanoparticles by co-treatment with autophagy inhibitor on breast cancer. *Theranostics* 4(11):1085–1095
69. Yang A, Liu Z, Yan B, Zhou M, Xiong X (2016) Preparation of camptothecin-loaded targeting nanoparticles and their antitumor effects on hepatocellular carcinoma cell line H22. *Drug Deliv* 23(5):1699–1706
70. Liu Y, Zhu YH, Mao CQ, Dou S, Shen S, Tan ZB, Wang J (2014) Triple negative breast cancer therapy with CDK1 siRNA delivered by cationic lipid assisted PEG-PLA nanoparticles. *J Control Release* 192:114–121
71. Yang XZ, Dou S, Sun TM, Mao CQ, Wang HX, Wang J (2011) Systemic delivery of siRNA with cationic lipid assisted PEG-PLA nanoparticles for cancer therapy. *J Control Release* 156(2):203–211
72. Contreras J, Xie J, Chen YJ, Pei H, Zhang G, Fraser CL, Hamm-Alvarez SF (2010) Intracellular uptake and trafficking of difluoroboron dibenzoylmethane-poly lactide nanoparticles in HeLa cells. *ACS Nano* 4(5):2735–2747
73. Laroui H, Viennois E, Xiao B, Canup BSB, Geem D, Denning TL, Merlin D (2014) Fab'-bearing siRNA TNF alpha-loaded nanoparticles targeted to colonic macrophages offer an effective therapy for experimental colitis. *J Control Release* 186:41–53
74. Kaffashi B, Davoodi S, Oliaei E (2016) Poly(epsilon-caprolactone)/triclosan loaded polylactic acid nanoparticles composite: a long-term antibacterial bionanocomposite with sustained release. *Int J Pharm* 508(1–2):10–21
75. Sun C, Wang X, Chen D, Lin X, Yu D, Wu H (2016) Dexamethasone loaded nanoparticles exert protective effects against cisplatin-induced hearing loss by systemic administration. *Neurosci Lett* 619:142–148
76. Pinon-Segundo E, Ganem-Quintanar A, Alonso-Perez V, Quintanar-Guerrero D (2005) Preparation and characterization of triclosan nanoparticles for periodontal treatment. *Int J Pharm* 294(1–2):217–232
77. Chen L, Liu L, Li C, Tan Y, Zhang G (2011) A new growth factor controlled drug release system to promote healing of bone fractures: nanospheres of recombinant human bone morphogenetic-2 and polylactic acid. *J Nanosci Nanotechnol* 11(4):3107–3114

78. Rancan F, Papakostas D, Hadam S, Hackbarth S, Delair T, Primard C, Verrier B, Sterry W, Blume-Peytavi U, Vogt A (2009) Investigation of polylactic acid (PLA) nanoparticles as drug delivery systems for local dermatotherapy. *Pharm Res* 26(8):2027–2036
79. Sakai T, Kohno H, Ishihara T, Higaki M, Saito S, Matsushima M, Mizushima Y, Kitahara K (2006) Treatment of experimental autoimmune uveoretinitis with poly(lactic acid) nanoparticles encapsulating betamethasone phosphate. *Exp Eye Res* 82(4):657–663
80. Molina J, Urbina J, Gref R, Brener Z, Rodrigues Junior JM (2001) Cure of experimental Chagas' disease by the bis-triazole DO870 incorporated into 'stealth' polyethyleneglycol-poly lactide nanospheres. *J Antimicrob Chemother* 47(1):101–104
81. Kohane DS (2007) Microparticles and nanoparticles for drug delivery. *Biotechnol Bioeng* 96(2):203–209
82. Freiberg S, Zhu XX (2004) Polymer microspheres for controlled drug release. *Int J Pharm* 282(1–2):1–18
83. Li S (1999) Hydrolytic degradation characteristics of aliphatic polyesters derived from lactic and glycolic acids. *J Biomed Mater Res* 48(3):342–353
84. Floyd JA, Galperin A, Ratner BD (2015) Drug encapsulated polymeric microspheres for intracranial tumor therapy: a review of the literature. *Adv Drug Deliv Rev* 91:23–37
85. Edlund U, Albertsson AC (2002) Degradable polymer microspheres for controlled drug delivery. In: *Degradable aliphatic polyesters, Advances in polymer science*, vol 157. Springer, Heidelberg, pp 67–112
86. Guan Q, Chen W, Hu X (2015) Development of lovastatin-loaded poly(lactic acid) microspheres for sustained oral delivery: in vitro and ex vivo evaluation. *Drug Des Devel Ther* 9:791–798
87. Lu J, Hou R, Yang Z, Tang Z (2015) Development and characterization of drug-loaded biodegradable PLA microcarriers prepared by the electro spraying technique. *Int J Mol Med* 36(1):249–254
88. Chen X, Yang Z, Sun R, Mo Z, Jin G, Wei F, Hu J, Guan W, Zhong N (2014) Preparation of lung-targeting, emodin-loaded polylactic acid microspheres and their properties. *Int J Mol Sci* 15(4):6241–6251
89. Falconi M, Focaroli S, Teti G, Salvatore V, Durante S, Nicolini B, Orienti I (2014) Novel PLA microspheres with hydrophilic and bioadhesive surfaces for the controlled delivery of fenretinide. *J Microencapsul* 31(1):41–48
90. Pinto E, Zhang B, Song S, Bodor N, Buchwald P, Hochhaus G (2010) Feasibility of localized immunosuppression: 2. PLA microspheres for the sustained local delivery of a soft immunosuppressant. *Pharmazie* 65(6):429–435
91. Umeki N, Sato T, Harada M, Takeda J, Saito S, Iwao Y, Itai S (2010) Preparation and evaluation of biodegradable microspheres containing a new potent osteogenic compound and new synthetic polymers for sustained release. *Int J Pharm* 392(1–2):42–50
92. Rafat M, Cleroux CA, Fong WG, Baker AN, Leonard BC, O'Connor MD, Tsilfidis C (2010) PEG-PLA microparticles for encapsulation and delivery of Tat-EGFP to retinal cells. *Biomaterials* 31(12):3414–3421
93. Sheshala R, Peh KK, Darwis Y (2009) Preparation, characterization, and in vivo evaluation of insulin-loaded PLA-PEG microspheres for controlled parenteral drug delivery. *Drug Dev Ind Pharm* 35(11):1364–1374
94. Ding LY, Xia PF, Yang CQ, Lin YL, Wang J (2007) Preparation and evaluation of sustained-release microsphere of Sanguis Draconis in vitro. *Zhongguo Zhong Yao Za Zhi* 32(5):388–390
95. Ren J, Yu X, Ren T, Hong H (2007) Preparation and characterization of fenofibrate-loaded PLA-PEG microspheres. *J Mater Sci Mater Med* 18(8):1481–1487
96. Matsumoto A, Matsukawa Y, Suzuki T, Yoshino H (2005) Drug release characteristics of multi-reservoir type microspheres with poly(DL-lactide-co-glycolide) and poly(DL-lactide). *J Control Release* 106(1–2):172–180

97. Chen A, Dang T, Wang S, Tang N, Liu Y, Wu W (2014) The in vitro and in vivo anti-tumor effects of MTX-Fe₃O₄-PLLA-PEG-PLLA microspheres prepared by suspension-enhanced dispersion by supercritical CO₂. *Sci China Life Sci* 57(7):698–709
98. Zhao H, Wu F, Cai Y, Chen Y, Wei L, Liu Z, Yuan W (2013) Local antitumor effects of intratumoral delivery of rIL-2 loaded sustained-release dextran/PLGA-PLA core/shell microspheres. *Int J Pharm* 450(1–2):235–240
99. Zhou JY, Wang XM, Zhang QQ, Ye SF (2009) Efficacy of intraperitoneally injected epirubicin-loaded poly (d, l)-lactic acid microspheres alone or combined with free epirubicin in treating hepatocellular carcinoma in mice. *Zhongguo Yi Xue Ke Xue Yuan Xue Bao* 31(5):603–606
100. Ciftci K, Hincal AA, Kas HS, Ercan TM, Sungur A, Guven O, Ruacan S (1997) Solid tumor chemotherapy and in vivo distribution of fluorouracil following administration in poly (L-lactic acid) microspheres. *Pharm Dev Technol* 2(2):151–160
101. Kuang LR, Yang DJ, Inoue T, Liu WC, Wallace S, Wright KC (1996) Percutaneous intratumoral injection of cisplatin microspheres in tumor-bearing rats to diminish acute nephrotoxicity. *Anti-Cancer Drugs* 7(2):220–227
102. Xia D, Yao H, Liu Q, Xu L (2012) Preparation of microspheres encapsulating a recombinant TIMP-1 adenovirus and their inhibition of proliferation of hepatocellular carcinoma cells. *Asian Pac J Cancer Prev* 13(12):6363–6368
103. Lu J, Jackson JK, Gleave ME, Burt HM (2008) The preparation and characterization of anti-VEGFR2 conjugated, paclitaxel-loaded PLLA or PLGA microspheres for the systemic targeting of human prostate tumors. *Cancer Chemother Pharmacol* 61(6):997–1005
104. Lu Y, Lin P, Lu B, Wang J, Zhang J, Huang X (2000) Studies on release characteristics and cytotoxicity of 5-fluorouracil loaded polylactide microspheres on lung cancer cell lines. *Zhongguo Fei Ai Za Zhi* 3(6):432–434
105. Burt HM, Jackson JK, Bains SK, Liggins RT, Oktaba AM, Arsenault AL, Hunter WL (1995) Controlled delivery of taxol from microspheres composed of a blend of ethylene-vinyl acetate copolymer and poly (D,L-lactic acid). *Cancer Lett* 88(1):73–79
106. Chandy T, Das GS, Rao GHR (2000) 5-Fluorouracil-loaded chitosan coated polylactic acid microspheres as biodegradable drug carriers for cerebral tumours. *J Microencapsul* 17(5):625–638
107. Macha IJ, Cazalbou S, Ben-Nissan B, Harvey KL, Milthorpe B (2015) Marine structure derived calcium phosphate-polymer biocomposites for local antibiotic delivery. *Mar Drugs* 13(1):666–680
108. Jain JP, Kumar N (2010) Development of amphotericin B loaded polymersomes based on (PEG)(3)-PLA co-polymers: factors affecting size and in vitro evaluation. *Eur J Pharm Sci* 40(5):456–465
109. Huang YY, Chung TW (2001) Microencapsulation of gentamicin in biodegradable PLA and/or PLA/PEG copolymer. *J Microencapsul* 18(4):457–465
110. Sharma R, Muttill P, Yadav AB, Rath SK, Bajpai VK, Mani U, Misra A (2007) Uptake of inhalable microparticles affects defence responses of macrophages infected with mycobacterium tuberculosis H37Ra. *J Antimicrob Chemother* 59(3):499–506
111. Seleik H, Sahin S, Ercan MT, Sargon M, Hincal AA, Kas HS (2003) Formulation and in vitro/ in vivo evaluation of terbutaline sulphate incorporated in PLGA (25/75) and L-PLA microspheres. *J Microencapsul* 20(2):261–271
112. Guiziou B, Armstrong DJ, Elliott PNC, Ford JL, Rostron C (1996) Investigation of in-vitro release characteristics of NSAID-loaded polylactic acid microspheres. *J Microencapsul* 13(6):701–708
113. Zha J, Chi XW, Yu XL, Liu XM, Liu DQ, Zhu J, Ji H, Liu RT (2016) Interleukin-1 beta-targeted vaccine improves glucose control and β -cell function in a diabetic KK-A(y) mouse model. *PLoS One* 11(5):16

114. Anugraha G, Madhumathi J, Prita PJJ, Kaliraj P (2015) Biodegradable poly-L-lactide based microparticles as controlled release delivery system for filarial vaccine candidate antigens. *Eur J Pharmacol* 747:174–180
115. Pavot V, Berthet M, Resseguier J, Legaz S, Handke N, Gilbert SC, Paul S, Verrier B (2014) Poly(lactic acid) and poly(lactic-co-glycolic acid) particles as versatile carrier platforms for vaccine delivery. *Nanomedicine* 9(17):2703–2718
116. Qiu SH, Wei Q, Liang ZL, Ma GH, Wang LY, An WQ, Ma XW, Fang X, He P, Li HM, Hu ZY (2014) Biodegradable polylactide microspheres enhance specific immune response induced by hepatitis B surface antigen. *Hum Vaccin Immunother* 10(8):2350–2356
117. Pandit S, Cevher E, Zariwala MG, Somavarapu S, Alpar HO (2007) Enhancement of immune response of HBsAg loaded poly(L-lactic acid) microspheres against hepatitis B through incorporation of alum and chitosan. *J Microencapsul* 24(6):539–552
118. Zhou SB, Liao XY, Li XH, Deng XM, Li H (2003) Poly-D,L-lactide-co-poly(ethylene glycol) microspheres as potential vaccine delivery systems. *J Control Release* 86(2–3):195–205
119. Wang K, Li WF, Xing JF, Dong K, Gao Y (2012) Preliminary assessment of the safety evaluation of novel pH-sensitive hydrogel. *Eur J Pharm Biopharm* 82(2):332–339
120. Markland P, Zhang Y, Amidon GL, Yang VC (1999) A pH- and ionic strength-responsive polypeptide hydrogel: synthesis, characterization, and preliminary protein release studies. *J Biomed Mater Res* 47(4):595–602
121. Gong C, Shi S, Dong P, Kan B, Gou M, Wang X, Li X, Luo F, Zhao X, Wei Y, Qian Z (2009) Synthesis and characterization of PEG-PCL-PEG thermosensitive hydrogel. *Int J Pharm* 365(1–2):89–99
122. Fu SZ, Li Z, Fan JM, Meng XH, Shi K, Qu Y, Yang LL, Wu JB, Fan J, Luot F, Qian ZY (2014) Biodegradable and thermosensitive monomethoxy poly(ethylene glycol)-poly(lactic acid) hydrogel as a barrier for prevention of post-operative abdominal adhesion. *J Biomed Nanotechnol* 10(3):427–435
123. Fan R, Deng X, Zhou L, Gao X, Fan M, Wang Y, Guo G (2014) Injectable thermosensitive hydrogel composite with surface-functionalized calcium phosphate as raw materials. *Int J Nanomedicine* 9:615–626
124. Basu A, Kunduru KR, Doppalapudi S, Domb AJ, Khan W (2016) Poly(lactic acid) based hydrogels. *Adv Drug Deliv Rev* 107:192–205
125. Lai PL, Hong DW, Ku KL, Lai ZT, Chu IM (2014) Novel thermosensitive hydrogels based on methoxy polyethylene glycol-co-poly(lactic acid-co-aromatic anhydride) for cefazolin delivery. *Nanomedicine* 10(3):553–560
126. Molina I, Li S, Martinez MB, Vert M (2001) Protein release from physically crosslinked hydrogels of the PLA/PEO/PLA triblock copolymer-type. *Biomaterials* 22(4):363–369
127. He X, Ma J, Jabbari E (2010) Migration of marrow stromal cells in response to sustained release of stromal-derived factor-1 α from poly(lactide ethylene oxide fumarate) hydrogels. *Int J Pharm* 390(2):107–116
128. Shen W, Luan J, Cao L, Sun J, Yu L, Ding J (2015) Thermogelling polymer-platinum(IV) conjugates for long-term delivery of cisplatin. *Biomacromolecules* 16(1):105–115
129. Fan R, Tong A, Li X, Gao X, Mei L, Zhou L, Zhang X, You C, Guo G (2015) Enhanced antitumor effects by docetaxel/LL37-loaded thermosensitive hydrogel nanoparticles in peritoneal carcinomatosis of colorectal cancer. *Int J Nanomedicine* 10:7291–7305
130. Manaka T, Suzuki A, Takayama K, Imai Y, Nakamura H, Takaoka K (2011) Local delivery of siRNA using a biodegradable polymer application to enhance BMP-induced bone formation. *Biomaterials* 32(36):9642–9648
131. Nelson DM, Hashizume R, Yoshizumi T, Blakney AK, Ma Z, Wagner WR (2014) Intramyocardial injection of a Yoshizumi hydrogel with delivery of bFGF and IGF1 in a rat model of ischemic cardiomyopathy. *Biomacromolecules* 15(1):1–11

132. Song Z, Shi B, Ding J, Zhuang X, Zhang X, Fu C, Chen X (2015) A comparative study of preventing postoperative tendon adhesion using electrospun polyester membranes with different degradation kinetics. *Sci China Chem* 58(7):1159–1168
133. Zhang ZZ, Jiang D, Wang SJ, Qi YS, Ding JX, Yu JK, Chen XS (2015) Scaffolds drive meniscus tissue engineering. *RSC Adv* 5(95):77851–77859
134. Wang X, Shan H, Wang J, Hou Y, Ding J, Chen Q, Guan J, Wang C, Chen X (2015) Characterization of nanostructured ureteral stent with gradient degradation in a porcine model. *Int J Nanomedicine* 10:3055–3064
135. Zhang J, Liu H, Ding JX, Zhuang XL, Chen XS, Li ZM (2015) Annealing regulates the performance of an electrospun poly(ϵ -caprolactone) membrane to accommodate tissue engineering. *RSC Adv* 5(41):32604–32608
136. Zhang J, Liu H, Xu H, Ding JX, Zhuang XL, Chen XS, Chang F, Xu JZ, Li ZM (2014) Molecular weight-modulated electrospun poly(ϵ -caprolactone) membranes for postoperative adhesion prevention. *RSC Adv* 4(79):41696–41704
137. Shi B, Ding J, Wei J, Fu C, Zhuang X, Chen X (2015) Drug-incorporated electrospun fibers efficiently prevent postoperative adhesion. *Curr Pharm Des* 21(15):1960–1966
138. Jin HJ, Fridrikh SV, Rutledge GC, Kaplan DL (2002) Electrospinning *Bombyx mori* silk with poly(ethylene oxide). *Biomacromolecules* 3(6):1233–1239
139. Chen M, Li YF, Besenbacher F (2014) Electrospun nanofibers-mediated on-demand drug release. *Adv Healthc Mater* 3(11):1721–1732
140. Zhang J, Wang X, Liu T, Liu S, Jing X (2016) Antitumor activity of electrospun polylactide nanofibers loaded with 5-fluorouracil and oxaliplatin against colorectal cancer. *Drug Deliv* 23(3):784–790
141. Zhang Z, Liu S, Xiong H, Jing X, Xie Z, Chen X, Huang Y (2015) Electrospun PLA/MWCNTs composite nanofibers for combined chemo- and photothermal therapy. *Acta Biomater* 26:115–123
142. Zong X, Li S, Chen E, Garlick B, Kim KS, Fang D, Chiu J, Zimmerman T, Brathwaite C, Hsiao BS, Chu B (2004) Prevention of postsurgery-induced abdominal adhesions by electrospun bioabsorbable nanofibrous poly(lactide-*co*-glycolide)-based membranes. *Ann Surg* 240(5):910–915
143. Chen CH, Chen SH, Shalumon KT, Chen JP (2015) Dual functional core-sheath electrospun hyaluronic acid/polycaprolactone nanofibrous membranes embedded with silver nanoparticles for prevention of peritendinous adhesion. *Acta Biomater* 26:225–235
144. Liu S, Zhao J, Ruan H, Wang W, Wu T, Cui W, Fan C (2013) Antibacterial and anti-adhesion effects of the silver nanoparticles-loaded poly(L-lactide) fibrous membrane. *Mater Sci Eng C* 33(3):1176–1182
145. Hu C, Liu S, Zhang Y, Li B, Yang H, Fan C, Cui W (2013) Long-term drug release from electrospun fibers for in vivo inflammation prevention in the prevention of peritendinous adhesions. *Acta Biomater* 9(7):7381–7388
146. Jiang S, Zhao X, Chen S, Pan G, Song J, He N, Li F, Cui W, Fan C (2014) Down-regulating ERK1/2 and SMAD2/3 phosphorylation by physical barrier of celecoxib-loaded electrospun fibrous membranes prevents tendon adhesions. *Biomaterials* 35(37):9920–9929
147. Liu S, Hu C, Li F, Li XJ, Cui W, Fan C (2013) Prevention of peritendinous adhesions with electrospun ibuprofen-loaded poly(L-lactic acid)-polyethylene glycol fibrous membranes. *Tissue Eng Part A* 19(3–4):529–537
148. Liu S, Qin M, Hu C, Wu F, Cui W, Jin T, Fan C (2013) Tendon healing and anti-adhesion properties of electrospun fibrous membranes containing bFGF loaded nanoparticles. *Biomaterials* 34(19):4690–4701
149. Wang H, Li M, Hu J, Wang C, Xu S, Han CC (2013) Multiple targeted drugs carrying biodegradable membrane barrier: anti-adhesion, hemostasis, and anti-infection. *Biomacromolecules* 14(4):954–961

150. Sreerexha PR, Menon D, Nair SV, Chennazhi KP (2013) Fabrication of electrospun poly (lactide-co-glycolide)-fibrin multiscale scaffold for myocardial regeneration in vitro. *Tissue Eng Part A* 19(7–8):849–859
151. Jia L, Prabhakaran MP, Qin X, Ramakrishna S (2013) Stem cell differentiation on electrospun nanofibrous substrates for vascular tissue engineering. *Mater Sci Eng C Mater Biol Appl* 33(8):4640–4650
152. Vadala G, Mozetic P, Rainer A, Centola M, Loppini M, Trombetta M, Denaro V (2012) Bioactive electrospun scaffold for annulus fibrosus repair and regeneration. *Eur Spine J* 21 (Suppl 1):S20–S26
153. Ahire JJ, Neppalli R, Heunis TD, van Reenen AJ, Dicks LM (2014) 2,3-Dihydroxybenzoic acid electrospun into poly(D,L-lactide) (PDLLA)/poly(ethylene oxide) (PEO) nanofibers inhibited the growth of gram-positive and gram-negative bacteria. *Curr Microbiol* 69 (5):587–593
154. Llorens E, Calderon S, del Valle LJ, Puiggali J (2015) Polybiguanide (PHMB) loaded in PLA scaffolds displaying high hydrophobic, biocompatibility and antibacterial properties. *Mater Sci Eng C Mater Biol Appl* 50:74–84
155. Spasova M, Manolova N, Paneva D, Mincheva R, Dubois P, Rashkov I, Maximova V, Danchev D (2010) Polylactide stereocomplex-based electrospun materials possessing surface with antibacterial and hemostatic properties. *Biomacromolecules* 11(1):151–159
156. Ni P, Fu S, Fan M, Guo G, Shi S, Peng J, Luo F, Qian Z (2011) Preparation of poly(ethylene glycol)/polylactide hybrid fibrous scaffolds for bone tissue engineering. *Int J Nanomedicine* 6:3065–3075
157. Seyedjafari E, Soleimani M, Ghaemi N, Shabani I (2010) Nanohydroxyapatite-coated electrospun poly(L-lactide) nanofibers enhance osteogenic differentiation of stem cells and induce ectopic bone formation. *Biomacromolecules* 11(11):3118–3125
158. Kobsa S, Kristofik NJ, Sawyer AJ, Bothwell AL, Kyriakides TR, Saltzman WM (2013) An electrospun scaffold integrating nucleic acid delivery for treatment of full-thickness wounds. *Biomaterials* 34(15):3891–3901
159. Canton I, McKean R, Charnley M, Blackwood KA, Fiorica C, Ryan AJ, MacNeil S (2010) Development of an ibuprofen-releasing biodegradable PLA/PGA electrospun scaffold for tissue regeneration. *Biotechnol Bioeng* 105(2):396–408
160. Santoro M, Shah SR, Walker JL, Mikos AG (2016) Poly(lactic acid) nanofibrous scaffolds for tissue engineering. *Adv Drug Deliv Rev* 107:206–212
161. Liu DH, Ding JX, Xu WG, Song XF, Zhuang XL, Chen XS (2014) Stereocomplex micelles based on 4-armed poly (ethylene glycol)-polylactide enantiomeric copolymers for drug delivery. *Acta Polym Sin* 9:1265–1273
162. Saffer EM, Tew GN, Bhatia SR (2011) Poly(lactic acid)-poly(ethylene oxide) block copolymers: new directions in self-assembly and biomedical applications. *Curr Med Chem* 18 (36):5676–5686
163. Zhou R, Xu W, Chen F, Qi C, Lu BQ, Zhang H, Wu J, Qian QR, Zhu YJ (2014) Amorphous calcium phosphate nanospheres/polylactide composite coated tantalum scaffold: facile preparation, fast biomineralization and subchondral bone defect repair application. *Colloids Surf B Biointerfaces* 123:236–245
164. Peltto J, Bjorninen M, Palli A, Talvitie E, Hyttinen J, Mannerstrom B, Suuronen Seppanen R, Kellomaki M, Miettinen S, Haimi S (2013) Novel polypyrrole-coated polylactide scaffolds enhance adipose stem cell proliferation and early osteogenic differentiation. *Tissue Eng Part A* 19(7–8):882–892
165. Niu X, Fan Y, Liu X, Li X, Li P, Wang J, Sha Z, Feng Q (2011) Repair of bone defect in femoral condyle using microencapsulated chitosan, nanohydroxyapatite/collagen and poly (L-lactide)-based microsphere-scaffold delivery system. *Artif Organs* 35(7):E119–E128
166. Hu J, Sun X, Ma H, Xie C, Chen YE, Ma PX (2010) Porous nanofibrous PLLA scaffolds for vascular tissue engineering. *Biomaterials* 31(31):7971–7977

167. Tsuji T, Tamai H, Igaki K, Kyo E, Kosuga K, Hata T, Nakamura T, Fujita S, Takeda S, Motohara S, Uehata H (2003) Biodegradable stents as a platform to drug loading. *Int J Cardiovasc Interv* 5(1):13–16
168. Haddad T, Noel S, Liberelle B, El Ayoubi R, Aji A, De Crescenzo G (2016) Fabrication and surface modification of poly lactic acid (PLA) scaffolds with epidermal growth factor for neural tissue engineering. *Biomatter* 6(1):e1231276
169. Zhao J, Han W, Tu M, Huan S, Zeng R, Wu H, Cha Z, Zhou C (2012) Preparation and properties of biomimetic porous nanofibrous poly(L-lactide) scaffold with chitosan nanofiber network by a dual thermally induced phase separation technique. *Mater Sci Eng C* 32(6):1496–1502
170. Lou T, Wang X, Song G, Gu Z, Yang Z (2014) Fabrication of PLLA/ β -TCP nanocomposite scaffolds with hierarchical porosity for bone tissue engineering. *Int J Biol Macromol* 69:464–470
171. Binan L, Tendey C, De Crescenzo G, El Ayoubi R, Aji A, Jolicoeur M (2014) Differentiation of neuronal stem cells into motor neurons using electrospun poly-L-lactic acid/gelatin scaffold. *Biomaterials* 35(2):664–674
172. Kontogiannopoulos KN, Assimopoulou AN, Tsvintzelis I, Panayiotou C, Papageorgiou VP (2011) Electrospun fiber mats containing shikonin and derivatives with potential biomedical applications. *Int J Pharm* 409(1–2):216–228
173. Nguyen TTT, Ghosh C, Hwang SG, Tran LD, Park JS (2013) Characteristics of curcumin-loaded poly(lactic acid) nanofibers for wound healing. *J Mater Sci* 48(20):7125–7133
174. Leroueil-Le Verger M, Fluckiger L, Kim YI, Hoffman M, Maincent P (1998) Preparation and characterization of nanoparticles containing an antihypertensive agent. *Eur J Pharm Biopharm* 46(2):137–143

3D Printing of Poly(lactic acid)



Michael Van den Eynde and Peter Van Puyvelde

Abstract Poly(lactic acid) has received considerable interest in biopolymer-related research because of its excellent biocompatibility and sustainability. With the advent of new processing routes based on additive manufacturing technologies – commonly called 3D printing – applications of PLA have become more and more widespread, especially in the biomedical field (e.g., as scaffolds for tissue engineering). This review focuses on three of the most important additive manufacturing routes: extrusion-based 3D printing techniques, powder-based laser sintering, and stereolithography. For each of these methods, we discuss the processing conditions and their effect on the end use of PLA.

Keywords 3D printing • Added manufacturing • Fused deposition modeling • PLA • Selective laser sintering • Stereolithography

Contents

1	Introduction	140
2	Different Printing Technologies	140
3	PLA in Extrusion-Based Printing Technologies	142
4	PLA in Powder-Based Additive Manufacturing Techniques	145
5	Photopolymerization-Based 3D Printing of PLA	151
6	Conclusion	153
	References	153

M. Van den Eynde and P. Van Puyvelde (✉)
Department of Chemical Engineering, Soft Matter: Rheology and Technology, KU Leuven,
Celestijnenlaan 200F, 3001 Leuven, Belgium
e-mail: peter.vanpuyvelde@kuleuven.be

1 Introduction

Poly(lactic acid) (PLA) is a linear aliphatic thermoplastic polymer produced by ring-opening polymerization of lactide, which can be obtained from the fermentation of sugar feedstock [1]. Its building block, lactic acid, exists in optically active D- and L-enantiomers and, depending on the ratio of D- to L-isomers, a broad range of material properties can be obtained. Since its commercial introduction in 2002, different potential applications of PLA have been explored, ranging from its use as a high-performance compostable material to applications as tissue engineering scaffolds in medical applications (e.g. [2, 3]). The reasons for its success are its reasonable barrier, mechanical, and optical properties compared with some of its petroleum-based counterparts [4, 5]. Because commercial PLAs are typically copolymers of poly(L-lactic acid) (PLLA) and poly(D,L-lactic acid) (PDLLA), their properties are to a large extent determined by the optical purity of PLA [6–9]. Moreover, in enantiomeric blends of PLLA and poly(D-lactic acid) (PDLA), multicenter hydrogen bonds can lead to PLA stereocomplex formation, which results in enhanced thermal and mechanical properties that could open new possible applications of PLA as an engineering material [10, 11]. Moreover, PLA can be processed using conventional polymer processing equipment with only minor equipment modification, which is an additional advantage of this biobased polymer [12]. Recently, new processing technologies for PLA have been introduced, such as supercritical foaming processes [13, 14] and electrospinning of PLA nanofibers [15–17], which are suitable for further expanding the use of this polymer. Newer processing technologies for PLA include the so-called additive manufacturing (AM) technologies – commonly called 3D printing techniques – that are the topic of this review. Originally, these production techniques were used to produce rapid prototype parts. However, the technology has now evolved to such an extent that end-use parts with sufficient mechanical and other properties can be produced. First, we briefly explain the different AM technologies and then discuss the production of PLA parts using some of the described 3D technologies.

2 Different Printing Technologies

An AM technique is defined by the joint ISO/ASTM standards as “a process that joins materials to make parts from 3D model data, usually layer upon layer” [18]. These technologies commonly start from a 3D computer representation of the desired part and produce end-use parts by building them layer by layer [19, 20]. One of the most important advantages of such additive production methods is the ability to manufacture parts that have a significantly greater geometrical complexity than possible with traditional processes such as injection molding, without the need for costly mold tooling (e.g. [21]). Geometries that are otherwise difficult to attain can be produced as effortlessly and at comparable cost as producing any simple shape.

Moreover, because expensive tooling is not required, the economics of production are dramatically changed, making low volume production and even fully customized products possible [22, 23]. According to the ISO standards, AM technologies are typically categorized into seven subgroups [18].

Of these groups, techniques based on *material extrusion* are probably the most popular AM technology. Here, the material under consideration is forced through a nozzle to extrude a semiliquid material that is used to create successive object layers. Typical materials used here are acrylonitrile-butadiene styrene (ABS) and PLA as commodity plastics, but some engineering and high-performance plastics such as nylon, polyetherimide (PEI), and polyphenylsulfone (PPSF) have also become available for this market. The technology is not limited to polymers because anything that can be pushed through a nozzle can, in principle, be printed. This has already led to some exotic applications of 3D printing such as the printing of concrete and even the printing of chocolate and other gastronomy-related products [24].

Related AM technologies are *binder jetting* and *material jetting* processes. In binder jetting, liquid droplets of an adhesive binder material are deposited to bind powder material by a process that has similarities to conventional inkjet processes. In some variations of the process, the binder becomes part of the component. In other variations, however, substantial post-treatment operations are required to remove the binder materials and to densify the resulting powder-based material to improve its mechanical properties. In material jetting, droplets of photosensitive thermoset polymers are deposited onto a build platform to create the desired shape by an in-situ curing operation after deposition. This process is a more modern variant of the oldest AM technology, *stereolithography*, which was developed in the mid-1980s [25]. In this approach, a liquid thermoset polymeric layer is deposited and is typically cured by passing a UV-laser beam onto the desired locations, after which a new liquid layer is spread.

Another important class of AM technologies is based on powder-bed fusion. Here, a solid powder layer is deposited and then exposed to a heat source, which is typically a laser (the so-called *laser sintering process*) or an electron beam. These technologies are popular for part manufacturing for several reasons [26–28]. First, different classes of materials can be sintered, ranging from metals to ceramics to polymers. Second, no support structures need to be printed because the unsintered solid powder bed serves as the structural support. Extrusion-based and lithography techniques have the drawback that they require support structures that need to be removed in a laborious (and thus expensive) postprocessing step.

A final class of AM technologies – according to the ISO standards – is based on *sheet lamination*, which includes processes in which the feedstock is in the form of a sheet that serves as a layer in the build. The different sheets are cut to shape before being stacked and adhered to previous layers. Alternatively, the different sheets can be bonded to previous layers before being cut and shaped to form the desired product. After 30 years of research and development, AM has evolved from a rapid prototyping process to a legitimate manufacturing method for end-use part production. PLA plays a significant role as a “printing material,” albeit not in all the

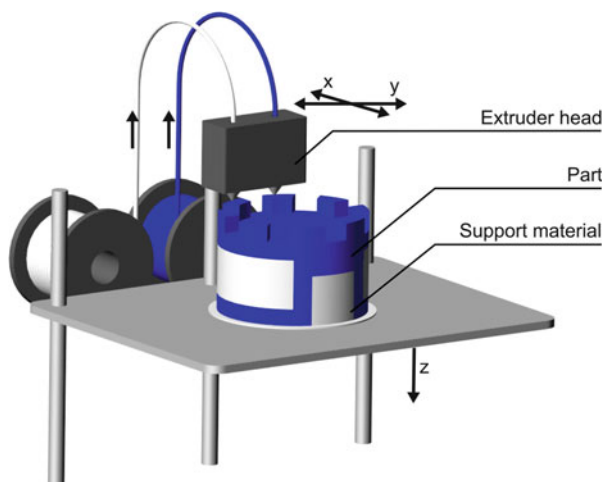
different technologies described above. In this review, we mainly focus on three application domains of PLA as a printing material: as feedstock for extrusion-based printing techniques, as a powder for sinter-based techniques, and as a liquid layer in stereolithographic applications.

3 PLA in Extrusion-Based Printing Technologies

Extrusion-based processes are among the most widely used and rapidly growing AM technologies [29] (<http://www.custompartnet.com/>). Within this category, fused deposition modeling (FDM), fused filament fabrication (FFF), and melt extrusion manufacturing (MEM) are commonly used terms to indicate technologies based on material extrusion. The difference between these processes can be traced back to differences in tradenames. In these processes, a filament of material is fed into the machine through a pinch roller mechanism (see Fig. 1). The filament is molten in a heated extrusion head and the solid portion of the filament acts as a piston to push the melt through the print nozzle. A simple mechanism moves the print nozzle along the horizontal xy plane. During this motion, the molten material is deposited on a build surface that can be moved in the vertical z -direction. After deposition, the material solidifies immediately. This process enables complex 3D objects to be manufactured.

The most common materials used in this type of process are amorphous thermoplastics, with ABS being the most widely used material, closely followed by PLA [30]. Applications of this technology are already versatile, especially in the area of prosumer goods. For instance, extrusion-based printing techniques (using PLA) have been widely used in the printing of teaching aides [31], science tools [32], farming tools [33], and surgical instruments [34]. Summarizing all the

Fig. 1 Typical fused deposition setup



different applications already using this technology is beyond the scope of this review. We focus here on the scientific challenges that are still faced with common 3D printing technologies, with an emphasis on PLA as the raw material.

The use of biopolymers such as PLA or polycaprolactone (PCL) is attractive for tissue engineering applications, as discussed later [35, 36]. A major factor that hinders further growth of this technology is the limited understanding of processing parameters [36]. However, with the growing popularity of 3D printers for consumer-level use, evaluation of the mechanical properties of parts produced with this technique is crucial. Several studies have already paid attention to different performance parameters, such as dimensional accuracy and compressive, tensile, flexural, and impact strengths [37–39]. For instance, Lee et al. [38] observed that the compressive strength of FDM parts was 24% higher in axially loaded samples than in transversally loaded specimens, showing the important effect of print orientation. Further effects of the processing properties were demonstrated by Panda et al. [39], who showed that both tensile and flexural strength increased with decreasing layer thickness. On the other hand, impact strength was improved by increasing the layer thickness. However, these studies have mostly been limited to ABS components rather than PLA, which is increasingly used in popular 3D printers.

As mentioned above, the biocompatibility of PLA has raised a lot of interest in the medical field for its use in applications such as tissue engineering and implants that are custom-made for a specific patient [40, 41]. Evidently, there is a great need to evaluate the properties of PLA FDM parts, especially regarding strength and fracture characteristics because these are critical properties for both industrial and general use. However, the situation is complex because the quality and strength of a component is affected by several machine-related factors. In addition to printing orientation and layer thickness, the material extrusion temperature also strongly influences the strength of FDM components [42, 43]. Combined with other printing settings such as print speed and building platform temperature, it is clear that the number of experiments needed to elucidate the effect of all these parameters on the mechanical performance can escalate drastically. To produce guidelines for optimal mechanical performance of PLA parts produced by FDM, Torres et al. used a design of experiments (DoE) approach [44]. Through testing of the tensile and fracture properties, guidelines were established for FDM printers using PLA print media. Recommendations were made for both tensile and fracture applications, as well as for generic applications that may not necessarily be constructed for a single loading situation. Although the given settings represent the best overall combination, as given by test results, some settings still depend on user preferences. For instance, if aesthetics are important, a lower layer thickness and slower speed result in a higher resolution with an improved surface finish. In such cases, layer thickness can be lowered with little concern for a loss in strength. Other statistical models have also been used to study the impact of process parameters on the mechanical properties of PLA parts produced by FDM [45, 46], as well as on the fatigue [47] and distortion properties [48]. However, there is a general consensus that the lack of published data and the high variability in experimental results, as well as the effect

of other less controllable factors such as humidity, require further investigations to improve knowledge of the mechanical behavior of PLA components manufactured by these melt extrusion-based printing techniques.

Despite the difficulties in controlling the mechanical properties, several attempts have already been made to enhance the intrinsic mechanical behavior of PLA and to create potential new synergies by 3D extrusion of composite materials. Regarding the latter, compounds of PLA with tricalcium phosphate (TCP) as a resorbable composite have already been prepared [41]. TCP is one of the main constituents of bone and is considered an ideal material for implants with osteoconductive properties that enable the regeneration of tissue [49]. Drummer et al. demonstrated that such compounds could be processed with FDM-based technologies and that adequate mechanical properties could be obtained [41]. However, there is still a long way to go to fulfill all requirements for medical scaffolds. For instance, the influence of processing parameters on porosity and pore size distribution, as well their effects on biocompatibility and in vivo degradation, are still largely unexamined.

To enhance mechanical properties, attempts have been made to create composite-like PLA materials. For instance, 3D printable PLA–graphene composites have recently been produced and could be used to explore enhanced mechanical behavior, flame retardancy, and electrical conductivity [50]. However, apart from a proof of principle, no systematic study of the properties has been made. Even continuous carbon fiber-reinforced PLA composites have been produced [51]. In this approach, impregnation of the fiber inside the PLA matrix and extrusion took place simultaneously in the extruder head of the printer. Similar to the case of printing pure PLA melt, the many processing parameters still hamper full exploitation of the potential of this process. Further experimental and modeling work is needed to make extrusion-based methods for PLA suitable for real structural and controlled applications.

Instead of depositing PLA materials from the melt, nozzle-based PLA printing techniques from solution have also been proposed. This technique has the advantage that the polymer can be printed at much lower temperatures, hence avoiding degradation. Typically, chloroform is used as the solvent. Such structures are of significant interest in regenerative medicine, where very promising applications of biodegradable templates for tissue regeneration can be envisaged [52, 53]. In addition, such 3D structures have interesting applications in 3D in vitro platforms for studying the cell response to different scaffold conditions or for screening different drug formulations [54]. One of the most challenging aspects of solution printing is to maintain the correct viscosity of the PLA printing ink. Either the processing temperature or the use of a plasticizer can be used to control viscosity. Of these methods, using the right plasticizer is probably more interesting because it allows the polymer to be processed at lower temperatures without risking thermal degradation of the polymer [55].

Different plasticizers have already been tested, but low molecular weight polyethylene glycol (PEG) seems to be the most efficient. PEG is a biocompatible, hydrophilic polymer that is (similarly to PLA) soluble in chloroform [56, 57]. Hence, it is possible to obtain homogeneous PLA/PEG blends for the fabrication of

3D scaffolds by this low temperature printing technique. For instance, Serra et al. [55] demonstrated that addition of PEG increased the surface roughness and wettability. However, the formed structures were not uniform and the mechanical properties were significantly decreased. This is further illustrated in Fig. 2, which shows SEM images of 3D-printed scaffolds. Figure 2a–c illustrates the effect of PEG concentration on the structures, which clearly reveals differences in pore size (quantified in Fig. 2e) and strut thickness of the three scaffolds. By increasing the PEG concentration from 5 to 20 wt%, the originally designed square pores turned into more rounded pores, which also affected porosity in general (Fig. 2g). In addition, as can be seen in Fig. 2f, the addition of PEG resulted in a decrease in mechanical properties, expressed here as the compressive strength. Figure 2d shows the effect of adding a bioactive glass (G5) on the resulting structure. In this case, the plasticizing effect of PEG yielded a good distribution of the glass particles in the polymeric matrix. This resulted in better reproduction of the originally orthogonal pores and in improved mechanical performance.

As demonstrated, the use of PLA for printing scaffolds by means of extrusion-based methods is becoming more widespread. Of course, printing a scaffold is one thing, but vascularization of large, solid, 3D polymer-based scaffolds is still an unsolved technological barrier in tissue engineering [58] and requires significant progress. In addition, for these applications, the use of PLA with this technology is questioned by some researchers. For instance, Liew et al. demonstrated that FDM and 3D printing of biodegradable polyesters might lead – because of the high temperatures – to the rapid formation of hydroxyacids, which can lead to local cell toxicity [59].

4 PLA in Powder-Based Additive Manufacturing Techniques

Powder-based AM processes, such as laser sintering, enable complex 3D objects to be built by selectively fusing together successive layers of powdered material (see Fig. 3).

In this process, a thin layer of powder (typically of the order of 100 μm) is spread over the build area to form the powder bed. A computer-controlled laser scans over this area and heats the powder in areas specified by the CAD model. The temperature of the powder particles that are hit by the laser rises above the melting temperature and the particles coalesce. Between layers, the build platform is lowered by a small increment (typically 100 μm) and a subsequent powder layer is deposited. This process is repeated until the entire plastic part is ready. An advantage of this technique with respect to extrusion-based methods is that the powder that has not been sintered by the laser remains in place in each layer to support subsequent layers, without the need to print support structures. The need for support is an important disadvantage of extrusion-based and photopolymerization-based

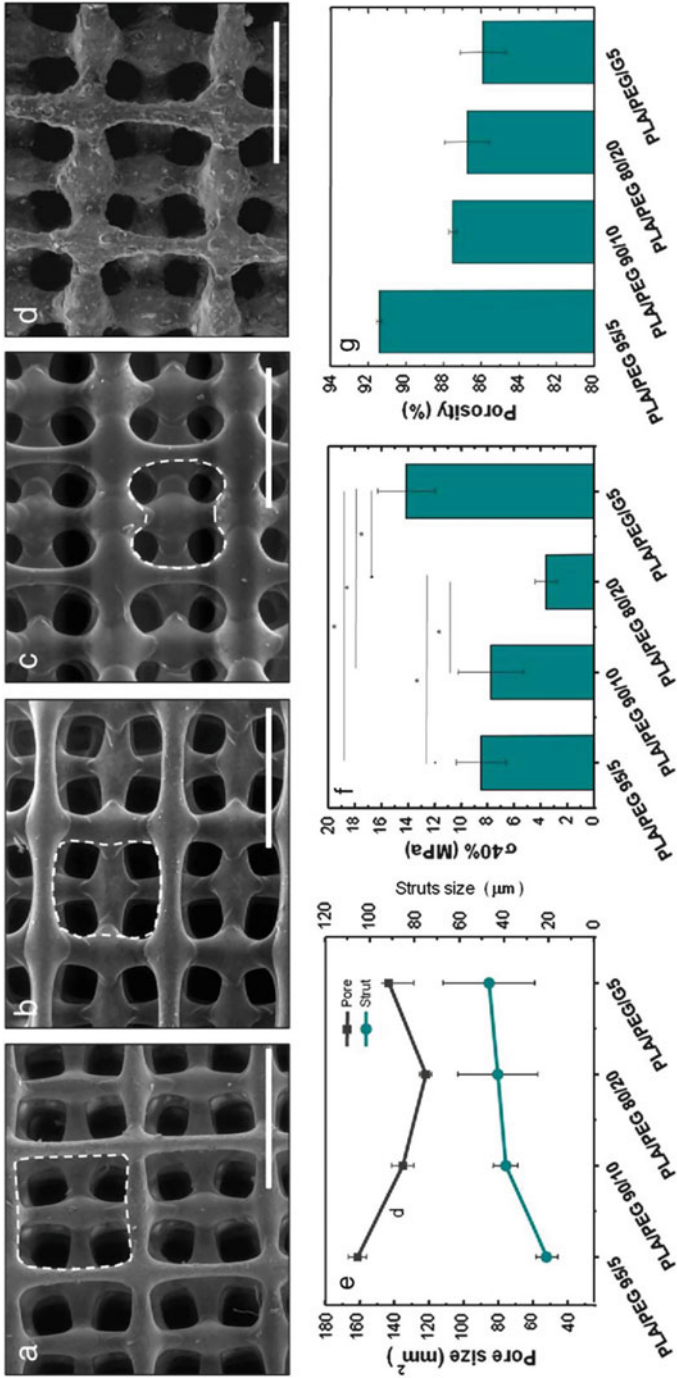


Fig. 2 SEM images of 3D-printed scaffolds: (a) PLA/PEG 95/5, (b) PLA/PEG 90/10, (c) PLA/PEG 80/20, (d) PLA/PEG 95/5/G5 (scale bar indicates 500 μm), (e) variation of struts and pore size, (f) compressive strength at 40% deformation, and (g) theoretical volume porosity percentage of the 3D-printed scaffolds with different blends [55]

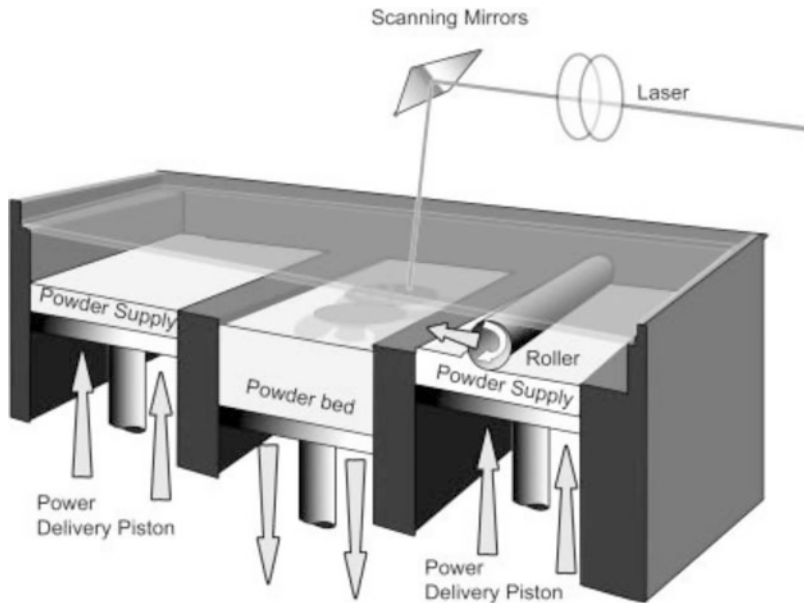


Fig. 3 The laser sintering process [20]

3D printing techniques. In laser sintering, the support is given by the surrounding unsintered powder. In extrusion-based methods, it is impossible to print overhanging structures without the use of support materials. The latter is also true for photopolymerization because printing is performed on a surrounding liquid. In laser sintering, upon completion of the build, the parts and surrounding supporting powder present in the build platform are removed from the machine. Unsintered powder can then, in principle, be recycled for subsequent new builds.

Despite its flexibility with respect to design, a widely acknowledged drawback of the method is the limited range of materials, particularly polymers, that can be used in this technique. To date, most of the market for laser sintering is dominated by polyamide 12, which is not necessarily the best material for every application. Hence, a lot of research effort is focused on elucidating the most important material properties for laser sintering [60–63]. This is not an easy task given the complexity of the laser sintering process. A first important step is to obtain a powder with good flow properties, which is typically obtained when interparticle adhesion and friction are low. Therefore, smooth powder particles with a high sphericity are typically preferred for laser sintering. Flow additives, often small silica particles, are typically added to enhance powder flow [20, 64–66].

In addition to the deposition of powders layers, a proper coalescence of the molten powder particles is crucial in obtaining dense parts. Because no mechanical force is applied during the process, this fusion is often restricted and full density is difficult to obtain. This part of the process is largely governed by the zero shear viscosity of the material and, to a more limited extent (because there is not so much

variation), by the surface tension of the polymer melt [67–69]. After processing, the sintered material cools and eventually solidifies. However, because of the layer-by-layer approach and the complex temperature distribution in this processing method, the resulting shrinkage is not always homogeneous. For semicrystalline materials in particular, large shrinkage during crystallization can be detrimental [70]. To postpone crystallization and, hence, minimize thermal gradients during laser sintering, each powder layer is typically preheated to just below the onset of melting. The more distant the onset of crystallization is with respect to this preheating temperature, the more supercooling is allowed before crystallization sets in, which could result in nonhomogeneous shrinkage. Therefore, the distance between melting and crystallization peaks in a typical DSC experiment is widely used to determine the processability of a polymer in laser sintering [20, 71–74].

Apart from postponing shrinkage, choosing a polymer with an inherently low shrinkage is also beneficial. However, shrinkage data for sintering materials is scarce, mainly because of the practical difficulties encountered in dilatometric measurements on molten polymers [74]. Most often, volume changes are measured under large pressures (*PVT* setups), which are extrapolated to atmospheric pressures in order to become relevant for laser sintering. Recently, a new dilatometer was developed in our group that allows measurement of shrinkage at ambient pressures starting from the melt, which is a feature in dilatometry. This setup can be used to determine and compare shrinkage of polymer grades relevant to laser sintering [75].

In summary, to evaluate the sinterability of a polymer, the polymer should fulfill the following requirements:

1. It has to be available in powder form with the correct particle size distribution (approximately 10–80 μm) and appropriate sphericity.
2. The powder has to flow smoothly.
3. Upon melting, the viscosity should be sufficiently low to have a good coalescence.
4. The melting and crystallization peaks should differ significantly so that the processing window to determine the bed temperature is as wide as possible.
5. The shrinkage should be small in order to avoid possible warpage problems.

An example of this screening methodology is shown in Fig. 4. Some of the relevant properties for laser sintering are given for the benchmark commercial sinter grade polyamide PA2200 (EOS GmbH). As can be seen in Fig. 4a, the powder particles are almost spherical, which is a result of the solution-precipitation process that is used to prepare these powders. This gives rise to a very good powder flow, as discussed by Van den Eynde et al. [66]. Figure 4b shows the melt rheology of the same polyamide for three different temperatures. As can be seen, the material shows significant postcondensation, especially at higher temperatures. This postcondensation is detrimental for recycling of the powder, because every treatment at high temperature leads to higher viscosity and, hence, more difficult coalescence. This eventually leads to very porous parts with very poor mechanical properties. Coalescence of the powder can be evaluated at the laboratory scale by

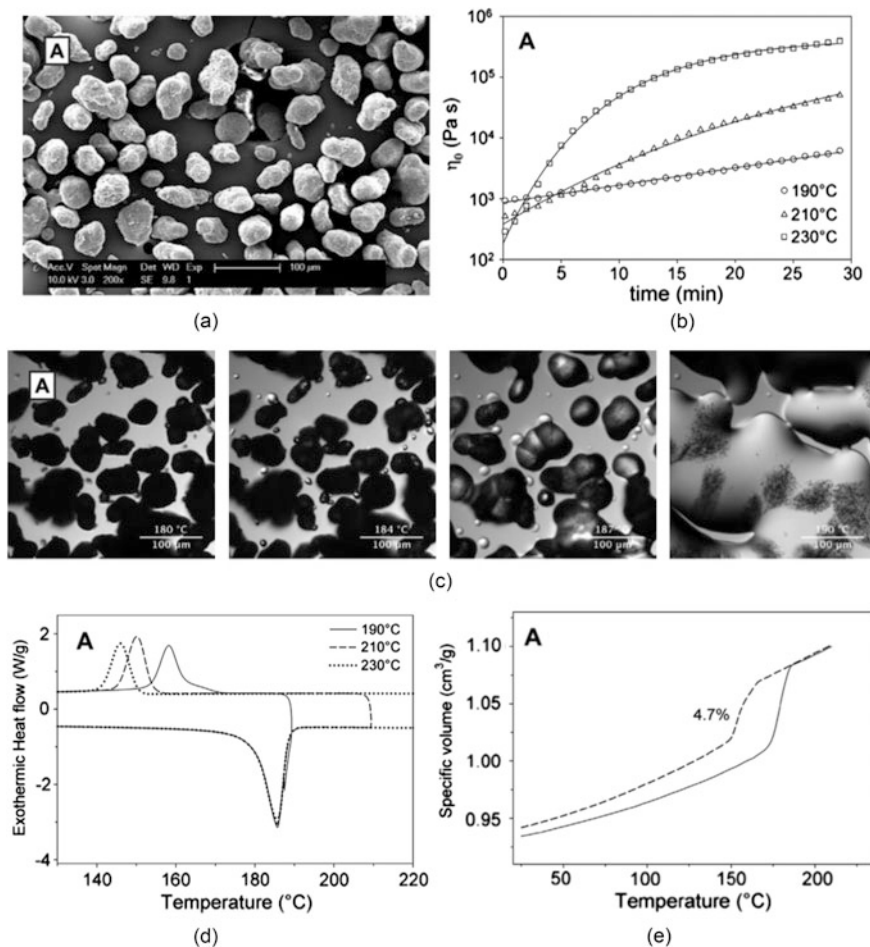


Fig. 4 Characteristics of the EOS commercial sinter grade polyamide PA2200: (a) SEM image of the powder, (b) zero shear viscosity at different temperatures as a function of time, (c) evolution of the coalescence process (heating rate of 10°C/min), (d) DSC curves upon heating and cooling (different heat treatments, measurements performed at 10°C/min), and (e) dilatometry performed at 0.5°C/min (adapted from [75])

means of a combination of a hot stage and microscopy, as seen in Fig. 4c. Coalescence of PA2200 is very sudden and a closed film is formed quite rapidly. Figure 4d shows the DSC curves for the material taken at 10°C/min. As stated, a large distance between melting and crystallization peaks in DSC is a good indication of the tendency of the material to warp during processing. For the polyamide shown in Fig. 4, an increased heating temperature results in significant postponing of the onset of crystallization. This is not surprising given the fact that a higher temperature also enhances postcondensation reactions, as shown in Fig. 4b. This postcondensation results in increased molecular weight and melt viscosity, hence

reducing the crystallization kinetics. In fact, the subtle difficulties of sintering a material are demonstrated here. On the one hand, the distance between the melting and crystallization peaks becomes large, which should broaden the processing window and reduce the risk of warping. On the other hand, an increased molecular weight decreases coalescence and leads to lower recyclability of the powder. Figure 4e shows the specific volume as a function of temperature, as measured using a new dilatometer setup developed by Verbelen [75]. This particular polyamide shows a rather large expansion step upon melting as a result of the high degree of crystallinity of the virgin powder. The crystallization shrinkage of 4.7% is low compared with other semicrystalline materials.

These results show that many different and often competitive material parameters are involved in the laser sinter process. Because of all these requirements (this list is a simplified summary of what is really required), few polymer grades have been identified as being sinterable. From the commercial point of view, the number of polymer sinter grades is very limited at present, although a polypropylene-based material, poly(ether ether keton) and thermoplastic polyurethanes have recently been introduced to the market [20]. However, very little published work has been carried out on new polymers. The available literature has mainly focused on non-load-bearing materials for medical applications [76–78].

Literature on the laser sintering of PLA is still scarce. A few reports link PLA and selective laser sintering in medical applications such as tissue engineering. Tissue engineering requires the implantation of a biocompatible and biodegradable porous scaffold that serves as a temporary template for cells to attach, develop, and subsequently generate tissue. The success of this approach depends largely on the performance of the scaffold. As a naturally derived biodegradable polymer, PLA has been investigated for this application [79, 80]. However, a major stumbling block is the lack of powder in sufficient quantities. Often, powders are produced ad hoc in small quantities by solution methods (e.g. [79]) that are impossible to use at a larger scale. A second drawback in the sintering of PLA for tissue engineering is the exposure to high temperatures, which can have two consequences. First, the heat provided by the laser could degrade the polymer, leading to changes in molecular weight and, hence, mechanical performance. Second, in tissue engineering applications, bioactive proteins are typically introduced to serve as seeding molecules for tissue creation. However, such bioactive components often do not withstand the heat provided by the laser [81]. To circumvent this, a modified laser sintering methodology (surface-selective laser sintering) was introduced [82, 83]. This technology is based on two modifications. The first modification is the use of a diode laser with a wavelength of 0.97 μm , rather than the conventional CO_2 laser that is normally used in laser sintering. This near-infrared laser radiation is not absorbed by the PLA. A second modification is the addition of a small quantity (<0.1 wt%) of biocompatible carbon microparticles, homogeneously distributed at the surface of the polymer particles [84, 85]. Because these particles are strong absorbers of the near-infrared laser radiation, only the surface of the particles becomes molten. As such, bioactive species trapped within each particle retain their activity during the processing step. A proof-of-concept of this approach was demonstrated by Antonov

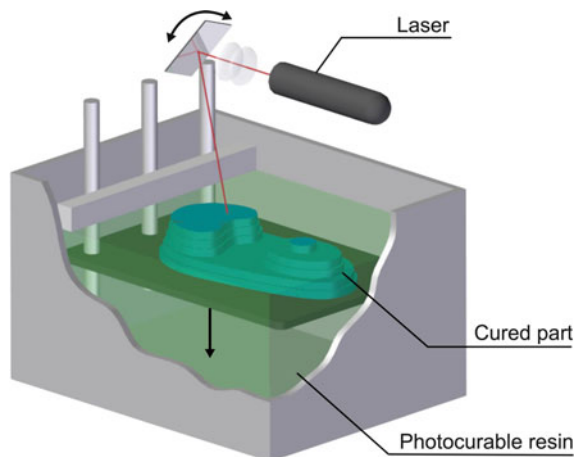
et al. [82] by incorporating the enzyme ribonuclease A in PLA particles. However, because the polymer partially melts, there is a delicate interplay between retaining sufficient bioactivity and obtaining appropriate mechanical properties of the sintered part.

For structural applications, laser sintering of PLA has not been extensively used. One of the stumbling blocks here is probably the lack of powders with sufficient flowability. PLA is known to be hard to mill, even in a cryogenic environment [75]. This automatically leads to a lack of sufficient sphericity and, hence, poor flow properties. Moreover, because PLA typically shows some cold crystallization, heating the material to the bed temperature induces stickiness of the powder, which makes it impossible to deposit a defect-free layer. Such cold crystallization can be eliminated by annealing the powder, but this would require an additional processing step before the feeding the powder to the sinter machine. Bai et al. [86] investigated the effect of adding nanoclay to PLA on the mechanical properties of sintered parts. They demonstrated that PLA parts could be produced by the method and that adding nanoclay improved the flexural modulus of the produced parts. However, flexural moduli were reported in the range of 100–700 MPa, which is dramatically lower than the reported moduli of standard injection-molded parts (about 3,000 MPa).

5 Photopolymerization-Based 3D Printing of PLA

One of the oldest AM techniques, developed in the late 1980s, is based on photopolymerization and is commonly called stereolithography (SLA). Originally, a HeCd laser system was used to spatially control the polymerization of a photocurable resin that had been deposited in a layer (see Fig. 5). The building

Fig. 5 A stereolithography setup



principle is similar to the laser sintering process, but a liquid layer is deposited instead of a solid powder layer. This causes a problem with sintering because uncured liquid cannot support the structure that is being built. Hence, to print complex parts, support structures also need to be manufactured and removed afterwards. When the part is ready, the unpolymerized resin is removed and, typically, the part is postcured in a UV oven to convert any unreacted groups and strengthen the part [87].

To produce parts within a decent time frame, the kinetics of the curing reaction is crucial because it affects the curing time and the thickness of the layer that can be polymerized. Typically, the kinetics can be controlled by the power of the light source, the scan speed, and the chemistry and amount of monomer and photoinitiator. In addition, UV absorbers can be added to the resin to control the degree of polymerization [88]. To ensure proper bonding between successive layers, the conversion at the interface should be slightly higher than the gel point. However, this local overexposure might result in further curing of the previous layer. Potentially, parts of the previous layer that were intended to remain uncured risk being partially polymerized. This effect might become significant when printing porous structures [89].

Regarding accuracy and resolution, SLA outperforms other AM techniques. In most of the above-mentioned methods, the smallest details are about 50–200 μm in size and many commercially available SLA setups can build objects at an accuracy of 20 μm . More sophisticated SLA setups can build structures with submicron resolution, which is impossible to achieve with the other technologies [90].

Materials that are used in SLA must contain photocurable moieties in order to undergo photocrosslinking. However, the amount of available resin is also relatively limited for this technique (cf. the laser sinter process). Typical resins for use in SLA are based on low molecular weight polyacrylate or epoxy-based materials that form glassy networks upon polymerization and crosslinking. Over the past decade, several resins have been developed and the resulting mechanical properties of the cured networks encompass a wide range, making them not only useful as prototypes but also as functional parts that can be used in more demanding end-use applications [91]. PLA is also finding its way into the SLA field, mainly in applications related to tissue engineering. The manufacture of precisely designed tissue engineering scaffolds by SLA is becoming a new standard.

A lot of work has been done in the development of biodegradable resins. These are typically based on poly(propylene fumarate), ϵ -caprolactone, or D,L-lactide [92–97]. For engineering tissue such as bone, strong and rigid biodegradable materials are required. The amorphous poly(D,L-lactide) has already been applied in bone fixation devices in clinical environments [98, 99] and in scaffolds suitable for bone tissue engineering [100–102]. The ability to process PLA by SLA opens many possibilities because a large variety of structures can be prepared with different mechanical properties, cell seeding possibilities, and culturing capabilities. Different chemical approaches have been followed to make PLA processable with SLA. PLA networks can be formed by photo-initiated radical polymerization of polylactide oligomers that are end-functionalized with an unsaturated group such

as methacrylate [103], fumarate [104], or acrylate [105]. However, to make such materials processable with SLA, a diluent is required to reduce the viscosity of the resin, which should be lower than approximately 5 Pa s [106]. Reactive diluents such as methyl methacrylate and *N*-vinyl-2-pyrrolidone have been used. However, the introduction of these diluents results in significant amounts of nondegradable material [92]. The latter can be overcome by using nonreactive diluents such as ethyl lactate [97].

6 Conclusion

This chapter reviews the use of PLA in AM (3D printing) processes. Three important 3D technologies have been considered: extrusion-based AM methods, methodologies based on powder sintering, and SLA. PLA can be processed by any of these techniques, but chemical modification is needed in the case of SLA. The main engineering application of PLA processed with these methods is the manufacturing of scaffolds for tissue engineering. All 3D printing techniques described here are eligible for this use, although differences in resolution have been reported. PLA functions very well in extrusion-based AM techniques and many applications in the prosumer area and in the medical field have already been reported. However, the use of PLA in more structurally demanding applications is still limited, but further development of specific material requirements targeted for a specific 3D-printing technology (e.g., powders with sufficient flow properties) could open up more applications for this versatile biodegradable polymer.

Acknowledgements The author acknowledges the financial support provided by the Strategic Initiative Materials (SIM) in Flanders.

References

1. Lunt J (1998) Large scale production, properties and commercial applications of polylactic acid polymers. *Polym Degrad Stab* 59:145–152
2. Gupta B, Revagade N, Hilborn J (2007) Poly(lactic) fiber: an overview. *Prog Polym Sci* 32:455–482
3. Ajiro H, Ito S, Kan K, Akashi M (2016) Catechin-modified polylactide stereocomplex at chain end improved antibiobacterial property. *Macromol Biosci* 16:694–704
4. Auras R, Harte B, Selke S, Hernandez R (2003) Mechanical, physical and barrier properties of poly(lactide-films). *J Plast Film Sheeting* 19:123–135
5. Lehermeier H, Dorgan J, Way JD (2000) Gas permeation properties of poly(lactic acid). *J Polym Environ* 8:1–9
6. Urayama H, Moon SI, Kimura Y (2003) Microstructure and thermal properties of polylactides with different L- and D-unit sequences: importance of the helical nature of the L-sequenced segments. *Macromol Mater Eng* 288:137–143
7. Tsuhii H, Okino R, Daimon H, Fujie K (2005) Water vapor permeability of poly(lactide)s: effects of molecular characteristics and crystallinity. *J Appl Polym Sci* 99:2245–2252

8. Sarasua JR, Arraiza AL, Baerlidi P, Maiza I (2005) Crystallinity and mechanical properties of optically pure polylactides and their blends. *Polym Eng Sci* 45:745–753
9. Tsuji H, Idada Y (1996) Crystallization from the melt of PLA with different optical purities and their blends. *Macromol Chem Phys* 197:3483–3499
10. Tan BH, Muiruri JK, Li Z, He C (2016) Recent progress in using stereocomplexation for enhancement of thermal and mechanical property of polylactide. *ACS Sustain Chem Eng* 4:5370–5391
11. Tsuji H (2005) Poly(lactide) stereocomplexes: formation, structure, properties, degradation and applications. *Macromol Biosci* 5:569–597
12. Lim LT, Auras R, Rubino M (2008) Processing technologies for poly(lactic acid). *Prog Polym Sci* 33:820–852
13. Nalawade S, Picchione F, Janssen LPBM (2006) Supercritical carbon dioxide as a green solvent for processing polymer melts: processing aspects and applications. *Prog Polym Sci* 31:19–43
14. Quirk RA, France RM, Shakesheff KM, Howdle SM (2004) Supercritical fluid technologies and tissue engineering scaffolds. *Curr Opin Solid State Mater Sci* 8:313–321
15. Yang F, Murugan R, Wang S, Ramakrishna S (2005) Electrospinning of nano/micro scale poly(L-lactic acid) aligned fibers and their potential in neural tissue engineering. *Biomaterials* 26:5330–5338
16. Xu X, Yang Q, Wang Y, Chen X, Jing X (2006) Biodegradable electrospun poly(L-lactide) fibers containing antibacterial silver nanoparticles. *Eur Polym J* 42:2081–2087
17. Jun Z, Hou H, Schaper A, Wendorff JH, Greiner A (2003) Poly-L-lactide nanofibers by electrospinning – influence of solution viscosity and electrical conductivity on fiber diameter and fiber morphology. *E-Polymers* 3:102–110
18. ISO/ASTM standard 52900 (2015) Standard terminology for additive manufacturing – general principles – part 1: terminology. ASTM, West Conshohocken
19. Hopkinson N, Hague R, Dickens P (2005) Rapid manufacturing: an industrial revolution for a digital age. Wiley-Blackwell, Berlin
20. Goodridge RD, Tuck CJ, Hague RJM (2012) Laser sintering of polyamides and other polymers. *Prog Mater Sci* 57:229–267
21. Campbell RI, Hague RJM, Sener B, Wormald PW (2004) The potential for the bespoke industrial designer. *Des J* 6:24–34
22. Hopkinson N, Dickens P (2001) Rapid prototyping for direct manufacture. *Rapid Prototyp J* 7:197–202
23. Chua CK, Leong KF, Lin CS (2010) Rapid prototyping: principles and applications, 3rd edn. World Scientific Publishing, Singapore
24. Van Puyvelde P (2016) 3D printing: the making of utopia. In: Achten V, Bouckaert G, Schokkaert E (eds) *A truly golden handbook: the scholarly quest for utopia*. Leuven University Press, Leuven, pp 442–451
25. Bourell DL (2016) Perspectives on additive manufacturing. *Ann Rev Mater Res* 46:1–18
26. Kruth JP (1991) Material in-process manufacturing by rapid prototyping techniques. *CIRP Ann Manuf Technol* 40:603–614
27. Kruth JP, Leu MC, Nakagawa T (1998) Progress in additive manufacturing and rapid prototyping. *CIRP Ann Manuf Technol* 47:525–540
28. Levy GN, Schindel R, Kruth JP (2003) Rapid manufacturing and rapid tooling with layer manufacturing (LM) technologies, State of the art and future perspectives. *CIRP Ann Manuf Technol* 52:589–609
29. Wohlers TT (2011) Wohlers report 2016: 3D printing and additive manufacturing State of the industry annual worldwide progress report. Wohlers Associates Inc., Fort Collins
30. Turner BN, Strong R, Gold SA (2014) A review of melt extrusion additive manufacturing processes: I. Process design and modeling. *Rapid Prototyp J* 20:192–204
31. Kostakis V, Niaros V, Giotitsas C (2015) Open source 3D printing as a means of learning: an educational experiment in two high schools in Greece. *Telematics Inform* 32:118–128

32. Baden T, Chagas AM, Gage G, Marzullo T, Prieto-Godino LL, Euler T (2015) Open labware: 3D printing your own lab equipment. *PLoS Biol* 13:e1002086
33. Pearce JM (2015) Application of open source 3D-printing on small farms. *Org Farming* 1:19–35
34. Rankin TM, Giovinco NA, Cucher DJ, Watts G, Hurwitz B, Armstrong DG (2014) Three-dimensional printing surgical instruments: are we there yet? *J Surg Res* 189:193–197
35. Yeong W-Y, Chua C-K, Leong K-F, Chandrasekaran M (2014) Rapid prototyping in tissue engineering: challenges and potential. *Trends Biotechnol* 22:643–652
36. Ortega Z, Aleman ME, Benitez AN, Monzon MD (2016) Theoretical-experimental evaluation of different biomaterials for parts obtained by fused deposition modeling. *Measurement* 89:137–144
37. Bourell DL, Leu MC, Rosen DW (2009) Roadmap for additive manufacturing: identifying the future of freeform processing. The university of Texas at Austin Laboratory for Freeform Fabrication Advanced Manufacturing Series, Austin, pp 11–15
38. Lee C, Kim S, Ahn S (2007) Measurement of anisotropic compressive strength of rapid prototyping parts. *J Mater Process Technol* 187/188:627–630
39. Panda SK, Padhee S, Sood AK, Mahapatra S (2009) Optimization of fused deposition modelling (FDM) process parameters using bacterial foraging technique. *Intell Inf Manag* 1:89–97
40. Zhang JW, Peng AH (2012) Process parameter optimization for fused deposition modeling based on Taguchi method. *Adv Mater Res* 538:444–447
41. Drummer D, Cifuentes-Cuellar S, Rietzel D (2012) Suitability of PLA/TCP for fused deposition modeling. *Rapid Protyp J* 18:500–507
42. Too M, Leong K, Chua C, Du Z, Yang S, Cheah C, Ho S (2002) Investigation of 3D non-random porous structures by fused deposition modeling. *Int J Adv Manuf Technol* 19:217–223
43. Sood AK, Ohdar R, Mahapatra S (2010) Parametric appraisal of mechanical property of fused deposition modelling processed parts. *Mater Des* 31:287–295
44. Torres J, Cole M, Owji A, DeMastry Z, Gordon AP (2016) An approach for mechanical property optimization of fused deposition modeling with polylactic acid via design of experiments. *Rapid Protyp J* 22:387–404
45. Lanzottin A, Grasso M, Staiano G, Martorelli M (2015) The impact of process parameters on mechanical properties of parts fabricated in PLA with an open-source printer. *Rapid Protyp J* 21:604–617
46. Stephen AO, Dalgarno KW, Munguai J (2014) Quality assurance and process monitoring of fused deposition modelling made parts. *Advanced research in virtual and rapid prototyping*. Taylor & Francis Group, London
47. Afrose MF, Masood SH, Lovenitti P, Nikzad M, Sbarski I (2016) Effects of part build orientations on fatigue behaviour of FDM-processed PLA material. *Prog Addit Manuf* 1:21–28
48. Liu X, Shengpeng L, Zhou L, Xianhua Z, Xiaohu C, Zhongbin W (2015) An investigation on distortion of PLA thin-plate part in the FDM process. *Int J Adv Manuf Technol* 79:1117–1126
49. Cao W, Hench LL (1996) Bioactive materials. *Ceram Int* 22:493–486
50. Wei X, Li D, Jiang W, Gu Z, Wang X, Zhang Z, Sun Z (2015) 3D printable graphene composite. *Sci Rep* 5:11181. doi:[10.1038/srep11181](https://doi.org/10.1038/srep11181)
51. Tian X, Liu T, Yang C, Wang Q, Li D (2016) Interface and performance of 3D printed continuous carbon fiber reinforced PLA composites. *Compos Part A* 88:198–205
52. Serra T, Mateos-Timoneda MA, Planell JA, Navarro M (2013) 3D printed PLA-based scaffolds. *Organogenesis* 9:239–244
53. Serra T, Planell JA, Navarro M (2013) High-resolution PLA-based composite scaffolds via 3D printing technology. *Acta Biomater* 9:5521–5530

54. Fong EL, Lamhamedi-Cherradi SE, Burdett E, Ramamoorthy V, Lazar AJ, Kasper FK, Farach-Carson MC, Vishwamitta D, Demicco EG, Menegaz BA (2013) Modeling Ewing sarcoma tumors in vitro with 3D scaffolds. *Proc Natl Acad Sci U S A* 110:6500–6505
55. Serra T, Ortiz-Hernandez M, Engel E, Planell JA, Navarro M (2014) Relevance of PEG in PLA-based blends for tissue engineering. *Mater Sci Eng C* 38:55–62
56. Zalipsky S, Harris JM (1997) Introduction of chemistry and biological applications of poly (ethylene) glycol. In: Harris JM, Zalipsky S (eds) *Poly(ethylene glycol): biomedical and biotechnological applications*, ACS symposium series, vol 680. American Chemical Society, Washington, pp 1–13
57. Inada Y, Furukawa M, Sasaki H, Kodera Y, Hiroto M, Nishimura H, Matsushima A (1995) Biomedical and biotechnological applications of PEG- and PM-modified proteins. *Trends Biotechnol* 13:86–91
58. Mironov V (2003) Printing technology to produce living tissue. *Expert Opin Biol Ther* 3:701–704
59. Liew CL, Leong KF, Chua CK, Du Z (2001) Dual material rapid prototyping techniques for the development of biomedical devices. Part A: space creation. *Int J Adv Manuf Technol* 18:717–723
60. Verbelen L, Dadbakhsh S, Van den Eynde M, Kruth J-P, Goderis B, Van Puyvelde P (2016) Characterization of polyamide powders for determination of laser sintering processability. *Eur Polym J* 75:163–174
61. Schmid M, Amado A, Wegener K (2014) Materials perspective of polymers for additive manufacturing with selective laser sintering. *J Mater Res* 29:1824–1832
62. Shi Y, Li Z, Sun H, Huang S, Zeng F (2004) Effect of the properties of the polymer materials on the quality of selective laser sintering parts. *J Mater Des Applic* 218:247–252
63. Evans RS, Bourell DL, Beaman JJ, Campbell MI (2005) SLS materials development for rapid manufacturing. In: *Proceedings of the 16th solid freeform fabrication symposium*, Austin, pp 184–196
64. Drummer D, Rietzel D, Kühnlein F (2010) Development of a characterization approach for the sintering behavior of new thermoplastics for selective laser sintering. *Phys Procedia* 5:533–542
65. Dupin S, Lame O, Barrès C, Charneau JY (2012) Microstructural origin of physical and mechanical properties of polyamide 12 processed by laser sintering. *Eur Polym J* 48:1611–1621
66. Van den Eynde M, Verbelen L, Van Puyvelde P (2015) Assessing polymer powder flow for the application of laser sintering. *Powder Technol* 286:151–155
67. Frenkel J (1945) Viscous flow of crystalline bodies under the action of surface tension. *J Phys* 9:358–391
68. Wouters M, de Ruiter B (2003) Contact angle development of polymer melts. *Prog Org Coat* 48:207–213
69. Brandrup J, Immergut EH, Grulke EA (1999) *Polymer handbook*, 4th edn. Wiley, New York
70. Gibson I, Shi D (1997) Material properties and fabrication parameters in selective laser sintering process. *Rapid Prototyp J* 3:129–136
71. Zarringhalam H, Hopkinson N, Kamperman NF, de Vlieter JJ (2006) Effects of processing on microstructure and properties of SLS nylon 12. *Mater Sci Eng A* 4325:172–180
72. Dotchev KD, Yusoff WA (2009) Recycling of polyamide 12 based powders in the laser sintering process. *Rapid Prototyp J* 15:192–203
73. Vasquez M, Haworth B, Hopkinson N (2013) Methods for quantifying the stable sintering region in laser sintered polyamide-12. *Polym Eng Sci* 53:1230–1240
74. Zoller P, Walsh D (1995) *Standard pressure-volume-temperature data for polymers*. CRC, Boca Raton
75. Verbelen L (2016) Towards scientifically based screening criteria for polymer laser sintering. PhD thesis, KU Leuven

76. Pohle D, Ponader S, Rechtenwald T, Schmidt M, Schlegel KA, Munstedt H (2007) Processing of three-dimensional laser sintered polyetheretherketone composites and testing of osteoblast proliferation in vitro. *Macromol Symp* 253:65–70
77. Partee B, Hollister SJ, Das S (2006) Selective laser sintering process optimisation of layered manufacturing of CAPA 6501 polycaprolactone bone tissue engineering scaffolds. *J Manuf Sci Eng* 128:531–540
78. Rimell JT, Marquis PM (2000) Selective laser sintering of ultra high molecular weight polyethylene for clinical applications. *J Biomed Mater Res* 53:414–420
79. Zhou WY, Lee SH, Wang M, Cheung WL, Ip WY (2008) Selective laser sintering of porous tissue engineering scaffolds from poly(L-lactide)/carbonated hydroxyapatite nanocomposite microspheres. *J Mater Sci Mater Med* 19:2535–2540
80. Chen VJ, Smith LA, Ma PX (2006) Bone regeneration on computer-designed nano-fibrous scaffolds. *Biomaterials* 27:3973–3979
81. Landers R, Hübner U, Schmelzeisen R, Mülhaupt R (2003) Rapid prototyping of scaffolds derived from thermoreversible hydrogels and tailored for applications in tissue engineering. *Biomaterials* 23:4437–4447
82. Antonov EN, Bagratashvili VN, Whitaker MJ, Barry JJA, Shakesheff KM, Konovalov AN, Popov VK, Howdle SM (2005) Three-dimensional bioactive and biodegradable scaffolds fabricated by surface-selective laser sintering. *Adv Mater* 17:327–330
83. Popov VK (2007) Laser technologies for fabricating individual implants and matrices for tissue engineering. *J Opt Technol* 74:636–640
84. Elias KL, Price RL, Webster TJ (2002) Enhanced functions of osteoblasts on nanometer diameter carbon fibers. *Biomaterials* 23:3279–3287
85. Price RL, Waid WC, Haberstroh KM, Webster TJ (2003) Selective bone cell adhesion on formulations containing carbon nanofibers. *Biomaterials* 24:1877–1887
86. Bai J, Goodridge RD, Hague RJM, Okamoto M (2015) Processing and characterization of a polylactic acid/nanoclay composite for laser sintering. *Polym Compos*. doi:10.1002/pc.23848
87. Wang WL, Cheah CM, Fuh JYH, Lu L (1996) Influence of process parameters on stereolithography part shrinkage. *Mater Des* 17:205–213
88. Heller C, Schwentenwein M, Russmueller G, Varga F, Stampfl J, Liska R (2009) Vinyl esters: low cytotoxicity monomers for the fabrication of biocompatible 3D scaffolds by lithography based additive manufacturing. *J Polym Sci A Polym Chem* 47:6941–6954
89. Melchels FPW, Feijen J, Grijpma DW (2010) A review on stereolithography and its applications in biomedical engineering. *Biomaterials* 31:6121–6130
90. Maruo S, Ikuta K (2002) Submicron stereolithography for the production of freely moldable mechanisms by using single-photon polymerizations. *Sens Actuators A Phys* 100:70–76
91. Mansour S, Gilbert A, Hague R (2007) A study of the impact of short-term ageing on the mechanical properties of a stereolithography resin. *Mater Sci Eng A* 447:277–284
92. Cooke MN, Fisher JP, Dean D, Rinnac C, Mikos AG (2003) Use of stereolithography to manufacture critical sized 3D biodegradable scaffolds for bone in growth. *J Biomed Mater Res B Appl Biomater* 64:65–69
93. Matsuda T, Mizutani M (2002) Liquid acrylate-terminated biodegradable poly(ϵ -caprolactone-co-trimethylene carbonate). II. Computer-aided stereolithographic microarchitectural surface photoconstructs. *J Biomed Mater Res* 62:395–403
94. Matsuda T, Mizutani M, Arnold SC (2000) Molecular design of photocurable liquid biodegradable copolymers. I. Synthesis and photocuring characteristics. *Macromolecules* 33:795–800
95. Lee SJ, Kang HW, Park JK, Rhie JW, Hahn SK, Cho DW (2008) Application of micro-stereolithography in the development of three-dimensional cartilage regeneration scaffolds. *Biomicrodevices* 10:233–241
96. Jansen J, Melchels FPW, Grijpma DW, Feijen J (2009) Fumaric acid monoethyl ester-functionalized poly(D,L-lactide)/N-vinyl-2-pyrrolidone resins for the preparation of tissue engineering scaffolds by stereolithography. *Biomacromolecules* 10:214–220

97. Melchels FPW, Feijen J, Grijpma DW (2009) A poly(D,L-lactide) resin for the preparation of tissue engineering scaffolds by stereolithography. *Biomaterials* 30:3801–3809
98. Raghoobar GM, Liem RSB, Bos RRM, van der Wal JE, Vissink A (2006) Resorbable screws for fixation of autologous bone grafts. *Clin Oral Implants Res* 17:288–293
99. Acosta HL, Stelnicki EJ, Rodriguez L, Slingbaum LA (2005) Use of absorbable poly(D,L) lactic acid plates in cranial-vault remodelling: presentation of the first case and lessons learned about its use. *Cleft Palate Craniofac J* 43:333–339
100. Silva M, Cyster LA, Barry JJA, Yang XB, Oreffo ROC, Grant DM (2006) The effect of anisotropic architecture on cell and tissue infiltration into tissue engineering scaffolds. *Biomaterials* 27:5909–5917
101. Tuli R, Nandi L, Li WJ, Tuli S, Huang XX, Manner PA (2004) Human mesenchymal progenitor cell-based tissue engineering of a single-unit osteochondral construct. *Tissue Eng* 10:1169–1179
102. Claase MB, de Riekering MB, de Bruijn JD, Grijpma DW, Engbers GHM, Feijen J (2003) Enhanced bone marrow stromal cell adhesion and growth on segmented poly(ether ester)s based on poly(ethylene oxide) and poly(butylene, terephthalate). *Biomacromolecules* 4:57–63
103. Storey RF, Warren SC, Allison CJ, Wiggins JS, Pucket AD (1993) Synthesis of bio-absorbable networks from methacrylate-endcapped polyesters. *Polymer* 34:4365–5372
104. Grijpma DW, Hou QP, Feijen J (2005) Preparation of biodegradable networks by photo-crosslinking lactide, epsilon-caprolactone and trimethylene carbonate-based oligomers functionalized with fumaric and monoethyl ester. *Biomaterials* 26:2795–2802
105. Sawhney AS, Pathak CP, Jubbell JA (1993) Bioerodible hydrogels based on photopolymerized poly(ethylene glycol)-co-poly(alpha-hydroxy acid) diacrylate macromers. *Macromolecules* 26:581–587
106. Hinczewski C, Corbel S, Chartier T (1998) Ceramic suspensions suitable for stereolithography. *J Eur Ceram Soc* 18:583–590

Poly(lactic acid) for Sensing Applications



Yoshiro Tajitsu

Abstract The piezoelectric responses of polymers in practical use are divided into the following classes with different piezoelectric characteristics: chiral polymers (optically active polymers), ferroelectric polymers, and cellular electrets. The piezoelectricity of chiral polymers is in response to shear strain, that of a ferroelectric polymer is in response to tensile strain, and that of cellular electrets is in response to strain perpendicular to the film surface. Study of the piezoelectricity of poly(L-lactic acid) (PLLA), which is a chiral polymer, has advanced in the last few decades, and its practical application to sensor devices has progressed accordingly. In this chapter, the piezoelectric characteristics of PLLA and its applications to sensor devices are systematically discussed.

Keywords Angle detection • Chirality • Fiber • Film • Piezoelectricity • PLLA • Sensing • Touch panel

Contents

1	Piezoelectricity in Polymers	160
2	Origin of PLLA Piezoelectricity	161
3	Macroscopic Piezoelectricity of PLLA Films	162
3.1	Helix Structure and Piezoelectricity	163
3.2	Macrosymmetry and Piezoelectricity	164
4	PLLA as Sensing Material	167
4.1	Deformation-Sensitive Touch Panel (PLLA Film Sensor)	167
4.2	Motion Capture with PLLA Fibers	170
5	Conclusion	174
	References	175

Y. Tajitsu (✉)

Department of Electrical and Electronic Engineering, Faculty of Engineering Science, Kansai University, 3-3-35 Yamate, Suita, Osaka 564-8680, Japan
e-mail: kenji_imoto@imonet.jp

1 Piezoelectricity in Polymers

The development of new human–machine interfaces (HMIs) for mobile devices such as smart phones has been actively progressing. As a key material of such HMIs, the piezoelectric element has attracted considerable attention. Piezoelectricity is the ability of dielectrics to generate an electric charge in response to mechanical stress. The opposite effect also occurs, that is, the application of voltage produces mechanical strain in piezoelectric materials. Both these effects can be measured, making piezoelectric materials suitable for use in sensors and transducers (actuators). Organic piezoelectric materials such as piezoelectric polymers are transparent, light, and flexible. Furthermore, the fabrication of thin films is simple, resulting in high expectation of their application as actuators and sensors [1–9].

First, a summary of the important discoveries in the history of piezoelectric polymers is given. The piezoelectricity of polymers was first investigated for wood and cellulose in 1955 and bone in 1957 [1]. Both materials exhibit shear piezoelectricity. Later, tensile piezoelectricity in the axial direction was found in bone and tendon in 1964 [7]. Pyroelectricity, which generates a state of electrical polarization by a change of temperature, was discovered in 1966 [6]. Tensile piezoelectricity in poly(vinylidene fluoride) (PVDF) was discovered by Kawai in 1969 [1, 3, 8] and shear piezoelectricity in poly(L-lactic acid) (PLLA) was found in 1991 [8]. Polymers that have chirality and a helix structure, such as α -helix polypeptides and optically active polymers such as PLLA, are well known to exhibit shear piezoelectricity [4]. In 2012, Li of the University of Washington discovered ferroelectricity in the aorta wall, which is a property of materials that have spontaneous polarization that can be reversed by the application of an external electric field. The piezoelectric charge constants, d , for various piezoelectric polymers are given in Table 1 [1, 3, 4, 7, 8]. The d -constant refers to the polarization (coulombs per square meter, C/m^2) generated per unit of mechanical stress (newtons per square meter, N/m^2) applied to a piezoelectric material. Table 1 demonstrates that PVDF and PLLA can be considered suitable polymer materials for forming practical elements.

Table 1 Magnitudes of piezoelectric d -constant

Biopolymers	d (pC/N)	Synthetic polymers	d (pC/N)
Polysaccharides		Polypeptides (shear)	
Cellulose	0.1	Poly- γ -methyl-L-glutamate (PMLG)	3.3
Chitin	1.5	Optically active polymers (shear)	
Amylose	3.0	Poly-L-lactic acid (PLLA)	10
Proteins		Polar polymer (tensile)	
Keratin	1.8	Polyvinylidene fluoride (PVDF)	20
Collagen	4.0	Porous electret (tensile)	
Fibrinogen	2.5	Porous polypropylene (pPP)	400
DNA (-100°C)	0.01	Quartz $d_{11} = 2.3$ pC/N	

2 Origin of PLLA Piezoelectricity

The piezoelectricity of dielectric materials having translation symmetry, such as single crystals, is capable of being predicted from the symmetry of the crystal system [10]. When considering the piezoelectricity of a dielectric material, the strain s_j (extension $j = 1-3$, shear strain $j = 4-6$) induced by an electric field E_i ($i = 1-3$) is represented by the equations below. The electric displacement D_i ($i = 1-3$) induced by stress T_j (tensile stress $j = 1-3$, shear stress $j = 4-6$) is also given:

$$D_i = d_{ij}T_j \quad (1)$$

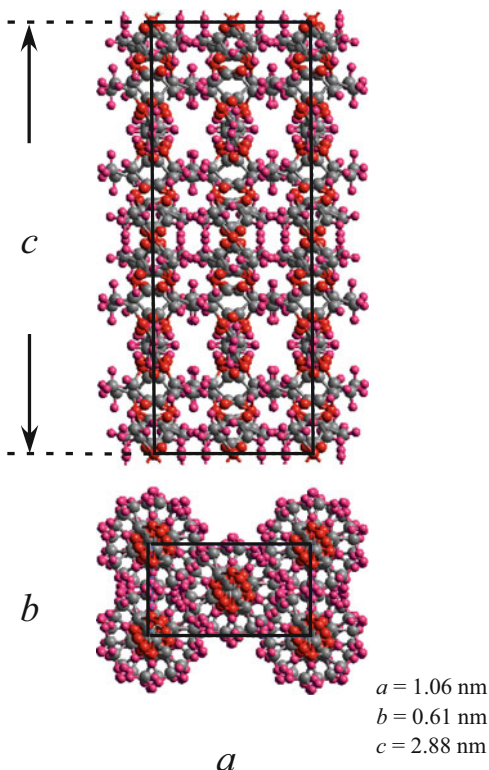
$$S_j = d_{ij}E_i \text{ (inverse effect)} \quad (2)$$

Here, d_{ij} ($i = 1-3, j = 1-6$) is a piezoelectric tensor. According to Eq. (1), an electric charge (D_i) is produced when a mechanical stress (T_j) is applied. This is the direct piezoelectric effect. Devices that use the direct piezoelectric effect include pressure sensors, hydrophones, and many other types of sensors. Also, according to Eq. (2), conversely, a mechanical deformation (S_j) is produced when an electric field (E_i) is applied. This is referred to as the inverse piezoelectric effect. Using the inverse piezoelectric effect, it is possible to produce devices that generate acoustic sound waves. Examples of piezoelectric acoustic devices are speakers or buzzers. Non-acoustic inverse piezoelectric devices include motors and actuators.

It is important to clarify the crystal system of PLLA [11, 12]. The PLLA crystal structure is based on a base-centered orthorhombic unit cell, as shown in Fig. 1. It contains two 10/3 helical chains in a PLLA crystal unit. The point group of the PLLA crystal system is D_2 and there are three independent shear piezoelectric tensors, d_{14} , d_{25} , and d_{36} . The origin and ultimate cause of the piezoelectricity is the cooperative motion of permanent dipoles existing on the helical chain molecules of PLLA. Here, it is emphasized that pyroelectricity (i.e., polarization resulting from a temperature change) is not anticipated in PLLA crystals because of its D_2 symmetry [12]. The existence of pyroelectricity is a very important factor in HMI applications for the following reason. If a piezoelectric sensor material exhibits pyroelectricity, then it can immediately detect heat from a finger when it is used as an HMI; therefore, it is not possible to distinguish whether the signal originates from the pressure or the heat of the operator's hand. Stable PLLA films with a sufficiently high piezoelectric constant to be used for sensing applications have been successfully produced and further developed into potential HMI devices (see Sect. 4).

Shear stress is applied to the chain molecules in PLLA with a 10/3 helical structure through its methyl groups [13]. All the atoms in the chain molecules are displaced, as shown in Fig. 2. In particular, the plane on which the C–O bond and carboxyl bond (C=O) exist is rotated. As a result, the C=O bond, which has a larger dipole moment than the other bond, is displaced. Rotation of the C=O bond changes the polarization of the entire long-chain molecule, resulting in the shear piezoelectricity of PLLA [14]. In summary, the origin of the observed macroscopic

Fig. 1 Crystal structure of PLLA



piezoelectricity, where charges are induced on a PLLA film surface when shear stress is applied, is understood to be the result of rotation of some C=O bonds [13, 14]. Thus, the macroscopic piezoelectricity of a drawn PLLA film is a result of its intrinsic piezoelectricity due to its crystal state. However, in general, translational symmetry does not exist in a PLLA film because of its complex high-order structure, as shown in Fig. 3. In other words, amorphous components are always present in the complex high-order structure. No one-to-one correspondence has been found between macroscopic piezoelectric properties and crystal characteristics. The mechanism of macroscopic piezoelectricity is made complicated by the existence of the complex high-order structure, as discussed in the next section.

3 Macroscopic Piezoelectricity of PLLA Films

This section first describes the piezoelectricity caused by the helix structure of PLLA chain molecules, in particular, the right- and left-hand helices. Furthermore, the macroscopic piezoelectricity of PLLA films is described on the basis of their high-order structure.

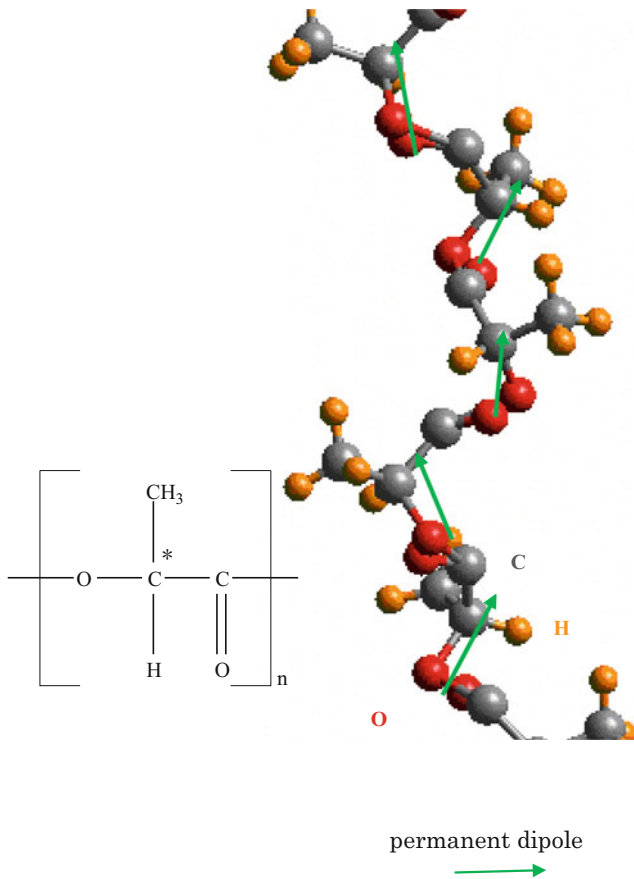


Fig. 2 PLLA molecule

3.1 Helix Structure and Piezoelectricity

Poly(lactic acid) is a chiral polymer with two optical isomers, and its chain molecules form a helical structure as a result of its chirality. One isomer is PLLA and the other is poly(D-lactic acid) (PDLA). The helical structure of PLLA is left-handed, as shown in Fig. 2, whereas the helical structure of PDLA is right-handed. It is emphasized that the sign of the piezoelectric constant of PDLA is opposite that of PLLA because of the clockwise and counterclockwise spiral structures of their helical structures, respectively. The internal displacement of the dipoles is the origin of the shear piezoelectricity. Shear piezoelectricity is observed in polypeptides with an α -helix structure and its sign depends on whether the optical activity is L or D [7]. A useful example of shear piezoelectricity in a polypeptide is poly(β -phenethyl L-aspartate) (PPLA), which undergoes helix inversion from right-hand

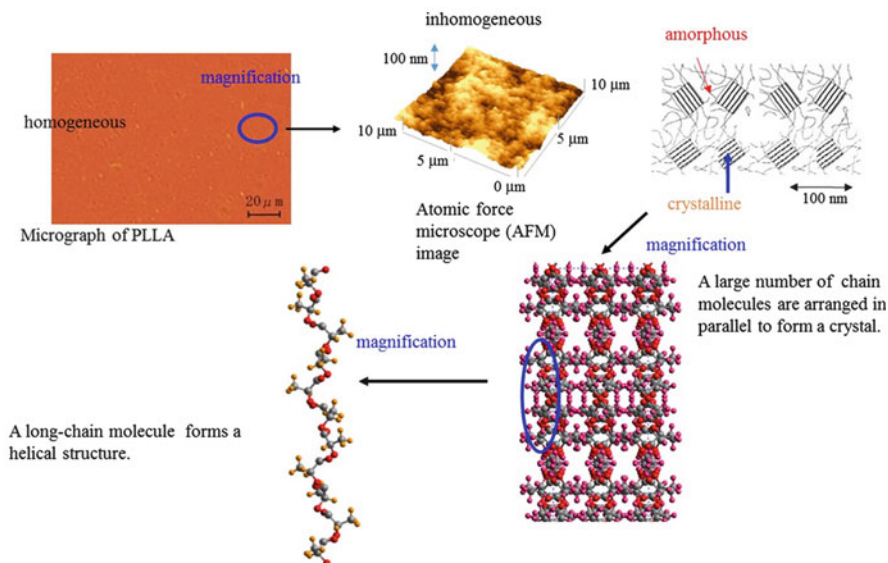


Fig. 3 High-order structure of PLLA shown at various scales

to left-hand in response to increasing temperature [15]. Macroscopic shear piezoelectric measurement of films of optically active PLLA and the change in piezoelectric constant during helix inversion have been investigated. It was found that PLLA exhibits shear piezoelectricity $d^* = d' - jd''$ and an irreversible sign inversion of d' at approximately 140°C, as shown in Fig. 4 [16]. It was confirmed that the inversion of PLLA from a right-hand to left-hand helix in the solid state progresses irreversibly at 130–140°C. This strongly implies that the macroscopic sign inversion of d' is a result of irreversible helix inversion. It is surprising that the macroscopic shear piezoelectricity remains even though a major change (i.e., helix inversion in the crystalline region) has occurred in the complex high-order structure, including the amorphous region. This unique property of shear piezoelectricity is expected to contribute to the analysis of complex molecular motion in basic science.

3.2 *Macrosymmetry and Piezoelectricity*

According to the definition of the piezoelectric effect in Eqs. (1) and (2), all components of the piezoelectric tensor (d_{ij}) should vanish in materials possessing a center of symmetry. In polymer films, amorphous components are always present in complex high-order structures, as shown in Fig. 3. In other words, polymer films have no translation symmetry and there is a possibility that a center of symmetry

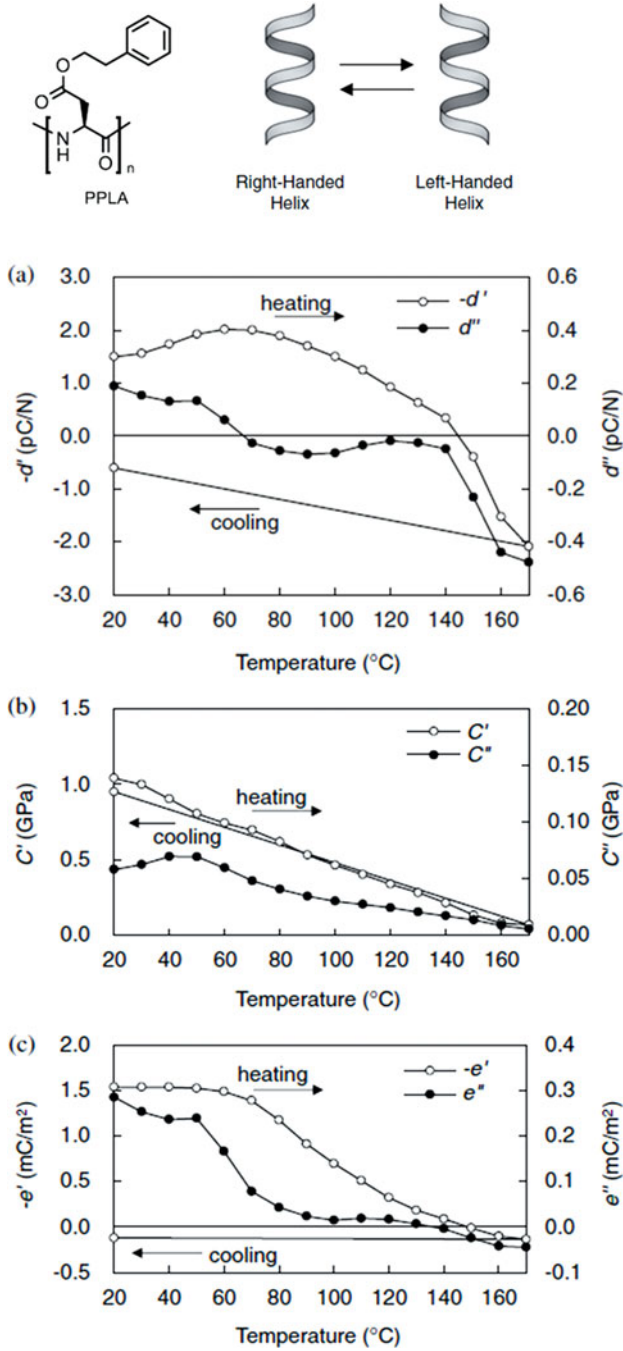


Fig. 4 Temperature dependences of (a) complex piezoelectric modulus $d^* = d' - jd''$, (b) complex Young's modulus $C^* = C' + jC''$, and (c) complex piezoelectric modulus $e^* = e' - je''$ of PPLA. Copyright The Japan Society of Applied Physics [16]

exists macroscopically. Therefore, for the piezoelectricity of polymer films, macroscopic symmetry must be considered on the basis of point group theory [12]. As shown in Fig. 5, asymmetry is imparted to a film by conventional methods such as drawing and poling. The purpose of the drawing process is to macroscopically arrange the chain molecules in a polymer film in the same direction in the entire film. The purpose of the poling process is to macroscopically arrange the dipole moments of molecules along the same direction in the entire film. Actually, piezoelectricity of an isotropic film does not occur, even though the piezoelectric tensor d_{ml} exists in the crystal state. The point group of drawn and poled films of ferroelectric polymers such as PVDF is C_{2v} as shown in Fig. 5. Thus, six independent piezoelectric constants exist. The symmetry of such films is the same as that for a PVDF crystal. A drawn and poled PVDF film is known to exhibit high tensile piezoelectricity at the macroscopic scale [3]. On the basis of its point group, PVDF is predicted to exhibit pyroelectricity. On the other hand, the point group of a drawn polymer film is $D_{\infty v}$, as shown in Fig. 5 [8]. In this case, it is important that a mirror plane perpendicular to the film surface exists. Furthermore, in this case, piezoelectricity does not arise. However, the PLLA molecule has chirality, as shown in Fig. 5. In this case, the mirror plane disappears, the point group becomes D_{∞} , and three independent piezoelectric constants exist. The shear piezoelectric constant of PLLA is high compared with those of other shear piezoelectric polymers, as shown in Table 1.

Thus, to clarify the piezoelectricity of PLLA, the shear piezoelectricity of other polymers is explained as follows. In wood, cellulose crystallites are uniaxially oriented with no preferential orientation of the polar axes [4]. The symmetry is D_{∞} . In this case, the macroscopic symmetry is the same as that of PLLA shown in Fig. 5. Thus, the piezoelectric matrix is relatively simple and only the shear piezoelectric coefficients d_{14} and d_{25} remain finite, which have the same value but opposite signs. The observed value of the piezoelectric constant is proportional to the average of the piezoelectric coefficients of the crystal, the degree of

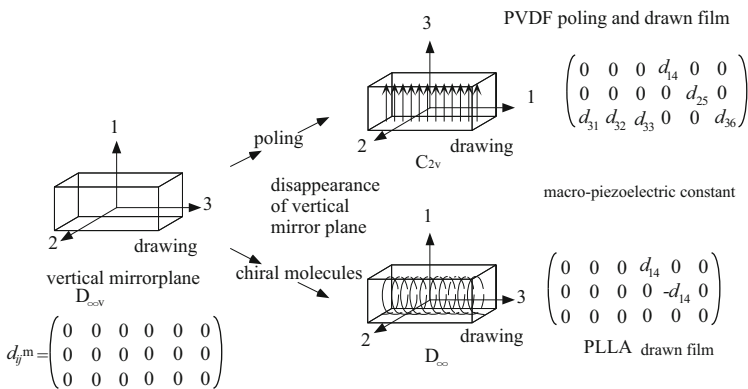


Fig. 5 Macroscopic symmetry of polymer film

orientation, and the degree of crystallization. On the other hand, tensile piezoelectricity together with shear piezoelectricity has been observed for bone and tendon. The tension or pressure in the orientation direction produces polarization in the same direction. The polar axes of collagen crystallites are preferentially oriented in the same direction. Thus, the piezoelectric constants d_{31} and d_{33} can be observed [4]. In this case, pyroelectricity can also be observed in the same way as for PVDF. The magnitude of the shear piezoelectric constant d_{14} is similar to that of quartz crystal, but the magnitude of the tensile piezoelectric constant is one order of magnitude smaller. Molecules of polypeptides such as collagen contain CONH dipoles with an asymmetric carbon atom [3]. A polypeptide forms an α -helical structure, which is one of the distinguishing secondary structures of polypeptides. This helical structure also plays a major role in the intramolecular hydrogen bonding between the peptide and the main chain, in which the CONH dipoles are aligned. The CONH dipoles are rotated under the application of shear stress. Here, the key word is “chirality.” When mechanical stress or an electric field is applied, the peptide dipoles undergo slight internal rotations, similar to those in PLLA, as shown in Fig. 2.

4 PLLA as Sensing Material

This section describes how a new PLLA sensor device was produced as an actual application of a PLLA film by a world-famous electronic device company, Murata Manufacturing Co., Ltd. Furthermore, the possibility of using PLLA fiber sensors as next-generation sensor devices is discussed.

4.1 Deformation-Sensitive Touch Panel (PLLA Film Sensor)

This section introduces the promising industrial applications of PLLA film sensor devices. PLLA films, which have a larger shear piezoelectric constant than the other polymers in Table 1 and no pyroelectricity, are anticipated to be used as sensors and actuators in unconventional HMIs because of their high flexibility and transparency. A PLLA sensor has been combined with a projected capacitive touch panel to realize a deformation-sensitive touch panel [17].

Two types of PLLA film were prepared. One film was cut from uniaxially oriented PLLA film at an angle of 45° from the orientation direction of the molecules (PLLA45). The other film was cut from uniaxially oriented PLLA film at an angle of 0° (PLLA0). It was confirmed that when PLLA45 was pasted onto a plate, it could detect the bending motion of the plate. When PLLA0 was pasted onto a plate it could detect twisting motion in the plate. Figure 6 [17] shows the test plate, with PLLA45 (thickness $35\ \mu\text{m}$) attached to the surface of a plastic plate (base plate). PLLA0 film with thickness of $35\ \mu\text{m}$ was attached to another surface and an

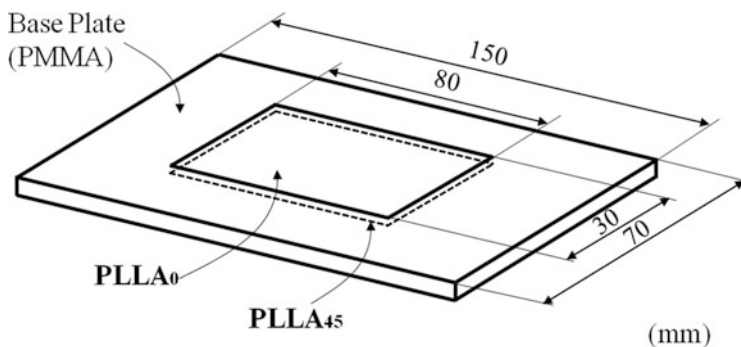


Fig. 6 Test plate for sensing motion. Copyright The Japan Society of Applied Physics [17]

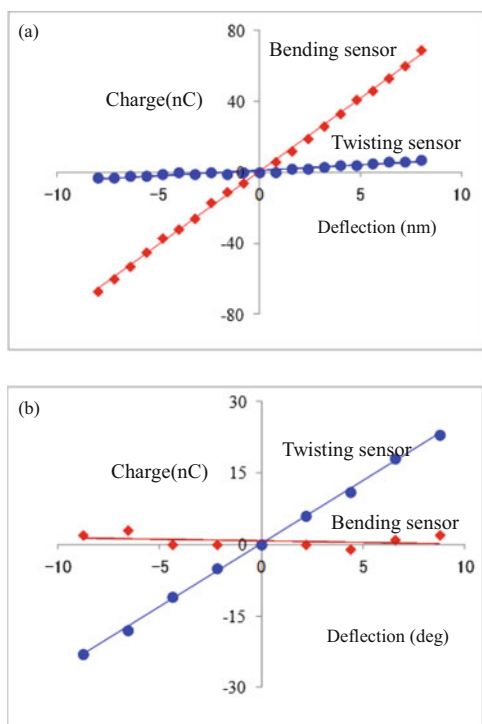


Fig. 7 Relationship between charge and deflection by (a) bending and (b) twisting. Copyright The Japan Society of Applied Physics [17]

organic electrode was placed on both surfaces of each sensor. Figure 7 [17] shows the relationship between the deformations of the base plates with PLLA45 and PLLA0 and the amount of electric charge generated. Figure 7a shows the deformation of the base plate and Fig. 7b shows the twisting. It is of major importance for sensor application of PLLA that sensing of the bending and twisting motions can be

performed independently. Furthermore, the relationship between the amount of electric charge generated and the displacement should be highly linear. The results indicate that PLLA45/PLLA0 can be used as a pressure sensor for a touch panel.

Another advantage of PPLA is that its piezoelectric voltage coefficient (piezoelectric g constant = piezoelectric d constant/dielectric constant ϵ , corresponding to sensing sensitivity) is high because its ϵ value of 2.7 is much lower than that of inorganic piezoelectric materials. In other words, the sensitivity of PLLA is very high.

A deformation-sensitive touch panel in which PLLA45 and PLLA0 were combined with a projected capacitive touch panel has been produced. The touch sensor comprises a PLLA film. A polycarbonate plate is used as the surface plate of the touch panel. The electrode consists of three layers, as shown in Fig. 8 [18]. Figure 8

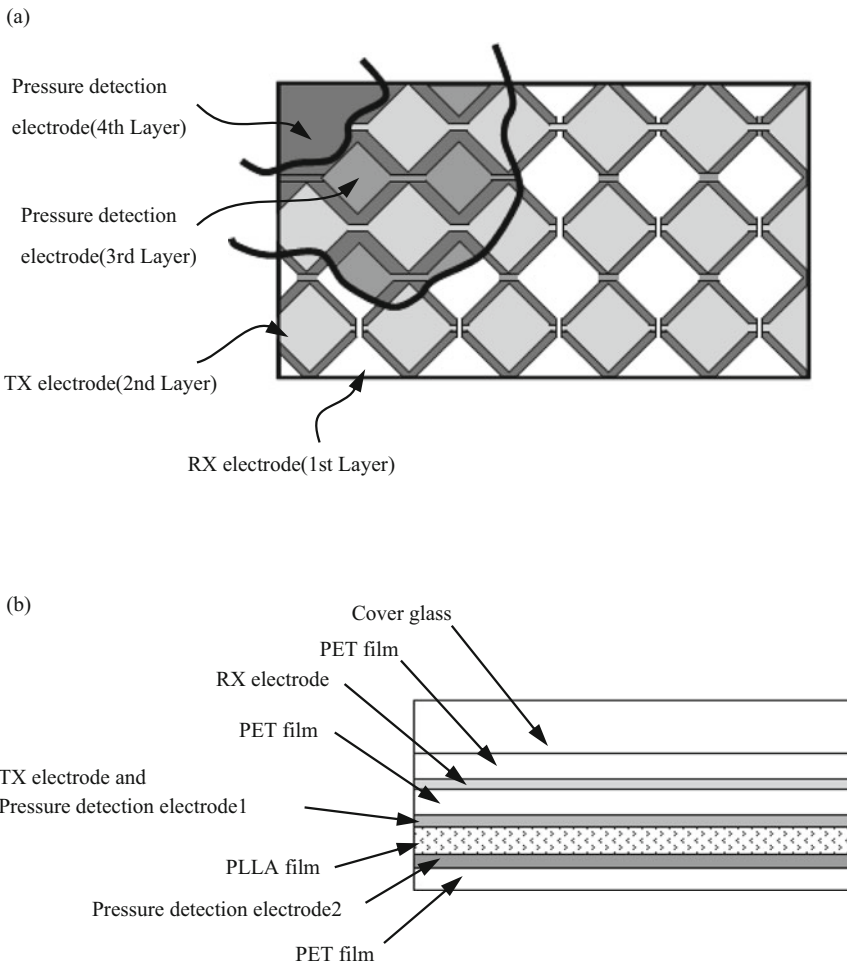


Fig. 8 Pressure-sensing electrode: (a) plan view and (b) layer structure. Copyright The Japan Society of Applied Physics [18]

shows a plan view of an electrode (Fig. 8a) and the electrode layer structure of a touch-sensing electrode (Fig. 8b). A diamond or rectangular structure is generally used for the electrodes, which are fabricated in a double layer system, with a drive electrode (TX) and a detection electrode (RX). An RX electrode is formed on the first layer and a TX electrode on the second layer. An electrode is formed directly under the RX electrode so that the TX and RX electrodes adjoin each other. Another electrode is formed on the third layer, and this electrode is separated into four portions. This sensor detects the moment of deformation. Furthermore, using an integrated circuit, the sensor can also detect absolute displacement. Murata Manufacturing released a prototype deformation detection touch panel as shown in Fig. 9 [18]. Multitouch functionality can be maintained, and three-axis (XYZ) detection can be achieved, while retaining all the advantages of projected capacitive touch panels, by using a simple three-layer electrode structure. The product was the first PLLA sensor device fabricated by Murata Manufacturing Co., Ltd. This flexible device was reported in television broadcasts worldwide in 2011, including those by the BBC (UK) and CBS (USA).

4.2 Motion Capture with PLLA Fibers

This section describes the potential use of PLLA fiber sensors in next-generation sensor applications.



Fig. 9 Prototype deformation detection touch panel (Murata Manufacturing Co., Ltd.)

4.2.1 PLLA Fiber Sensor

Our aim was to realize PLLA fibers with high orientation of the fiber axis and a high degree of crystallinity. PLLA with a D-isomer content of 0.1% was prepared. We first attempted to obtain an axis-oriented PLLA fiber by a high-speed spinning process. To make the PLLA fiber sensor, two types of helical torsion coil were prepared, one with a PLLA fiber wound spirally in the counterclockwise direction (PLLA fiber left-hand coil) and one with a PLLA fiber wound spirally in the clockwise direction (PLLA fiber right-hand coil). To fabricate each coil, a PLLA fiber was formed around a metallic bar in an oven, then annealed at 120°C for 10 min and quenched to obtain a soft and flexible PLLA fiber coil, as shown in Fig. 10 [19].

4.2.2 Sensing of Expansion and Twisting

Figure 11 [19] shows the sensing device used for simultaneous sensing with two PLLA fiber coils. Both ends of the PLLA fiber left-hand coil and the PLLA fiber right-hand coil were tightly bonded to an epoxy-plastic block [19]. When expansion and constriction strains were induced in the two PLLA fiber coils, a response signal caused by the piezoelectricity of the PLLA fiber was subsequently detected, as shown in the upper part of Fig. 12 [19]. A positive peak signal was obtained from both the PLLA fiber left-hand coil and the PLLA fiber right-hand coil when expansion strain was induced. Also, a negative peak signal from both coils was obtained when the constriction strain was induced. In these cases, the peak signals from the two coils had the same sign. Typical experimental results for twisting motion are shown in the lower part of Fig. 12. It was found that the signals from the two coils differed in sign when the coils were twisted. In other words, it is possible to differentiate between counterclockwise twisting and clockwise twisting simultaneously using the two coils.

Fig. 10 PLLA fiber coil.
Copyright The Japan
Society of Applied Physics
[19]

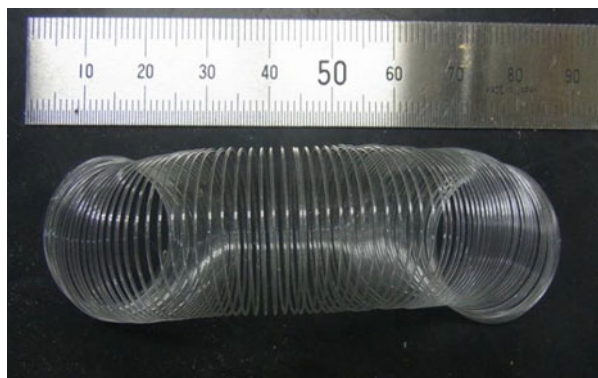
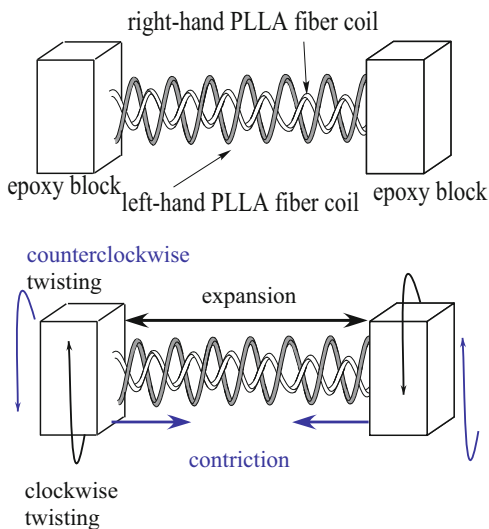


Fig. 11 Experimental setup used for the sensing demonstration employing PLLA fiber left- and right-hand coils. Copyright The Japan Society of Applied Physics [19]



4.2.3 Sensing of Rotation Angle

An experimental system was produced for sensing rotation angle using a PLLA fiber coil, as shown in Fig. 13. The signal produced in response to rotation was processed via a charge amplifier and an LED display that displayed the angle. Figure 14 shows a plot of the output voltage against rotation angle. A linear relationship was found between the rotation angle and the induced voltage. On the basis of the experimental results, a device for measuring rotation angle that has a simple structure and provides high reliability and high precision can be provided using PLLA fiber coils.

4.2.4 Visual Demonstration of Sensing of Human Motion Using PLLA Fiber Left-Hand and Right-Hand Coils

Using the PLLA fiber coils, we attempted to simultaneously detect human pulse rate and arm motion. A PLLA fiber sensor system was prepared in which a PLLA fiber coil was linked to a personal computer (PC) used for simple image processing [19]. Still images of various types of motion of the arm of a subject were prepared in advance. The response signal generated by each PLLA fiber coil was processed by the PC to determine which of the still images most closely matched the motion of the arm. In the demonstration, PLLA fiber left- and right-hand coils were placed on the forearm of a subject on the outside of his coat sleeves, as shown in Fig. 15 [19]. The arm was flexed, extended, and rotated. This demonstration was recorded with a video camera. Typical examples of images selected by the PC for different

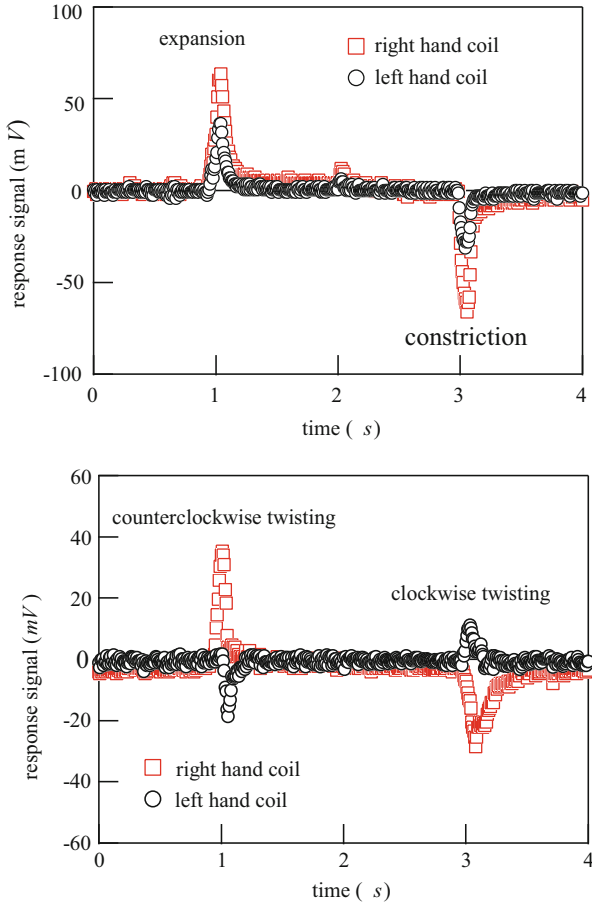


Fig. 12 Response signal from PLLA fiber left- and right-hand coils generated by strains. Copyright The Japan Society of Applied Physics [19]

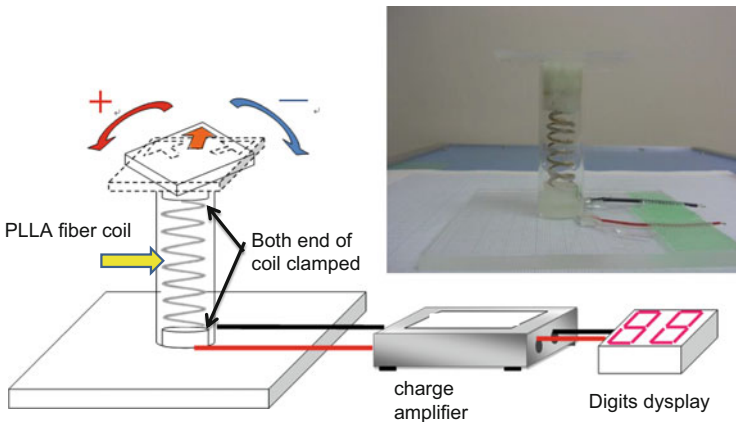


Fig. 13 Experimental setup used for sensing rotation angle

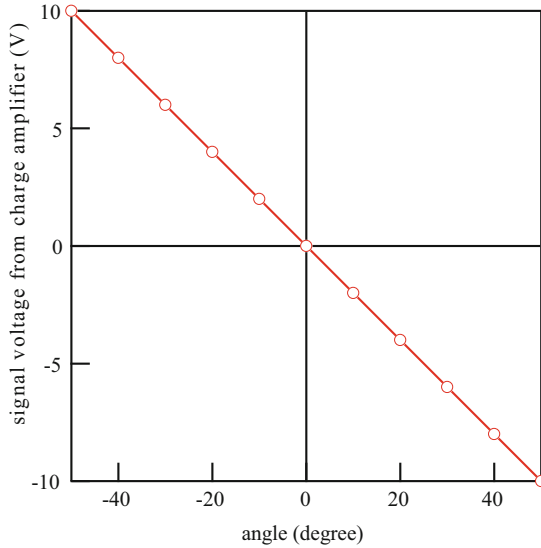


Fig. 14 Plot of signal voltage from charge amplifier against rotation angle

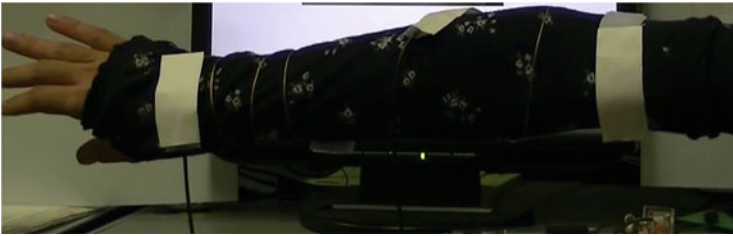


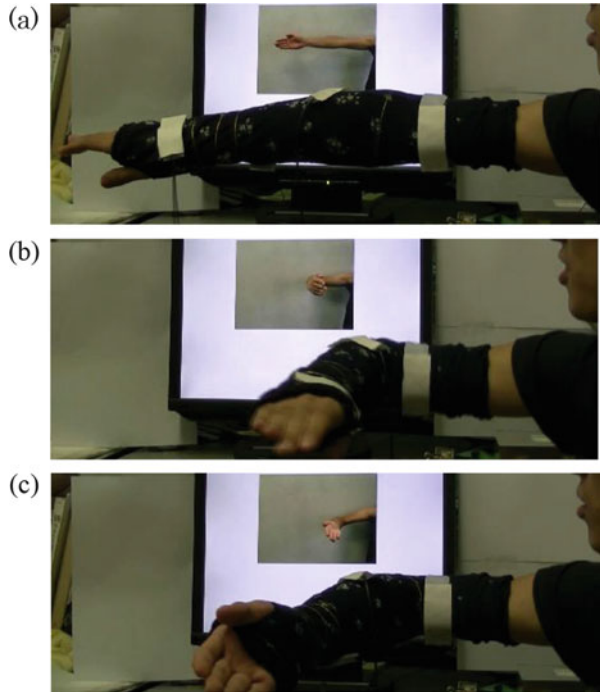
Fig. 15 PLLA fiber left-hand and right-hand coils, respectively, placed on the wrist and arm of a subject. Copyright The Japan Society of Applied Physics [19]

movements of the arm are shown in Fig. 16 [19]. We were able to visualize the inward rotation and outward rotation of the forearm and upper arm by means of computer graphics.

5 Conclusion

PLLA exhibit unique shear piezoelectricity and no pyroelectricity. Furthermore, it exhibits flexibility and transparency. All these characteristics satisfy the requirements of new HMIs such as flexible smart phones and wearable devices. A deformation detection touch panel using a piezoelectric PLLA film sensor has been produced in combination with a projected capacitive touch panel. This touch panel can detect both bending and twisting motion, as well as the degree of

Fig. 16 Visual demonstration of sensing of human motion using PLLA fiber left-hand and right-hand coils. (a) extending, (b) flexing, and (c) inward rotation. Copyright The Japan Society of Applied Physics [19]



deformation resulting from such motion. The basic function of the sensor is the same as that of current projected capacitive touch panels; therefore, the operations of touching, stroking, and multitouch gestures can be used. This touch panel shows great promise for future applications requiring flexible sensor devices. We have described a soft sensor using the PLLA fiber coil and a new technique for sensing using a shear piezoelectric PLLA fiber. Our results indicate the strong possibility of realizing a new soft sensor using biodegradable chiral piezoelectric polymers such as PLLA fibers. In particular, piezoelectric PLLA fibers are expected to have a wide range of applications.

Acknowledgments This work was supported in part by a Grant-in-Aid for Scientific Research from the Ministry of Education, Culture, Sports, Science and Technology, Japan. We appreciate receiving a 2016 Commendation for Science and Technology (Prizes for Science and Technology: Development) from the Minister of Education, Culture, Sports, Science and Technology, Japan.

References

1. Galetti P, DeRossi D, DeReggi A (eds) (1988) Medical applications of piezoelectric polymers. Gordon and Breach, New York

2. Wang T, Herbert J, Glass A (1988) The applications of ferroelectric polymers. Blackie, Glasgow
3. Nalwa H, Fukada E (eds) (1995) Ferroelectric polymers. Marcel Dekker, New York
4. Fukada E (2000) History and recent progress in piezoelectric polymers. *IEEE Trans Ultrason Ferroelectr Freq Control* 47:1110–1119
5. Uchino K (eds) (2000) Ferroelectric devices. Marcel Dekker, New York
6. Lang SB (2005) Guide to the literature of piezoelectricity and pyroelectricity. *Ferroelectrics* 321:91–204
7. Fukada E (2006) Recent developments of polar piezoelectric polymers. *IEEE Trans Dielectr Electr Insul* 13:1110–1119
8. Carpi F, Smela E (eds) (2009) Biomedical applications of electroactive polymer actuators. Wiley, Chichester
9. Tajitsu Y (2013) Fundamental study on improvement of piezoelectricity of poly(L-lactic acid) and its application to film actuators. *IEEE Trans Ultrason Ferroelectr Freq Control* 60:1625–1629
10. Nye J (ed) (1985) Physical properties of crystals. Clarendon Press, Oxford
11. Kobayashi J, Fukada E, Shikinami Y, et al (1995) Structural and optical properties of polylactic acid. *J Appl Phys* 77:2957–2972
12. Aleman C, Lotz B, Puiggali J (2001) Crystal structure of the alpha-form of poly(L-lactide). *Macromolecules* 34:4795–4801
13. Tajitsu Y (2002) Giant optical rotatory power and light modulation by polylactic acid film. In: Zhang Q, Fukada E (eds) Materials Research Society symposium proceedings book vol. 698. pp. 125–136
14. Tajitsu Y (2010) Basic study on controlling piezoelectric motion of chiral polymeric fiber. *IEEE Trans Dielectr Electr Insul* 17:1050–1055
15. Abe A, Maeda Y, Furuya H, Hiromoto A, Kondo T (2012) Thermodynamic studies on the helix-sense inversion of polyaspartates in the solid state. *Polymer* 53:2673–2680
16. Tanimoto K, Furuya H, Tajitsu Y (2014) Effect of helix inversion of poly(β -phenethyl L-aspartate) on macroscopic piezoelectricity. *Jpn J Appl Phys* 53:09PC01
17. Ando M, Kawamura H, Tajitsu Y, et al (2012) Film sensor device fabricated by a piezoelectric poly-L-lactic acid film. *Jpn J Appl Phys* 51:09LD14-1
18. Ando M, Kawamura H, Tajitsu Y et al (2013) A deformation detection touch panel using a piezoelectric poly(L-lactic acid) film. In: Proceedings of the 20th International Display Workshop, Sapporo Convention Center, Sapporo, Japan, 4–6 Dec 2013
19. Ito S, Imoto K, Takai K, Kuroda S, Kamimura Y, Kawai N, Date M, Fukada E, Tajitsu Y (2012) Sensing using piezoelectric chiral polymer fiber. *Jpn J Appl Phys* 51:09LD16

Poly(lactic acid)-Based Materials for Automotive Applications



**Amani Bouzouita, Delphine Notta-Cuvier, Jean-Marie Raquez,
Franck Lauro, and Philippe Dubois**

Abstract As a result of increasingly stringent environmental regulations being imposed on the automotive sector, ecofriendly alternative solutions are being sought through the use of next-generation bioplastics and biocomposites as novel vehicle components. Thanks to its renewability, low cost, high strength, and rigidity, poly(lactic acid), PLLA, is considered a key material for such applications. Nevertheless, to compete with traditional petroleum-sourced plastics some of the properties of PLLA must be improved to fulfill the requirements of the automotive industry, such as heat resistance, mechanical performance (especially in terms of ductility and impact toughness), and durability. This review focuses on the properties required for plastics used in the automotive industry and discusses recent breakthroughs regarding PLLA and PLLA-based materials in this field.

A. Bouzouita (✉)

Laboratory of Polymeric and Composite Materials (LPCM), Center of Innovation and Research in Materials and Polymers (CIRMAP), University of Mons (UMONS), Place du Parc 23, 7000 Mons, Belgium

Industrial and Human Automatic Control and Mechanical Engineering Laboratory (LAMIH), UMR CNRS 8201, University of Valenciennes and Hainaut-Cambrésis, Le Mont Houy, 59313 Valenciennes, Cedex 9, France
e-mail: amani.bouzouita@umonts.ac.be

D. Notta-Cuvier and F. Lauro

Industrial and Human Automatic Control and Mechanical Engineering Laboratory (LAMIH), UMR CNRS 8201, University of Valenciennes and Hainaut-Cambrésis, Le Mont Houy, 59313 Valenciennes, Cedex 9, France

J.-M. Raquez (✉) and P. Dubois

Laboratory of Polymeric and Composite Materials (LPCM), Center of Innovation and Research in Materials and Polymers (CIRMAP), University of Mons (UMONS), Place du Parc 23, 7000 Mons, Belgium
e-mail: jean-marie.raquez@umonts.ac.be

Keywords Automotive industry • Bioplastic • Injection molding • Poly(lactic acid)

Contents

1	Introduction	179
2	(Bio)plastics in the Automotive Industry	180
2.1	Technical Requirements for Plastics Used in Car Applications	181
2.2	Why PLLA Is Being Viewed as a Key Material for Cars	183
3	Development of High-Performance PLLA-Based Materials	186
3.1	Tough and/or Ductile PLLA-Based Blends	187
3.2	Heat-Resistant PLLA-Based Blends	195
3.3	Mold-Injected PLLA Materials for Automotive Applications	202
3.4	Durable PLLA/Polymer Blends	205
4	PLLA in the Automotive Industry: Current Applications	207
4.1	PLLA-Based Plastics and Reinforced Plastics for Automotive Interior Parts	207
4.2	PLLA-Based Fabrics and Nonwovens Products	211
5	Conclusions and Perspectives	212
	References	212

Abbreviation

ABS	Acrylate-butadiene-styrene
ATBC	Acetyltributylcitrate
BioPA	Bio-polyamide
BioPE	Bio-polyethylene
BS	Biomax [®] Strong (Commercial impact modifier)
CE	Chain extender
CL25A	Cloisite [®] 25A
DEHA	Bis(2-ethylhexyl) adipate
DOA	Diethyl adipate
DSC	Differential scanning calorimetry
EBS	Ethylene bis-stearamide (nucleating agent)
EMA-GMA	Ethylene-methyl acrylate-glycidyl methacrylate
ENR	Epoxidized natural rubber
GTA	Glyceryl triacetate
HDT	Heat deflection temperature
HNT	Halloysite nanotube
NCH	Nylon-clay hybrid
OEM	Original equipment manufacturer
OMC	Organic modified clay
OMLS	Organically modified layered silicate
PA	Polyamide
PBGA	Oligomericpoly(1,3-butylene glycol adipate)
PC	Polycarbonate
PCL	Polycaprolactone

PDLA	Poly(D-lactic acid)
PEBA	Polyether block amide
PEG	Polyethylene glycol
PET	Polyethylene terephthalate
PHA	Polyhydroxyalkanoate
PLLA	Poly(L,D-lactic acid)
PLS	Polymer-layered silicate nanocomposites
PMMA	Poly(methyl methacrylate)
PP	Polypropylene
PPA	Poly(1,2-propylene glycol adipate)
PS	Polystyrene
PTT	Polytrimethylene terephthalate
PU	Polyurethane
RH	Relative humidity
sc-PLA	Stereocomplex of polylactide
TAC	Triacetin
TBC	Tributylcitrate
TPU	Thermoplastic polyurethane

1 Introduction

Reducing vehicle weight is an important issue for the automotive industry, and plastics are attractive materials for addressing this challenge. Because of their renewable origin, bioplastics help minimize the environmental impact of car production by further reducing CO₂ emissions and energy consumption [1, 2]. Besides, it is crucial for the industry to develop sustainable alternatives to products derived from petroleum oil, because the price of petroleum oil is unstable and its feedstock is expected to run out in the near future. Of the bioplastics existing today on the market, some are already suitable for the automotive sector, particularly formulations based on poly(lactic acid) (PLLA) and its composites [3]. Several key points contribute to the success of PLLA, especially its excellent (bio)degradability/recyclability and attractive physical and mechanical properties such as high rigidity, strength, and easy processability using conventional processing techniques such as extrusion and injection molding [4, 5]. However, although PLLA can fulfill environmental regulations regarding the automotive sector, the development of technical PLLA-based materials for automotive applications still encompasses some thresholds that have not yet been achieved. These requirements include high toughness, durability, processability at high temperature, and high production rate at affordable cost [6].

Several strategies such as blending with petroleum-based polymers, plasticizers, impact-modifiers, and micro- and/or nanosized fillers have thereby been proposed in efforts to overcome these drawbacks [7]. This chapter describes the great potential of PLLA-based materials and their future trends, while mentioning their

current drawbacks and the improvements required to sustain their successful implementation in the automotive sector. Special emphasis is placed on the current and future use of PLLA-based materials for some automobile parts as both bulk and fibrous materials.

2 (Bio)plastics in the Automotive Industry

The plastics industry plays a significant role in the environmental, societal, and economic dimensions of sustainable development. Plastics meet the societal demands of today’s products in packaging, lightweight components for cars and aircraft, electronic housing, insulating materials for buildings, medical devices, etc. Yet, the plastics industry still has to face up to great challenges concerning improvements in safety, protection of the environment, and energy-saving in plastics manufacturing processes as well as during their lifetime. In the automotive sector, plastics and polymer composites are more and more appealing because their light weight can help decrease the fuel consumption of vehicles, without adversely affecting safety issues. Indeed, automotive manufacturers are tending to replace traditional materials such as metals and metal alloys for lightweight materials such as plastics and composites [8, 9]. As an illustration, the contribution of plastics to the average weight of a vehicle is presented in Fig. 1. Today, plastics typically make up 16% of the average weight of a new vehicle and will account for 18% by 2020, with more than 50% of a modern vehicle’s volume. This renders cars lighter and more fuel efficient, resulting in lower greenhouse gas emissions [10, 11].

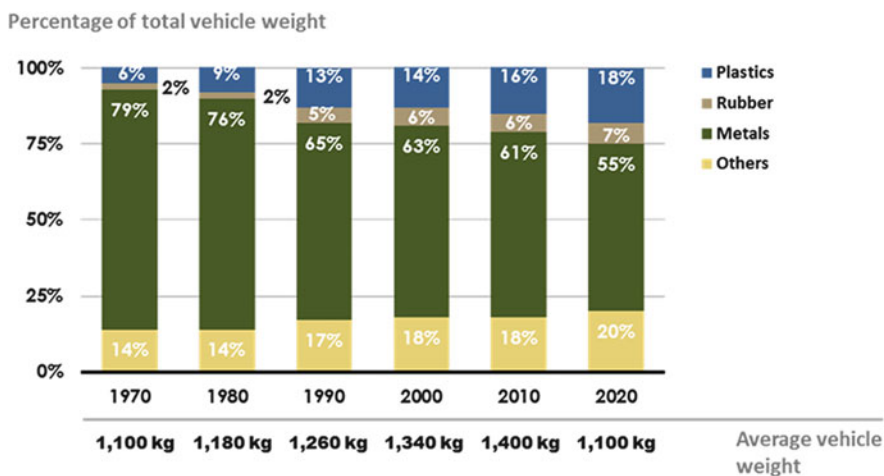


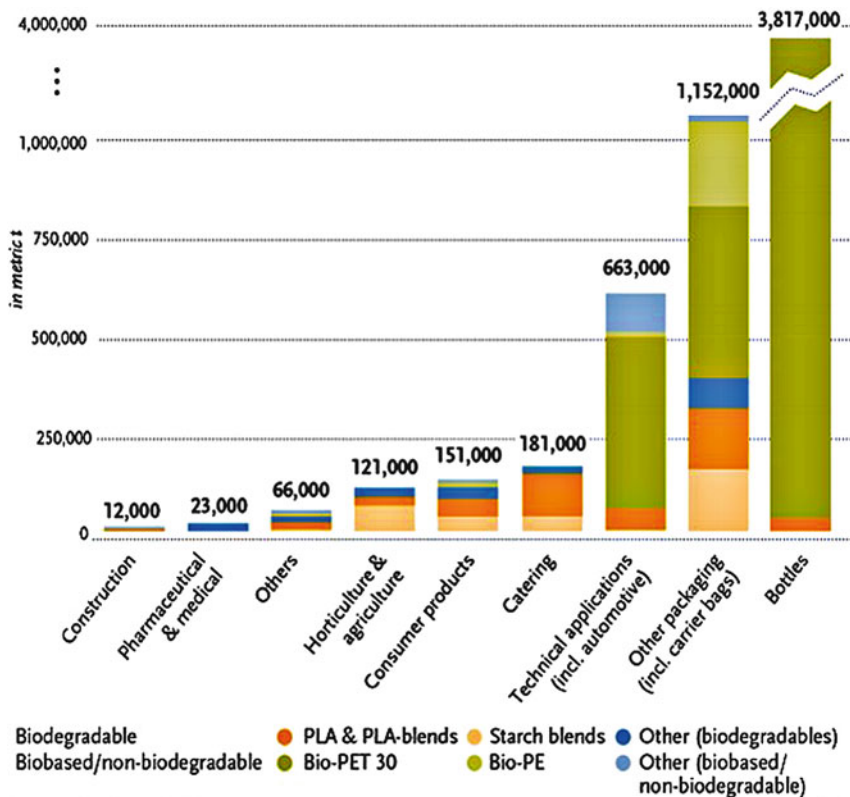
Fig. 1 Evolution of the percentage of plastics in vehicles by weight. Reproduced with permission from [10] Copyright © 2012, A.T. Kearney, Inc

Furthermore, an important challenge for the twenty-first century is undoubtedly sustainable management of resources, accompanied by new environmental regulations and a strengthening bioeconomy. This latter refers to the sustainable production and conversion of renewable resources from agriculture into energy and a large range of food, health, fiber, and industrial products [12]. This trend is pushing automotive manufacturers to propose renewable alternatives to traditional plastics, while fulfilling current and new specifications for automotive parts, the aim being production of smarter, lighter, greener and, if possible, low cost cars. In that context, bioplastics meet these requirements because they have similar structural and functional characteristics as their petroleum-sourced counterparts. Note that the term “bioplastics” covers materials that are both partially and fully biosourced. Beyond their initial use for packaging applications [13–15], bioplastics have reached a very high level of maturity for a large range of automotive applications, offering high performance together with reduced environmental impact. It is therefore not surprising that the use of bioplastics is continuously increasing in technical applications, including for the automotive sector (Fig. 2).

2.1 Technical Requirements for Plastics Used in Car Applications

Today, plastics are employed not only to build internal parts in cars but also external components such as bumpers, body panels, laminated safety glass, trims, and many others (Fig. 3). In exterior applications, plastics are not only used for their light weight, but also because they give designers the freedom to create innovative concepts, for instance parts of a complex shape that could not be massively manufactured using other materials such as metals. In other words, plastics are nothing less than revolutionary. They have shown to be great materials for creating comfortable, durable, and aesthetically pleasing interior components, while preserving occupant protection and reducing noise and vibration levels. Furthermore, they have proven to be strong, durable, corrosion-resistant, and able to withstand high temperatures under harsh engine environments. These properties make plastics suitable for electrical, powertrain, fuel, chassis, and engine applications.

Usually, the choice of materials made by vehicle manufacturers depends on a combination of several criteria. Some of the criteria are the result of regulation and legislation on environmental and safety concerns. Other criteria relate to production costs, mechanical and physical properties, and weight reduction. Different characteristics are often mentioned as material selection criteria for the automotive industry (Fig. 4) [17–21]. These criteria vary according to the type of vehicle and component application. In many cases, different factors may conflict with each other and therefore a successful design is only possible through an optimum and balanced solution.



Source: European Bioplastics | Institute for Bioplastics and Biocomposites (December 2013)

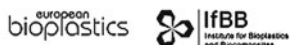


Fig. 2 Global production capacities of bioplastics 2017 by market segment. Reproduced with permission from [16]

Many types of petroleum-based plastics that can provide the technical requirements for the automotive sector are employed in more than 1,000 different parts of all shapes and sizes. The most important polymers in the automotive industry are polypropylene (PP), used for instance in body panel bumpers and fuel systems; polyamide (PA), used in seats and electrical components; poly(methyl) methacrylate (PMMA) and polyurethane (PU) used in lighting; and polycarbonate (PC) used in bumpers, dashboards, and interior and exterior trim and usually associated with acrylate-butadiene-styrene (ABS) [22].

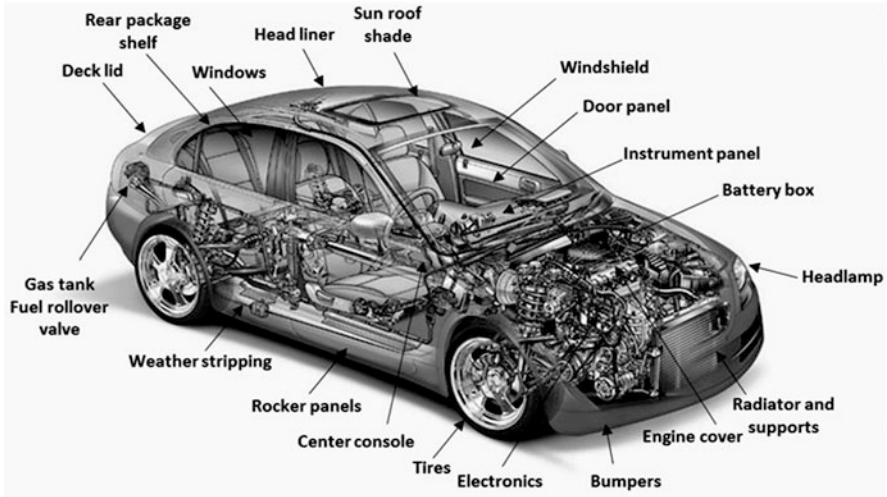


Fig. 3 Autoparts of lightweight plastics and rubber

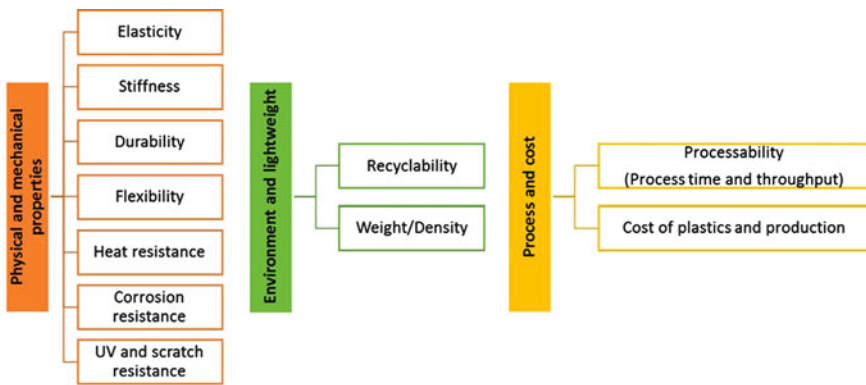


Fig. 4 Criteria used in automotive plastics selection and component design

2.2 Why PLLA Is Being Viewed as a Key Material for Cars

Together with other bioplastic polymers such as polyhydroxyalkanoate (PHA), polycaprolactone (PCL), polytrimethylene terephthalate (PTT), biopolyamide (BioPA), and biopolyethylene (BioPE) [23], one of most popular alternatives to traditional petroleum-based plastics in automotive applications is poly(L-lactic acid) (PLLA), as currently derived from cornstarch. In spite of intensive R&D on PLLA science and new technology to enable large-scale production, the industrial application of unmodified PLLA is currently limited to short-term goods such as packaging, cold drink cups, bottles, and textiles [24–26]. Nevertheless, a number of factors can help extend the application of PLLA to more durable goods: high

Table 1 Selected data on mechanical and physical properties of various plastics [28–32]

	PP	PA	PMMA	ABS	PC	PU	PVC	PLLA
Young's modulus (GPa)	0.896–1.55	2.62–3.2	2.24–2.8	1.1–2.9	2–2.44	1.31–2.07	2.14–4.14	3.55–3.75
Tensile strength (MPa)	27.6–41.4	90–165	48.3–79.6	28–55	60–72.4	31–62	40.7–65.1	65–70
Impact strength (J/m) at 24°C	26.7–106.8	53.4–160.2	21.4–26.7	53.4–534	640.8–961.2	800	21.4–160.2	19–26
HDT (°C) load at 1.8 MPa	67	75	97	100	143	46–96	64	50–57
Density (g/cm ³)	0.89–0.91	1.12–1.14	1.16–1.22	1.1–1.2	1.14–1.21	1.12–1.24	1.3–1.58	1.25
CO ₂ Footprint (kg/kg)	2.6–2.8	5.5–5.6	3.4–3.8	3.3–3.6	5.4–5.9	4.6–5.3	2.2–2.6	<1
Cost (\$US/kg)	1.2–1.3	3.3–3.6	2.6–2.8	2.1–2.5	3.7–4	4.1–5.6	0.93–1	~2

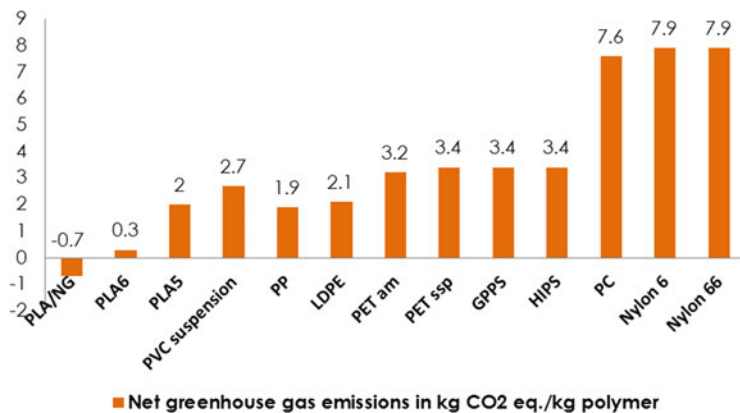


Fig. 5 Net greenhouse gas emission of commercial PLAs and other polymers. *PLA/NG* NatureWorks® PLA next-generation, *PLA5* NatureWorks® PLA in 2005, *PLA6* NatureWorks® in 2006, *HIPS* high impact poly(styrene), *PC* poly(carbonate), *GPPS* general purpose poly(styrene), *PET am* PET amorphous, *PET ssp*. PET solid state polycondensed. Reproduced with permission from [29] Copyright © 2010 Institute of Food Technologists®

strength, rigidity, compostability, and recyclability [27]. To assess the strengths and weaknesses of PLLA, its physical and mechanical properties can be compared with those of the most commonly used plastics in automotive applications (see Table 1). The mechanical properties of PLLA appear very attractive, particularly its Young's modulus (>3.5 GPa), making it an excellent alternative to commonly used stiff polymers.

In the context of designing ecofriendly products, both to satisfy customer demand and increasingly strict legislation [33], PLLA possesses undeniable assets compared with petroleum-based polymers. First, it is derived from bioresources (starch plants), which are abundant and renewable. Moreover, one of the most positive points of PLLA production in comparison with the other hydrocarbon-based polymers is its low CO₂ emission. Carbon dioxide is the most important contributor to global climate change. Because CO₂ from air is readily transformed when plants grow, the use of PLLA has the potential to reduce the environmental impact of greenhouse gases compared with petroleum-based polymers. In addition, emerging green technologies enable a decrease in greenhouse gas emissions during PLLA production processes. Vink et al. [28] showed that the net greenhouse gas emission of NatureWorks PLLA decreased from 2 kg CO₂ equivalents/kg polymer in 2003 to 0.3 kg in 2006. Furthermore, Jamshidian et al. [29] estimated that the net greenhouse gas emissions for next-generation PLLA using wind energy can achieve -0.7 kg CO₂/kg polymer (Fig. 5).

PLLA has also received some interest from other industrial sectors because of its relatively low price and commercial availability compared with other bioplastics. This is certainly the key point for any successful polymer application. In fact, the average price of commercial PLLA in 2015 was less than 1.8 €/kg, which is sufficiently close to other petroleum-based polymers such as PET and is the lowest

among biodegradable polymers [30]. Clearly, the PLLA market is still in its infancy, but it is expected that a decrease in production costs and improvement in product performance will result in a clear breakthrough in PLLA industrial use. Many researchers have developed a more efficient and economic route for cheaper and greener PLA production [31, 32, 34]. It is estimated that PLLA production capacity, currently around 180,000 tons/year, should exceed more than 1×10^6 tons in 2020 [35]. In addition to lower gas emissions, increasingly affordable cost, and appealing mechanical properties, PLLA possesses other assets not generally available with petroleum-based plastics. Among those assets are excellent biocompatibility, (bio)degradability, and recyclability; furthermore, it can be readily processed in large-scale processing equipment such as injection molding units [36, 37]. More particularly, PLLA can be processed by injection molding, sheet-extrusion, blow molding, thermoforming, and film forming and is one of the few plastics suitable for 3D printing [38].

This new technology process for plastics is very important for the automotive industry and aftermarket because it allows the realization of automotive parts of incredibly complex geometry and enables production of spare parts on demand [39, 40]. Recently, an electric Street Scooter C16 short-distance vehicle was built by a team at Aachen University [41]. 3D printing using ABS polymer was used for all the vehicle's exterior plastic parts, including the large front and back panels, door panels, bumper systems, side skirts, wheel arches, and lamp masks and for interior components such as the retainer instrument board and a host of smaller parts [41]. Local Motors made a car called the "Strati" by building the chassis and body of its cars using giant 3D printers and raw materials [42].

Referring to Table 1 and comparing PLLA with the traditional plastics used in automotive applications, neat PLLA has many appealing properties such as high rigidity but cannot fulfill all the criteria required by the automotive sector, most importantly in terms of brittleness and heat resistance. Several strategies have been studied in efforts to overcome these drawbacks.

3 Development of High-Performance PLLA-Based Materials

As discussed, the major drawbacks of PLLA that hamper its application in the automotive industry are its inherent brittleness, low heat resistance, limited flexibility in design, and poor durability. In order to make PLLA suitable for such applications, many studies have focused on modifications of PLLA, mainly of its bulk properties. These modifications have involved control of crystallinity and processability via blending, plasticizing, stereocomplexing, and other modifications depending on the properties to be improved. There is no unique way to improve PLLA properties and the most interesting solutions are generally a combination of different routes; however, not many have been successful as a result of antagonist

effects when combined. Those modifications are described in detail in the next sections, with an emphasis on PLLA-based materials that fit automotive requirements in terms of processing (e.g., injection molding), properties (e.g., stiffness), and durability.

3.1 Tough and/or Ductile PLLA-Based Blends

In cases that require a high level of impact strength and ductility, especially for a vehicle's exterior parts, the impact toughness and ductility of PLLA in its pristine state is often insufficient. Therefore, there have been tremendous efforts to develop ways to improve these mechanical properties. These approaches are summarized next, with a focus on how the protocols also influence other mechanical properties in the resultant materials.

3.1.1 Plasticized PLLA Blends

Plasticization is a widely used technique for improving the processability of thermoplastics. The main role of plasticizers is to decrease the glass transition temperature (T_g). In addition, plasticization frequently opens new possibilities for material processing by lowering degradation rate, which enables processing of materials in equipment with reduced extrusion pressure and mixing time [43]. Furthermore, it can also increase polymer ductility and flexibility, which is related to the decrease in T_g . The choice of plasticizer for PLLA is dictated by factors relating to the intended application (e.g., nontoxicity of plasticizer for food and medical applications) as well as by general criteria such as non-volatility to avoid evaporation under the high temperature conditions used during processing, and miscibility for creating homogenous blends with PLLA. Another point is that the plasticizer must migrate as little as possible from the material bulk, otherwise plasticized PLLA blends can rapidly regain the inherent brittle properties of neat PLLA [44].

Many different molecules and classes of plasticizer have been tested for PLLA [45, 46], the three main types being monomeric plasticizers, oligomeric and polymeric plasticizers, and mixed plasticizers. Only plasticizers designed for injection-molded parts are selected here for discussion. Examples of the thermal and mechanical properties of PLLA plasticized with these three classes of plasticizers are given in Table 2 and described in more detail.

Jacobsen and Fritz [47] used glucose monoester (DehydatVPA 1726), partial fatty esters (LoxioIVR GMS95), and polyethylene glycol (PEG) with a molecular weight of 1,500 g/mol (PEG1500), to plasticize PLLA and examined the effect on the tensile strength and unnotched Charpy impact strength of injection-molded PLLA specimens. A significant improvement in both elongation (180%) and impact resistance (unbroken specimens under unnotched Charpy impact tests) was reported with the addition of 10 wt% PEG1500. In the case of glucose monoester and partial

Table 2 Thermal and mechanical properties of plasticized PLLA blends

Plasticized PLLA blends	Molecular weight (g/mol)	Content (wt%)	T_g ($^{\circ}$ C)	σ (MPa)	E (GPa)	ϵ (%)	Reference	
<i>Monomeric plasticizers</i>								
PLLA	74,000	100	54	57	3.75	5	[47]	
Loxiol GMS95	–	2.5	–	52	3.4	14		
		5	–	48	3.2	7		
		10	45	45	3	8		
Dehydatt VPA 1726	–	2.5	–	53	3.3	5		
		5	–	47	3	6		
		10	40	38	2.5	13		
PLLA	74,500	100	62	66	1.02	11		[48]
ATBC	402.5	10	44	51	0.97	11		
		20	38	30	0.27	317		
DOA	370.6	10	45	29	0.72	36		
		20	45	21	0.67	78		
GTA	218.2	10	48	38	0.76	8		
		20	29	24	0.01	443		
<i>Polymeric plasticizers</i>								
PEG	1,500	2.5	–	50	3.2	5	[47]	
		5	–	44	2.5	7		
		10	28	38	1.3	180		
PLLA	121,400	100	58.6	69.8	1.77	6	[49]	
PPA	1,900	5	49.3	63.2	1.39	6		
		10	40.6	49.6	1.3	157		
		15	33.3	39.8	0.882	315		
		20	27	25.7	0.554	362		
		25	24.3	14.4	0.374	410		
<i>Mixed plasticizers</i>								
PLLA	207,400	100	–	58	–	4	[50]	
TAC/PBGA	–	5	–	48	–	4		
		9	–	36	–	180		
		13	–	24	–	349		
		29	–	17	–	327		

T_g is the glass transition temperature; σ , E , and ϵ refer to the tensile strength, elastic modulus, and tensile elongation at break, respectively

fatty acid ester, elongation of PLLA was improved but impact strength was slightly decreased at all concentrations examined (i.e., 2.5–10 wt%). Murariu et al. [48] studied the plasticization of PLLA using three low molecular weight ester-type plasticizers, bis(2-ethylhexyl) adipate (DOA), glyceryl triacetate (GTA), and acetyltributylcitrate (ATBC). Addition of up to 20 wt% plasticizer led to a gradual decrease in Young's modulus and increased ductility in the following order of efficiency, $GTA > ATBC > DOA$. The best notched impact performance was seen in PLLA plasticized with 20 wt% GTA, with unbroken specimens. By comparison,

addition of ATBC led to the lowest improvement in the impact strength of the three plasticizers, with “only” an increase of 77% at 20 wt % ATBC.

The main drawback of monomeric plasticizers is their tendency to migrate out of the polymer bulk [51]. This drawback can be overcome by using polymeric plasticizers [47, 49]. Recently, it has been shown that PLLA can be efficiently plasticized and toughened by melt-blending with poly(1,2-propylene glycol adipate) (PPA) [49]. Thermal and dynamic mechanical analysis revealed that PPA was partially miscible with PLLA, and morphological investigation of the blends showed that PPA was compatible with PLLA. As a result, the blends showed a decrease in the tensile strength and Young’s modulus with an increase in PPA content (5–25 wt%) (Table 2). However, the elongation at break and impact strength dramatically increased as a result of plastic deformation. The notched Izod impact strength reached 100 J/m with 25 wt% of PPA. The results show that polymeric plasticizers can cause an additional increase in impact strength. Nevertheless, increasing the molecular mass of plasticizers can lead to poor miscibility with the polymer, causing phase separation [52].

Mixed plasticizers combine an oligomeric or polymeric plasticizer with a small-molecule plasticizer. Therefore, they can lead to a medium drop in T_g and more balanced mechanical properties (in terms of elongation, tensile modulus, and strength) than the individual plasticizers. Mixed plasticizers combining low molecular weight triacetin (TAC) and oligomeric poly(1,3-butylene glycol adipate) (PBGA) have been employed to improve the ductility of PLLA, as reported by Ren et al. [50]. They found that this combination led to significant improvement in the elastic properties (for plasticizer content higher than 5 wt%), with a dramatic decrease in tensile strength as the content of plasticizer increased (Table 2).

To enhance mechanical properties without altering the rigidity of PLLA too much and to improve flexibility and toughness, Notta-cuvier et al. [53] had the idea of combining plasticizers with Halloysite nanotubes (HNT) as reinforcing nanofillers, leading to more attractive properties for automotive applications. In particular, this composition achieved the right combination of good rigidity and tensile flexural strength imparted by HNT with better ductility and toughness provided by tributylcitrate (TBC) plasticizer. Tensile behavior and impact results are represented in Fig. 6 and show that the ductility and impact resistance of PLLA/HNT/TBC ternary blends were improved to an extent that depended on the amount of plasticizer. Moreover, a high content of TBC (12.5–15%wt) enhanced the impact resistance of the blend, but led to a drop in rigidity and flexural strength. For a good balance of properties, an optimized PLLA/HNT/TBC composition containing 10 wt% of plasticizer was proposed as a biosourced alternative blend for automotive application.

In summary, several studies have demonstrated that plasticizers can play a significant role in tuning the properties of PLLA plastics, mainly to improve the flexibility and ductility of PLLA blends, and could also pave the way to novel applications. However, there are still some limitations associated with plasticization, including leaching during use, lack of thermal stability, and substantial reductions in strength and modulus. This illustrates the need to carefully estimate

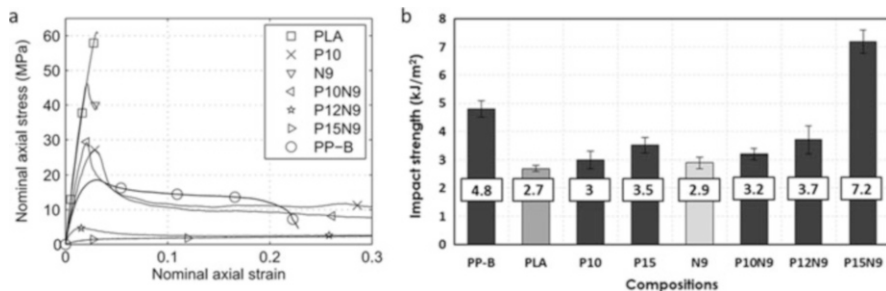


Fig. 6 (a) Nominal behavior of PLLA/TBC/HNT compositions and PP-B in tensile tests at 1 mm min^{-1} . (b) Izod impact resistance (notched specimens) of PLLA/TBC/HNT compositions and PP-B. Sample codes refers to the following weight contents (PLLA/TBC/HNT): *N9* (91/0/9); *P10* (90/10/0); *P15* (85/15/0); *P10N9* (81/10/9); ***P12N9*** (78.5/12.5/9); and *P15N9* (76/15/9). Reproduced with permission from [53] Copyright © 2015 WILEY-VCH Verlag GmbH & Co. KGaA, Weinheim

plasticizer content to reach a better compromise between ductility and strength, especially for automotive applications.

3.1.2 Rubber-Toughened PLLA Blends

Several successful strategies have been proposed to improve the ductility and toughness of PLLA. Of these, melt-blending with rubbers has proved to be efficient, thanks to its remarkable toughening effect and the fact that is based on easy-to-perform and cost-effective techniques. A variety of biodegradable and nonbiodegradable flexible polymers have been used as toughening modifiers for PLLA to improve the balance between stiffness and toughness. Various reviews report the most commonly used polymeric additives to be effective PLLA impact modifiers [45, 54–59]. However, this section is strictly limited to recent and noteworthy studies concerned with developing rubber-toughened PLLA blends for engineering applications requiring high ductility and impact toughness.

When aiming to improve PLLA ductility and impact toughness, the use of impact modifiers can be of great interest because they allow an increase in energy dissipation through the material during deformation, without affecting stiffness and thermal stability [60]. Several commercial impact modifiers have been specifically designed to toughen PLLA. When dispersed in the form of rubbery microdomains (with an average size of $0.1\text{--}1.0 \mu\text{m}$) within the PLLA matrix, they enable a significant increase in energy absorption during impact [61, 62]. However, it is well known that their toughening effect is of varying magnitude, depending on their miscibility with the PLLA matrix, thermal stability under PLLA processing temperatures, interfacial adhesion between the dispersed rubbery phase and continuous PLLA matrix within the blend, etc. Of the impact modifiers compatible with PLLA, Biomax[®] Strong (BS) from Dupont Company is probably the most investigated because it was specifically designed to improve PLLA toughness. In this regard, BS

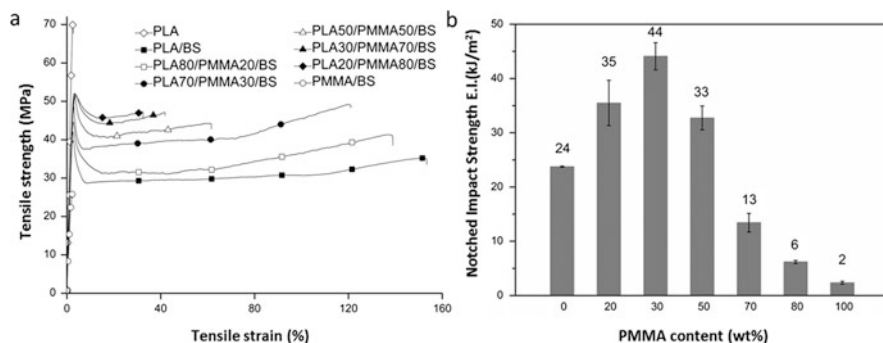


Fig. 7 (a) Tensile stress–strain curves for PLLA and PLLA/PMMA/BS blends. (b) Effect of relative content of PMMA on the notched impact strength of PLLA/PMMA/BS blends. Adapted with the permission from [64] Copyright © 2016 Wiley Periodicals, Inc

was used by Taib et al. [63], who noted a significant improvement in notched Izod impact strength of PLLA from 3.6 to 14 kJ/m² with use of 10% BS, and to 28 kJ/m² with 20 wt% BS. For more suitable PLLA blends in automotive applications with simultaneously enhanced impact and thermal resistance, ethylene acrylate BS impact modifier was used by Bouzouita et al. [64] to develop a PLLA/PMMA/BS ternary blend capable of competing with commercial ABS/PC blends for the manufacture of injection-molded automotive parts. Thermal mechanical analysis revealed that ternary blends showed a miscible PLLA/PMMA matrix, but the impact modifier was phase-separated and formed immiscible blends. The effect of PMMA content on the notched impact strength and tensile mechanical properties of ternary PLLA-based blends showed that a significant gain in tensile elongation and impact toughness was achieved ($116 \pm 4\%$ and 44 ± 2.5 kJ/m², respectively, with addition of 25 wt% PMMA and 17 wt% BS) with only a slight decrease in tensile rigidity and strength (Fig. 7). To understand the evolution of toughness in PLLA/PMMA/BS blends, the average size and distribution of rubber microdomains were analyzed. Results revealed that blend impact toughness and fracture mechanisms depend on rubber particle size, with an optimum of 0.5–0.55 μm achieved at 25 wt% PMMA content. However, PMMA content higher than 50% led to poor mechanical properties and low interfacial adhesion between PLLA/PMMA matrix and BS nodules as a result of the low affinity of impact modifier with PMMA. To conclude the study, the authors selected PLLA/PMMA/BS (58/25/17) as the most promising composition made of at least 50% biosourced polymer in terms of ductility/stiffness balance and characterized by competitive mechanical properties, compared with commercial ABC/PC blends, for use in automotive applications (Table 3).

Using BS impact modifier, Notta-Cuvier et al. [65] prepared PLLA/plasticizer/impact modifier/nanoclay quaternary compositions designed for automotive applications. Good ductility and toughness were achieved with the binary blend (PLLA/BS) at a resiliency of 16.5 kJ/m². A synergistic effect of BS (10 wt%), plasticizer TBC (10 wt%), and the nanoclay Cloisite[®] 25A (1 wt%) was surprisingly seen, with

Table 3 Summary of all mechanical properties of PLLA70/PMMA30/BS compared with those of ABS/PC (tensile tests performed at a displacement rate of 1 mm/min, ASTM-D-638 norm)

Compounds	ABS/PC	PLLA70/PMMA30/BS
Tensile modulus (GPa)	2.3 (0.1)	2.5 (0.1)
Ultimate tensile strength (MPa)	52 (1)	49 (3)
Tensile elongation at break (%)	19 (5)	116 (4)
Impact strength (KJ/m ²)	20 (1)	44 (2)

Reproduced with the permission from [64] Copyright © 2016 Wiley Periodicals, Inc

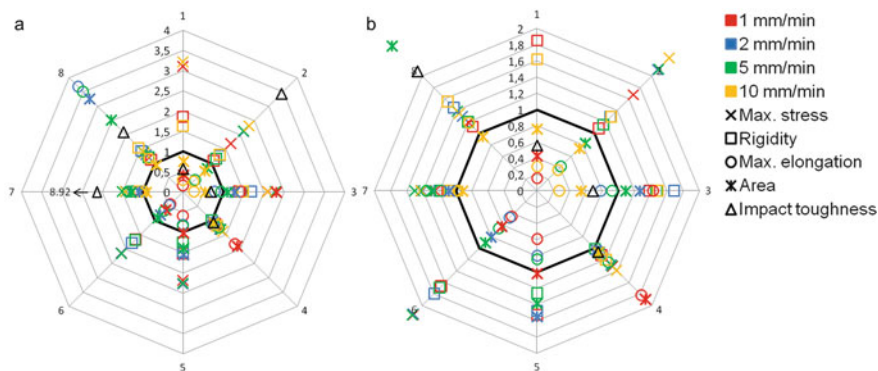


Fig. 8 (a) Summary of all mechanical properties compared with those of PP-B. Numbers refer to PLLA/TBC/BS/CL25A composition codes: 1 (100/0/0/0); 2 (90/0/10/0); 3 (90/10/0/0); 4 (80/10/10/0); 5 (90/0/10/1); 6 (90/0/10/3); 7 (80/10/10/1); 8 (80/10/10/3), in weight percentages. Values presented are ratios of properties of compositions 1–8 divided by those of PP-talc, so that qualitative comparisons are immediate (a value higher than 1.0 stands for a mechanical property higher than that of PP-talc). (b) Summary of all mechanical properties compared with those of PP-B (focus on lower values). Adapted with permission from [65] Copyright © 2016 Elsevier Ltd

an optimal toughness of 42.8 kJ/m². Analysis also revealed that a compromise is needed between high tensile rigidity and strength on one hand, and high ductility on the other hand, as illustrated in Fig. 8. In Fig. 8, the mechanical properties of a mineral (talc)-filled polypropylene (PP-talc), commonly used in automotive applications, were taken as reference. The composition PLLA + 10 wt% BS + 10 wt% TBC + 3 wt% CL25A (composition 8 in Fig. 8) has, globally, the most interesting properties compared with PP-talc. In particular, this composition was characterized by an interesting level of ductility, while its rigidity and strength were higher than those of the mineral-filled PP (10 kJ/m² compared with 4.8 kJ/m² for PP-talc).

Zhang et al. [66] developed super-toughened PLLA multiphase reactive blends using a commercial class of renewable elastomeric copolymers. Polyether block amide PEBA (Pebax[®]) offered high impact resistance and excellent elasticity, and an ethylene-methyl acrylate-glycidyl methacrylate (EMA-GMA) terpolymer impact modifier (commercialized under the name of Lotader[®] AX8900; Arkema Ltd.) improved the interfacial adhesion of PLLA/PEBA blends and enhanced toughness. As shown in Fig. 9b, only limited improvement in impact strength was

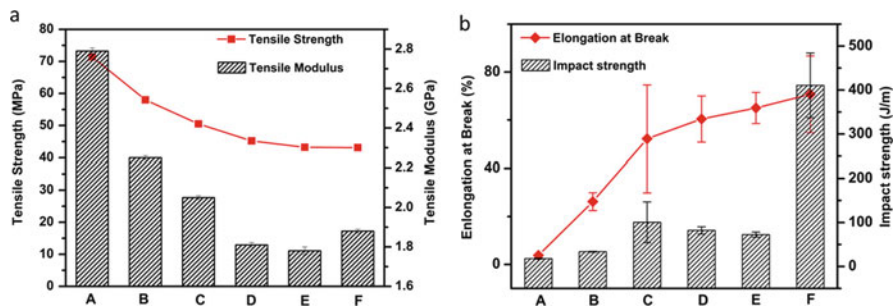


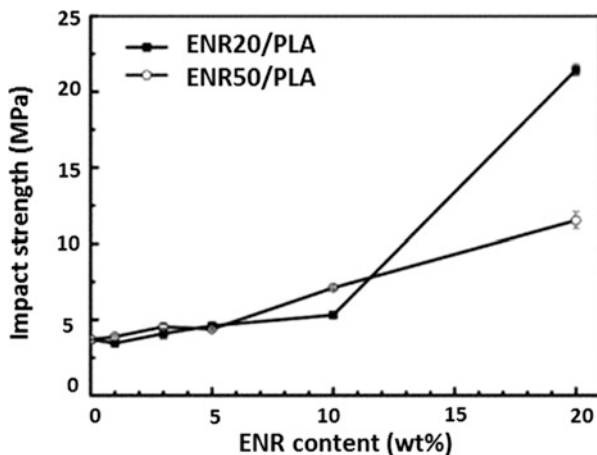
Fig. 9 (a) Tensile properties of PLLA/EMA-GMA/PEBA ternary blends as a function of the weight fraction. (b) Notched Izod impact strength and percentage elongation at break of PLLA/EMA-GMA/PEBA ternary blends as a function of the weight fraction: (A) neat PLLA; (B) PLLA/PEBA (80/20); (C) PLLA/EMA-GMA (80/20); (D) PLLA/EMA-GMA/PEBA (70/10/20); (E) PLLA/EMA-GMA/PEBA (70/15/15); and (F) PLLA/EMA-GMA/PEBA (70/20/10). Adapted with the permission from [66] Copyright © 2014 American Chemical Society

achieved for binary PLLA/PEBA blends but significant enhancement of PLLA impact toughness, together with higher elongation at break, thanks to addition of the impact modifier. Elongation at break increased with the EMA-GMA content, reaching almost 73% with 20 wt% of impact modifier (20 times higher than that of the neat PLLA). Nevertheless, a decrease in tensile strength and modulus for ternary blends was noticed with an increase in EMA-GMA content (Fig. 9a). This result can be attributed to the presence of soft PEBA and EMA-GMA elastomers.

Good interfacial adhesion was achieved by addition of Lotader AX8900. A supertough PLLA ternary blend was thus developed, exhibiting an impact strength of 500 J/m with only partial break of impact specimens, therefore allowing this blend to be used in automotive interior parts.

Although many of the solutions investigated for achieving a decrease in PLLA brittleness and/or an improvement in PLLA impact strength are not fully ecofriendly, blending PLLA with ecofriendly rubber modifiers [67–72], elastomers [73, 74], and biodegradable polymers [75, 76] has gained momentum in recent years. Zhang et al. [67] reported an improvement in the impact strength of PLLA with the incorporation of 20 wt% of epoxidized natural rubber containing 20 mol% (ENR20) and 50 mol% (ENR50) of epoxidation content. ENR20 was found to impart higher impact strength to the PLLA matrix than ENR50 (Fig. 10). Moreover, the higher content of epoxy groups in ENR50 led to an increase in viscosity and therefore decreased deformability of the blends. Interchain crosslinking reactions and molecular entanglements were more pronounced in PLLA/ENR50 blends and, in turn, increased the tensile strength.

Fig. 10 Impact strength of pure PLLA, ENR20/PLLA, and ENR50/PLLA blends. Reproduced with permission from [67] Copyright © 2012 Elsevier Ltd



3.1.3 Annealing Process

Of the additional approaches related to process modification, the literature shows that annealing is an effective method for improving the mechanical properties of PLLA blends (rigidity and impact strength), in particular for injection-molded parts. Annealing modifies the inherent crystalline structure and crystal polymorphism, which have a deep impact on the mechanical properties of PLLA [77–84].

Perego et al. [83] studied the effect of crystallinity on the mechanical properties of PLLA of different molecular weights. To promote further crystallization, PLLA injection-molded specimens were annealed at 105°C for 90 min under nitrogen. DSC analysis demonstrated that the crystallinity degree of PLLA reached 42–65 J/g, instead of 3–13 J/g for nonannealed PLLA, as a function of molecular weight (\bar{M}_v). Annealing PLLA samples also led to some increase in impact strength, depending on the evolution of crystallinity and molecular weight. Values of notched impact strength ranged from 66 to 70 J/m, following the molecular weight of PLLA. The highest tensile elastic modulus attained was 4.15 GPa, resulting from the higher crystallinity degree of annealed materials (Table 4).

From a general viewpoint, in the automotive industry, annealing is mainly used for semifinished components after shaping or cold-forming, with the aims of producing a uniform material structure that offers softness and removing any residual stresses for both alloy and plastic components [85, 86]. Annealing is carried out after heating the material at a specific temperature for a definite period of time, followed by slow cooling to room temperature. This process is used to control the degree of crystallinity and/or orientation of the material and to remove any internal stresses within the product that were created during primary processing. Annealing can also improve impact resistance and reduce the tendency to crazing and cracking during service. It can also offer additional value to the final alloy, such as improved welding properties, better corrosion resistance, and good dimensional and shape accuracy. Unfortunately, this post-process is expensive and

Table 4 Mechanical properties of nonannealed and annealed PLLA

Property Specimen	Molecular weight (\bar{M}_v)	ΔH_m^a (J/g)	Notched strength (J/m)	Modulus of elasticity (GPa)
PLLA-I	23,000	8	19	3.65
Annealed PLLA-I	20,000	65	32	4.2
PLLA-II	31,000	13	22	3.6
Annealed PLLA-II	33,500	59	55	4.0
PLLA-III	58,000	8	25	3.6
Annealed PLLA-III	47,000	48	70	4.15
PLLA-IV	67,000	3	26	3.65
Annealed PLLA-IV	71,000	42	66	4.15

Adapted with permission from [83] Copyright © 1996 John Wiley & Sons, Inc

^aEnthalpy of melting

involves longer production times. Moreover, annealing can induce some structural defects within the part, making it difficult to control shrinking and complicating part ejection. Therefore, it cannot be seen as a promising solution for mass-production processes currently used in the automotive industry.

3.2 Heat-Resistant PLLA-Based Blends

In some applications, heat resistance over extended periods of time is compulsory. Yet, heat resistance is an important issue for plastics used in engineering applications. Indeed, all polymers exhibit a wide variation in mechanical and physical properties as a function of temperature. Apart from the extreme temperature attained in combustion chambers, automotive parts may face service temperatures ranging from -40°C for a car parked outdoors in a cold country to 85°C for the driver interior, and even 125°C under the bonnet [87]. With increasing temperature, polymer strength and rigidity tend to decrease dramatically. Above a given temperature, rigidity drops in a more pronounced way and becomes too low to enable the use of the material in these technical parts. In this regard, the heat deflection temperature (HDT) is defined as the temperature at which a standardized test bar deflects a specified distance under an imposed load value (see ASTM D648 procedure). HDT is therefore an effective way to evaluate the thermal stability, or heat resistance, of plastics [88]. Many researchers have studied the improvement in heat-resistance of PLLA by manufacturing, for example, PLLA-based green composites containing reinforcing fibers. Fibers from wood [89], banana [90], kenaf [91], bamboo [92], and cellulose [93] can all increase HDT, but the resulting composites is brittle.

By contrast, nanofilled PLLA/petroleum-based thermoplastic blends can offer a good balance between thermal stability and ductility, allowing their use in the automotive sector.

3.2.1 PLLA-Based Nanocomposites with High Thermal Properties

Polymer nanocomposites are commonly defined as the combination of a polymer matrix and nanofillers that have at least one dimension in the nanometer range. The nanofillers can be one-dimensional (1D; nanofibers or whiskers), two-dimensional (2D; plate-like nanofillers) or three-dimensional (3D; nanoparticles). The use of nanocomposites in vehicle parts and systems is expected to enhance manufacturing speed, improve thermal stability, and reduce weight. Applying this technology only to structurally noncritical parts such as front and rear panels, cowl ventilator grids, and valve/timing covers could allow a reduction in weight. Indeed, nanocomposite plastic parts offer a 25% weight savings on average compared with highly (micro) filled plastics and as much as 80% compared with steel [94, 95]. As important as the process advantages and weight and energy savings are, nanocomposites can also offer enhanced physical properties. Depending on composition, nanocomposites show stiffness and strength comparable to, or even better than, metals [96–102]. Nanofillers can also improve the corrosion resistance, noise dampening, thermal stability, and dimensional stability of a material. However, as a relatively new approach, it is still unknown whether the cost/performance ratio of nanocomposites is superior to that of materials currently used by the automotive industry.

Layered silicate (clay) nanocomposites (PLS) are among the best-known nanocomposites. Their interesting properties at low nanofiller content make them appealing in both academic and industrial realms [103]. Three main methods have been proposed for preparation of nanocomposites: in situ intercalative polymerization, solution intercalation, and melt intercalation [104, 105]. Clay materials can be dispersed and exfoliated into polymers by conventional melt-compounding or solution methods. Toyota Motor Company successfully pioneered an in situ intercalation polymerization method to create a Nylon–clay hybrid (NCH) for manufacture of an automotive timing belt cover [106]. Although in situ intercalative polymerization is the most efficient technique for obtaining an exfoliated structure, it is not the most viable option for current industrial challenges [104, 107]. Alternatively, the melt-intercalation technique is more versatile and less environmentally harmful. Therefore, it is the most efficient method for the preparation of polymer nanocomposites from an industrial viewpoint. The main advantages in comparison with other approaches are the utilization of elevated shearing force and the absence of solvent during preparation. The applied shear force during mixing readily promotes the diffusion of polymer chains from the bulk to the clay gallery spacing, resulting in further nanoplatelet delamination and improved nanofiller distribution and dispersion [105].

Table 5 Heat deflection temperatures of PLLA, PLLA/TPU blends, and their nanocomposites

Specimen	Content (wt%)				HDT of injection-molded specimens (°C)	HDT of annealed specimens (°C)
	PLLA	TPU	Talc	OMC		
LA	100	0	0	0	59.2	–
LAT4C0	96.0	0	4.0	0	61.1	129.5
LAT4C02	94.0	0	4.0	2.0	63.9	133.3
LAT4C06	90.0	0	4.0	6.0	60.1	133.4
LAT4C10	86.0	0	4.0	10.0	63.1	126.1
LAT4C14	82.0	0	4.0	14.0	61.7	130.6
LU	90	10	0	0	60.6	–
LUT4C0	86.4	9.6	4.0	0	60.1	130.3
LUT4C02	84.6	9.4	4.0	2.0	58.9	122.7
LUT4C06	81.0	9.0	4.0	6.0	60.6	115.3
LUT4C10	77.4	8.6	4.0	10.0	59.2	123.1
LUT4C14	73.8	8.2	4.0	14.0	59.1	128.1

Adapted with permission from [61] Copyright © 2013 Society of Plastics Engineers

Addition of layered silicates can potentially achieve enhanced barrier properties, high heat deflection temperatures, improved rate of biodegradation, good optical properties, and antimicrobial properties; therefore, numerous research studies have focused on the development of PLLA-based nanocomposite blends for food packaging and medical applications [96–102]. However, only limited studies deal with PLLA-based nanocomposites for automotive applications, for instance in the form of PLLA nanocomposite foams and injection-molded PLLA nanocomposites [61, 108–117]. Liu et al. [61] developed a nanocomposite of thermoplastic polyurethane (TPU)-toughened PLLA/talc/organic modified clay (OMC) and demonstrated that the annealing process is necessary for improving the heat resistance of PLLA. As shown in Table 5, the differences between compositions of injection-molded specimens were negligible before annealing, with HDT values of about 60°C. Annealing increased HDT values to more than 120°C, mostly due to the increase in crystallinity resulting from thermal treatment and, to a lesser extent, to some interactions between PLLA and TPU molecular chains.

Thermal stability, mechanical performance, and added-value properties such as flame retardancy are among the most targeted properties for PLLA materials intended for the automotive sector. Sinha Ray et al. [110] reported the flexural properties of neat PLLA and various PLLA nanocomposites prepared with organically modified layered silicate (OMLS) (injection-molded samples). The flexural modulus, flexural strength, and distortion at break of neat PLLA and various PLLA nanocomposites were measured at 25°C and the results showed a significant increase in flexural modulus for PLLA nanocomposites with 4 wt% of OMLS (5.5 GPa) compared with that of neat PLLA (4.8 GPa). This was followed by a much slower increase with OMLS content, and a maximum at 5.8 GPa (increase of 21%) for 7 wt% OMLS. In addition, the flexural strength and distortion at break remarkably increased for 4 wt% OMLS, then gradually decreased with increased

Table 6 Flame-retardant properties of PLLA nanocomposites compared with pristine PLLA, as determined by calorimeter testing at a heating flux of 35 kW/m²

Composition (% by weight)	TTI (s)	pHRR (kW/m ²)	Decrease in pHRR (%)
PLLA (reference)	75	374	Reference
PLLA-43% AII	98	319	[15]
PLLA-3% B104	75	285	[24]
PLLA-3% C30B	62	244	[35]
PLLA-40% AII-3% C30B	88	230	[39]
PLLA-40% II-3% B104	91	217	[42]

Reproduced with permission from [109] Copyright © 2009 Elsevier Ltd

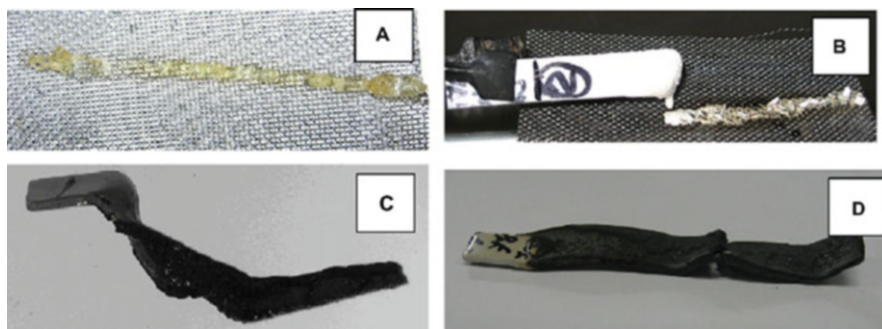


Fig. 11 Behavior of specimens during UL94 HB testing: (a) PLLA and (b) PLLA-43% AII burned with drips; (c) PLLA-40% AII-3% C30B and (d) PLLA-40% AII-3% B104 burned without drips. Reproduced with permission from [109] Copyright © 2009 Elsevier Ltd

OMLS loading. The study revealed that a high content of OMLS leads to brittleness in the material and that there is an optimal amount of OMLS in nanocomposites, which must be carefully adjusted to achieve the most significant improvement in mechanical properties. Murariu et al. [109] developed a calcium sulfate-containing PLLA-based nanocomposite with flame-retardant properties for technical applications requiring rigidity, heat resistance, and dimensional stability. Accordingly, composites of PLLA and β -anhydrite II (AII) characterized by specific end-use flame-retardant properties were added together with selected OMLS. Co-addition of AII and OMLS led to PLLA nanocomposites characterized by good nanofiller dispersion, thermal stability, and adequate mechanical resistance. The flame-retardant properties, as measured by cone calorimetry (Table 6), displayed a significant increase in ignition time (TTI) compared with neat PLLA and a substantial decrease (about 40%) in the maximum (peak) rate of heat release (pHRR). The composite successfully passed the UL94 HB standard flammability test in terms of nondripping effect and extensive char formation (Fig. 11).

In summary, PLLA-based nanocomposites show very interesting properties that should enable their more widespread use in automotive applications in the near future, in particular for reduced energy consumption resulting from weight reduction. The high strength and rigidity of these materials are also undeniable assets.

Table 7 Heat deflection temperatures of PLLA/PC blends and/or chain extender (CE) blends (HDT normalized measurement test) [124]

Compound	HDT (°C)
PLLA	55
PLLA + 30% PC	57
PLLA + 50% PC	62
PLLA + 50% PC + 1.1%CE	106
PC	136

However, nanofilled PLLA blends still have low heat resistance in the absence of additional heat processes such as annealing.

3.2.2 PLLA/Petroleum-Sourced Polymer Blends of High Thermal Stability

The comparatively high thermal stability of commonly used petroleum-based thermoplastics, as indicated by their HDT values (Table 1), has encouraged interest in compounding PLLA with petroleum- or biosourced polymers to improve the HDT [118, 119]. In some cases, compounding in association with toughening modifiers also achieved high impact properties, leading to a competitive partially biobased material with enhanced thermal stability and mechanical performance that is suitable for use in vehicle parts. PLLA/PC blends have been widely reported [120–125] as a simple binary blends or with addition of some additives such as chain extenders and compatibilizers to significantly enhance toughness and heat resistance, while minimizing the reduction in stiffness. Recently, Srihep et al. [124] developed a PLLA/PC blend with the addition of epoxy-based chain extender (CE) to improve compatibility of the blend by reaction between the epoxide groups in the CE and the hydroxyl/carboxylic end groups of PLLA and PC. The HDT value of PLLA/PC blends without and with addition of CE was improved from 62°C for PLLA + 50%PC to 106°C after mixing with CE (Table 7).

PMMA is often viewed as an excellent polymer partner for PLLA, resulting in blends exhibiting high miscibility, excellent thermal stability, increased HDT, high sustainability, and good ageing behavior [126–129]. Recently, Samuel et al. [128] prepared miscible PLLA/PMMA blends of enhanced thermomechanical properties and confirmed that the addition of even a moderate amount of PMMA can deeply modify the thermal properties of PLLA (in terms of T_g and HDT values), which were easily adjusted between those of neat PLLA and neat PMMA. More particularly, the HDT progressively increased from 51.5 to 54.8°C with 20 wt% PMMA and up to 61.9°C with 50 wt% PMMA. Similarly, Bouzouita et al. [64] reported the design of PLLA/PMMA blends with incorporation of impact modifier. The authors confirmed that the addition of impact modifier led to a supertough ternary blend (33 kJ/m² with 50 wt% PMMA) but also noticed that the impact modifier had a slight influence on HDT, which reached 63°C for ternary PLLA/PMMA/BS blends with 50 wt% PMMA.

Table 8 Thermal properties and heat deflection temperatures of sc-PLA blends with or without impact modifiers [137]

Compounds	$\Delta H_m, H^a$ (J/g)	$\Delta H_m, SC^b$ (J/g)	HDT (°C)
PLLA	37	–	56
PLLA/PDLA (92/8)	30	8	110
PLLA/PDLA (85/15)	28	17	110
PLLA/PDLA (75/25)	17	30	110
PDLA	54	–	53
PLLA/PDLA (92/8) + 10 wt% Strong 120	31	5	70
PLLA/PDLA (92/8) + 20 wt% Strong 120	29	6	65
PLLA/PDLA (85/15) + 10 wt% Strong 120	27	15	87
PLLA/PDLA (85/15) + 20 wt% Strong 120	31	10	79
PLLA/PDLA (92/8) + 10 wt% Elvaloy	30	8	90
PLLA/PDLA (92/8) + 20 wt% Elvaloy	26	7	81
PLLA/PDLA (85/15) + 10 wt% Elvaloy	24	13	101
PLLA/PDLA (85/15) + 20 wt% Elvaloy	23	12	97

^aMelting Enthalpy of homopolymer

^bMelting Enthalpy of stereocomplex

3.2.3 Heat-Resistant PLLA-Based Stereocomplexes

Together with the development of PLLA/petroleum-sourced polymer associations, other studies have focused on making PLA stereocomplexes (sc-PLA) [130], as stereocomplexing is generally judged to be an effective method for increasing material crystallinity. Poly(L-lactic acid) (PLLA) and poly(D-lactic acid) (PDLA) readily form stereocomplexed crystallites with a distinct crystal structure that leads to a high melting point in the range of 220–230°C, that is, values that are significantly higher than those of PLLA homocrystallites (approximately 170°C) [131, 132]. Stereocomplexing can therefore enhance PLLA properties in terms of resistance to heat and hydrolysis, in particular. A drawback of stereocomplexing is that it can lead to brittle PLLA-based materials, which could dramatically reduce their industrial implementation, as shown by Torres et al. [133]. Other research has aimed at simultaneously improving the HDT and toughness of PLLA using stereocomplexing [134–136]. Similarly, Nam et al. [137] prepared sc-PLA by extruding PLLA with various amounts of PDLA and 10–20 wt% of two types of commercial impact modifiers (BioStrong 120, Elvaloy) to enhance both thermal (Table 8) and mechanical properties.

As shown in Table 8, HDT dramatically increased to over 100°C as a result of incorporation of different amounts of PDLA. Nevertheless, impact strength decreased with addition of PDLA (18 J/m for neat PLLA to 11 J/m with 15 wt% of PDLA). Once impact modifiers were added, HDT decreased with the increase in impact modifier content (Table 8). Taking all results into account, a well-balanced composition of toughened sc-PLA with 10 wt% of impact modifier could compete with petroleum-based polymers. In this context, Corbion Purac [138] created a developmental grade of highly heat-resistant PLLA (not commercialized yet) that

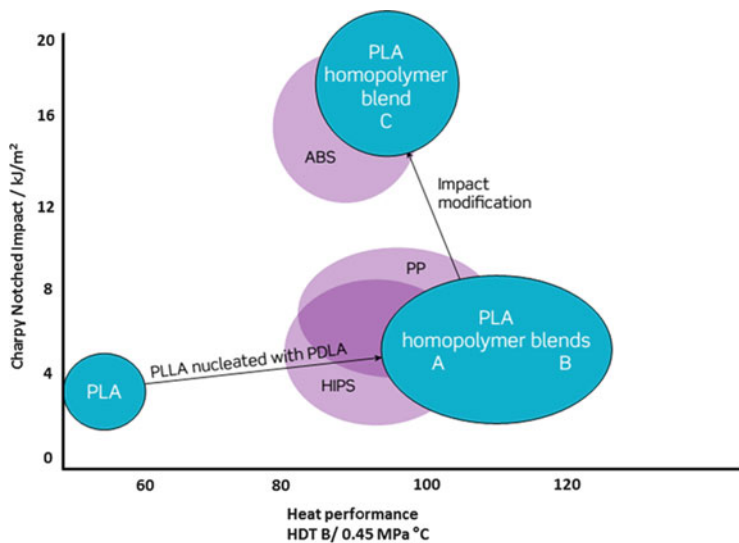


Fig. 12 Typical results of using PLLA homopolymer blends, showing heat performances similar to those of PS, PP, and ABS. Reproduced with permission from [139]© Copyright 2015 Corbion

in a given stereocomplex form could replace polystyrene (PS), PP, and ABS-type materials in applications where heat performance is compulsory.

As shown in Fig. 12, the key driver behind the improvement of HDT in blend A is the presence of PLLA homopolymers that are nucleated with a small amount of PDLA homopolymers and a traditional nucleating agent. The improved heat performance of blend A was obtained without adding a significant amount of filler. To achieve a higher modulus, and an even higher temperature resistance, talc was added to blend A to form blend B (4 GPa and 120°C for blend B instead of 3 GPa and 105°C for blend A), leading to better performance than those of PP and PS blends. To achieve an impact resistance comparable to that of ABS, blend A was impact-modified and, to minimize the drop in modulus, talc was added to obtain blend C, which was characterized by a good balance of properties (33 kJ/m² for impact resistance, 3.5 GPa for tensile modulus, and 95°C for HDT).

Sections 3.1 and 3.2 presented the most efficient way to improve PLLA impact strength, ductility, and thermal stability in order to obtain PLLA-based materials with properties compatible with their implementation as automotive components. Another key point when developing materials for use in the automotive industry is to ensure their good processability through mass production methods, typically by injection molding. This subject is discussed in the next section.

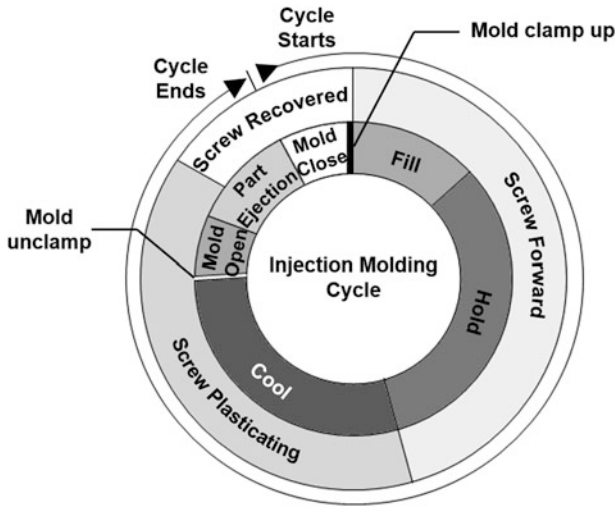


Fig. 13 Typical cycle for an injection molding process. Reproduced with permission from [141] Copyright ©2008 Elsevier Ltd

3.3 *Mold-Injected PLLA Materials for Automotive Applications*

In the automotive industry, PLLA components are generally produced by injection molding, similarly to other thermoplastics. The advantage of injection molding is continuous production capability with minimal maintenance and labor, allowing significant economies for large-scale production. Several factors are involved in the injection molding process and have a great influence on the injected part; these include material formability, characteristics of the molding machine, mold design, and process conditions [139, 140].

The typical cycle for an injection molding process has been detailed by Lim et al. [141] (Fig. 13). The authors described the different steps of the cycle and gave some advice on how to avoid defects in injection-molded products. Although the cooling time must be sufficient to ensure a dimensionally stable injected part, cycle time should be minimized to maximize production throughput.

The slow crystallization rate of PLLA compared with that of commonly used injection-molded thermoplastics is a major obstacle to its use in the automotive industry (i.e., at high production rate). Indeed, the injection molding cycle time in the automotive industry is typically within the range of 20–60 s [142], which implies a high cooling rate. However, the crystallization half-time, $t_{1/2}$, of a pure sample of PLLA was reported in the literature as being in the range of 17–45 min, depending on crystallization temperature, stereochemistry, and molecular weight [143]. Therefore, injection molding of PLLA for automotive parts is limited to the manufacture of parts for which a high degree of crystallinity is not required. Indeed, using a post-annealing step or longer cycle time to obtain sufficient crystallinity for PLLA components would be impractical for high volume automotive use. In

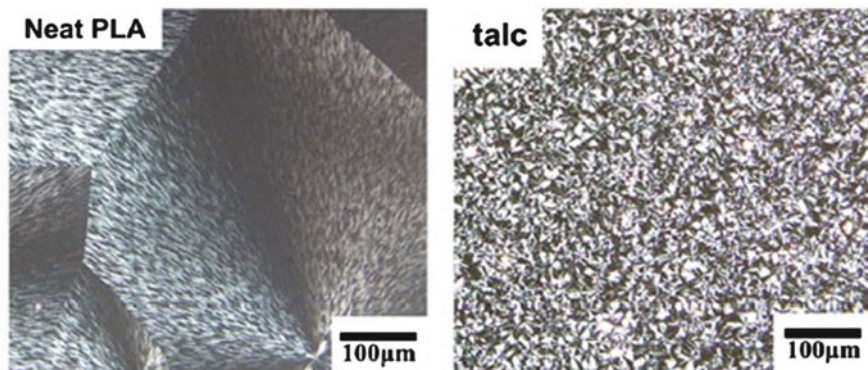


Fig. 14 Polarized optical micrographs of neat PLLA (*left*) and PLLA containing 5 wt% talc (*right*) at 122°C after quenching from 180°C. Adapted with permission from [147] Copyright ©The Royal Society of Chemistry 2013

addition, the slow crystallization rate of PLLA also causes difficulties during part ejection, again increasing molding cycle duration.

An efficient way to accelerate crystallization of PLLA is by incorporation of nucleating agents. In polymers, nucleating agents provide additional sites for initiation of crystallization and influence crystalline morphology and crystallization kinetics [144–146]. For example, blending PLLA with 5 wt% talc can fundamentally change the crystalline morphology of the blend (Fig. 14). Judging from polarized optical micrographs of PLLA formulations, spherulite concentration increases after nonisothermal crystallization from the melt, whereas spherulite size decreases in PLLA/talc compared with neat PLLA. Therefore, talc addition can lead to much more heterogeneous nuclei and can reduce the size of spherulites [147]. Nucleating agents have a remarkable effect on the kinetics of crystallization by reducing $t_{1/2}$, leading to better processability of PLLA. In some cases, they may also lead to enhanced mechanical properties [116].

Shi et al. [148] demonstrated that the addition of 1 wt% aromatic sulfonate derivative LAK-301 (Takemoto Oil & Fat Co) to PLLA as an effective nucleating agent led to a dramatic reduction in $t_{1/2}$ of up to 2 min, with a crystallinity content reaching 27%. Kolstad [149] showed that talc can be added to PLLA to effectively modify the crystallization rate of the polymer. The $t_{1/2}$ of the polymer reduced from 3 min at 110°C to approximately 25 s with the addition of 6% talc to PLLA. At the same content of talc, for 3% mesolactide copolymerized with L-lactide, the $t_{1/2}$ value reduced from 7 to 1 min. The stereocomplexation of PLLA and PDLA was previously mentioned as an effective way to increase PLLA HDT (see Sect. 3.2.3). It can also be regarded as a potential tool for self-nucleation of PLLA. Schmidt and Hillmyer [150] investigated self-nucleation of PLLA, in which small crystallites of the stereocomplex were formed by blending up to 15% PDLA into PLLA. They compared the effectiveness of self-nucleation with the heterogeneous nucleation obtained after addition of talc, finding self-nucleation to be more

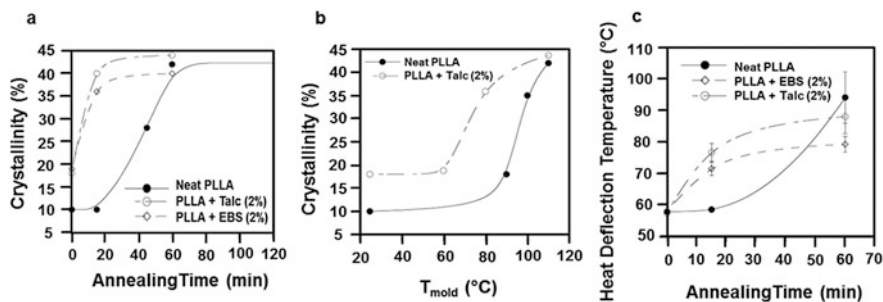


Fig. 15 (a) Crystallinity versus annealing time at 80°C for neat PLLA, PLLA + talc, and PLLA + EBS samples. (b) Crystallinity as a function of injection molding mold temperature for neat PLLA and PLLA + talc samples. (c) Dependence of HDT on annealing time at 80°C for neat PLLA, PLLA + talc, and PLLA + EBS samples. Adapted with permission from [143] Copyright © 2007 Wiley Periodicals, Inc

efficient. Self-nucleation reduced $t_{1/2}$ by nearly 40-fold, in the best case, whereas a similar loading of talc only decreased $t_{1/2}$ by twofold under the same conditions. The majority of works dealing with nucleation of PLLA are focused on the study of crystallization kinetics, morphology, and some mechanical properties, but Harris and Lee [143] pushed forward the study of nucleated PLLA using talc and ethylene bis-stearamide (EBS) by optimizing the parameters for injection molding and post-processing in order to increase crystallinity within the finished injected part. Furthermore, HDT and flexural strength were both analyzed. The authors showed that the addition of 2% of nucleating agent (talc or EBS) improved the crystallization rate by over 20 times and 65 times for EBS and talc, respectively, compared with neat PLLA. The authors then worked on the optimization of processing conditions, especially for nucleated samples, aiming to increase PLLA crystallinity and mechanical performance.

Post-annealing processing of both nucleated and neat PLLA materials was found to increase the crystallinity of PLLA to a maximum level of 42% (Fig. 15a). Interestingly, annealing is significantly faster in the presence of nucleating agent. Injection molding the PLLA materials into a preheated mold (110°C) was found to significantly increase the crystalline content of the molded specimens to their maximum level (41–43%) in both neat and nucleated PLLA materials (Fig. 15b). Furthermore, the same crystallinity was reached at a lower temperature in the nucleated samples than for neat PLLA; for instance, a crystallinity ratio of 35% was reached at a mold temperature of about 80°C for nucleated samples, compared with about 100°C for neat PLLA. The combination of nucleating agents and process optimization therefore resulted in an increase in crystallinity level in the final injection-molded part, together with a decrease in processing time. Moreover, an increase of 30°C in the HDT (Fig. 15c) and an improvement in flexural modulus by over 25% were achieved thanks to material nucleation and process optimization.

Previous research has demonstrate that PLLA crystallization kinetics can be improved to make PLLA-based materials suitable for high-rate production

processes by injection molding, which is a typical process in the automotive industry. Furthermore, the increase in crystallization rates achieved in these works and discussed in this section can result in reductions in both cycle time and energy consumption during injection molding. Moreover, materials with higher crystallinity degree show increased mechanical properties, especially in terms of rigidity and strength (and sometimes thermal resistance) and are thought to have better durability. The issue of the durability of PLLA blends is the subject of the next section.

3.4 Durable PLLA/Polymer Blends

The plastics and polymer composites developed recently can provide mechanical performances that can withstand the stresses related to many applications, including those applied to loaded parts. However, some operating conditions, such as high temperature, corrosive chemicals in fluids and lubricants, electric currents, weather variations, or minerals from roadways, can be too harsh to be sustained by some plastics and polymer composites over a vehicle's lifetime. Both interior and exterior parts can be exposed to a large range of temperatures (-40 to 125°C), together with high humidity levels, throughout the vehicle's lifetime (possibly more than 10 years). Obviously, these conditions can have long-term detrimental effects on the durability, performance, and aesthetics of the materials in automotive components. The suitability of a material for automotive application must therefore be evaluated regarding long-term performance.

Under specific conditions, PLLA presents a fast degradation rate, which makes it appealing for disposable applications but inadequate for applications requiring long-term durability. This explains why the majority of current commercial applications for PLLA blends are oriented toward clothing and linens and disposable packaging and objects (e.g., water cups). Unfortunately, very few research studies or applications concern the use of PLLA in durable goods [151, 152], and even less in cases of the severe environmental conditions that can be encountered in automotive applications. Among the few available works, Harris and Lee [153] investigated the durability of a commercial injection molding grade of PLLA through its crystallization behavior. Commercially available injection molding grade PLLA and annealed PLLA were conditioned at a temperature of 50°C and 90% relative humidity for 12 weeks, which corresponds to a simulated environment for automotive interiors. Moisture absorption, molecular weight, and mechanical performances were investigated. Both amorphous and crystalline PLLA showed significant moisture absorption, allowing hydrolysis to occur. The linear regression of average molecular weight was more accentuated for amorphous PLLA than for crystalline PLLA (Fig. 16a, b). The effects of moisture and heat-conditioning on mechanical performance were examined through the evolution of flexural strength (Fig. 16c). This decreased significantly for both amorphous and annealed PLLA. In conclusion, the properties of the conditioned samples were not maintained, even for

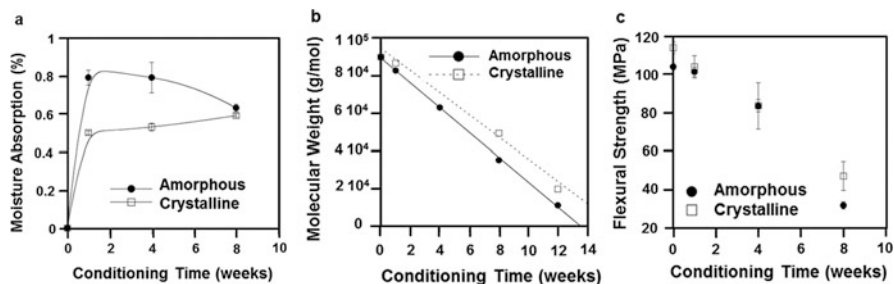


Fig. 16 (a) Moisture absorption as a function of conditioning time for amorphous and crystalline PLLA. (b) Dependence of molecular weight on conditioning time for amorphous and crystalline PLLA. (c) Dependence of flexural strength on conditioning time for amorphous and crystalline PLLA. Adapted with permission from [153] Copyright © 2009 Wiley Periodicals, Inc

crystallized PLLA, and commercial PLLA grades remain inadequate for durable use in automotive parts.

However, different approaches have proved to improve the durability of PLLA-based materials. A possible approach is to blend PLLA with resins that are not susceptible to hydrolysis and could therefore prevent contact between PLLA and water by acting as moisture barrier [154, 155]. In this regard, Harris and Lee [155] studied the durability of PLLA/PC blends (100, 45, 30, and 25 wt% PLLA) for use in injection-molded automotive interior parts. Harsh conditions were set up to study the durability of the blends, namely 70°C and 90% relative humidity for 62 days, corresponding to 10 years of in-field exposure for an automotive interior component in the climate of southern Florida. The durability of ABS/PC was used as a basis for comparison. Results demonstrated that the presence of PC can improve the long-term performance of blends compared with neat PLLA (durability increase for one in-field exposure year). Nevertheless, all samples containing PLLA exhibited extreme degradation after 14 conditioning days, resulting in a drop in mechanical performance (in terms of flexural strength; see Fig. 17a) together with the formation of a large amount of brown liquid residue at the sample surface as a result of hydrolysis of the PC phase (accompanied by the appearance of potentially health-harmful bisphenol-A (BPA); see Fig. 17b, c). Although PC was initially blended to stabilize PLLA and improve overall durability, the final durability of the blend was only marginally improved because of the hydrolytic degradation of PC. It should be noted that PC suffered more from hydrolysis when blended with PLLA than with ABS.

In conclusion, the formation of PC/PLLA blends has not yet achieved a durability level high enough for automotive applications, regardless of PC content. However, blending PLLA with more durable polymer resins in order to enhance the durability of blends constitutes a promising research field.

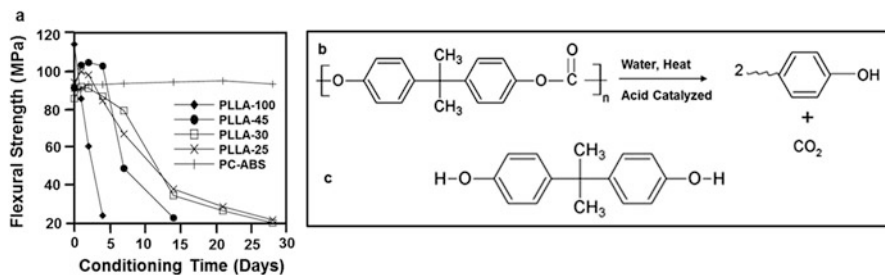


Fig. 17 (a) Flexural strength as a function of conditioning time of PLLA/PC blends. (b) Hydrolysis of PC. (c) Chemical structure of bisphenol-A (BPA). Adapted with permission from [155] Copyright© 2012 Wiley Periodicals, Inc

4 PLLA in the Automotive Industry: Current Applications



Corporate environmental responsibility has to become reconciled with business economics. Therefore, original equipment manufacturers (OEMs) must adopt the use of biobased materials. However, before biobased materials can replace conventional nonrenewable materials in the automotive industry, different criteria must be fulfilled, in addition to environmental benefits, namely cost, suitable physical and mechanical properties, processability, and continuous supply. The willingness for a more widespread use of biobased materials by the automotive OEMs is heavily influenced by those criteria, as is already the case for currently used conventional materials.


The previous sections showed PLLA to be an environmentally friendly polymer that can respond to the requirements of car manufacturers for some applications. In particular, PLLA-based materials can be tailor-made for different manufacturing processes, including injection molding, sheet extrusion, blow molding, thermoforming, film forming, and fiber-spinning. This is an undeniable asset for the use of PLLA in products of different forms and applications [141, 156].

4.1 PLLA-Based Plastics and Reinforced Plastics for Automotive Interior Parts

Thanks to technological breakthroughs in recent years, significant progress has been made in the development of PLLA-based blends, not only at the laboratory scale but also at industrial scale, which makes PLLA biopolymers suitable for a growing number of automotive components, in particular vehicle interior parts. Indeed, biobased PLLA blends are used today by many automobile manufacturers, including Mazda, Toyota, Ford, and Hyundai Motors for the manufacture of various components (see Table 9). Some car manufacturers (or their suppliers) have developed their own blends based on PLLA or some other biobased or

Table 9 Current application of PLLA-based blends (plastics, fabrics, and nonwovens) in interior parts of vehicles

PLLA compound	Company	Properties	Vehicle part	Reference
PLLA/kenaf	Toyota Boshoku Corporation	High heat resistance Shock resistance	 Door trim ornamentation	[157]
PLLA/PP	Toyota Motor Corporation	–	 Spare tire cover (up to 2009) (Reproduced with permission from [157] Copyright © Toyota Boshoku Corporation)	[158]
PLLA/PP	Hyundai Motor Company	–	Interior part for Hyundai Blue Will concept car	[159]
Biofront TM Bioplastic: Stereocomplex PLA	Tejin and Mazda	High heat resistance equal to PBT Superior transparency equal to PET	Electric/electronic parts and chassis requiring heat resistance, molding, dashboard, door trim	[160]
PLLA/Nylon fiber	Mitsubishi Motors, in cooperation with Toray Industries	High durability	Car floor mat	[161]

<p>Plantura™ biobased PLA Plantura™_30% wood fiber</p>	<p>Röchling Automotive</p>	<p>Excellent hydrolysis resistance at 70°C and 100% relative humidity Scratch and UV resistant Good colorability</p>	 <p>Air filter part, interior trim parts (Reproduced with permission from [162] Copyright © Corbion)</p>	<p>[162]</p>
<p>Biofront™ fiber: stereocomplex PLA</p>	<p>Teijin and Mazda</p>	<p>High heat resistance Possibility to iron Dye-affinity and anti-bacterial properties Resistant to abrasion and damage from sunlight</p>	<p>Seat fabric in Premacy Hydrogen RE Hybrid vehicle</p>	<p>[163]</p>
<p>Flax-PLLA biocomposites PLLA/PET (nonwovens)</p>	<p>Project Nature Wins (Centexbel, SLC-Lab, ITA) Toyota Motor Corporation</p>	<p>Anti-odor Fire retardance –</p>	<p>Race car seat demonstrator</p>	<p>[164, 165]</p>
<p>PLLA fibers (Ingeo, NatureWorks)</p>	<p>Ford Company</p>	<p>–</p>	<p>Trunk liner, luggage side trims in Toyota's Sai vehicle Canvas roof and carpet mats for Ford model U</p>	<p>[158] [166]</p>
<p>PLLA-based fibers (melt spinning technique)</p>	<p>BIOFIBROCAR project: Aitex/Aimplas/Addcomp/Avanzere</p>	<p>Thermal resistance Antimicrobial resistance</p>	<p>Composite: two nonwoven layers + woven fabric for automotive interior application: molded door panel (fabrics and nonwovens)</p>	<p>[167]</p>

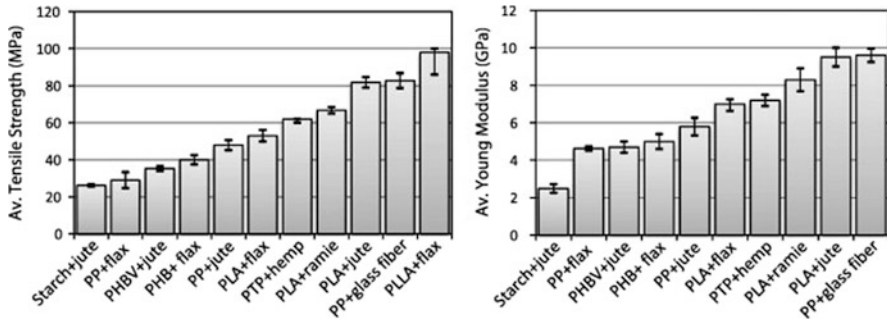


Fig. 18 Mechanical performance of several fiber-based composites. Reproduced with permission from [169] Copyright © 2012 Elsevier Ltd

petroleum-based thermoplastics or fibers for use in interior automotive parts. For instance, Teijin has developed in cooperation with Mazda a new brand of high-performance stereocomplexed PLA, called BIOFRONT, by utilizing superior polymerization techniques and molecular structure control techniques (stereocomplexation). Major quality improvements were achieved compared with conventional PLLA, and BIOFRONT can be found in car dashboards and door tread plates [160].

Another major revolution in biobased materials for automotive application was the introduction by Toyota of a PLLA/kenaf fiber biocomposite in the Raum mini-MPV [157]. Specifically, Toyota substituted the PP matrix used within its kenaf fiber-based composite with a PLLA resin, thanks to a unique technology that optimizes the raw material mixture and molding conditions to achieve a high level of heat and shock resistance. This 100% plant-derived composite is particularly used in door trims. It is worth noting that increasing use of composites made of natural fibers coincides with attempts to reduce the use of expensive glass [168], aramid, and carbon fibers and also lighten the car body considerably by taking advantage of the low density of most natural fibers. Renewable fibers as reinforcements are increasingly used in composites for the interior parts of many passenger and commercial vehicles. When regrouping different studies, it is noticeable that in most cases “green composites” made of PLA, semicrystalline PLLA, and natural fibers such as flax, ramie, or jute have mechanical properties that can compete with those of the traditional PP/glass fiber composites (Fig. 18 shows performance in terms of tensile strength and Young’s modulus) [169].

Following the pioneering work by Toyota, many automotive OEMs and suppliers have launched research aimed at introducing biocomposites into their vehicles. For instance, Röchling Automotive produces a wide range of automotive plastic parts such as air filter box and interior trim parts using a PLLA-based biopolymer called Planutra™ [162]. This biopolymer, developed by Corbion Purac, is an ecological and economic alternative to traditional thermoplastics and could replace PP, ABS, and polyamide. Composites made of modified PLA Planutra™ and wood fiber reinforcement are already undergoing tests and are

being exposed to temperatures well above 100°C. These materials are claimed to show improved hydrolysis and thermal resistance up to 140°C, as well as a good scratch and UV resistance.

4.2 PLLA-Based Fabrics and Nonwovens Products

The use of fabrics in cars is increasing as a promising strategy for production of lighter vehicles that consume less fuel. In that context, more and more applications using tissues and nonwoven composites are being developed in the automotive industry. Depending on the formulation, such materials can offer flexibility, low weight, sound absorption, improved aesthetics, cost-efficiency, and ecofriendliness. From nonwoven interior and trunk carpets to knitted or woven upholstery, package trays, and dash panels, textile producers are finding innovative ways to keep the momentum going. There are now more than 40 applications for inner automobile seat upholstery, belts, airbags, cladding, filters, and insulating materials. More than 35 m² of flat textile surfaces can be found inside one of today's cars [170]. Recently, there has been a gradual switch in many automotive applications toward the use of recycled materials or materials made of natural fibers, instead of conventional fabrics. Many current applications are described in Table 9. Mazda Motor Corporation, with the cooperation of Teijin Fibers Limited, has developed a heat-resistant PLA-based fabric (commercialized under the name BIOFRONT, see Sect. 4.1), which was initially used for the manufacture of a high-quality and highly durable car-seat fabric for the new Premacy Hydrogen RE Hybrid vehicle [163]. During manufacture of BIOFRONT, the molecular architecture of the polymer is controlled to improve fiber strength until the fabric attains sufficient resistance to abrasion and light damage. Recently, the project "Nature Wins" succeeded in producing a 100% biobased composite with biopolymer PLLA as matrix and mix of hemp and flax fibers as reinforcement [164]. The fibers were assembled into various structures such as yarn and woven and nonwoven fabrics and the flax/PLLA nonwoven composite used to make a molded demonstration model of a race car seat. Recently, the BIOFIBROCAR project has focused on the development of PLLA-based fibers to be used as an alternative to PET and PP fibers in car interiors [167]. The developed PLLA compound was shown to fulfill the requirements of automotive interior applications in terms of thermal resistance, antimicrobial resistance, and odor emission. Its conversion into fabric and nonwoven samples allowed fabrication of a prototype of a 100% biobased molded door panel, with the association of two nonwoven layers and a woven fabric.

5 Conclusions and Perspectives

The automotive industry is one of the mainsprings for the development of bioplastics and biocomposites in durable applications, due to its well-structured network of car manufacturers, OEMs, and raw material suppliers. All have shown significant need for bioplastics and biocomposites to meet joint objectives in terms of reduction of vehicle weight combined with increasing demands for environmentally friendly materials.

In this review, the technical requirements for plastics used in automotive applications are presented, with a special emphasis on renewable PLLA-based materials. Attention is paid to the development of PLLA-based blends and the different modifications that make PLLA suitable for automotive applications in terms of mechanical properties (ductility combined with high rigidity and strength), high heat resistance, durability, and good processability, even under high-rate production. Some of these modifications can provide relevant PLLA-based materials for intensive use in the automotive sector, allowing car makers to invest in ecofriendly vehicles using developed PLLA-based bioplastics and biocomposites. For instance, Koronis et al. [169] judiciously mentioned that “the application of green composites in automobile body panels seems to be feasible as far as green composites have comparable mechanical performances with the synthetic ones.” However, up to now, automotive application of tailored PLLA compounds has been limited to interior parts, particularly because of long-term durability issues under the severe environmental conditions that exterior parts have to withstand. However, in near future, research efforts can offer PLLA-based blends suitable for the exterior parts of vehicles. One issue to be investigated now concerns the recyclability and to some extent biodegradability of these novel parts in the end-life scenario. A final question here is, why not using 3D printing processes to print full size cars? PLLA is proven to be a good candidate for use in 3D printing, and it would improve the need for storage facilities in the case of spare parts.

Acknowledgements LAMIH authors are grateful to CISIT, the Nord-Pas-de-Calais Region, the European Community, the Regional Delegation for Research and Technology, the Ministry of Higher Education and Research, and the National Center for Scientific Research for their financial support. UMONS and Materia Nova authors are grateful to the “Region Wallonne” and the European Community (FEDER, FSE) in the frame of “Pole d’Excellence Materia Nova” INTERREG IV—NANOLAC project and in the excellence program OPTI²MAT for their financial support. CIRMAP thanks the “Belgian Federal Government Office Policy of Science (SSTC)” for general support in the frame of the PAI-7/05. J.O. thanks F.R.I.A. for its financial support thesis grant. J.-M. Raquez is a “Chercheur Qualifié” by the F.R.S.-FNRS (Belgium).

References

1. Brostow W, Datashvili T (2016) Environmental impact of natural polymers. In: Natural polymers. Springer, Berlin, pp 315–338

2. Akampumuza O et al (2016) Review of the applications of biocomposites in the automotive industry. *Polym Compos.* doi:[10.1002/pc.23847](https://doi.org/10.1002/pc.23847)
3. Niaounakis M (2015) Automotive applications. In: *Biopolymers: applications and trends.* William Andrew, Oxford, pp. 257–289
4. Garlotta DA (2001) Literature review of poly(lactic acid). *J Polym Environ* 9(2):63–84
5. Avérous L (2008) Polylactic acid: synthesis, properties and applications. In: Gandini MNB (ed) *Monomers, polymers and composites from renewable resources.* Elsevier, Amsterdam, pp. 433–450
6. Maxwell J (1994) *Plastics in the automotive industry.* Elsevier, Amsterdam
7. Auras RA et al (2011) *Poly(lactic acid): synthesis, structures, properties, processing, and applications,* vol 10. Wiley, Hoboken
8. Reynolds N, Ramamohan AB (2013) High-volume thermoplastic composite technology for automotive structures. In: *Advanced composite materials for automotive applications.* Wiley, Hoboken, pp 29–50
9. Rowe J (2012) *Advanced materials in automotive engineering.* Elsevier, Amsterdam
10. Götz Klink GR, Znojek B, Wadivkar O (2012) *Plastics. The future for automakers and chemical companies.* A.T. Kearney, Korea
11. Swift TK, Moore M, Sanchez E (2015) *Plastics and polymer composites in light vehicles.* Economics and Statistics Department/American Chemistry Council
12. Philp JC et al (2013) Biobased plastics in a bioeconomy. *Trends Biotechnol* 31(2):65–67
13. Thielen M (2012) *Bioplastics: basics, applications, markets.* Polymedia, Mönchengladbach
14. Pilla S (2011) *Handbook of bioplastics and biocomposites engineering applications,* vol 81. Wiley, Hoboken
15. Siracusa V et al (2008) Biodegradable polymers for food packaging: a review. *Trends Food Sci Technol* 19(12):634–643
16. *European Bioplastics* (2013) *Applications for bioplastics.* European Bioplastics, Berlin. <http://www.european-bioplastics.org/market/applications-sectors/>
17. Lee E, Flanigan C (2012) *Automotive plastics and composites.* In: *Encyclopedia of polymer science and technology.* Wiley, Hoboken
18. Szteiová K (2010) *Automotive materials: plastics in automotive markets today.* Institute of Production Technologies, Slovak University of Technology, Bratislava
19. Andrea DJ, Brown WR (1993) *Material selection processes in the automotive industry.* OSAT, Michigan
20. Ghassemieh E (2011). *Materials in automotive application, state of the art and prospects.* In: Chiaberge M (ed) *New trends and developments in automotive industry.* Intech, Rijeka, pp 366–394. doi:[10.5772/13286](https://doi.org/10.5772/13286)
21. Weber M, Weisbrod J (2003) Requirements engineering in automotive development-experiences and challenges. In: *IEEE joint international conference on requirements engineering, 2002.* IEEE, pp 331–340. doi:[10.1109/MS.2003.1159025](https://doi.org/10.1109/MS.2003.1159025)
22. Biron M (2012) *Thermoplastics and thermoplastic composites.* William Andrew, Oxford
23. Babu RP et al (2013) Current progress on bio-based polymers and their future trends. *Prog Biomater* 2(1):1–16
24. Fiori S (2014) Industrial uses of PLA. In: Jiménez A, Peltzer M, Ruseckaite R (eds) *Poly(lactic acid) science and technology: processing, properties, additives and applications.* Royal Society of Chemistry, London, pp 315–333. doi:[10.1039/9781782624806-00315](https://doi.org/10.1039/9781782624806-00315)
25. Lunt J (1998) Large-scale production, properties and commercial applications of polylactic acid polymers. *Polym Degrad Stab* 59(1–3):145–152
26. Signori F et al (2009) Thermal degradation of poly(lactic acid) (PLA) and poly(butylene adipate-co-terephthalate) (PBAT) and their blends upon melt processing. *Polym Degrad Stab* 94(1):74–82
27. Song J et al (2009) Biodegradable and compostable alternatives to conventional plastics. *Philos Trans R Soc Lond B Biol Sci* 364(1526):2127–2139

28. Vink ET et al (2007) Original research: the eco-profiles for current and near-future NatureWorks[®] polylactide (PLA) production. *Ind Biotechnol* 3(1):58–81
29. Jamshidian M et al (2010) Poly-lactic acid: production, applications, nanocomposites, and release studies. *Compr Rev Food Sci Food Saf* 9(5):552–571
30. Sin LT et al (2012) Polylactic acid: PLA biopolymer technology and applications. William Andrew, Oxford
31. Dusselier M et al (2015) Shape-selective zeolite catalysis for bioplastics production. *Science* 349(6243):78–80
32. Achmad F et al (2009) Synthesis of polylactic acid by direct polycondensation under vacuum without catalysts, solvents and initiators. *Chem Eng J* 151(1–3):342–350
33. Gerrard J, Kandlikar M (2007) Is European end-of-life vehicle legislation living up to expectations? Assessing the impact of the ELV directive on ‘green’ innovation and vehicle recovery. *J Clean Prod* 15(1):17–27
34. Madhavan Nampoothiri K et al (2010) An overview of the recent developments in polylactide (PLA) research. *Bioresour Technol* 101(22):8493–8501
35. Nova Institute (2012) Growth in PLA bioplastics: a production capacity of over 800,000 tonnes expected by 2020. *Bio-based News*, 7 Aug 2012
36. Nair LS, Laurencin CT (2007) Biodegradable polymers as biomaterials. *Prog Polym Sci* 32(8–9):762–798
37. Bhardwaj R, Mohanty AK (2007) Advances in the properties of polylactides based materials: a review. *J Biobased Mater Bioenergy* 1(2):191–209
38. Canessa E et al (2013) Low-cost 3D printing for science, education and sustainable development. ICPT, Trieste. <http://sdu.ictp.it/3D/book.html>
39. Campbell T et al (2011) Could 3D printing change the world. Technologies, potential, and implications of additive manufacturing. Atlantic Council, Washington
40. Reeves P, Mendis D (2015) The current status and impact of 3D printing within the industrial sector: an analysis of six case studies. Intellectual Property Office, Newport
41. Staff S (2014) Revolutionary new electric car built and tested in one year with Objet1000 multi-material 3D production system. *Stratasys*. <http://blog.stratasys.com/2014/11/18/streetscooter-3d-printing/>. Accessed 14 Jan 2016
42. Bunkley N (2014) “World’s first” 3D printed car created and driven by Local Motors. *Automotive News*. <http://www.autonews.com/article/20141027/OEM06/310279987/auto-industry-uses-3-d-printing-heavily-in-product-development>. Accessed 14 Jan 2016
43. Wypych G (2012) *Handbook of plasticizers*, 2nd edn. William Andrew, Boston
44. Ljungberg N, Wesslén B (2005) Preparation and properties of plasticized poly(lactic acid) films. *Biomacromolecules* 6(3):1789–1796
45. Liu H, Zhang J (2011) Research progress in toughening modification of poly(lactic acid). *J Polym Sci B Polym Phys* 49(15):1051–1083
46. Ruellan A et al (2015) Plasticization of poly(lactide). In: Jiménez A, Peltzer M, Ruseckaite R (eds) *Poly(lactic acid) science and technology: processing, properties, additives and applications*. The Royal Society of Chemistry, London, pp. 124–170
47. Jacobsen S, Fritz HG (1999) Plasticizing polylactide—the effect of different plasticizers on the mechanical properties. *Polym Eng Sci* 39(7):1303–1310
48. Murariu M et al (2008) Polylactide (PLA) designed with desired end-use properties: 1. PLA compositions with low molecular weight ester-like plasticizers and related performances. *Polym Adv Technol* 19(6):636–646
49. Zhang H et al (2013) Thermal, mechanical, and rheological properties of polylactide/poly(1,2-propylene glycol adipate). *Polym Eng Sci* 53(1):112–118
50. Ren Z et al (2006) Dynamic mechanical and thermal properties of plasticized poly(lactic acid). *J Appl Polym Sci* 101(3):1583–1590
51. Wojciechowska P (2012) The effect of concentration and type of plasticizer on the mechanical properties of cellulose acetate butyrate organic-inorganic hybrids. In: Luqman M (ed) *Recent advances in plasticizers*. Intech, Rijeka, pp. 141–164

52. Suvorova AI et al (1993) Chemical structure of plasticizers, compatibility of components and phase equilibrium in plasticized cellulose diacetate. *Makromol Chem Rapid* 194 (5):1315–1321
53. Notta-Cuvier D et al (2015) Tailoring polylactide properties for automotive applications: effects of co-addition of halloysite nanotubes and selected plasticizer. *Macromol Mater Eng*. doi:[10.1002/mame.201500032](https://doi.org/10.1002/mame.201500032)
54. Kfoury G et al (2013) Recent advances in high performance poly (lactide): from “green” plasticization to super-tough materials via (reactive) compounding. *Front Chem* 1:1
55. Sangeetha VH et al (2016) State of the art and future prospectives of poly(lactic acid) based blends and composites. *Polym Compos*. doi:[10.1002/pc.23906](https://doi.org/10.1002/pc.23906)
56. Odent J et al (2015) Highly toughened polylactide-based materials through melt-blending techniques. In: *Biodegradable polyesters*. Wiley-VCH, Weinheim, pp. 235–274
57. Anderson KS et al (2008) Toughening polylactide. *Polym Rev* 48(1):85–108
58. Hongzhi L, Jinwen Z (2012) Toughening Modification of Poly(lactic acid) via melt blending. In: *Biobased monomers, polymers, and material*. ACS Symposium Series, vol 1105, pp 27–46
59. Detyothin S et al (2010) Poly(lactic acid) blends. In: *Poly(lactic acid)*. Wiley, Hoboken, pp. 227–271
60. Perkins WG (1999) Polymer toughness and impact resistance. *Polym Eng Sci* 39 (12):2445–2460
61. Liu Z-W et al (2014) Mechanical and thermal properties of thermoplastic polyurethane-toughened polylactide-based nanocomposites. *Polym Compos* 35(9):1744–1757
62. NatureWorks (2007) Technology focus report: toughened PLA. NatureWorks, Minnetonka
63. Taib RM et al (2012) Thermal, mechanical, and morphological properties of polylactic acid toughened with an impact modifier. *J Appl Polym Sci* 123(5):2715–2725
64. Bouzouita A et al (2016) Design of highly tough poly(l-lactide)-based ternary blends for automotive applications. *J Appl Polym Sci*. doi:[10.1002/app.43402](https://doi.org/10.1002/app.43402)
65. Notta-Cuvier D et al (2014) Tailoring polylactide (PLA) properties for automotive applications: effect of addition of designed additives on main mechanical properties. *Polym Test* 36 (0):1–9
66. Zhang K et al (2014) Supertoughened renewable PLA reactive multiphase blends system: phase morphology and performance. *ACS Appl Mater Interface* 6(15):12436–12448u
67. Zhang C et al (2013) Thermal, mechanical and rheological properties of polylactide toughened by epoxidized natural rubber. *Mater Des* 45:198–205
68. Pattamaprom C et al (2016) Improvement in impact resistance of polylactic acid by masticated and compatibilized natural rubber. *Iran Polym J* 25(2):169–178
69. Pongtanayut K et al (2013) The effect of rubber on morphology, thermal properties and mechanical properties of PLA/NR and PLA/ENR blends. *Energy Procedia* 34:888–897
70. Desa M et al (2015) Mechanical and thermal properties of rubber toughened poly(lactic acid). In: *Advanced materials research*, vol 1125. Trans Tech Publications, pp 222–226
71. Sun Y, He C (2013) Biodegradable “core-shell” rubber nanoparticles and their toughening of poly(lactides). *Macromolecules* 46(24):9625–9633
72. Odent J et al (2013) Toughening of polylactide by tailoring phase-morphology with P[CL-co-LA] random copolyesters as biodegradable impact modifiers. *Eur Polym J* 49(4):914–922
73. Meyva Y, Kaynak C (2015) Toughening of polylactide by bio-based and petroleum-based thermoplastic elastomers. *Int Polym Process* 30(5):593–602
74. Li Y, Shimizu H (2007) Toughening of polylactide by melt blending with a biodegradable poly(ether) urethane elastomer. *Macromol Biosci* 7(7):921–928
75. Todo M, Takayama T (2014) Fracture mechanisms of biodegradable PLA and PLA/PCL blends. In: Pignatello R (ed) *Biomaterials – physics and chemistry*. InTech, Rijeka, pp 375–394
76. Todo M, Takayama T (2007) Toughening of bioabsorbable polymer blend by microstructural modification. In: Watanabe M, Okuno O, Sasaki K, Takahashi N, Suzuki O, Takada H (eds)

- Proceedings of the 2nd international symposium for Interface oral health science, Sendai, Japan, 18–19 February, 2007. Springer Japan, Tokyo, pp. 95–104
77. Turng L-S, Srithep Y (2014) Annealing conditions for injection molded poly (lactic acid). Society of Plastics Engineers (SPE). doi:10.2417/spepro.005392. <http://www.4spepro.org/pdf/005392/005392.pdf>
 78. Grijpma DW et al (2002) Improvement of the mechanical properties of poly(D,L-lactide) by orientation. *Polym Int* 51(10):845–851
 79. Carrasco F et al (2010) Processing of poly(lactic acid): characterization of chemical structure, thermal stability and mechanical properties. *Polym Degrad Stab* 95(2):116–125
 80. Nascimento L et al (2010) Effect of the recycling and annealing on the mechanical and fracture properties of poly(lactic acid). *J Polym Environ* 18(4):654–660
 81. Gámez-Pérez J et al (2011) Fracture behavior of quenched poly (lactic acid). *Express Polym Lett* 5(1):82–91
 82. Yang G et al (2012) Toughening of poly (L-lactic acid) by annealing: the effect of crystal morphologies and modifications. *J Macromol Sci B* 51(1):184–196
 83. Perego G et al (1996) Effect of molecular weight and crystallinity on poly(lactic acid) mechanical properties. *J Appl Polym Sci* 59(1):37–43
 84. Cocca M et al (2011) Influence of crystal polymorphism on mechanical and barrier properties of poly(l-lactic acid). *Eur Polym J* 47(5):1073–1080
 85. Edenhofer B et al (2006) The flexible heat treatment of automotive components in a novel type of pusher furnace. *La Metallurgia Italiana* (2):39–45. <http://www.fracturae.com/index.php/aim/article/download/633/602>
 86. Funatani K (2004) Heat treatment of automotive components: current status and future trends. *Trans Indian Inst Metals* 57(4):381–396
 87. Johnson RW et al (2004) The changing automotive environment: high-temperature electronics. *IEEE Trans Electron Packag Manuf* 27(3):164–176
 88. ASTM (2016) ASTM standard test method for deflection temperature of plastics under flexural load in the edgewise position. ASTM. <http://www.astm.org/Standards/D648.htm>
 89. Huda MS et al (2006) Wood-fiber-reinforced poly(lactic acid) composites: evaluation of the physicomechanical and morphological properties. *J Appl Polym Sci* 102(5):4856–4869
 90. Shih Y-F, Huang C-C (2011) Poly(lactic acid) (PLA)/banana fiber (BF) biodegradable green composites. *J Polym Res* 18(6):2335–2340
 91. Lee B-H et al (2009) Bio-composites of kenaf fibers in polylactide: role of improved interfacial adhesion in the carding process. *Compos Sci Technol* 69(15–16):2573–2579
 92. Shi QF et al (2012) Influence of heat treatment on the heat distortion temperature of poly (lactic acid)/bamboo fiber/talc hybrid biocomposites. *J Appl Polym Sci* 123(5):2828–2836
 93. Ganster J, Fink H-P (2006) Novel cellulose fibre reinforced thermoplastic materials. *Cellulose* 13(3):271–280
 94. Chanda M, Roy SK (2008) Industrial polymers, specialty polymers, and their applications, vol 74. CRC, Boca Raton
 95. Coelho MC et al (2012) Nanotechnology in automotive industry: research strategy and trends for the future—small objects, big impacts. *J Nanosci Nanotechnol* 12(8):6621–6630
 96. Mai Y-W, Yu Z-Z (2006) Polymer nanocomposites. Woodhead, Cambridge
 97. Huang J-W et al (2009) Poly(lactide)/nano and microscale silica composite films. I. Preparation and characterization. *J Appl Polym Sci* 112(3):1688–1694
 98. Frone AN et al (2011) Cellulose fiber-reinforced poly(lactic acid). *Polym Compos* 32(6):976–985
 99. Li ZQ et al (2010) Preparation and characterization of bacterial cellulose/polylactide nanocomposites. *Polym-Plast Technol Eng* 49(2):141–146
 100. Shamel K et al (2010) Silver/poly(lactic acid) nanocomposites: preparation, characterization, and antibacterial activity. *Int J Nanomedicine* 5:573–579
 101. Xu X et al (2006) Biodegradable electrospun poly(l-lactide) fibers containing antibacterial silver nanoparticles. *Eur Polym J* 42(9):2081–2087

102. González A et al (2012) Fire retardancy behavior of PLA based nanocomposites. *Polym Degrad Stab* 97(3):248–256
103. Sinha Ray S, Okamoto M (2003) Polymer/layered silicate nanocomposites: a review from preparation to processing. *Prog Polym Sci* 28(11):1539–1641
104. Alexandre M, Dubois P (2000) Polymer-layered silicate nanocomposites: preparation, properties and uses of a new class of materials. *Mater Sci Eng R Rep* 28(1–2):1–63
105. Sinha Ray S, Bousmina M (2005) Biodegradable polymers and their layered silicate nanocomposites: in greening the 21st century materials world. *Prog Mater Sci* 50(8):962–1079
106. Kurauchi T et al (1991) Nylon 6-clay hybrid-synthesis, properties and application to automotive timing belt cover. SAE Technical Paper 910584. doi:[10.4271/910584](https://doi.org/10.4271/910584)
107. Paul M-A et al (2003) Exfoliated polylactide/clay nanocomposites by In-situ coordination-insertion polymerization. *Macromol Rapid Commun* 24(9):561–566
108. Khankrua R et al (2013) Thermal and mechanical properties of biodegradable polyester/silica nanocomposites. *Energy Procedia* 34:705–713109
109. Murariu M et al (2010) New trends in polylactide (PLA)-based materials: “green” PLA–calcium sulfate (nano)composites tailored with flame retardant properties. *Polym Degrad Stab* 95(3):374–381
110. Sinha Ray S et al (2003) New polylactide-layered silicate nanocomposites. 2. Concurrent improvements of material properties, biodegradability and melt rheology. *Polymer* 44(3):857–866
111. Pilla S et al (2010) Microcellular processing of polylactide–hyperbranched polyester–nanoclay composites. *J Mater Sci* 45(10):2732–2746
112. Ameli A et al (2014) Development of high void fraction polylactide composite foams using injection molding: mechanical and thermal insulation properties. *Compos Sci Technol* 90:88–95
113. Pilla S et al (2007) Solid and microcellular polylactide-carbon nanotube nanocomposites. *Int Polym Process* 22(5):418–428
114. Kramschuster A et al (2007) Injection molded solid and microcellular polylactide compounded with recycled paper shopping bag fibers. *Int Polym Process* 22(5):436–445
115. Seo J-H et al (2012) Combined effects of chemical and microcellular foaming on foaming characteristics of PLA (poly lactic acid) in injection molding process. *Polym-Plast Technol Eng* 51(5):455–460
116. Harris AM, Lee EC (2006) Injection molded polylactide (PLA) composites for automotive applications. SPE ACCE Paper Draft 62906
117. Najafi Chaloupli N (2015) Development of polylactide (PLA) and PLA nanocomposite foams in injection molding for automotive applications. Doctoral dissertation, École Polytechnique de Montréal
118. NatureWorks (2007) Technology focus report: blends of PLA with other thermoplastics. NatureWorks, Minnetonka
119. Guo X et al (2015) Poly(lactic acid)/polyoxymethylene blends: morphology, crystallization, rheology, and thermal mechanical properties. *Polymer* 69:103–109
120. Hashima K et al (2010) Structure-properties of super-tough PLA alloy with excellent heat resistance. *Polymer* 51(17):3934–3939
121. Wang Y et al (2012) Improvement in toughness and heat resistance of poly(lactic acid)/ polycarbonate blend through twin-screw blending: influence of compatibilizer type. *J Appl Polym Sci* 125(S2):E402–E412
122. Lin L et al (2015) Improving the impact property and heat-resistance of PLA/PC blends through coupling molecular chains at the interface. *Polym Adv Technol* 26(10):1247–1258
123. Lin L et al (2015) Super toughened and high heat-resistant poly(lactic acid) (PLA)-based blends by enhancing interfacial bonding and PLA phase crystallization. *Ind Eng Chem Res* 54(21):5643–5655

124. Srithep Y et al (2014) Processing and characterization of poly(lactic acid) blended with polycarbonate and chain extender. *J Polym Eng* 34:665–672
125. Liu J (2014) Heat resistant, flame retardant polylactic acid compounds. Patent WO2014113453 A1
126. Eguiburu JL et al (1998) Blends of amorphous and crystalline polylactides with poly(methyl methacrylate) and poly(methyl acrylate): a miscibility study. *Polymer* 39(26):6891–6897
127. Li S-H, Woo EM (2008) Immiscibility–miscibility phase transitions in blends of poly(L-lactide) with poly(methyl methacrylate). *Polym Int* 57(11):1242–1251
128. Samuel C et al (2013) PLLA/PMMA blends: a shear-induced miscibility with tunable morphologies and properties? *Polymer* 54(15):3931–3939
129. Zhang G et al (2003) Miscibility and phase structure of binary blends of polylactide and poly(methyl methacrylate). *J Polym Sci B Polym Phys* 41(1):23–30
130. Tsuji H (2007) Poly(lactide) stereocomplexes: formation, structure, properties, degradation, and applications. *Macromol Biosci* 7(12):1299–1299
131. Ikada Y et al (1987) Stereocomplex formation between enantiomeric poly(lactides). *Macromolecules* 20(4):904–906
132. Tsuji H et al (1991) Stereocomplex formation between enantiomeric poly(lactic acid)s. 4. Differential scanning calorimetric studies on precipitates from mixed solutions of poly(D-lactic acid) and poly(L-lactic acid). *Macromolecules* 24(20):5657–5662
133. Torres L et al (2016) Effect of multi-branched PDLA additives on the mechanical and thermomechanical properties of blends with PLLA. *J Appl Polym Sci* 133(1). doi:10.1002/app.42858
134. Zou J et al (2012) Effects of poly(D-lactide acid) on the properties of crystallization and thermal behavior of poly(L-lactide acid). *Adv Info Sci Service Sci* 4(10):382
135. Oyama HT, Abe S (2015) Stereocomplex poly(lactic acid) alloys with superb heat resistance and toughness. *ACS Sustain Chem Eng* 3(12):3245–3252
136. Sun B et al (2016) Enhanced toughness and strength of poly(d-lactide) by stereocomplexation with 5-arm poly(l-lactide). *J Appl Polym Sci* 133(1). doi:10.1002/app.42857
137. Nam B-U, Lee B-S (2012) Toughening of PLA stereocomplex by impact modifiers. *J Korea Acad Industr Coop Soc* 13(2):919–925
138. Corbion Purac (2015) high heat PLA: unlocking bioplastic potential for durable applications. <http://www.corbion.com/media/77166/corbion-puracpla-high-heat-themesheet.pdf>. Accessed Jan 2016
139. Min BH (2003) A study on quality monitoring of injection-molded parts. *J Mater Process Technol* 136(1–3):1–6
140. Spina R (2004) Injection moulding of automotive components: comparison between hot runner systems for a case study. *J Mater Process Technol* 155–156:1497–1504
141. Lim LT et al (2008) Processing technologies for poly(lactic acid). *Prog Polym Sci* 33(8):820–852
142. Mazumder SK (ed) (2002) Composites manufacturing, materials, product and process engineering. CRC Taylor & Francis, London. ISBN 0-8493-0585-3
143. Harris AM, Lee EC (2008) Improving mechanical performance of injection molded PLA by controlling crystallinity. *J Appl Polym Sci* 107(4):2246–2255
144. Li M et al (2010) Nonisothermal crystallization kinetics of poly(lactic acid) formulations comprising talc with poly(ethylene glycol). *Polym Eng Sci* 50(12):2298–2305
145. Urayama H et al (2003) Controlled crystal nucleation in the melt-crystallization of poly(l-lactide) and poly(l-lactide)/poly(d-lactide) stereocomplex. *Polymer* 44(19):5635–5641
146. Petchwattana N et al (2014) Influence of talc particle size and content on crystallization behavior, mechanical properties and morphology of poly(lactic acid). *Polym Bull* 71(8):1947–1959
147. Zhou J et al (2013) Synthesis and characterization of triblock copolymer PLA-b-PBT-b-PLA and its effect on the crystallization of PLA. *RSC Adv* 3(40):18464–18473

148. Shi X et al (2015) Synergistic effects of nucleating agents and plasticizers on the crystallization behavior of poly (lactic acid). *Molecules* 20(1):1579–1593
149. Kolstad JJ (1996) Crystallization kinetics of poly(L-lactide-co-meso-lactide). *J Appl Polym Sci* 62(7):1079–1091
150. Schmidt SC, Hillmyer MA (2001) Polylactide stereocomplex crystallites as nucleating agents for isotactic polylactide. *J Polym Sci B Polym Phys* 39(3):300–313
151. NEC (2006) NEC & UNITIKA Realize bioplastic reinforced with Kenaf fiber for mobile phone use. <http://www.nec.co.jp/press/en/0603/2001.html>
152. Fujitsu Limited, Fujitsu Laboratories Ltd., Toray Industries, Inc. (2005) Fujitsu and Toray develop world's first environmentally-friendly large-size plastic housing for notebook PCs [Press release]. Retrieved from <http://www.fujitsu.com/global/about/resources/news/press-releases/2005/0113-01.html>
153. Harris AM, Lee EC (2010) Heat and humidity performance of injection molded PLA for durable applications. *J Appl Polym Sci* 115(3):1380–1389
154. Finnis A (2014) Poly(lactic acid)-based polymer blends for durable applications. West Virginia University, Morgantown
155. Harris AM, Lee EC (2013) Durability of polylactide-based polymer blends for injection-molded applications. *J Appl Polym Sci* 128(3):2136–2144
156. Jiménez A et al (2014) Poly (lactic acid) science and technology: processing, properties, additives and applications, vol 12. Royal Society of Chemistry, London
157. Toyota Motor Corporation (2000) Utilising plant-derived materials in automotive interior parts. <http://www.toyota-boshoku.com/global/about/development/eco/index.html>. Accessed 19 Feb 2016
158. Toyota Motor Corporation (2008) Toyota to increase 'ecological plastic' in vehicle interiors. <http://www.toyota.co.jp/en/news/08/1217.html>. Accessed 21 Feb 2016
159. Thielen M (2010) Hyundai Blue-Will concept to feature PLA and PA 11. *Bioplastics Magazine*, Jan/Feb 2010
160. Teijin Ltd. (2007) Highly heat-resistant bioplastic. <http://www.teijin.com/rd/technology/bioplastic/>. Accessed 22 Feb 2016
161. Motors M (2006) Mitsubishi Motors develops plant-based green plastic floor mat. <http://www.mitsubishi-motors.com/en/corporate/pressrelease/corporate/detail1475.html>. Accessed 20 Feb 016
162. Corbion Purac (2013) PLA bioplastics: a driving force in automotive. Corbion Purac. <http://www.corbion.com/bioplastics/pla-markets/automotive>. Accessed 05 Jan 2016
163. Kitamura H (2007) Teijin Launches BIOFRONT heat-resistant bioplastic - 100% BIOFRONT car seat fabrics developed with Mazda
164. Ramaswamy S, Aslan B, Gries T, Urbanus M (2015) Biobased thermoplastic composites for automotive interiors. *Bioplastics Magazine*, Jan/Feb 2015
165. Aslan B et al (2012) Bio-composites: processing of thermoplastic biopolymers and industrial natural fibres from Staple fibre blends up to fabric for composite applications. *J Textile Eng* 19(85)
166. Ichhaporia PK (2008) Composites from natural fibers. Dissertation, North Carolina State University, Raleigh
167. Ampro Verdù Solis A (2015) New biobased fibres for automotive interior applications. *Bioplastics Magazine*, Sept/Oct 2015
168. Wambua P et al (2003) Natural fibres: can they replace glass in fibre reinforced plastics? *Compos Sci Technol* 63(9):1259–1264
169. Koronis G et al (2013) Green composites: a review of adequate materials for automotive applications. *Compos Part B* 44(1):120–127
170. Edana (2013) Nonwovens in automotive applications. Edana, Brussels. <http://www.edana.org/discover-nonwovens/products-applications/automotive>

Index

A

- ABA triblock copolymers, 87
- Additive manufacturing (AM)
 - advantages, 140
 - binder jetting, 141
 - definition, 140
 - extrusion-based printing technologies
 - amorphous thermoplastics, 142
 - biocompatibility, 143
 - DoE approach, 143
 - FDM, 142
 - FFF, 142
 - fused deposition setup, 142
 - intrinsic mechanical behavior, 144
 - MEM, 142
 - PEG, 144–145
 - TCP, 144
 - 3D printable PLA–graphene composites, 144
 - 3D-printed scaffolds, 145, 146
 - tissue engineering applications, 143
 - FFF, 26–28
 - laser sintering process, 141
 - material extrusion, 141
 - material jetting, 141
 - photopolymerization-based 3D printing, 151–153
 - powder-based AM processes, 25
 - advantage, 145
 - coalescence, 148, 149
 - cold crystallization, 151
 - complex temperature distribution, 148
 - crystallization, 148–150
 - disadvantage, 147, 150
 - EOS commercial sinter grade polyamide PA2200, 148, 149
 - laser sintering process, 145, 147–150
 - layer-by-layer approach, 148
 - melting, 148–150
 - nonhomogeneous shrinkage, 148
 - sinterability, 148
 - surface-selective laser sintering, 150–151
 - tissue engineering applications, 150
 - sheet lamination, 141
 - stereolithography, 141
 - vat photopolymerization, 28–29
- Agriculture applications, 47
- Alkaline phosphatase (ALP) assay, 97
- Alvelac™, 94
- AM, *see* Additive manufacturing
- Amorphous polymers, 7–8
- Amphiphilic copolymers, 87
- Automotive industry
 - bioplastics
 - bioeconomy, 181
 - evolution of plastics, 180
 - global production capacities, 181, 182
 - technical requirements, car applications, 181–183
 - PLLA (*see* PLLA, automotive industry)

B

- BBB, *see* Blood–brain barrier
- Bell-shaped crystallization growth curves, 4, 5
- Bilayered electrospun vascular graft, 63–64
- Bioactivity, 91–92

- Bio-based materials, *see* Poly(lactic acid)
- Biodegradable mulching, 47
- Biomaterial, 53–54
- Biomax[®] Strong (BS), 190–191
- Bioplastics, automotive industry
- bioeconomy, 181
 - evolution of plastics, 180
 - global production capacities, 181, 182
 - PLLA
 - net greenhouse gas emission, 185
 - vs.* petroleum-based polymers, 183, 185
 - physical and mechanical properties, 184, 185
 - production capacity, 186
 - short-term goods, 183
 - Strati car, 186
 - 3D printing, 186
 - technical requirements, car applications, 181–183
- Biopolymers, *see* Poly(lactic acid)
- Bioresorbable vascular scaffolds (BVSs), 56–58
- BioSeed[®]-C, 94
- Blends, polylactides, 88–89
- Block copolymers, 87–88
- Blood–brain barrier (BBB), 114, 117
- Breviscapine (BVP), 114, 117
- BVSs, *see* Bioresorbable vascular scaffolds
- C**
- Carbon nanotubes (CNTs), 67
- Cardiac patches, tissue-engineered, 65–68
- Cardiovascular applications
- coronary stents
 - bioresorbable vascular scaffolds, 56–58
 - coronary artery disease, 55
 - drug-eluting stents, 55
 - in-stent restenosis, 55
 - tissue engineering
 - ECM function, 59
 - RM approach, 58
 - TEHV, 61–63
 - TEVG, 63–65
 - 3D scaffolds, 59–60
 - tissue-engineered cardiac patches, 65–68
- CDDP-loaded PDLLA microspheres, 121
- Central nervous system (CNS), 114, 117
- Chemical grafting, 92
- Chitosan (CHI), 89
- CNS, *see* Central nervous system
- Composites, organic–inorganic, 91–94
- Controlled DDSs
- carriers, 110
 - biodegradable polymers, 110
 - PLA (*see* Poly(lactic acid), controlled drug release)
 - SMD solubility, 110
- Copolymers, block, 87–88
- Coronary artery disease (CAD), 55
- Crosslinking, 89–90
- Crystallization
- bell-shaped growth curve, 4, 5
 - cold, 5, 6
 - exothermic, 4
 - growth rate, 4
 - isothermal, 4, 5
 - temperature, 4
- D**
- DDSs, *see* Drug delivery systems
- Dechloro-4-iodo-fenofibrate (IFF), 117
- Design of experiments (DoE) approach, 143
- Difluoroboron dibenzoylmethane dye (BF₂dbmPLA), 118
- Dimethyl sulfoxide (DMSO), 89
- Docetaxel (DTX), 120
- Doxorubicin (DOX), 124, 125
- Drug delivery systems (DDSs)
- controlled (*see* Controlled DDSs)
 - definition, 110
 - packaging, 110
- Drug-eluting stents (DESs), 55
- E**
- Electrospinning technique, 66–67
- Electrospun fibers
- applications, 124–126
 - properties, 124
- Electrospun scaffolds, 67
- Emodin (ED)-loaded PLA microspheres, 120
- Ethylene bis-stearamide (EBS), 204
- Extracellular matrix (ECM) function, 59
- Extrusion-based printing technologies
- amorphous thermoplastics, 142
 - biocompatibility, 143
 - DoE approach, 143
 - FDM, 142
 - FFF, 142
 - fused deposition setup, 142
 - intrinsic mechanical behavior, 144
 - MEM, 142
 - PEG, 144–145

TCP, 144
3D printable PLA–graphene
composites, 144
3D-printed scaffolds, 145, 146
tissue engineering applications, 143
Extrusion process, 8–9

F

FFF, *see* Fused filament fabrication
Fiber yarns
and filament, 14–16
shrinkage tension, 13–14
shrinkage *vs.* temperature, 13–14
tensile strength *vs.* elongation
offline drawn fiber yarns, 12, 13
online drawn fiber yarns, 12, 13
5-Fluorouracil (5-FU), 120
Freeze-dry fabricated PLGA/collagen
scaffolds, 63
Fused deposition modeling (FDM), 142
Fused filament fabrication (FFF), 26–28, 142

G

Gelatine (GEL), 89
Global carbon cycle, 39–40

H

Halloysite nanotubes (HNT), 189
HAp, *see* Hydroxyapatite
Heart valves, tissue-engineered, 61–63
Heat deflection temperature (HDT), 195
Hepatocellular carcinoma (HCC), 120
Hot recoverable (HR) strain test, 19–20
Hydrogel networks, 90
Hydrogels
applications, 122–124
properties, 122
Hydroxyapatite (HAp), 91–94
Hyperbranched polyglycerol (HPG), 113

I

Immiscible blends, 3
Injection molding
advantages, 17
crystalline morphology and properties,
19–21
crystallinity, process influence, 20–22

interfaces formation, 22–25
steps, 18–19
In situ intercalative polymerization, 196
In-stent restenosis (ISR), 55
Inverse piezoelectric effect, 161
Isothermal crystallization, 4, 5

L

Lactic acid monomer, 2
Lactic acid polymerization, 2
Laser sintering process, 145, 147–150
Layer-by-layer (LbL) technique, 95, 98
L-C Ligament[®], 94
Lovastatin (LVT), 120
Low molecular weight protamine (LMWP), 117

M

Macroscopic piezoelectricity, PLLA films
helix structure, 163–165
macrosymmetry
chirality, 167
drawing process, 166
ferroelectric polymers, 166
high-order structures, 164
poling process, 166
polypeptide molecules, 167
shear piezoelectric constant, 167
shear stress, 161–162
Medical applications, 46
Melt extrusion manufacturing (MEM), 142
Melt intercalation, 196
Melt spinning
advantages, 10
equipment, 11
fiber-grade pellets, 10–11
filament and fiber yarns, 14–16
mechanical properties, fiber yarns, 12–14
micro- and nanofibrillar PLA structures
from blends, 16–17
process parameters, 11–12
Methacrylate end-capped PLA macromers, 90
Microspheres
applications, 120–121
properties, 119–120
Monomeric plasticizers, 187–189
MTX-loaded Fe₃O₄-PLLA-PEG-PLLA
(MMCMs), 120
Multiwalled carbon nanotubes (MWCNTs),
124, 125

N

Nanoparticles (NPs)
 applications
 BBB, 114, 117
 BF₂dbmPLA, 118
 BVP-loaded PDLLA NPs, 114, 117
 cancer diagnosis and treatment, 117
 CNS, 114, 117
 micelle composition and metabolism
 in vivo, 117, 118
 TAT-conjugated NPs, 117
 TC-loaded PLA NPs, 118–119
 TNF α -siRNA-loaded NP, 118
 HP–PLA NP group, 113
 PEG–PLA NP group, 113
 PLA NP group, 113
 properties, 114
 Natural polymers, 60
 Non-acoustic inverse piezoelectric devices, 161
 NPs, *see* Nanoparticles

O

Oligomeric plasticizers, 187–189
 Organic–inorganic composites, 91–94
 Original equipment manufacturers
 (OEMs), 207
 Oxaliplatin (OXA), 113

P

Packaging applications, 47–48
 PCL/PLLA blends, 88
 PDLA, *see* Poly(D-lactic acid)
 PEG dimethacrylate–PLA, 61–62
 PEG/PLA blends, 88
 PEI, *see* Poly(ethylene imine)
 PEM, *see* Polyelectrolyte multilayers
 PGA/PLLA (50:50 blend) scaffolds, 61
 Pharmaceutical applications, 46
 Photopolymerization-based 3D printing,
 151–153
 Piezoelectric *d*-constant, 160
 Piezoelectricity
 PLLA (*see* Poly(L-lactic acid),
 piezoelectricity)
 in polymers, 160
 PLA, *see* Poly(lactic acid)
 PLA-based carriers, controlled drug release,
 110–111
 biomedical applications, 114–116
 electrospun fibers, 124–126
 hydrogels, 122–124

 microspheres, 119–121
 NPs (*see* Nanoparticles)
 scaffolds, 126–128
 PLA-based hydrogels, 62–63
 PLA/CHI networks, 90
 PLA/CHI solution, 89
 PLA INGEO, carbon footprint (case study)
 global carbon cycle, 39–40
 GWP-cradle-to-polymer factory-gate,
 43, 45
 Ingeo production process flow diagram,
 41–42
 Ingeo production steps, 43, 44
 lactic acid production process, 43
 NatureWorks' lactide formation process, 43
 polylactide polymerization process, 43
 primary energy of non-renewable resources,
 43, 45
 production system, 41
 up-to-date life cycle inventory data, 41
 PLA–PCL-based scaffolds, 67
 PLA–PCL copolymers, 64
 PLA–PCL/PLA scaffolds, 65
 PLA/PGA blends, 88
 PLA-reinforced PCL–PLA sponges, 67
 Plasticization
 with HNT, 189
 mixed plasticizers, 189
 monomeric plasticizers, 187–189
 oligomeric plasticizers, 187–189
 PLLA/TBC/HNT compositions, 189, 190
 polymeric plasticizers, 187–189
 PP-B, 189, 190
 thermal and mechanical properties, 187, 188
 thermoplastics, 187
 PLGA/PANi fibrous scaffolds, 68
 PLGA/PGA scaffolds, 65
 PLLA, *see* Poly(L-lactic acid)
 PLLA-based materials
 disadvantages, 186
 durable PLLA/polymer blends, 205–207
 heat-resistant PLLA-based blends
 HDT, 195
 nanocomposites with high thermal
 properties (*see* Polymer
 nanocomposites)
 petroleum-sourced polymer blends, 199
 stereocomplexes, 200–201
 modifications, 186
 mold-injected PLLA materials
 crystallinity vs. annealing time, 204
 crystallization kinetics, 204
 crystallization rate, 202, 205

- EBS, 204
- injection molding process cycle, 202
- polarized optical micrographs, 203
- post-annealing processing, 204
- self-nucleation, 203–204
- PLLA-based fabrics and nonwovens
 - products, 211
- PLLA-based plastics and reinforced plastics
 - biobased materials, 207, 210
 - current application, 207–209
 - green composites, 210
 - hydrolysis and thermal resistance, 211
 - kenaf fiber-based composite, 210
 - Planutra™, 210
 - PP/glass fiber composites, 210
 - renewable fibers, 210
- tough/ductile PLLA-based blends
 - annealing process, 194–195
 - plasticization (*see* Plasticization)
 - rubber-toughened PLLA blends (*see* Rubber-toughened PLLA blends)
- PLLA film sensors
 - deformation-sensitive touch panel
 - bending and twisting motions, 168
 - charge and deflection, 168
 - film types, 167
 - piezoelectric voltage coefficient, 169
 - pressure-sensing electrode, 169–170
 - prototype, 170
 - sensing motion, test plate, 167, 168
 - fiber sensors, motion capture, 170
 - expansion and twist detection, 171–173
 - fiber coil, 171
 - helical torsion coil, 171
 - human motion detection, 172, 174, 175
 - rotation angle detection, 172–174
- PLLA/HAp nanocomposite scaffolds, 91–93
- PLLA/HAp/SBF scaffolds, 91, 93
- PLLA/PDLA blends, 21–22, 88
- Poly(D-lactic acid) (PDLA), 111–112
 - helix structure, 163
 - stereocomplex, 140
- Poly(D,L-lactic acid) (PDLLA), 111–112
- Polyelectrolyte multilayers (PEM), 98–101
- Poly-electrolytes (PEL), 98–99
- Poly(ethylene glycol) (PEG), 113
 - block copolymers, 87
 - plasticizers, 144–145
- Poly(ethylene imine) (PEI), 95–97
- Poly(lactic acid) (PLA)
 - AM (*see* Additive manufacturing)
 - applications
 - agriculture, 47
 - future of PLA-based materials, 48
 - medical and pharmaceutical industry, 46
 - packaging, 47–48
 - textile industry, 46
 - world-wide demand, 43, 45
 - biodegradation, 38
 - as biomaterial, 53–54
 - carbon footprint of PLA INGENEO, 39–43
 - cardiovascular applications
 - coronary stents, 55–58
 - tissue engineering, 58–68
 - controlled drug release
 - advantage, 112
 - biocompatibility, 112
 - biodegradability, 112
 - chemical and physical properties, 113
 - formulation factors, 113
 - green biomaterial, 111
 - L and D isomers, 111–112
 - OXA concentration, 113
 - PEG, 113
 - peptide- and protein-based therapeutics, 128
 - PLA-based carriers (*see* PLA-based carriers, controlled drug release)
 - preparation, 111
 - from renewable sources, 111
 - D- and L-enantiomers, 140
 - environmental characteristics, 39
 - extrusion process, 8–9
 - flow behavior, 6–7
 - immiscible blends, 3
 - injection molding
 - advantages, 17
 - crystalline morphology and properties, 19–20
 - crystallinity, process influence, 20–22
 - interfaces formation, 22–25
 - steps, 18–19
 - lactic acid monomer, 2
 - linear aliphatic thermoplastic polymer, 140
 - market status, 68–69
 - melt spinning
 - advantages, 10
 - fiber-grade pellets, 10–11
 - filament and fiber yarns, 14–16
 - mechanical properties, fiber yarns, 12–14
 - micro- and nanofibrillar PLA structures from blends, 16–17
 - process parameters, 11–12
 - polymer blends, 3
 - polymerization, 2

- Poly(lactic acid) (PLA) (*cont.*)
- properties
 - biodegradable polymer properties, 37–38
 - general considerations, 36
 - hydroxy acid precursor, 37
 - limitations, 37
 - mechanical properties, 37
 - pVT behavior, 7–8
 - stereocomplex, 140
 - technical properties, 3
 - thermal behavior, 4–6
- Poly(lactic-co-glycolic acid) (PLGA), 28, 120
- Poly lactides
- advantages and disadvantages, 82–85
 - surface modification, 95
 - covalent activation *vs.* adsorptive binding, 95–97
 - PLLA with polyelectrolyte multilayers, 98–101
 - tailoring bulk composition
 - blends, 88–89
 - block copolymers, 87–88
 - commercially available products, 94
 - organic–inorganic composites, 91–94
 - polymer network, 89–90
- Poly(L-lactic acid) (PLLA), 111–113
- advantages, 84
 - apparent Young's moduli, 92, 94
 - automotive industry (*see also* PLLA-based materials)
 - bioplastics (*see* Bioplastics)
 - OEMs, 207
 - PLLA-based fabrics and nonwovens products, 211
 - PLLA-based plastics and reinforced plastics, 207–211
 - biocompatibility, 85
 - blends, 88–89
 - crystallization behavior, 4, 21–22
 - degradation, 83
 - drug-free high molecular weight PLLA, 56
 - fibrous scaffolds, 68
 - films
 - macroscopic piezoelectricity (*see* Macroscopic piezoelectricity, PLLA films)
 - sensor (*see* PLLA film sensors)
 - stable films, 161
 - heating curves, 4–5
 - nanofibrous scaffolds, 64, 66
 - physical surface modification techniques, 98–100
 - piezoelectricity
 - crystal structure, 161, 162
 - direct piezoelectric effect, 161
 - electric displacement, 161
 - high-order structure, 162, 164
 - inverse piezoelectric effect, 161
 - molecule, 161, 163
 - PLGA scaffolds, 66
 - PLLA/HAp scaffolds, 91
 - PLLA/PDLA, 21–22
 - polymerization, 82
 - processing–property relationships, 19–20
 - scanning electron micrographs, 84, 91–92
 - semi-crystalline, 53
 - stereocomplex, 140
 - surface properties, 95–96
 - tailoring bulk composition, 86–94
 - of variable molecular weight, 53
- Polymer blends(ing), 3, 88
- Polymeric plasticizers, 187–189
- Polymerization, lactic acid, 2
- Polymer nanocomposites
- flame-retardant properties, 198
 - HDT values, 197
 - injection-molded PLLA nanocomposites, 197
 - layered silicate nanocomposites, 196
 - nanofillers, 196
 - OMLS, 197–198
 - PLLA nanocomposite foams, 197
 - polymer matrix, 196
 - preparation methods, 196
 - specimen behavior, UL94 HB testing, 198
- Polymer network, 89–90
- Powder-based AM processes, 25
- advantage, 145
 - coalescence, 148, 149
 - cold crystallization, 151
 - complex temperature distribution, 148
 - crystallization, 148–150
 - disadvantage, 147, 150
 - EOS commercial sinter grade polyamide PA2200, 148, 149
 - laser sintering process, 145, 147–150
 - layer-by-layer approach, 148
 - melting, 148–150
 - nonhomogeneous shrinkage, 148
 - sinterability, 148
 - surface-selective laser sintering, 150–151
 - tissue engineering applications, 150

R

- Rapid prototyping, 25
- Regenerative medicine, *see* Tissue engineering
- Reticuloendothelial system (RES), 117
- Rubber-toughened PLLA blends
 - biodegradable and nonbiodegradable flexible polymers, 190
 - Biomax[®] Strong, 190–191
 - ductility and impact toughness, 190
 - ENR20/PLLA blends, 193, 194
 - ENR50/PLLA blends, 193, 194
 - melt-blending, 190
 - PLLA/EMA-GMA/PEBA ternary blends, 193
 - PLLA/PEBA blends, 192–193
 - PLLA/PMMA/BS blend, 191, 192
 - PP-B, mechanical properties, 192
 - tensile stress–strain curves, 191
 - thermal mechanical analysis, 191

S

- Scaffolds
 - applications, 127–128
 - properties, 126
 - 3D-printed scaffolds, 145, 146
- Semi-crystalline polymers, 4, 7–8
- Shear controlled orientation in injection molding (SCORIM), 20–21
- Shear piezoelectricity, 160, 163, 167
- Skeletal tissues engineering
 - bone and cartilage, 81
 - commercially available products, 94
 - ideal scaffold material, 80
 - synthetic biodegradable poly(α -hydroxy ester)s, 81
 - 3D networks of cells and matrix, 81
- SLA, *see* Stereolithography
- Small molecule drugs (SMDs), 110
- Solution intercalation, 196
- Stents, coronary
 - bioresorbable vascular scaffolds, 56–58
 - coronary artery disease, 55
 - drug-eluting stents, 55
 - in-stent restenosis, 55
- Stereolithography (SLA), 141, 151–153
- Surface modification, polylactides, 95
 - adsorption of ECM proteins, 95
 - ALP assay, 97
 - covalent activation *vs.* adsorptive binding, 95–97

- LbL technique, 95, 98
- plasma treatment, 95
- of PLLA with polyelectrolyte multilayers
 - Alizarin Red staining, hMSCs, 100, 101
 - SPR curves, 98–99
 - WCA, 98–99
- surface properties of PLLA films, 96
- Surface plasmon resonance (SPR) curves, 98–99

T

- TEHV, *see* Tissue-engineered heart valves
- Tensile piezoelectricity, 160, 167
- TEVG, *see* Tissue-engineered vascular grafts
- Textile applications, 46
- Three-dimensional (3D) printing, 25, 62
 - See also* Additive manufacturing
- Tissue-engineered heart valves (TEHV), 61–63
- Tissue-engineered vascular grafts (TEVG), 63–65
- Tissue engineering (TE)
 - ECM function, 59
 - polylactides
 - advantages and disadvantages, 82–85
 - surface modification, 95–101
 - tailoring bulk composition, 86–94
 - RM approach, 58
 - of skeletal tissues
 - bone and cartilage, 81
 - ideal scaffold material, 80
 - synthetic biodegradable poly(α -hydroxy ester)s, 81
 - 3D networks of cells and matrix, 81
 - TEHV, 61–63
 - TEVG, 63–65
 - 3D scaffolds, 59–60
 - tissue-engineered cardiac patches, 65–68
- Tough/ductile PLLA-based blends
 - annealing process, 194–195
 - plasticization
 - with HNT, 189
 - mixed plasticizers, 189
 - monomeric plasticizers, 187–189
 - oligomeric plasticizers, 187–189
 - PLLA/TBC/HNT compositions, 189, 190
 - polymeric plasticizers, 187–189
 - PP-B, 189, 190
 - thermal and mechanical properties, 187, 188
 - thermoplastics, 187

Tough/ductile PLLA-based blends (*cont.*)
 rubber-toughened PLLA blends
 biodegradable and nonbiodegradable
 flexible polymers, 190
 Biomax[®] Strong, 190–191
 ductility and impact toughness, 190
 ENR20/PLLA blends, 193, 194
 ENR50/PLLA blends, 193, 194
 melt-blending, 190
 PLLA/EMA-GMA/PEBA ternary
 blends, 193
 PLLA/PEBA blends, 192–193
 PLLA/PMMA/BS blend, 191, 192
 PP-B, mechanical properties, 192
 tensile stress–strain curves, 191

 thermal mechanical analysis, 191
Trans-activating transcriptional activator (TAT)
 peptide, 117
Tributylcitrate (TBC) plasticizer, 189
Tricalcium phosphate (TCP), 144
Triclosan (TC), 118–119

V

Vascular grafts, tissue-engineered, 63–65
Vat photopolymerization (VP), 28–29

W

Water contact angles (WCA), 98–99